№ 4(88)/2017

ХИМИЯ сериясы

Серия ХИМИЯ

CHEMISTRY Series

ҚАРАҒАНДЫ
УНИВЕРСИТЕТІНІҢ
ХАБАРШЫСЫ

ВЕСТНИК
КАРАГАНДИНСКОГО
УНИВЕРСИТЕТА

BULLETIN
OF THE KARAGANDA
UNIVERSITY

Bulletin of the Karaganda University. «Chemistry» series.

ISSN 2518-718X.

Proprietary: RSE «Academician Ye.A. Buketov Karaganda State University».

Registered by the Ministry of Culture and Information of the Republic of Kazakhstan. Registration certificate No. 13110–Zh from 23.10.2012.

Signed in print 28.12.2017. Format 60×84 1/8. Offset paper. Volume 15,4 p.sh. Circulation 300 copies. Price upon request. Order № 124.
Printed in the Ye.A. Buketov Karaganda State University Publishing house.
38, Gogol Str., Karaganda, 100012, Kazakhstan. Tel.: (7212) 51-38-20. E-mail: izd_kargu@mail.ru

МАЗМҰНЫ

ОРГАНИКАЛЫҚ ХИМИЯ

ФИЗИКАЛЫҚ ЖӘНЕ АНАЛИТИКАЛЫҚ ХИМИЯ

БЕЙОРГАНИКАЛЫҚ ХИМИЯ

ХИМИЯЛЫҚ ТЕХНОЛОГИЯ

ХИМИЯНЫ ОҚЫТУ ӘДІСТЕМЕСІ

СОДЕРЖАНИЕ

ОРГАНИЧЕСКАЯ ХИМИЯ

ФИЗИЧЕСКАЯ И АНАЛИТИЧЕСКАЯ ХИМИЯ

НЕОРГАНИЧЕСКАЯ ХИМИЯ

ХИМИЧЕСКАЯ ТЕХНОЛОГИЯ

МЕТОДИКА ОБУЧЕНИЯ ХИМИИ

CONTENTS

ORGANIC CHEMISTRY

PHYSICAL AND ANALYTICAL CHEMISTRY

INORGANIC CHEMISTRY

CHEMICAL TECHNOLOGY

METHODS OF TEACHING CHEMISTRY

UDC 554.02

J. Klimentova, M. Madlova, P. Nemeckova, L. Palatinusova, P. Vojtisek, I. Lukes

Charles University, Praha, Czech Republic
(E-mail: pavojt@natur.cuni.cz)

Conformations of calix[4]arenes — an investigation based on CSD data. Part II. Partial cone, 1,2-alternate and 1,3-alternate conformers of methylene- and heteroatom-bridged calix[4]arenes

In the first part of this investigation (Part I), cone conformers of calix[4]arenes with methylene and heteroatom bridges from the Cambridge Structural Database (CSD) were investigated. Previously introduced parameters α, β and δ were utilized in describing the conformations of the hydrocarbon base frame of the above mentined compounds. In this part of the investigation, partial cone, 1,2- and 1,3-alternate conformers of methylene- and heteroatom-bridged calix[4]arenes are studied and the influence of inter- and intramolecular interactions on the conformations of these compounds is evaluated.

Keywords: calix[4]arene, conformation, torsion angle, distorsion parameter.

Introduction

Calix[4]arenes with methylene or heteroatom bridges and calix[4]resorcinarenes are interesting classes of macrocyclic compounds which have recently attracted a lot of interest because of their ability to form host-guest complexes and act as enzyme mimics [1–3]. However, design of functional hosts for cations, anions and neutral molecules often requires that the calixarene scaffold adopts a specific geometry. The factors affecting the geometry of the calixarene base frame are numerous [1–6] and the knowledge of how the calixarene base frame is deformed in response on these inter- and intramolecular interactions is essential in molecular design of functional molecules. In the first part of this work (Part I [7]), the previously introduced parameters α, β and δ [8, 9] have been utilized to describe the geometry of the calixarene base frame. Furthermore, the influence of various inter/intramolecular interactions on the value of the parameters α, β and δ (and therefore, on the geometry of the calixarene scaffold) in the *cone* conformers of methylene- and heteroatom-bridged calix[4]arenes was studied.

In the second part this work, the influence of inter/intramolecular interactions on the geometry of the *partial cone*, *1,2-alternate* and *1,3-alternate* moiety in calix[4]arenes with methylene and heteroatom bridges is investigated. As in the *cone* conformers, the previously introduced parameters α, β and δ [8, 9] and data from the Cambridge Structural Database [10] are utilized for this purpose.

The main difference between *partial cone*, *1,2-alternate* and *1,3-alternate* conformers and the previously described *cone* conformers (Part I [7]) is the presence of cavity formed by four calix[4]arene phenyl rings in the case of *cone* conformers. This cavity is nonexistent in *partial cone*, *1,2-alternate* and *1,3-alternate* conformers. In the case of *partial cone* structures, the 'cavity' is formed by three calix[4]arene phenyl rings only; the guest cannot be therefore completely encapsulated and, due to diminished intermolecular van der Waals interactions (three phenyl rings instead of four participate on the guest binding), weaker binding of the guest in the cavity can be expected. This effect is even more pronounced in *1,2-alternate* conformers, which possess a 'half-cavity' formed by two adjacent calix[4]arene phenyl rings only. On the other hand, in

1,3-alternate conformers the 'cavity' is formed by two opposite calix[4]arene phenyl rings, so stronger binding of the guest than in the case of *1,2-alternate* conformers is expected. Furthermore, *1,2-alternate* and *1,3-alternate* conformers contain two such 'cavities' compared to *cone* and *partial cone* conformers. The illustration of the above mentioned effects is summarized in Figure 1.
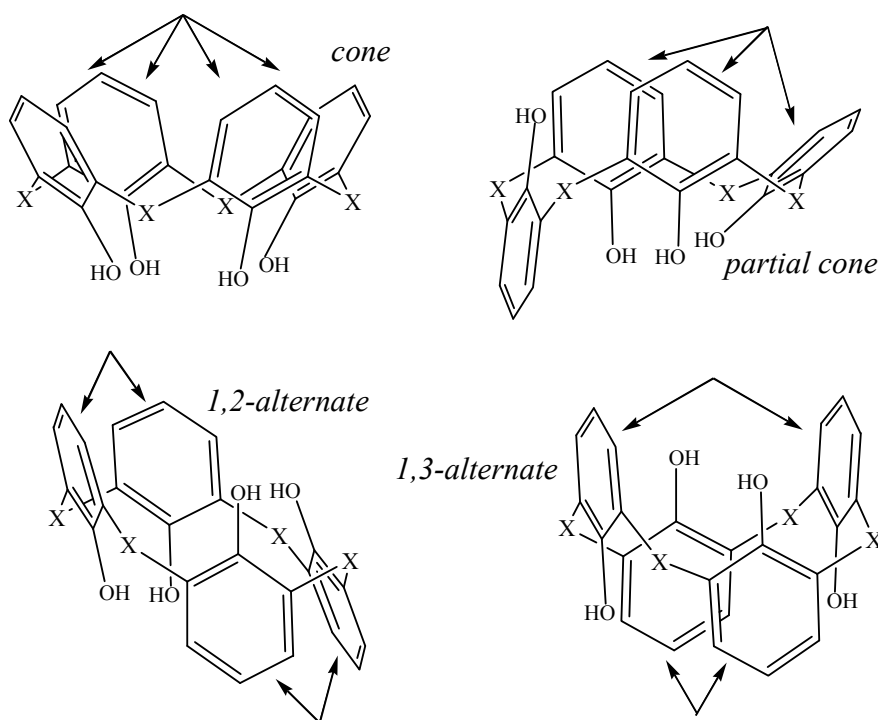
Figure 1. Cavities in cone, partial cone 1,2-alternate and 1,3-alternate calix[4]arenes
(X … CH$_2$ or heteroatom/heterogroup)

In the next part of this article, the influence of inter- and intramolecular interactions on the geometry of *partial cone*, *1,2-alternate* and *1,3-alternate* structures will be investigated.

Partial cone structures

Methylene-bridged partial cone calix[4]arenes

The group of *partial cone* conformers of calix[4]arenes with methylene bridge groups contains relatively few hits (93 complete cif files with 106 independent molecules, and 3 incomplete cif files) compared to other groups, especially *cone* (see Part I, [7]), the substitution patterns are also fewer symmetrical than in the *cone* group. Important ones and their corresponding percentages of the *partial cone* group are given in Table 1.

T a b l e   1

**The substitution patterns and the corresponding percentages
of the methylene-bridged partial cone group from [10]**

Type	Hits	%	Independent molecules	%
Symmetrically tetrasubstituted	24	25.0	27	25.5
Distally substituted lower rim, symmetrically tetrasubstituted upper rim	17	17.7	20	18.9
Single atom 'triple bridge'	15	15.6	15	14.1
Other	40	41.7	44	41.5
Total	**96**	**100**	**106**	**100**

The α-β and β-δ plots (Fig. 2, 3) depict the distribution of the *partial cone* calix[4]arenes according to their substitution. Since only 16 % of all cif files belong to complexes, metal-coordinated structures are not distinguished in these plots.
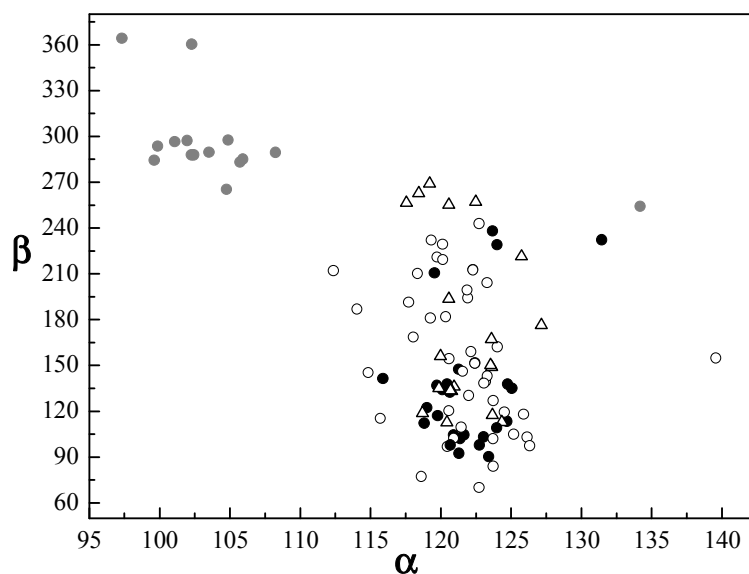
● — symmetrically tetrasubstituted; ● — single atom 'triple bridge' at the lower rim;
Δ — distally substituted lower rim and symmetrically tetrasubstituted upper rim; ○ — other substitution patterns

Figure 2. The α-β plot of the group of partial cone methylene-bridged calix[4]arenes

From Figure 2 it can be clearly seen that the symmetrically tetrasubstituted and single atom 'triple-bridged' groups are relatively uniform in parameters α, β with the symmetrically tetrasubstituted group closer to average values of α, β (see Table 4 in Part I [7]). There are two groups of lower rim distally disubstituted structures: one at β < 210° and one at β ~ 240°. Other substitution patterns (relatively uniform in α but distributed in the β parameter) are less important because each of them contains only a few molecules and these substitution patterns are therefore not distinguished.

The α-δ plot (Fig. 3) shows that almost all *partial cone* conformers are uniform in these two parameters regardless of their substitution pattern with the notable exception of lower rim single atom 'triple-bridged' structures which form a very distinct group. Lower rim distally substituted structures are not distinguished in this plot.
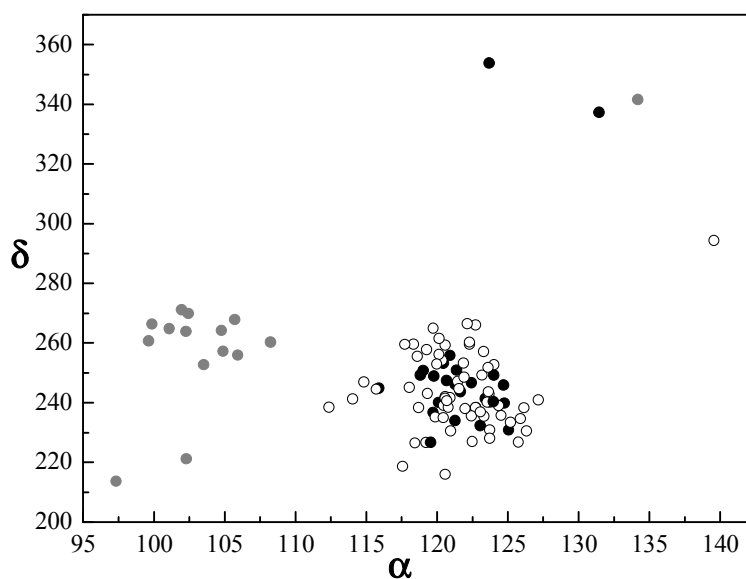
● — symmetrically tetrasubstituted; ● — single atom 'triple bridge' at the lower rim; ○ —other substitution patterns

Figure 3. The α-δ plot of the group of partial cone methylene-bridged calix[4]arenes

The main group of the single atom 'triple-bridged' structures ('cluster' 2-I, 15 cif files with 15 independent molecules) is centered at the values [α, β, δ] of [103.35; 288.17; 262.95] with a standard deviation of [2.51; 8.40; 5.44]. There are three deviating structures not included in this group: one at $\delta \sim 340°$ and two at $\delta < 230°$.

The main group of the symmetrically tetrasubstituted structures ('cluster' 2-II, 20 cif files with 23 independent molecules) is centered at [121.55; 118.78; 243.39] with a standard deviation of [2.19; 18.35; 6.49]. The four deviating structures with $\beta > 180°$ in Figure 2 have been excluded from this cluster.

There are two clusters in the lower rim distally disubstituted group: 'cluster' 2-III containing structures with $\beta < 210°$ (11 cif files with 14 independent molecules) centered at [121.99; 142.33; 240.83] with standard deviation of [2.25; 23.70; 5.78] and 'cluster' 2-IV containing structures with $\beta > 210°$ (5 cif files with 6 independent molecules) centered at [120.67; 253.64; 223.61] with standard deviation of [2.76; 15.17; 4.50].

The binding mode in 'cluster' 2-I of the single atom 'triple-bridged' group requires bringing of three phenolic oxygen atoms to close proximity because of three relatively short covalent bonds to a single heteroatom and therefore a certain degree of forced opening of the structure reflected by low α, high β and $\delta \sim 260°$. Deformation of the calix[4]arene moiety is very significant in this case and causes the observed separation of this group in parameters α, β (see Fig. 2). Typical example of 'cluster' 2-I structures is structure ABIHIC [10] (see Fig. II-1). All structures from this cluster have the '*partial cone*' phenyl ring not bound to the heteroatom. On the other hand, in the structure ZALGOI [10], the '*partial cone*' phenyl ring is the ring opposite to the unbound ring; this type of lower rim substitution leads to $\delta < 230°$ (the two deviating structures in Fig. 3). The one structure with $\delta \sim 340°$ (KOCQEY [10], Fig. II-1) has the '*partial cone*' phenyl ring positioned next to the unbound ring. The parameter δ can thus distinguish between the different binding modes within the 'triple-bridged' structures.
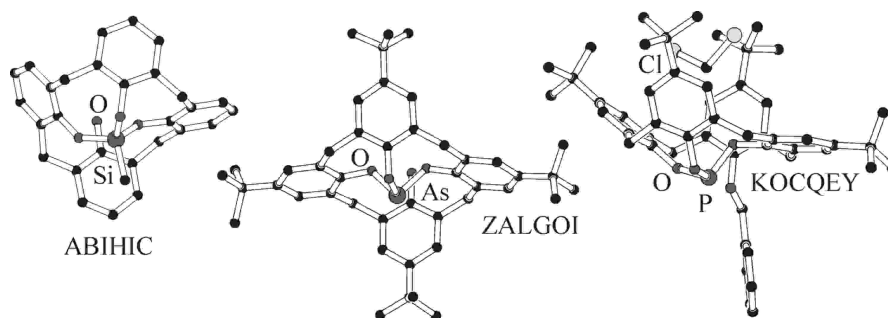
Figure II-1. Structures ABIHIC, ZALGOI and KOCQEY [10]

In Figure 2, there are four symmetrically tetrasubstituted structures with $\beta > 200°$ which do not fall into 'cluster' 2-II. Two of them are clathrates with solvent molecule or one lower rim substituent inside the 'cavity' formed by three calixarene phenyl rings; see structure JOYHIO [10], Fig. II-4. Because of the filled 'cavity' formed by three calixarene phenyl rings, these structures have more open 'cavity' and therefore higher β.

The other two symmetrically tetrasubstituted structures with parameters $\beta > 200°$ and $\delta > 290°$ are metal complexes and they are out of our discussion now (see Fig. II-2).
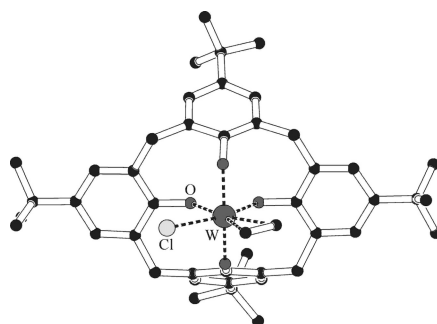
Figure II-2. Structure of tungsten complex GUBTAY [10]

In 'cluster' 2-II, there are relatively few structures which differ from each other significantly in upper/lower rim substitution, occupation of the cavity, possible upper/lower rim coordination etc. Since it is difficult to find common trends within this cluster, these structures will not be explicitly discussed.

From Figure 2, it is obvious that there are two 'clusters' within the lower rim distally disubstituted, upper rim symmetrically tetrasubstituted structures: 'cluster' 2-III at $\beta \sim 140°$, $\delta \sim 240°$ and smaller 'cluster' 2-IV at $\beta \sim 250°$, $\delta \sim 220°$. Structures from 'cluster' 2-IV contain bulky upper rim t-butyl groups and are lower rim-bridged by a relatively short crown ether moiety; compared to structure XOZBAP [10] from 'cluster' 2-III with unsubstituted upper rim, longer and more flexible crown ether chain and average geometry ($\beta \sim 110°$, $\delta \sim 240°$). The position of the '*partial cone*' phenyl ring differs in the above-mentioned bridged group and in structure XOZBAP in dependence on sterical hindrance between the p-substituent on the '*partial cone*' phenyl ring and lower rim bridge (Fig. II-3). Other structures from 'cluster' 2-III have nonbridged lower rim and are therefore not included in this comparison.
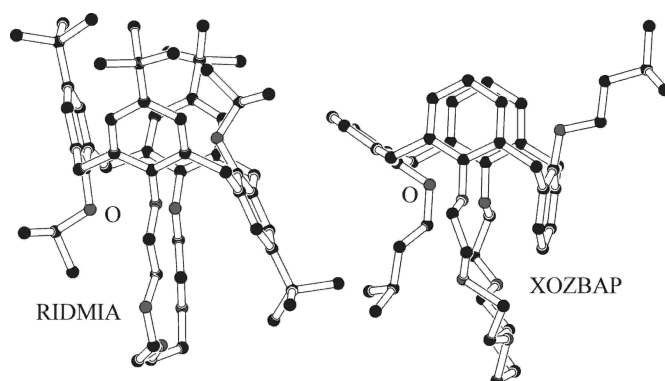
Figure II-3. Structures RIDMIA and XOZBAP [10].
The main difference is the position of the 'partial cone' phenyl ring

As shown previously (structure JOYHIO [10], Fig. II-4), the occupation of the calixarene 'cavity' can have some effect on its geometry. The dependence of parameters α, β on the type of the 'clathrate' for all *partial cone* calix[4]arenes (complexes included) is depicted in Figure 4; 'clathrates' tend to have more open 'cavity' and therefore bigger β than molecules with empty 'cavity'.
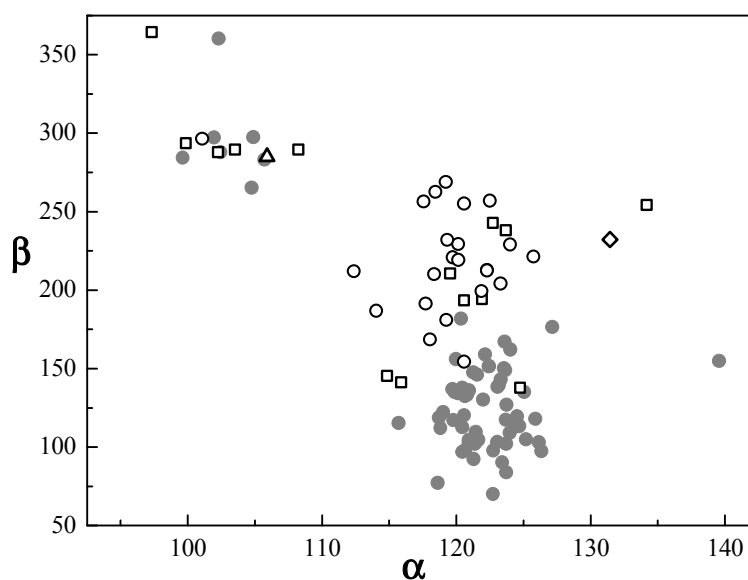
□ — solvent molecule inside the 'cavity'; ○ — lower rim substituent inside the 'cavity'; Δ — unsubstituted upper rim from another calixarene molecule inside the 'cavity'; ◊ — metal ion inside the 'cavity'; ● — nothing inside the 'cavity'

Figure 4. The dependence of the partial cone calix[4]arene geometry on the type of the 'clathrate'

Compared to *cone* structures (Part I, [7]), there are a relatively large number of structures which contain lower rim substituent inside the 'cavity'; this substituent usually comes from the same molecule which is rare in *cone* structures. As a rule, structures which contain another molecule or lower rim substituent inside the 'cavity' tend to be more open and therefore have bigger β; similar but not so profound effect have bulky nonpolar upper rim substituents (*t*-butyl). On the other hand, structures where π,π-interaction between the calix[4]arene opposite phenyl rings is not disrupted (empty 'cavity', no upper rim substituents or polar upper rim substituents capable of some type of interaction) have low β and more closed structures. This effect can be observed primarily on structures with π,π-interaction between aromatic upper rim substituents; π,π-interaction between two opposite calix[4]arene phenyl rings or interaction of polar upper rim substituents (see structure HAWYUZ [10], Fig. II-4). The above-mentioned effect of upper rim substituents is depicted in Figure 5.
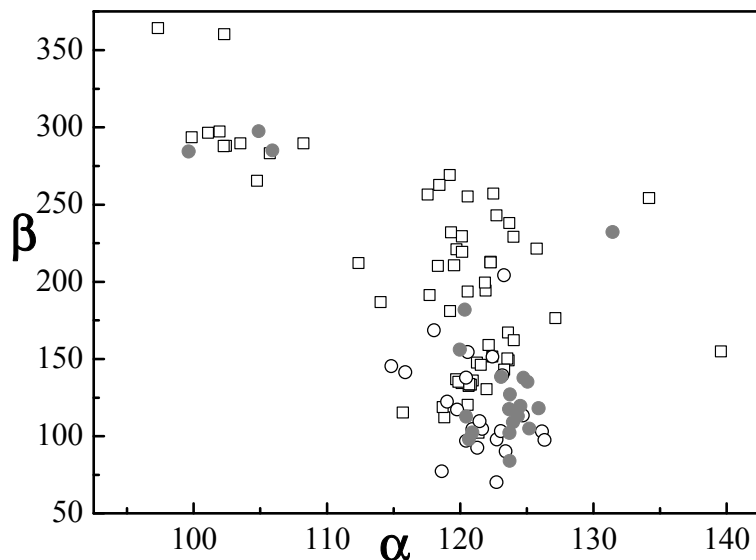
□ — nonpolar substituent at the upper rim; ○ — polar substituent at the upper rim; ● — unsubstituted upper rim

Figure 5. Effect of upper rim substituents on the geometry of partial cone calix[4]arenes

The influence of the lower rim substituents on the geometry of the symmetrically tetrasubstituted calix[4]arene base frame is less transparent and probably much less significant than the above-described effects.

Figure II-4 depicts the arrangement of the calix[4]arene moiety in the previously-mentioned structures HAWYUZ and JOYHIO [10].
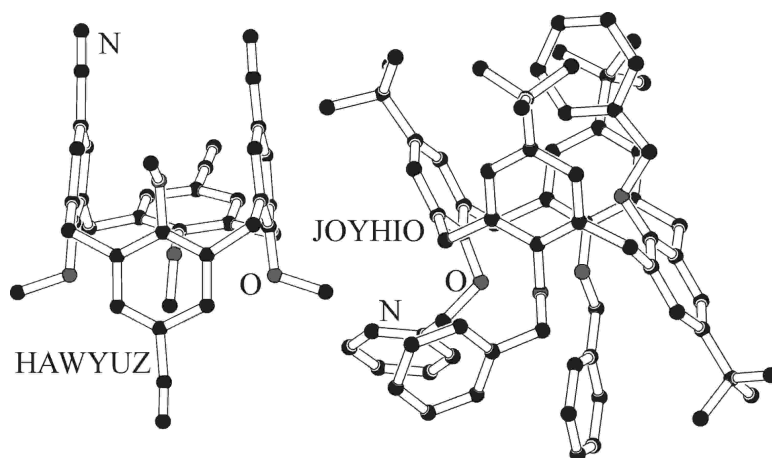
Figure II-4. Structures HAWYUZ and JOYHIO [10]

Heteroatom-bridged partial cone calix[4]arenes

The group of *partial cone* heteroatom-bridged calix[4]arenes comprises of a few hits only (9 cif files containing 9 symmetrically tetrasubstituted independent molecules, 3 cif files containing 5 independent molecules with other substitution patterns). Since there are not enough data and therefore no distinct trends could be observed, no division according to the respective substitution patterns was performed. Likewise, complexes are not distinguished because there are only three such structures in this group. The only bridge groups that occur in this group are S and SO; structures containing the SO bridges are emphasized in text.

The α-β plot regarding the group of all *partial cone* heteroatom-bridged calix[4]arenes (Fig. 6) shows two distinct groups. Structures with α < 110° (SEBZEE, YAQKAD and VAVRAM [10]) are 'clathrates' which possess more open 'cavity' (similar effect as in the methylene-bridged *partial cone* group). The more open 'cavity' in these structures is also reflected in higher value of parameter β. In the second group with α > 120° ('cluster' 6-I containing 8 cif files with 9 independent molecules, centered at [121.67; 125.82; 238.77] with standard deviation of [1.09; 10.82; 12.89]), no such effects are involved; these structures have empty 'cavity' and unhindered intramolecular π, π-interaction between two opposite calix[4]arene phenyl rings.

● — no molecule inside the 'cavity'; □ — solvent molecule inside the 'cavity';
○ — ligand from a complex inside the 'cavity'
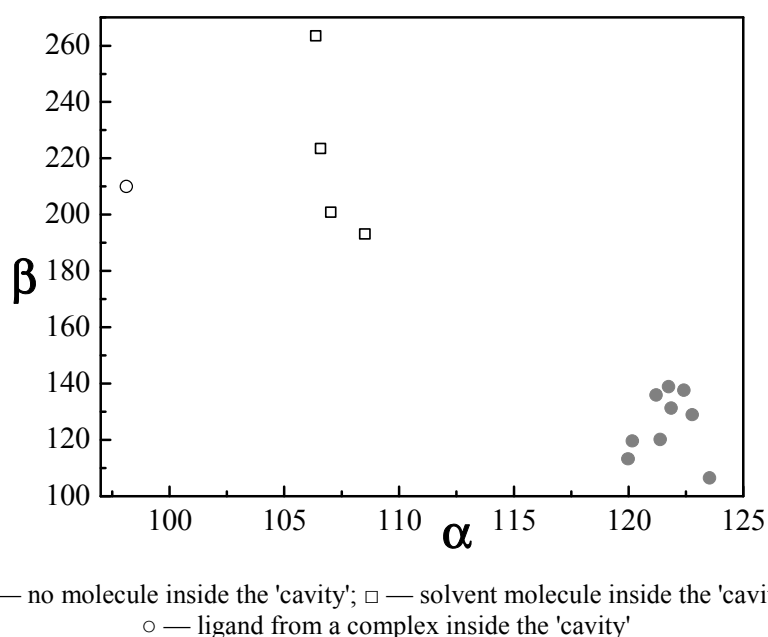
Figure 6. The α-β plot displaying the group of all partial cone heteroatom-bridged calix[4]arenes

Structure VAVRAM [10] which displays intramolecular π,π-interaction between one calixarene phenyl ring and an aromatic ligand from a complex is depicted in Figure II-5.
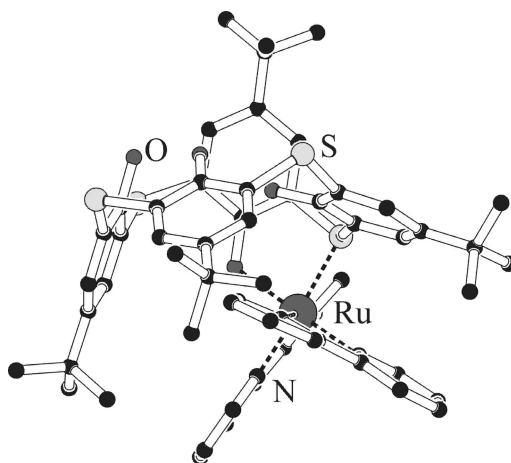
Figure II-5. Structure VAVRAM [10]

In the group of structures with empty 'cavity', the structures are distributed in the δ parameter. It is very difficult to find dependences of the distorsion parameters on the substitution of the calixarene platform because of a small number of structures in this group. However, the only upper rim unsubstituted structure in this group YANBUL [10] has the lowest β (~ 106°) probably because of π, π-interaction between two opposite calixarene phenyl rings unhindered by any upper rim substituents (Fig. II-6). Other structures contain bulky *t*-butyl groups at the upper rim and the resulting sterical hindrance leads to a somewhat more open 'cavity' and slightly increased β. This effect is very similar to that observed in the methylene-bridged group.
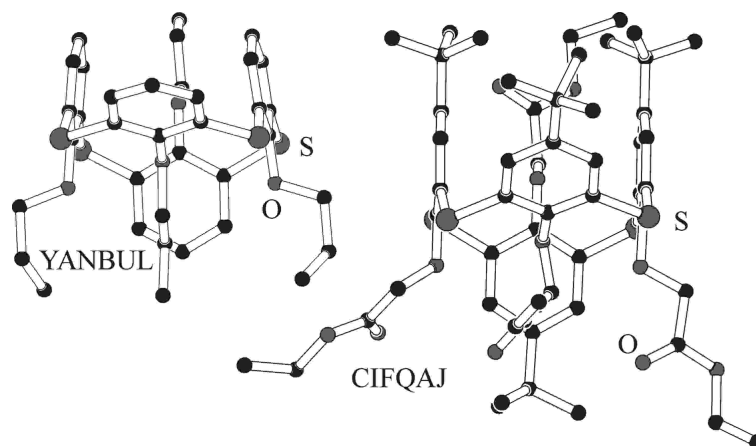
Figure II-6. Structures YANBUL and CIFQAJ [10]

Since there are only a few structures in this group, The values of the parameter δ are not discussed. There are four SO-bridged structures with empty 'cavity': trimeric lower rim tetragonally coordinated SUWNAZ [10] (β ~ 120°) and uncomplexed structures LUXYEI, LUXYIM and LUXXUX [10] (two proximal SO and two S bridges) with β > 130°. Structure LUXYEI [10] is depicted on Figure II-7. One interesting feature of the SO-bridged structures is the arrangement of the sulfinyl bridge groups. The structure LUXYEI has these bridges arranged in a *down-*, *up-*, *up-*, *up-* fashion (aeee in clockwise direction beginning at the bridge adjacent to the '*partial cone*' phenyl ring), LUXYIM in a *down-*, *up-*, *up-*, *down-* fashion (aeea), SUWNAZ in a *down-*, *up-*, *down-*, *up-* fashion (aeae) and LUXXUX has its two SO groups arranged in a *up-*, *up-* (ee) fashion (compare to *cone* SO-bridged structures LUXYAE, MAZNEG(01) and OKUKOU (eeee) and the complex RAWLIL (aaaa) [10]).
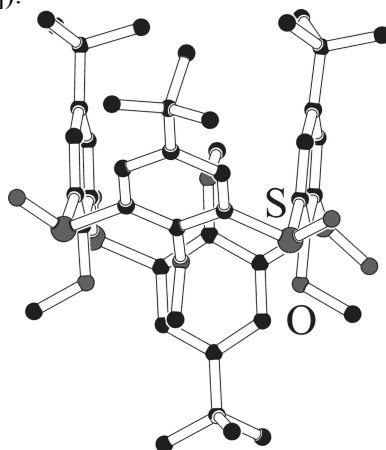
Figure II-7. Structure LUXYEI [10]

Unlike the methylene-bridged structures, there are no single atom 'triple-bridged' structures in this group. Unlike the methylene-bridged structures, there are also quite a number of structures containing hydroxyl groups at the lower rim in this group (4 out of 9 structures). The arrangement of hydrogen bonds at the lower rim therefore seems to be somewhat weaker than in the methylene-bridged group, the reason being probably larger cavity in heteroatom-bridged calix[4]arenes.

Since this group contains only a few structures, no conclusions regarding the effect of substitution and/or coordination beyond those already mentioned in the text were made.

Conclusion — partial cone structures

The arrangement of the *partial cone* base frame is best reflected in parameter β. Very open structures (single atom 'triple-bridged' at the lower rim, 'clathrates') tend to have high β whereas structures with unhindered π, π-interaction between two calixarene opposite phenyl rings have closed 'cavity' and low β. Because of the forced opening of the structure imposed by tetrahedral arrangement of bonds on the heteroatom, single atom 'triple-bridged' structures also have low α. The vast majority of *partial cone* structures are uniform in δ; the role of this parameter is therefore not discussed.

To sum up, the best way to deform the base frame of *partial cone* methylene-bridged molecules seems to be direct substitution of the calix[4]arene phenolic oxygen atoms either by a single atom 'triple bridge' or by lower rim *cis*-coordination by a transition metal ion. (there have been observed no molecules with this substitution or coordination patterns in the heteroatom-bridged group). Substitution at the upper rim significantly affects the *partial cone* calix[4]arene geometry only in the case when one pair of opposite phenyl rings is brought to a close proximity (e.g. upper rim polar substituents capable of some type of interaction).

Compared to *cone* structures, *partial cone* methylene-bridged structures which contain four lower rim hydroxyl groups are rare. Cyclic hydrogen bond arrangement at the lower rim is known to stabilize *cone* conformation (see e.g. [1–3]); *partial cone* conformation is therefore favored by molecules containing alkylated or acylated lower rim hydroxyl groups. On the other hand, heteroatom-bridged *partial cone* calix[4]arenes contain a relatively large number of structures which have four hydroxyl groups at the lower rim; the reason behind this behavior is probably larger cavity and therefore weakening of the hydrogen bonds present at the lower rim.

1,2-alternate structures

Methylene-bridged 1,2-alternate calix[4]arenes

The group of *1,2-alternate* conformers of calix[4]arenes with methylene bridge groups contains relatively few hits (56 complete cif files with 65 independent molecules, 5 incomplete cif files) compared to other groups (especially *cone*, see Part I [7]). Similarly to *partial cone* conformers, the molecules of these entries are also less symmetrically substituted than the *cone* group; the percentage of symmetrically tetrasubstituted molecules is less than 30 % compared to almost 50 % of symmetrically tetrasubstituted molecules in the *cone* conformation. The substitution patterns and the corresponding percentages of the *1,2-alternate* group are given in Table 2.

Since there is a large number of complexes in this group (41 % of cif files belong to metal-coordinated structures), these structures are distinguished.

Table 2

The substitution patterns and the corresponding percentages of the 1,2-alternate group

Type	No. of cif files	%	No. of independent molecules	%
Symmetrically tetrasubstituted	16	26.2	17	26.1
Single atom proximal bridge	17	27.9	19	29.2
Other	28	45.9	29	44.7
Total	61	100	65	100

The distribution of important groups of *1,2-alternate* calix[4]arenes is given in Figure 7 (α-β plot). The vast majority of symmetrically tetrasubstituted *1,2-alternate* calix[4]arenes falls to the point [180, 0]. The *1,2-alternate* calix[4]arenes with a single atom proximal bridge at the lower rim form a diffuse group. Other substitution patterns contain only a few molecules each and do not form distinct groups.
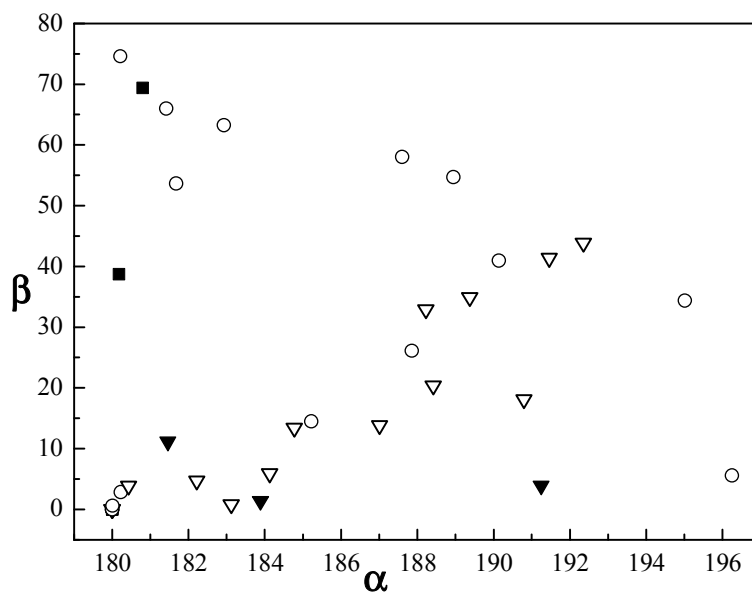
α-β plot; ■ — symmetrically tetrasubstituted — uncomplexed; □ — symmetrically tetrasubstituted — complex; ▼ — single atom proximally bridged lower rim — uncomplexed; ▽ — single atom proximally bridged lower rim — complex; ○ — other substitution patterns — complexes not distinguished

Figure 7. The distribution of important groups of 1,2-alternate methylene-bridged calix[4]arenes

The β-δ plot (Fig. 8) depicts more closely the group of symmetrically tetrasubstituted molecules. *1,2-alternate* calix[4]arenes with a single atom proximal bridge at the lower rim form again quite a distinct group. Other substitution patterns do not have such a significant distribution and do not form distinct groups. α-δ plot is very similar to the β-δ one and is therefore not reported.
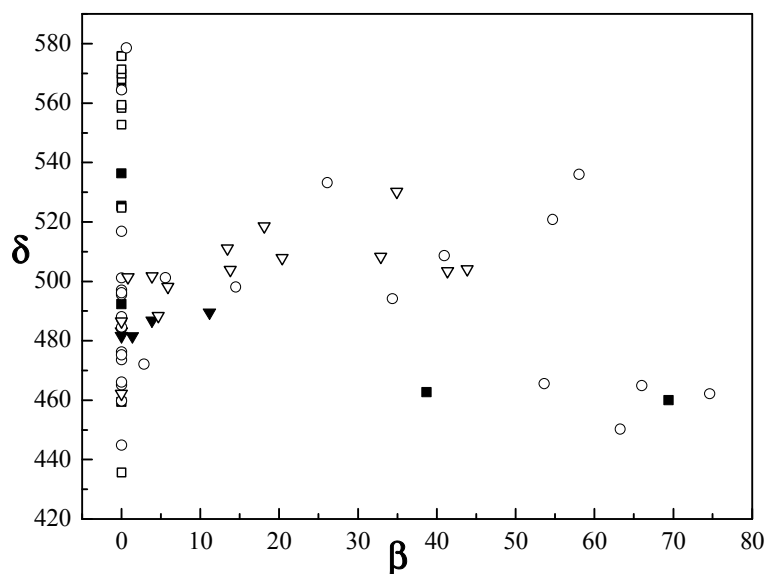
β-δ plot; ■ — symmetrically tetrasubstituted — uncomplexed; □ — symmetrically tetrasubstituted — complex; ▼ — single atom proximally bridged lower rim — uncomplexed; ▽ — single atom proximally bridged lower rim — complex; ○ — other substitution patterns — complexes not distinguished

Figure 8. The distribution of important groups of 1,2-alternate methylene-bridged calix[4]arenes

In the group of symmetrically tetrasubstituted molecules, there are two distinct 'clusters' (see Fig. 8): 'cluster' 8-I at δ < 500° (5 cif files, 5 independent molecules) formed mostly by uncomplexed molecules and 'cluster' 8-II (9 cif files, 12 independent molecules) at δ > 500° formed mostly by complexes. 'Cluster' 8-I is

centered at [180.20; 21.62; 462.01] with a standard deviation of [0.31; 28.20; 18.02], 'cluster' 8-II is centered at [180.00; 0.00; 556.88] with a standard deviation of [0.00; 0.00; 17.70]. Two symmetrically tetrasubstituted molecules with $\beta > 30°$ were not included in these groups.

In the group of single atom proximally bridged molecules in Figure 8, there are two clusters observable: 'cluster' 8-III with $\beta < 10°$ containing both complexes and uncomplexed molecules and 'cluster' 8-IV formed mainly by complexes with $\beta > 10°$. 'Cluster' 8-III contains 10 cif files with 10 independent molecules, is centered at [182.50; 2.06; 487.17] with a standard deviation of [3.33; 2.17; 11.14]. 'Cluster' 9-IV contains 8 cif files with 9 independent molecules, is centered at [188.21; 25.55; 508.53] with a standard deviation of [3.24; 12.02; 10.56].

In the group of single atom proximally bridged *1,2-alternate* calix[4]arenes, there are 5 uncomplexed structures and 12 complexes. The group of single atom (X) proximally bridged *1,2-alternate* calix[4]arenes is relatively uniform in parameter δ; however, its structures differ significantly in α, β. This behavior probably reflects the rigidity of the lower rim O-X-O frame which depends on bond lengths between atom X and calix[4]arene phenolic oxygen atom and on bond angle on atom X. Smaller atoms (especially B, to a lesser extent Si, P) with short X-O bond lengths and relatively rigid bond angles tend to warp the calix[4]arene base frame more than «coordinated metaloid» atoms (see Fig. II-8). Because this deformation reflects both the rigidity of bond length and angle and because a large number of structures from this group contain mixed metal/non-metal bridges at the lower rim, no correlation and explanation of the two 'clusters' 8-III and 8-IV was attempted. However, structures with larger β from 'cluster' 8-IV are mostly structures with nonsymmetrical proximal substitution (e.g one metal ion and one heteroatom, usually Si). The changes in the calix[4]arene base frame in dependence on atom X seem to be less significant than those in the case of lower rim single atom 'triple-bridged' structures (see *cone* [7] and *partial cone* structures).
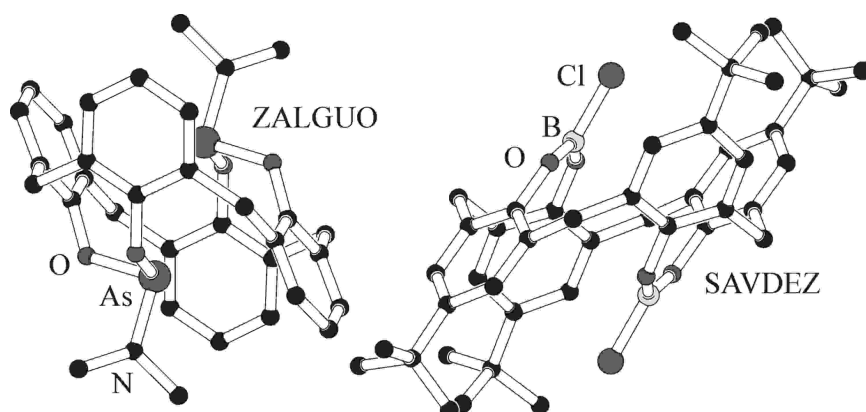
Figure II-8. Single atom proximally bridged 1,2-alternate calix[4]arenes ZALGUO, SAVDEZ [10]

The rigidity of the single atom proximal bridge can be further demonstrated on the values of β and δ parameters of this group and a group of *1,2-alternate* calix[4]arenes which contain longer proximal bridges. Single atom proximally bridged structures have relatively high δ parameter and low β ($\beta < 40°$, $\delta \sim 500°$) whereas in the group with longer proximal bridges (four structures) where the calix[4]arene base frame is less restrained the situation is exactly the opposite ($\beta \sim 60°$, $\delta \sim 460°$). The values of the β and δ parameters can therefore serve as a rough estimation of the rigidity of proximally bridged structures.

The group of symmetrically tetrasubstituted *1,2-alternate* calix[4]arenes (8 uncomplexed structures, 8 complexes) is uniform in α and β parameters with the exception of two structures with $\beta > 30°$. Since no significant intra- or intermolecular interactions exist in the crystal structures of these compounds (beyond relatively weak CH-π interactions), this behavior remains unexplained.

However, the group of symmetrically tetrasubstituted structures varies significantly in the δ parameter. As a rule, structures with one or more lower rim phenolic oxygen atoms missing tend to have higher δ parameter because of the lack of sterical hindrance at the lower rim (structure YIRGAH [10], Fig. II-9); the resulting arrangement of the calix[4]arene moiety is very similar to the *chair* arrangement of resorcinarenes [1–3]. Sterical hindrance stemming from larger substituents at the lower rim is reflected in lower δ because of less open structure as in the case of structure CAZSEC with four carboxymethoxy groups at the lower rim [10].
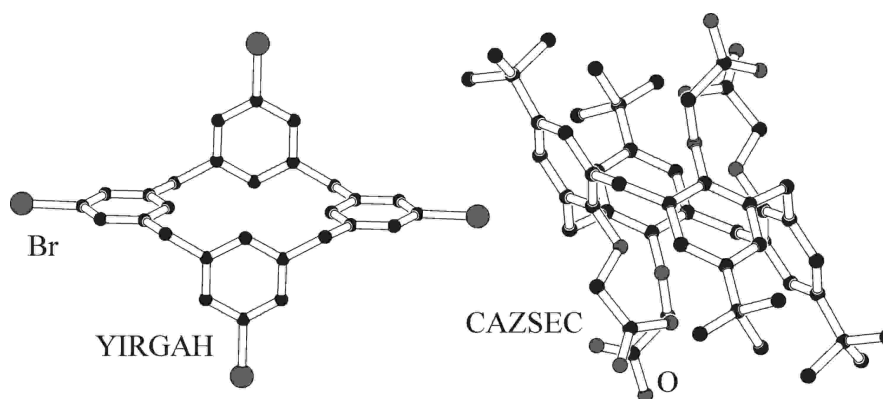
Figure II-9. Structures YIRGAH and CAZSEC [10]

Other substitution patterns with the notable exception of lower rim distally disubstituted structures (16 hits including three complexes) contain each a few molecules only and are therefore not discussed. The only interesting structures within this group are three lower rim single atom 'triple-bridged' structures (3 hits) which have very high value of δ parameter. The influence of this motif on the calixarene base frame is similar to *partial cone* structures described in previous chapter; these structures essentially form the transition between *partial cone* and *1,2-alternate* groups. Representative example is structure POSJUC [10] (Fig. II-10).
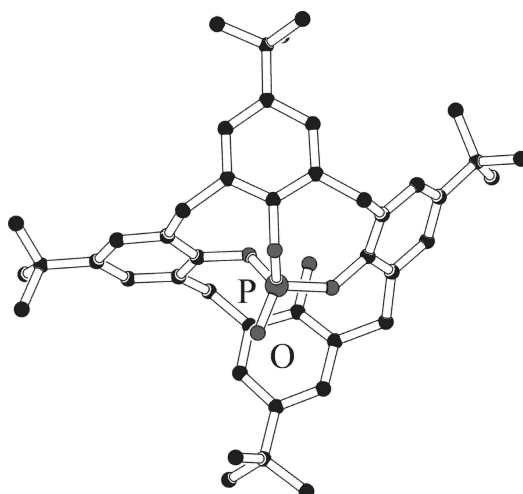
Figure II-10. Single atom 'triple-bridged' 1,2-alternate calix[4]arene POSJUC [10]
(the fourth lower rim substituent has been omitted for clarity)

Since the *1,2-alternate* calix[4]arenes lack cavity, clathrates cannot be defined. However, quite a large variety of inter/intramolecular interactions can be observed in this group. CH-π; π,π- and van der Waals interaction exist between lower rim substituents, ligands from complex or solvent molecules and the calixarene 'half-cavity' in almost all these structures. In addition, structures lacking lower rim hydroxyl groups tend to stack in a chair-like fashion in solid state (intermolecular π, π-interactions between calixarene molecules). Since the structures in this group are few and the effects are usually mixed, no clear dependence of parameters α, β, δ on the type of interaction has been observed. Similarly, because there are only a few structures and these structures vary widely in substitution, no dependence of the calix[4]arene geometry on the type of upper rim substituent was observed.

Complexes of *1,2-alternate* calix[4]arenes generally fall into two categories: metal ion(s) coordinated in a single atom proximal bridge fashion or metal ion(s) coordinated in a single atom 'triple bridge' fashion (Fig. II-11). These structures tend to have high δ because of the forced opening of the calixarene base frame. For comparison, see previous chapter on similar (both coordinated and uncomplexed) *partial cone* structures.
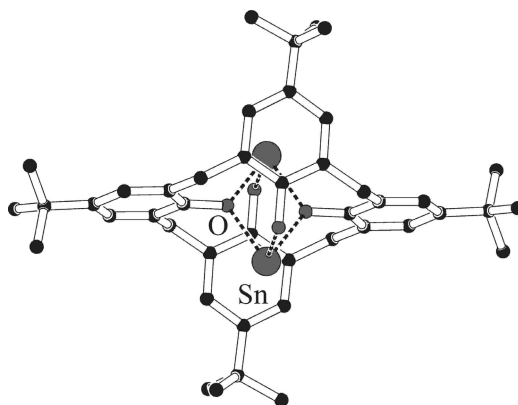
Figure II-11. Structure JOQBEW [10]

Heteroatom-bridged 1,2-alternate calix[4]arenes

The group of *1,2-alternate* heteroatom-bridged calix[4]arenes consists of relatively few hits (23 cif files containing 23 symmetrically tetrasubstituted independent molecules, 6 cif files containing 6 independent molecules with other substitution patterns). Since there are only a few molecules of other substitution patterns than the symmetrically tetrasubstituted one, separation according to substitution patterns was not performed. This group contains a relatively large number of complexes (9 complete cif files, all of them belong to the symmetrically tetrasubstituted group) which are distinguished. Moreover, there are only two structures containing complete cif files with bridge groups other than S (oxygen-bridged ACUNAO and SO_2-bridged OCUFUO [10]; discussed in text below).

Figures 9, 10 show α-δ and β-δ plots of this group. α-β plot is the least informative one (as in the group of methylene-bridged *1,2-alternate* calix[4]arenes, the majority of structures fall to the point [180, 0]) and is therefore not displayed.

In Figures 9, 10, no distinct 'clusters' can be observed. As in the group of methylene-bridged *1,2-alternate* calix[4]arenes, structures are distributed in the δ parameter. Likewise, there is quite a large number of inter/intramolecular interactions between calixarene molecules, upper or lower rim substituents and calixarene phenyl rings or solvent molecules and the calixarene 'half-cavity'. No distinct dependence of the calix[4]arene symmetry on the type of interaction has been observed, however. Similarly, no dependence on the type of upper/lower rim substituents was observed in this group.

■ — uncomplexed structures; □ — complexes
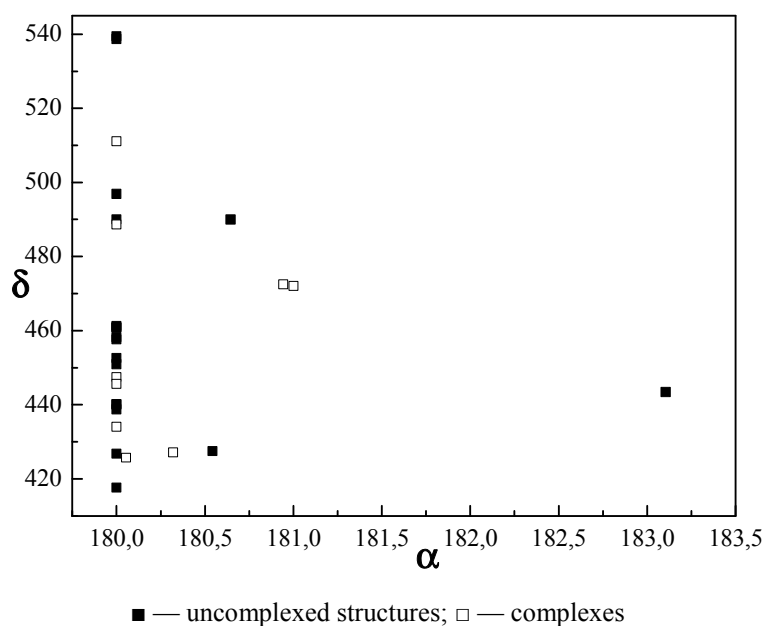
Figure 9. The α-δ plot of the group of 1,2-alternate heteroatom-bridged calix[4]arenes
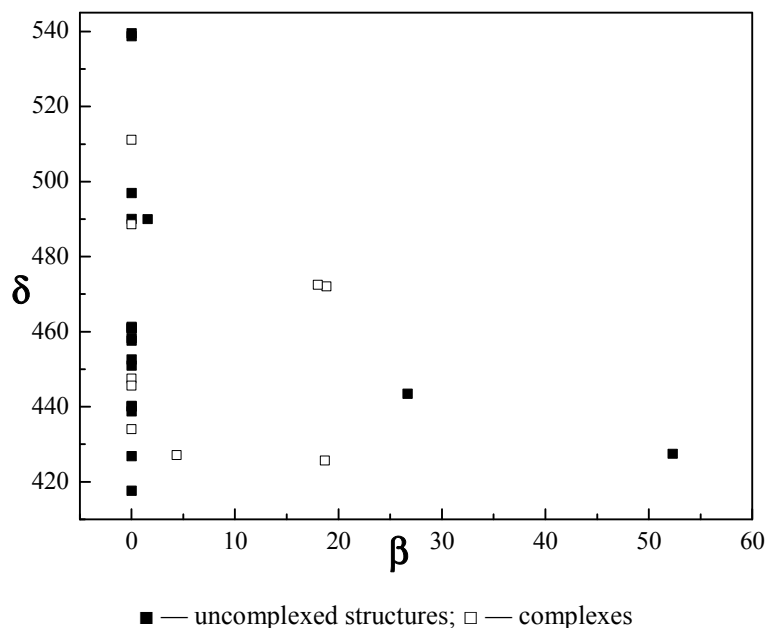
Figure 10. The β-δ plot of the group of 1,2-alternate heteroatom-bridged calix[4]arenes

There are two deviating hits in Figure 11 with $\delta > 520°$. One of them is structure ACUNAO [10], a unique structure containing oxygen bridges, *m*-substituted phenyl rings, two hydrogen atoms and two carbon atom substituents at the lower rim. The geometry of this structure is close to that of *chair* resorcinarenes. The other deviating hit in Figure 11 is structure FUDXAD (Fig. II-12), which contains very short one atom proximal bridges at the lower rim and therefore a very open structure. The only other proximally bridged lower rim structure in this group is structure BALNOS (two crown-5 bridges) with significantly more average geometry owing to longer and more flexible lower rim substituents. Figure II-12 depicts structures FUDXAD and BALNOS [10] showing the dependence of the calixarene geometry on the length of the proximal bridge. Structure BALNOS has very low δ (426°) which reflects a relatively closed 'cavity' in this case. Similar effects have been observed previously in the group of methylene-bridged *1,2-alternate* structures.
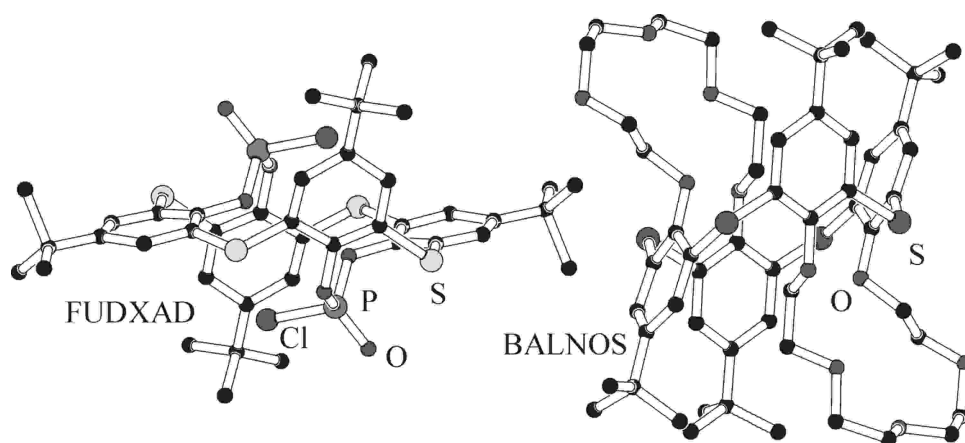
Figure II-12. Structures FUDXAD and BALNOS [10]

The deviating hit in Figures 9, 10 with $\alpha > 183°$ and $\beta \sim 27°$ is structure ETUQAL [10]. The hit with $\beta \sim 52°$ in Figure 10 is a similar tetrasubstituted structure ETUQOZ [10]. Bulky lower rim substituents (three in ETUQAL, four in ETUQOZ) cause deformation of the base calixarene skeleton mostly because of sterical hindrance; both structures possess CH-π interaction between upper rim *t*-butyl substituent and one calixarene phenyl ring from different calixarene molecule which is probably behind increased β. Both structures have low δ (430–440°) which indicates a relatively closed structure (Fig. II-13).
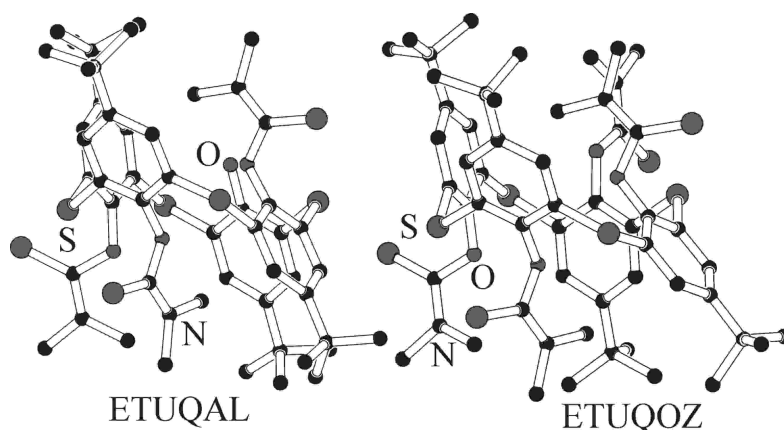
Figure II-13: Structures ETUQAL, ETUQOZ [10]

It is obvious that the geometry of the calix[4]arene base frame regarding opening of the structure is dependent on the substitution of the calixarene skeleton and is reflected by parameter δ as in the group of methylene-bridged *1,2-alternate* structures. This dependence is demonstrated on a group of symmetrically tetrasubstituted uncomplexed *1,2-alternate* heteroatom-bridged calix[4]arenes with upper rim *t*-butyl substituents with $\alpha \sim 180°$, $\beta \sim 0°$ (the main group in Figures 9, 10 with δ between 410–460°).

The dependence of the geometry of these molecules on the size of lower rim substituents (and henceforth the sterical hindrance) is depicted in Figure 11; it shows the plot of the δ parameter against the 'length' of the lower rim substituents expressed as a number of atoms in chain from the calixarene phenyl oxygen (included) to the most distant atom on the substituent (also included).
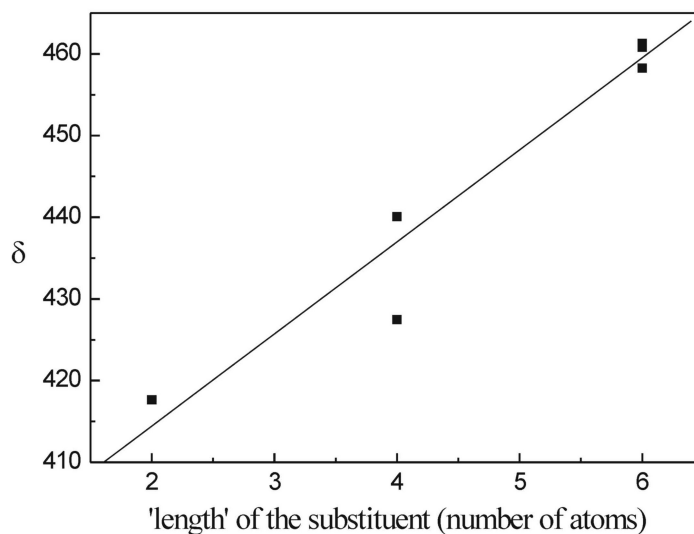
Figure 11. Dependence of the δ parameter on the 'length' of the lower rim substituents

The group of *1,2-alternate* heteroatom-bridged calix[4]arenes contains relatively large number of complexes (compared to the *partial cone* group). All complexes are derived from symmetrically tetrasubstituted calixarenes, which simplifies evaluation of inter- and/or intramolecular interactions on their geometry.

The two deviating hits with $\beta \sim 18°$ and $\delta \sim 470°$ in Figure 11 (β-δ plot) are structures containing proximally coordinated two oxygen atoms at the lower rim (and the bridge between them) compared to other structures in this chapter with none or all lower rim oxygen atoms coordinated. This type of coordination forces the structures more open as demonstrated by higher δ value; nonsymmetrical coordination at the lower rim is probably behind slightly increased β. The representative structure MOTMUD [10] is shown on Figure II-14.
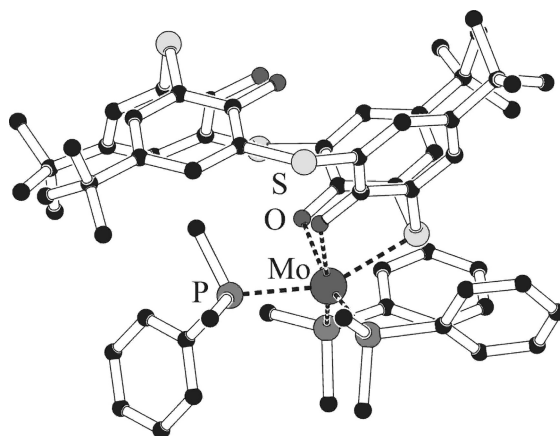
Figure II-14. Structure MOTMUD [10]

The two deviating hits with β = 0° and δ > 480° in Figure 11 are structures OCUFUO and TARFIC [10] (Fig. II-15). Structure OCUFUO is the only structure among *1,2-alternate* calix[4]arenes which contains sulfone bridges, one oxygen atom from each of two distal bridges participates on the octahedral coordination of two Cu(II) ions. The coordination is similar to the proximal coordination mentioned above and the value of the δ parameter is therefore larger. The structure TARFIC contains four proximally Rh(III) complexed thiolato groups at the lower rim; there is a structure with the same coordination pattern (TARFAU, Ir(III) complex) possessing an average geometry (δ ~ 445°). These structures show only weak intermolecular CH-π interactions; the difference in δ therefore seems to arise from different ionic radii of Rh and Ir. The size of the calixarene lower rim is obviously better suited for larger Ir(III), the coordination polyhedron is therefore less strained and the influence on the calixarene base frame not so profound. On the other hand, smaller Rh(III) forces the lower rim oxygen atoms closer and the structure is therefore more open as confirmed by higher δ.

The coordination of all mentioned lower rim complexes (two proximal oxygen atoms and the bridge between them) is very close to one of coordination patterns occurring in the *cone* group (see Part I, [7]).
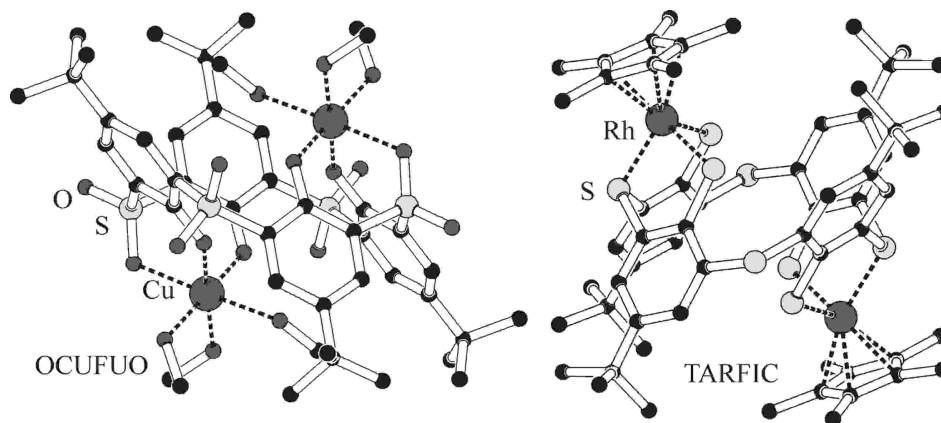
Figure II-15. Structures OCUFUO and TARFIC [10]

Other complexes from the average group with δ ~ 440° in Figure 11 belong to polymeric upper rim coordinated sulfonato calix[4]arenes. In conclusion, upper rim complexation does not seem to affect the geometry of the calixarene base frame as significantly as the lower rim and/or bridge coordination.

Conclusion — 1,2-alternate structures

Calix[4]arenes lacking lower rim substituents tend to have their base frame deformed towards that of *chair* calix[4]resorcinarenes (average α, β; δ ~ 500° and more). On the other hand, structures with very large lower rim substituents tend to have low δ because of a more closed structure caused by sterical hindrance at the lower rim. The parameter δ can therefore serve as an indicator for the degree of opening of the structure.

Single atom proximally or 'triple-bridged' structures have also very open structures as reflected by high δ along with somewhat increased α and β.

To sum up, the best way to immobilize and 'open' the *1,2-alternate* calix[4]arene base frame is to proximally bridge the lower rim by a single atom (preferably from the second period) or to form a single atom 'triple bridge' as in the *partial cone* group. A variety of atoms and cations can be utilized for this purpose; the single atom 'triple bridge' appears to be the more efficient way to open structures. Another method of opening the calixarene base frame is removal of lower rim phenolic oxygen atoms and the resulting decrease of sterical hindrance at the lower rim. On the other hand, large substituents on the lower rim phenolic oxygen atoms tend to produce more closed structures (opposite effect). Direct coordination at the lower rim phenolic oxygen atoms can also significantly affect the calixarene geometry; little influence has been observed in the case of coordination at the upper rim substituents.

As in the group of *partial cone* structures, *1,2-alternate* methylene-bridged calix[4]arenes which contain four lower rim hydroxyl groups are uncommon. On the other hand, in the group of heteroatom-bridged structures there is quite a number of structures with lower rim hydroxyl groups in this group which confirms that the hydrogen bonds at the lower rim in heteroatom-bridged structures are weaker than in their methylene-bridged counterparts.

1,3-alternate structures

Methylene-bridged 1,3-alternate calix[4]arenes

This group contains relatively small number of symmetrically tetrasubstituted structures (42 out of 184 cif files, which correspond to about 23 %). On the other hand, the number of lower rim distally bridged structures in this conformation is the largest of all methylene-bridged calix[4]arenes (81 from the total of 184 cif files, 44 %). For further details, see Table 3.

There are also quite a large number of complexes in this group (30 %); the complexes are therefore distinguished.

T a b l e 3

1,3-alternate methylene-bridged calix[4]arenes from [10]

Type	No. of cif files	%	No. of independent molecules	%
Symmetrically tetrasubstituted	42	22.8	43	22.4
Distally bridged lower rim	81	44.0	84	43.8
Other	61	33.2	65	33.9
Total	184	100	192	100

α-β plot (Fig. 12) and β-δ plot (Fig. 13) depict almost continuous distribution of all substitution patterns; no pattern forms a distinct group and only little amounts of trends can be deducted. First, symmetrically tetrasubstituted structures are all uniform in α parameter, differing significantly in β. No distinct 'clusters' can be observed in this group.

On the other hand, lower rim distally bridged structures form a small group at β < 350° ('cluster' 12-I) and a significantly larger group at higher β ('cluster' 12-II). 'Cluster' 12-I contains 10 cif files with 11 independent molecules; this cluster is centered at [180.92; 326.75; 4.54] with a standard deviation of [0.86; 4.98; 3.45]. 'Cluster' 12-II contains 58 cif files with 67 independent molecules; this 'cluster' is centered at [181.54; 424.64; 11.20] with a standard deviation of [1.48; 21.18; 9.15].

Several trends can be observed within the β-δ plot. The group of symmetrically tetrasubstituted molecules remains uniform even in the δ parameter; only a few structures have δ > 10°. The two distinct groups at lower/higher β ('clusters' 13-I, 13-II) of molecules with distally bridged lower rim remain even in this plot. However, the group of other substitution patterns distributed almost evenly in the δ parameter.

In the group of symmetrically tetrasubstituted structures in Fig. 13, several hits deviate from the main group. Some of the structures with δ > 15° contain large and flexible lower rim substituents one of which reaches into the 'cavity' formed by the two opposite phenyl rings (CH-π interactions; structure AFEFUM [10], Fig. II-16). Since the substituents are large, it is impossible for both distal substituents to be inside the 'cavity' and the structure is therefore deformed in the δ parameter. Deformation in the δ parameter may also arise from sterical hindrance by four bulky lower rim substituents; the substituents are simply too large to fit

inside the 'cavity'. In the case of complexes, the deformation in the δ parameter is caused by nonsymmetrical proximal coordination of the lower rim by two metal ions (structure FUTKAG [10], Fig. II-18). The effect of the proximal coordination can be demonstrated on the fact that other complexes of this group which contain more symmetrical distal lower or upper rim coordination have low δ. Other structures in the symmetrically tetrasubstituted group have more symmetrical arrangement with δ < 15°.
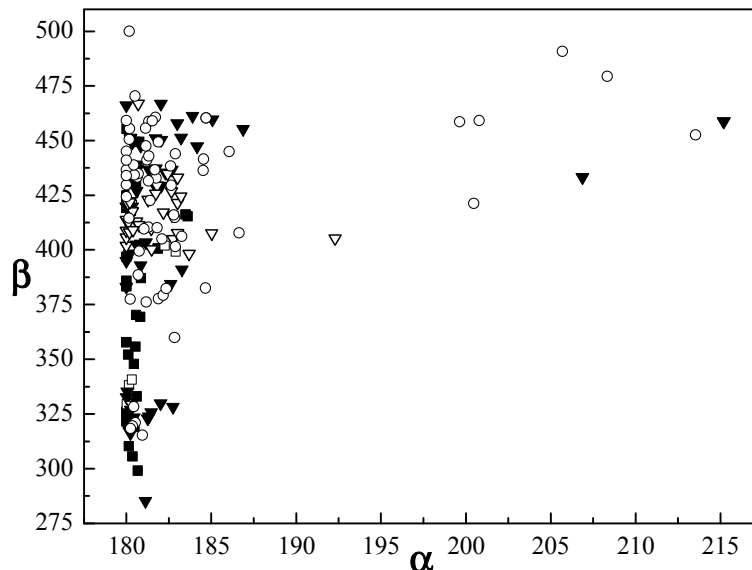
■ — symmetrically tetrasubstituted — uncomplexed; □ — symmetrically tetrasubstituted — complex;
▼ — distally bridged lower rim — uncomplexed; ▽ — distally bridged lower rim — complex;
○ — other substitution patterns — complexes not distinguished

Figure 12. The α-β plot of the group of 1,3-alternate methylene-bridged calix[4]arenes
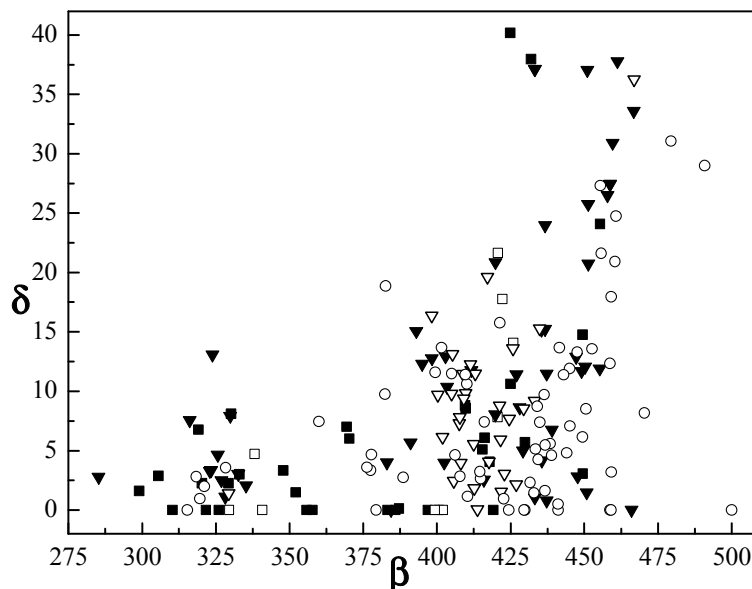
■ — symmetrically tetrasubstituted — uncomplexed; □ — symmetrically tetrasubstituted — complex;
▼ — distally bridged lower rim — uncomplexed; ▽ — distally bridged lower rim — complex;
○ — other substitution patterns — complexes not distinguished

Figure 13. The β-δ plot of the group of 1,3-alternate methylene-bridged calix[4]arenes

The β parameter reflects the degree of opening of the calix[4]arene 'cavity' (see Fig. II-16, II-17) and can be therefore used to describe the geometry of uncomplexed calix[4]arenes from this group. As a rule, structures with low β parameter have more closed 'cavities' which corresponds to the presence of π, π-interactions between the opposite calix[4]arene phenyl rings (e.g. structure FAZFAO [10], Fig. II-16). Bringing of the calixarene opposite phenyl rings to close proximity is often facilitated by lower rim sterical hindrance caused by presence of bulky lower rim substituents in these structures. On the other hand, if the lower rim substituent (AFEFUM [10], Fig. II-16) or other molecule (GOTHAY [10], Fig. II-16) enters the calixarene 'cavity', π, π-interaction between the opposite rings is disrupted and as a result the structure is more open as reflected by higher value of the β parameter (see Fig. II-16). Similar effect has been already observed in *partial cone* structures.
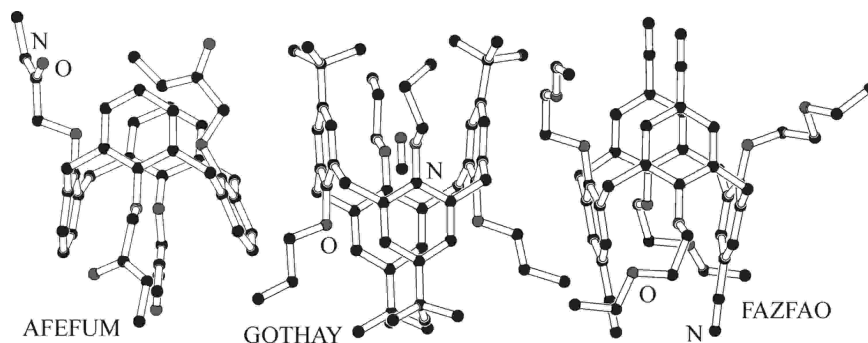
Figure II-16. Structures AFEFUM (β ~ 425°), GOTHAY (β ~ 370°) and FAZFAO (β ~ 320°) [10] demonstrating effects of a filled and empty 'cavity' on the geometry of the calix[4]arene base frame

The type of the upper rim substituent plays less transparent role; structures with nonpolar bulky upper rim substituent (*t*-butyl) tend to have more open structures with larger β parameter probably because of the sterical hindrance at the upper rim. On the other hand, in structures which contain upper rim polar substituents capable of π, π- and/or dipolar interaction the β parameter differs in dependence whether the π, π-interaction takes place between the calixarene opposite phenyl rings bearing these substituents or whether there is an interaction between the upper rim substituents and some other molecule inserted into the calixarene 'cavity' (this molecule may be even similar substituent from another calixarene molecule). An example of these three effects is the trio of structures KARNEX, KARNIB, KARNUN [10] (Fig. II-17).

Structure KARNEX contains phenyl groups at the upper rim; however, the π, π-interaction of the calixarene opposite phenyl rings is disrupted by interfence of lower rim substituents and phenyl group from another calixarene molecule (not depicted, β ~ 449°). Structure KARNIB contains bromine atoms at the upper rim; nothing prevents π, π-interaction of the calixarene opposite phenyl rings in this case (β ~ 329°). Structure KARNUN with bulky *t*-butyl groups at the upper rim adopts less deformed conformation because of sterical hindrance at the upper rim and the contribution of lower rim substituents which partially reach into the 'cavity' (β ~ 449°).
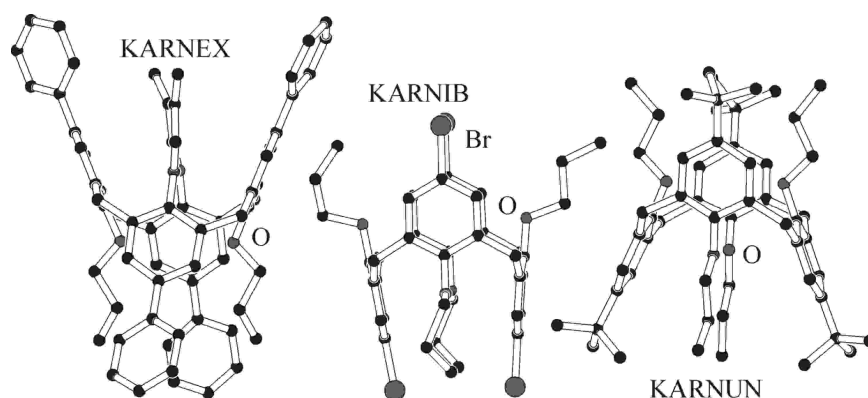
Figure II-17: Structures KARNEX, KARNIB and KARNUN [10]

There are several possible modes of metal ion coordination within the symmetrically tetrasubstituted group: lower rim phenolic oxygen or sulfur atoms as in structures FUTKAG, HELYAY [10] (proximal or distal coordination, Fig. II-18), lower rim phenolic oxygen atoms combined with donor atoms from the corresponding lower rim substituent (distal coordination), lower rim substituents (distal coordination), upper rim distal coordination (AHUCEL [10]) or distal coordination on a rigid upper rim substituent. Since there are only a few structures of coordinated calix[4]arenes in this group, drawing extensive conclusions is impossible. However, the upper rim coordinated structures have all very low β parameter which is caused by bringing of the opposite phenyl rings to close proximity by their distal coordination; lower rim coordinated structures where this restraint is absent have all more open structures as demonstrated by higher values of the β parameter.
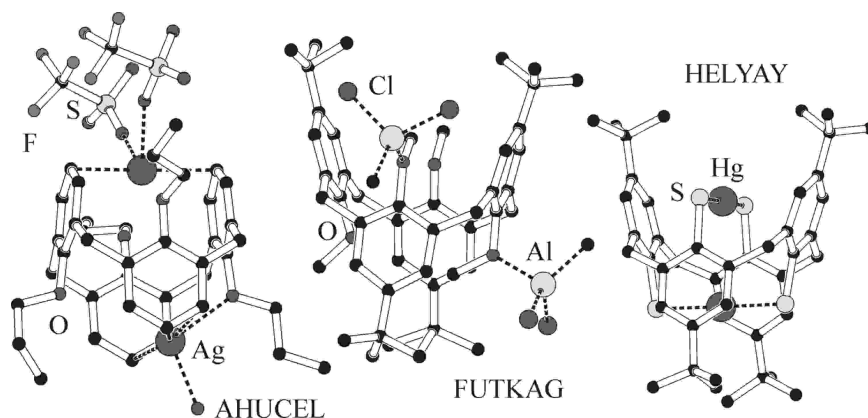
Figure II-18. Structures of the Ag(I) complex AHUCEL (β ~ 338°), Al(III) complex FUTKAG (β ~ 422°) and Hg(II) complex HELYAY (β ~ 426°) [10] demonstrating the influence of different types of upper/lower rim coordination on the geometry of the calix[4]arene

Lower rim bridged structures (49 uncomplexed, 32 complexes) in the group of *1,3-alternate* calix[4]arenes have a few unique specifics. First, proximal bridges are impossible within this group unless these bridges were very large. Single atom proximal or 'triple-bridging' at the lower rim described in the groups of *partial cone* or *1,2-alternate* calix[4]arenes which can significantly affect the geometry of the calix[4]arene base frame is impossible from sterical reasons. The remaining possibility is distal lower rim bridge; according to Table 3, this form of lower rim substitution is very popular within this group. For the most part, flexible lower rim bridges with insignificant sterical demands have been utilized in the vast majority of these structures and the length of these lower rim bridges (number of atoms in the bridge) has little effect on the geometry of the calix[4]arene base frame. In the case of more rigid lower rim bridges, some effect on the geometry of the calix[4]arene moiety has been observed (see next paragraph).

The group of lower rim distally bridged *1,3-alternate* calix[4]arenes formed two distinct groups in parameter β ('clusters' 13-I, 13-II; Fig. 12, 13). The larger/lower β seems to reflect the same effects as in the group of symmetrically tetrasubstituted molecules (namely reaching of lower rim substituent into the calixarene cavity). The group with lower β also contains more molecules with more rigid lower rim bridges compared to the group with larger β.

Complexes of the lower rim bridged *1,3-alternate* calix[4]arenes form a uniform group because the coordination takes place at the lower rim substituent and mostly even at lower rim phenolic oxygen atoms; the resulting cation-π interaction between this metal ion and two opposite calixarene phenyl rings ensures a relatively open structure and therefore higher β (see structure AVERUO, Fig. II-19). As a rule, the coordination at the lower rim does not significantly affect the geometry of the calix[4]arene base frame as described by relatively uniform values of the β parameter; all these structures belong to 'cluster' 13-II. The only notable exception within this group is one structure coordinated distally at the rigid upper rim substituents; this structure falls into the 'cluster' 13-I. The low value of β in this case reflects the π, π-interaction present between the calix[4]arene opposite phenyl rings and the resulting deformation of the calix[4]arene moiety towards a more closed structure.
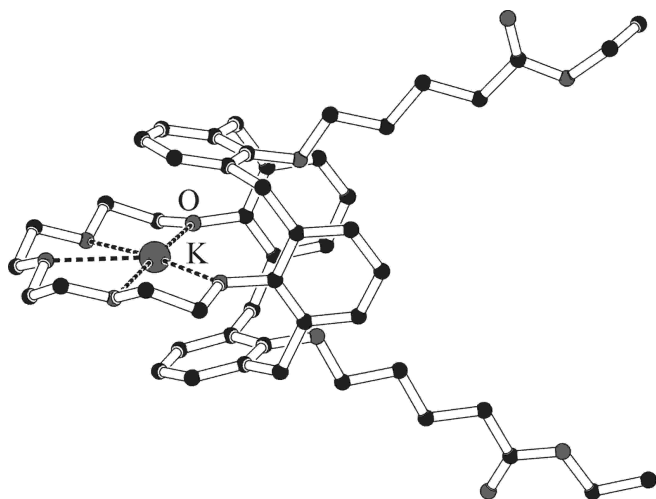
Figure II-19. Structure AVERUO [10]
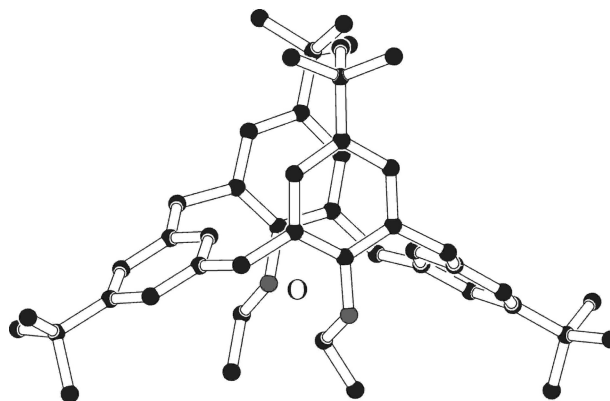
Figure II-20. Structure YUYYOG [10]

Among *1,3-alternate* calix[4]arenes with other substitution patterns, the only relatively numerous group is the group of lower rim distally disubstituted structures (19 hits including 6 complexes). The values of the β in the calix[4]arenes with other substitution patterns generally seem to follow the same rules as those for the symmetrically tetrasubstituted group. However, there are several structures with relatively high α parameter. Structures with α > 200° (e.g. YUYYOG [10], Fig. II-20) lack lower rim phenolic oxygen atoms and, because of missing sterical hindrance at the lower rim, their conformation is similar to that of *saddle* conformers of calix[4]resorcinarenes (for comparison, see the effect of missing phenolic oxygen atoms in the *1,2-alternate* group). Slightly increased α parameter is also present in the structures of calix[4]quinones.

Effect of a filled/empty 'cavity' in the group of *1,3-alternate* methylene-bridged calix[4]arenes is depicted in Fig. 14 and 15. The main difference from the *cone* and *partial cone* conformers is that *1,3-alternate* calix[4]arenes have two 'cavities'; each of these may be filled or empty.
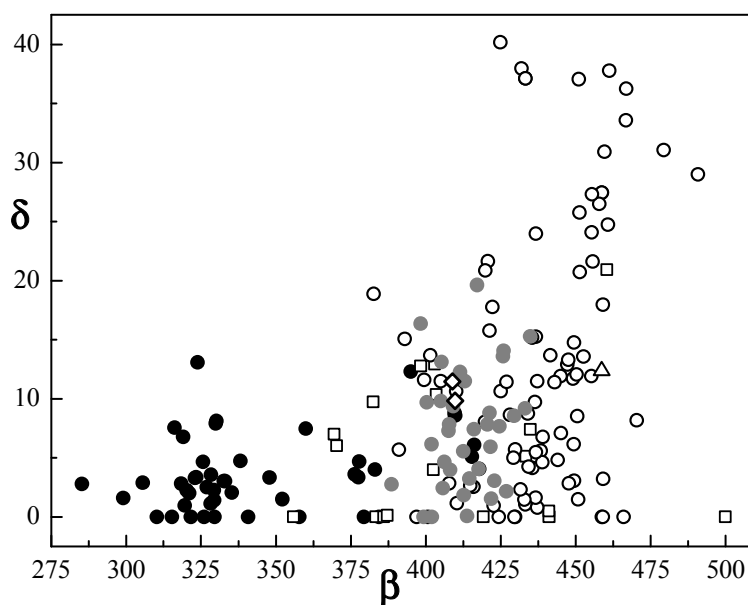
β-δ plot; ● — no molecule inside any 'cavity'; ● — metal ion inside at least one 'cavity';
□ — solvent molecule inside at least one 'cavity'; ○ — lower rim substituent inside at least one 'cavity';
Δ — upper rim substituent from another molecule inside the 'cavity'; ◊ — ligand from a complex inside the 'cavity'

Figure 14. Dependence of the geometry of 1,3-alternate methylene-bridged calix[4]arenes on the type of clathrate

From Figure 14, it is obvious that structures with empty 'cavities' have low β whereas for clathrates the reverse is true. Empty 'cavities' allow undisturbed π, π-interaction between two opposite calix[4]arene phenyl

rings; the structure is therefore more closed and the parameter β lies below 400° (see similar effect in *partial cone* structures). Filled 'cavities' result in more open structures. Uncomplexed structures with both 'cavities' filled have β usually above 430°; when only one 'cavity' is filled this parameter drops to about 400°. These effects are depicted in Fig. 15. The group of complexes with one or two metal ions inside the 'cavities' is relatively uniform; the number of encapsulated metal ions does not seem to matter.

A large number of structures with lower rim substituent inside the 'cavity/ies' have δ > 20° (Fig. 14). The reason for this behavior is probably that in case of bulky lower rim substituents only one of these distal substituents can be encapsulated; the other one lies necessarily outside the 'cavity' because of sterical reasons. This arrangement at the lower rim may lead to deformations in δ.

● — 0; ● — 1; ○ — 2 filled 'cavities'
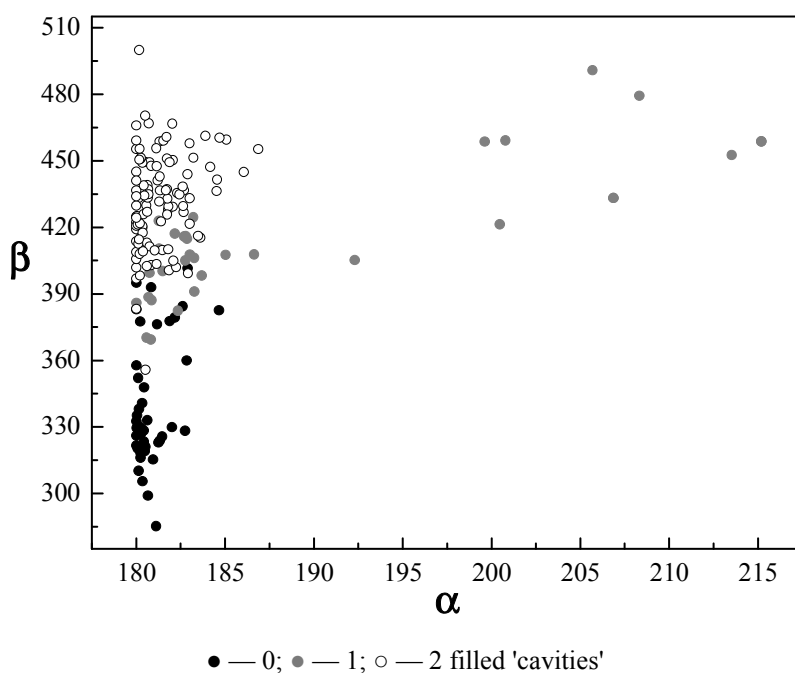
Figure 15. Effect of the number of filled 'cavities' on the geometry of 1,3-alternate methylene-bridged calix[4]arenes

There are three 'clusters' in Figure 15: the first one ('cluster' 15-I, 44 cif files with 47 independent molecules) centered at [180.80; 344.34; 4.48] with a standard deviation of [1.00; 32.13; 4.50] which contains molecules with empty 'cavities'; the second one ('cluster' 15-II, 21 cif files with 24 independent molecules) centered at [182.16; 402.86; 7.27] with a standard deviation of [1.60; 15.55; 5.45] containing molecules with one 'cavity' filled and α < 190° and the third 'cluster' ('cluster' 15-III, 99 cif files with 110 independent molecules) centered at [181.33; 432.16; 10.00] with a standard deviation of [1.46; 21.30; 9.72] containing molecules with both 'cavities' filled.

Heteroatom-bridged 1,3-alternate calix[4]arenes

The group of *1,3-alternate* heteroatom-bridged calix[4]arenes contains 63 cif files with 73 independent molecules (significantly more than the *partial cone* and *1,2-alternate* groups). However, complexes are scarce (4 complete cif files with 5 independent molecules, 2 incomplete cif files compared to its methylene-bridged counterpart). The complexes are therefore not distinguished. In addition, all types of bridges (S, SO, SO_2, N, Si, O) were observed in this group (compared to the *cone*, *partial cone* and *1,2-alternate* groups).

Figure 16 depicts α-β plot of all calixarenes from this group divided according to their substitution patterns. No distinct groups among the symmetrically tetrasubstituted structures can be observed. On the other hand, lower rim distally substituted, upper rim symmetrically tetrasubstituted structures form a distinct group at β ~ 440° with several structures located at lower β. Other substitution patterns apart from these two ones contain only a few structures each and are therefore not distinguished.

The main group of lower rim distally substituted, upper rim symmetrically tetrasubstituted structures ('cluster' 16-I) with β > 400° contains 6 cif files with 8 independent molecules and is centered at [182.11; 437.39; 10.92] with a standard deviation of [2.54; 15.98; 6.96]. Structures from 'cluster' 16-I are lower rim

bridged with crown 5 bridge(s). There are three structures with $\beta < 400°$ which do not fall into this group; these structures are either not bridged at the lower rim or are bridged with longer crown ether chain (e.g. crown 6).

■ — symmetrically tetrasubstituted molecules; ▼ — distally substituted lower rim, symmetrically tetrasubstituted upper rim; ○ — other substitution patterns
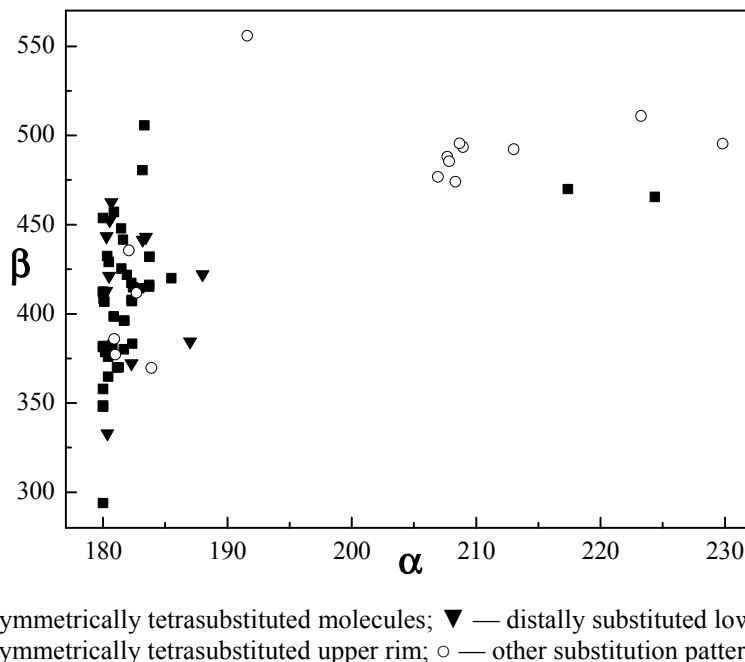
Figure 16. The α-β plot of all 1,3-alternate heteroatom-bridged calix[4]arenes

Figures 17, 18 (α-β plots) depict dependence of the calix[4]arene symmetry on the type of clathrate. Similar effects have been already observed for the methylene-bridged group.

● — no molecule inside the 'cavity', □ solvent molecule inside the 'cavity'; ● — metal ion inside the 'cavity';
○ — lower rim substituent inside the 'cavity'; Δ — other calix[4]arene molecule inside the 'cavity'
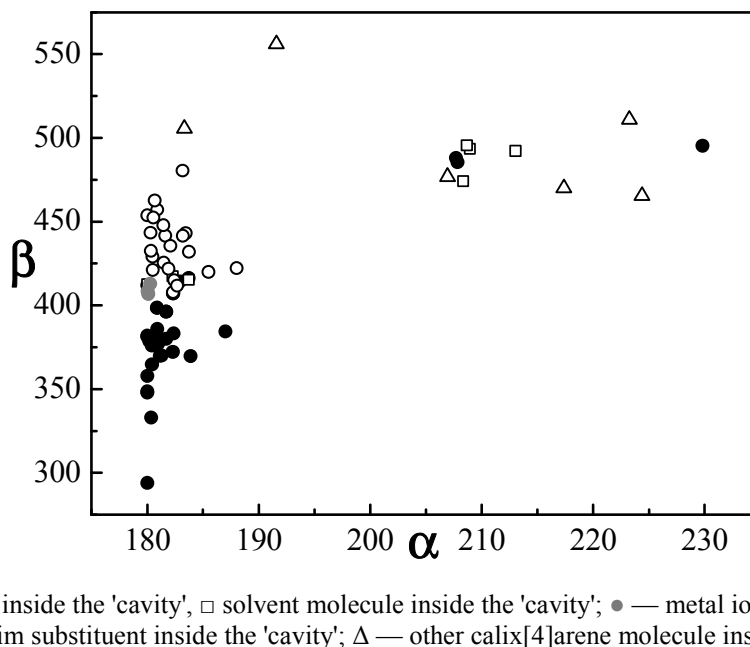
Figure 17. Dependence of the symmetry of the calix[4]arene scaffold on the type of the clathrate

As *1,3-alternate* calixarenes have two 'cavities', only one or both of them can be filled or empty. Structures which have both 'cavities' empty have $\beta < 400°$; or $\alpha > 200°$ and large β if they lack substituents at the lower rim. Structures with only one 'cavity' filled have generally $\beta \sim 410°$, structures with both 'cavities' filled have larger β because of a more open structure (see Fig. 18). Similar effect has been observed within

the methylene-bridged group. Since there are only a few molecules in each group, calculation of 'clusters' was not performed.

● — 0; ● — 1; ○ — 2 filled 'cavities'
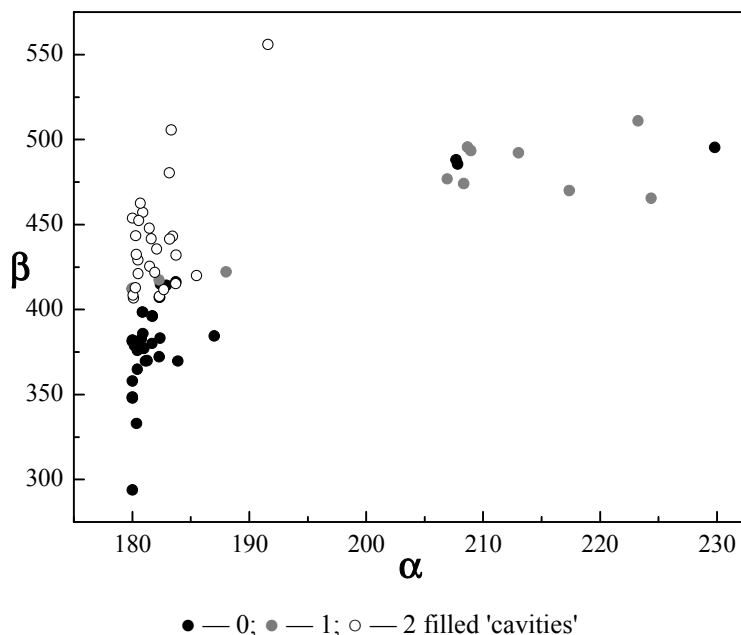
Figure 18. Effect of a filled 'cavity' on the geometry of 1,3-alternate heteroatom-bridged calix[4]arenes

Figure 19 shows effects of upper/lower rim substitution on the geometry of the calix[4]arene scaffold. From Figure 19, it can be seen that structures which contain alkylated or acylated lower rim hydroxyl groups are all relatively uniform. Unlike other previously described groups, there are a large number of structures with missing hydroxyl groups at the lower rim in the *1,3-alternate* heteroatom-bridged group; these structures have $\alpha > 200°$ and/or $\beta > 500°$ in Figure 19.

■ — nonpolar substituent at the upper rim, hydroxyl or no substituent at the lower rim;
● — polar substituent at the upper rim, hydroxyl or no substituent at the lower rim;
▲ — no substituent at the upper rim, hydroxyl or no substituent at the lower rim;
□ — nonpolar substituent at the upper rim, substituted lower rim hydroxyl groups;
○ — polar substituent at the upper rim, substituted lower rim hydroxyl groups;
△ — no substituent at the upper rim, substituted lower rim hydroxyl groups

Figure 19. Dependence of the symmetry of the calix[4]arene scaffold on the type of the substitution

Since there are altogether six possible types of bridge in the group of *1,3-alternate* heteroatom-bridged calix[4]arenes, Figure 20 depicts this group divided according to the type of the bridge.

● — S; ● — SO; ○ — SO$_2$; Δ — Si; ◊ — N; ▽ — O
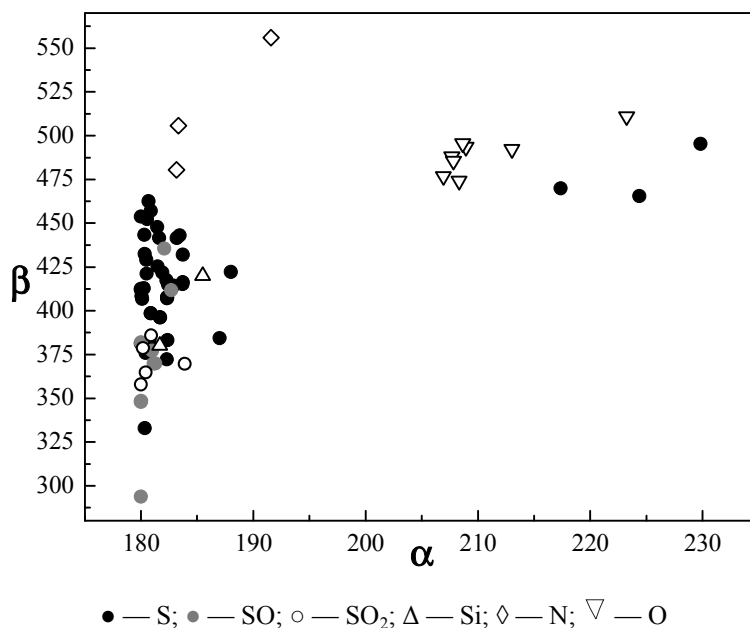
Figure 20. The α-β plot of all 1,3-alternate heteroatom-bridged calix[4]arenes
divided according to the type of the bridge

The type of the bridge seems to have some effect on the calixarene stereochemistry (Fig. 20). It can be clearly seen that the nitrogen- and oxygen-bridged calix[4]arenes form distinct groups. Likewise, all sulfone-bridged calix[4]arenes are very close to each other. Thanks to the symmetrical SO$_2$ bridge, these structures are very symmetrical with all phenyl ring angles to the reference plane of about 90° (the opposite calixarene phenyl rings are almost parallel in all these structures, see Fig. II-21). These values of the phenyl ring angles account for the relatively low β value. The sulfone-bridged group is uniform in α and β and differs slightly in δ ('cluster' 20-I; 5 cif files with 5 independent molecules; center at [181.08; 371.41; 9.85], standard deviation [1.44; 9.93; 7.91]); no dependence of the δ parameter in the sulfone group on the size and type of substituents was observed.
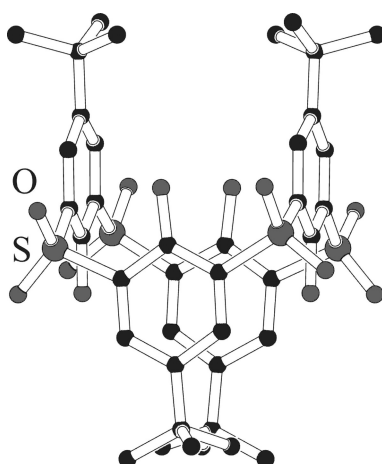
Figure II-21. Structure NUHFOL [10]

The group of SO-bridged calix[4]arenes is relatively uniform in parameter α; however, in the β parameter there are significant differences. No correlations between this parameter and the substitution and/or size of the upper and lower rim substituents were found. The hit with β < 300° is structure LEQMID [10], a structure with SO bridges and unsubstituted upper rim. All structures possessing SO bridges in this group (includ-

ing the structure LEQMID) have these bridges arranged in an *up-*, *down-*, *up-*, *down-* (aeae) fashion but only the structure LEQMID has unsubstituted upper rim which allows for a more efficient π, π — stacking of two opposite calixarene rings (and CH-π interaction between upper rims from different molecules) and has therefore lower β (Fig. II-22).
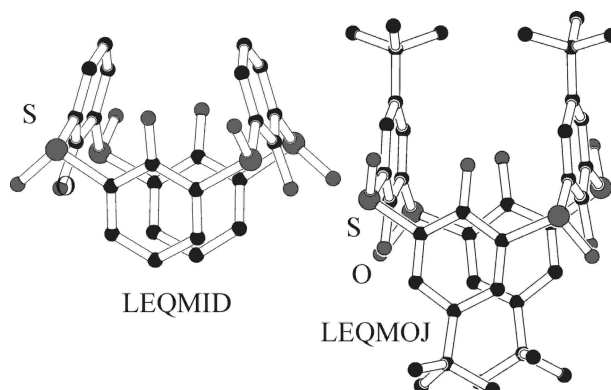
Figure II-22. Structures LEQMID and LEQMOJ [10]

The oxygen-bridged group is likewise uniform in α, β and varies in δ; because of the complexity of the substitution patterns in this group, no conclusions concerning dependence of the δ parameter on the type and size of the substituents could be made. This group contains 6 cif files with 8 independent molecules ('cluster' 20-II) and is centered at [210.58; 489.59; 11.50] with a standard deviation of [5.09; 10.82; 9.11]. The conformation of these structures is very similar to those of *saddle* resorcinarenes. An example of an oxygen-bridged structure shows Figure II-23.

Nitrogen-bridged structures are NANREA, SUDMOT and TAZMEN [10], Figure II-24. Structure TAZMEN is a clathrate with *m*-substituted phenyl rings (the lonely hit with α ~ 190° and β ~ 550°). The common feature of all these structures is a very open cavity (no intramolecular π, π-stacking). The factors affecting the calixarene stereochemistry coming into play are numerous: substitution of N bridges, filled or empty cavity, intermolecular π, π- and CH-π interaction and substitution of the upper and lower rim and possible *m*-substitution. Because of too few structures of this type, these stereochemical factors are very difficult to evaluate.
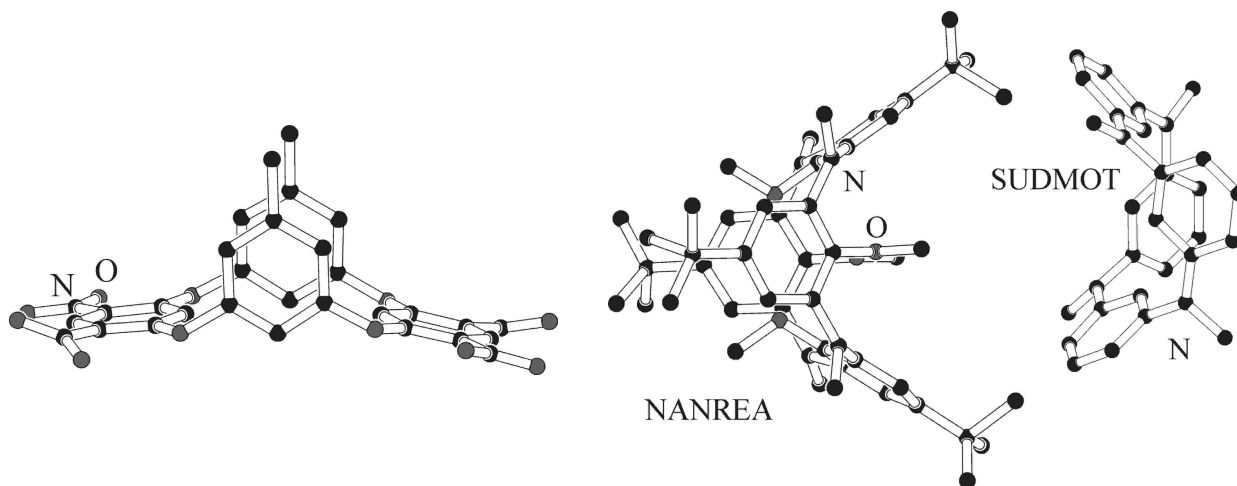
Figure II-23. Structure FEZZIU [10]

Figure II-24. Structures NANREA, SUDMOT [10]

Since in the silicon-bridged group there are only two structures it is difficult to draw any conclusions here. Conformations of these structures are similar to those of the sulfone-bridged group.

Dependence of the β parameter on the type of the bridge can be shown on the example of lower rim methoxy, upper rim *t*-butyl tetrasubstituted *1,3-alternate* calix[4]arenes with different bridge groups (all these structures are uncomplexed). The α-β plot is given in Figure 21. The majority of relevant structures are

discussed elsewhere in this chapter. No similar uncomplexed methylene-bridged structure was found in the CSD [10] for comparison.
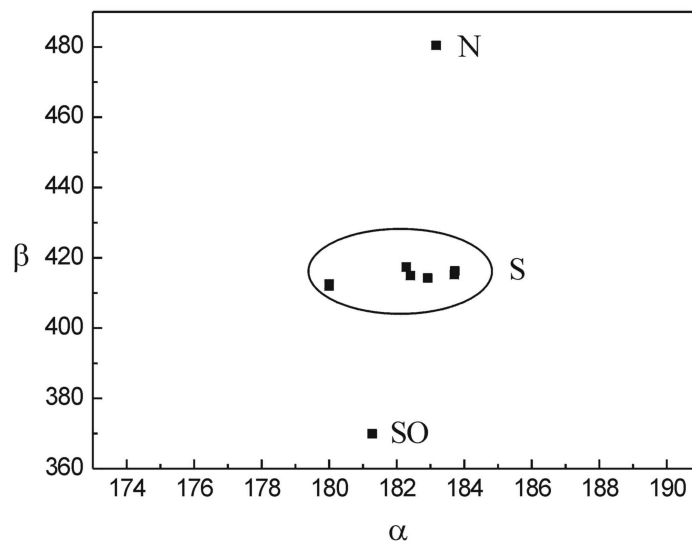
Figure 21: α-β plot showing dependence on the bridge

By far the most common bridge among *1,3-alternate* heteroatom-bridged calix[4]arenes is the sulfur one. The following text will deal exclusively with these structures.

In the group of symmetrically tetrasubstituted molecules, several hits deviate from the main group. The two hits from the symmetrically tetrasubstituted group with $\alpha > 210°$ are structures SAXJEG(01) [10]. These structures lack substituents on both upper and lower rim and their conformation is similar to that of *saddle* resorcinarenes. There is intramolecular π,π-stacking (Fig. II-25) present in these structures and intermolecular CH-π interaction between calixarene phenyl rings. The intramolecular π,π-stacking is not present in similar structure SUDMOT (Fig. II-24) because there is another calixarene molecule positioned inside the cavity in this structure; the intramolecular π,π–stacking cannot be therefore present.
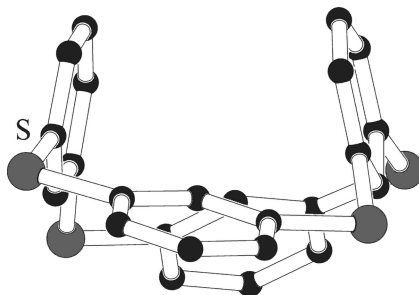
Figure II-25. Structure SAXJEG [10]

The remaining hit with $\alpha > 205°$ belongs to structure NODJOF [10], long chain *m*- substituted, S-bridged structure with missing lower rim substituents. Because of the lack of sterical hindrance at the lower rim, the conformation of this structure is similar to that of *saddle* resorcinarenes.

The rest of the sulfur-bridged group ('cluster' 20-III, 28 cif files, 41 independent molecules, centered at [181.70; 413.64; 5.92], standard deviation [1.75; 26.70; 8.41]) is relatively uniform with regard to both α and β. Structures with two identical crown ether bridges at the lower rim have been included in the lower rim distally substituted group, therefore there are no lower rim distally bridged structures within the symmetrically tetrasubstituted group. The trends within this group are similar to those observed within the methylene-bridged group.

For example, structure ALETUG01 [10] similar to the structure ALETEQ ($\beta = 377°$) is substituted by *t*-butyl groups at the upper rim and has a more open structure ($\beta \sim 415°$) which reflects sterical hindrance caused by bulky upper rim substituents. Structures ALETEQ, ALETUG01 are depicted in Fig. II-26. Four

other lower rim methoxy, upper rim *t*-butyl-substituted structures are very similar to the structure ALETUG01 (β ~ 415°).
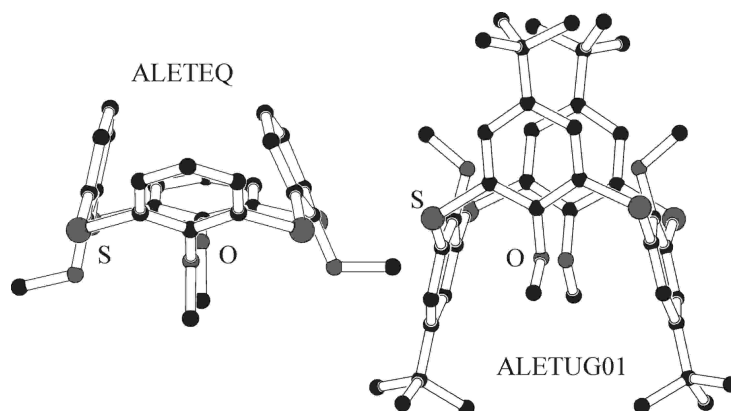
Figure II-26. Structures ALETEQ, ALETUG01 [10]

Upper rim ethynyl-substituted structure HAGVAN (β ~ 430°) has a relatively open structure because of coordination of the ethynyl groups and bulky phosphine ligands on Pt(II). On the other hand, similar structure HAGTUF with 4-pentylphenylethynyl substituents at the upper rim is not so open because there is hydrophobic interaction between two 1-pentyl chains on the upper rim substituents on the opposite calixarene rings and CH-π interaction between upper and lower rim substituents (Fig. II-27). Therefore, the β value for this structure lies beneath 410°.
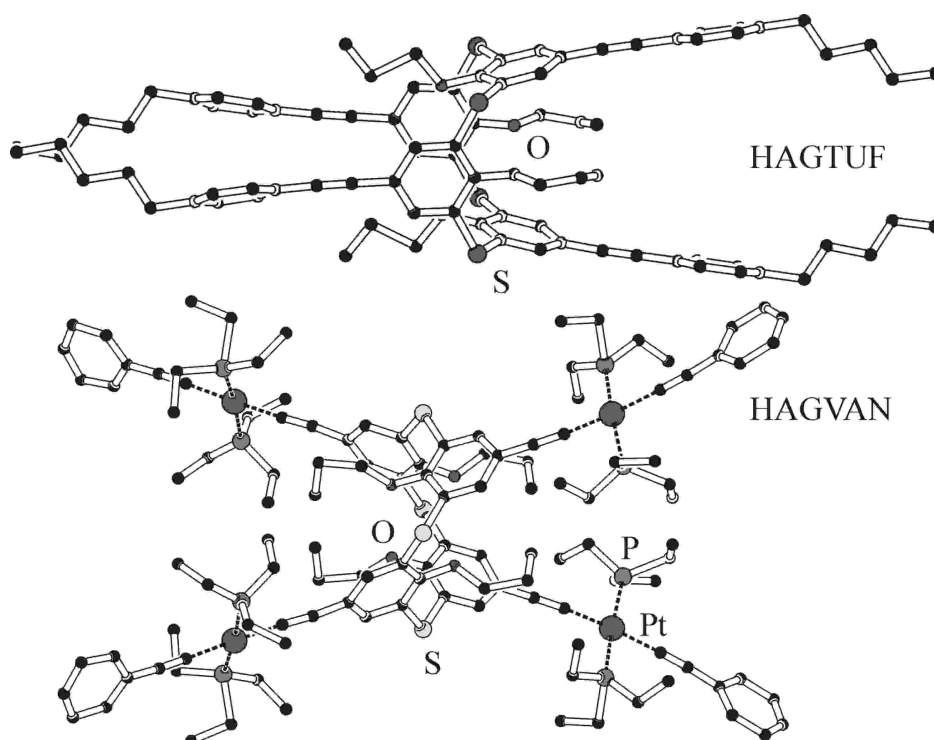
Figure II-27. Structures HAGTUF and HAGVAN [10]

The only interesting structures in the group of lower rim distally substituted heteroatom-bridged *1,3-alternate* calix[4]arenes are crown-6 bridged BOXWEQ and ERUWET01 [10], its Cs(I) complex (the only complex in this group). The long crown-6 chain allows for π, π-interaction between the opposite calixarene rings in the structure BOXWEQ but this interaction is broken in the structure ERUWET01 because of Cs(I) complexation and the resulting cation-π interaction with the two opposite calixarene rings. The structure ERUWET01 is therefore more open (Fig. II-28) and has larger β value.
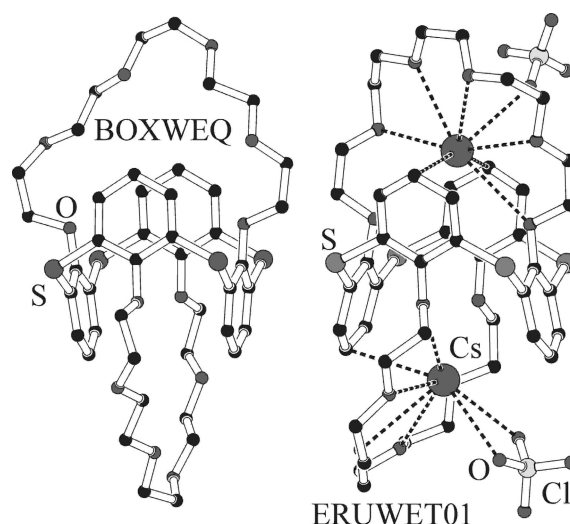
Figure II-28. Structures BOXWEQ and ERUWET01 [10]

Crown-5 bridged calixarenes from this group tend to have larger β value (more open cavities) because of shorter bridge which partially reaches into the ′cavities′; these structures are therefore not able to form intramolecular π, π-interaction like the crown-6 bridged structure BOXWEQ [10]. Representative example is structure BOXQUA (Fig. II-29; compare to structures BOXWEQ and ERUWET01 on Fig. II-28).
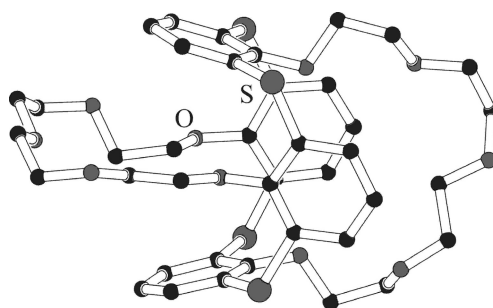
Figure II-29. Structure BOXQUA [10]

Conclusion — 1,3-alternate structures

The parameter β seems to be the best one to describe the base frame geometry of *1,3-alternate* ca-lix[4]arenes. Structures with parallel or closer opposite calixarene rings (more closed cavities) have low β whereas structures with more open cavities have high β. Structures lacking lower rim substituents and there-fore deformed towards the *saddle* geometry common among *saddle* resorcinarenes also have higher β but this type of deformation affects predominantly α (> 200°). Because the δ parameter is below 15° in the vast majority of *1,3-alternate* structures, it is relatively insignificant for this group. Heteroatom-bridged ca-lix[4]arenes containing oxygen bridge substituents are also deformed towards the *saddle* geometry common among *saddle* resorcinarenes (short C-O bond length 1.43 Å compared to C-C 1.54 Å).

To sum up, the best way to significantly influence the geometry of the *1,3-alternate* methylene-bridged calix[4]arenes seems to be distal upper rim coordination which leads invariably to more closed structures. Removal of lower rim phenolic oxygen atoms also has significant impact on the calix[4]arene geometry. Other effects (filled/empty cavity; effects of upper rim substitution and lower rim coordination; length, flexi-bility or rigidity of the lower rim bridge) do not seem to affect the geometry of the calix[4]arene moiety so significantly and/or the result cannot be reasonably foreseen by the chemist.

The best way to immobilize the *1,3-alternate* conformation in heteroatom-bridged calix[4]arenes is a double distal bridge at the lower rim. The length of the bridge seems to affect the geometry of the calixarene base frame; shorter bridges tend to produce more open structures with higher β whereas longer ones do not disrupt intramolecular π,π-interaction between the opposite calixarene phenyl rings and therefore tend to produce more closed cavities with lower β.

As in the group of *partial cone* structures, *1,3-alternate* methylene-bridged calix[4]arenes which contain four lower rim hydroxyl groups are few. Unlike the groups of *partial cone* and *1,2-alternate* structures, there are not so many structures containing unsubstituted lower rim hydroxyl groups among the *1,3-alternate* heteroatom-bridged structures.

Conclusion

To sum up, the parameters α, β, δ are very useful in describing the geometry of the base frame of methylene- and heteroatom-bridged calix[4]arenes. The values of these parameters reflect not only the base conformation (e.g. *cone*, *partial cone*, *1,2-alternate* or *1,3-alternate*) of the calix[4]arene base frame but react to inter- and/or intramolecular interactions present in the structure as well (see discussions at the end of each chapter). Dependence of the parameters α, β, δ on several types of inter- and/or intramolecular interactions has been demonstrated. However, as these results were obtained from solid state data, no conclusion concerning conformations and behavior of calix[4]arene molecules in solution can be stated.

Acknowledgements

References

1   Gutsche C.D. Calixarenes: Monographs in Supramolecular Chemistry. — Cambridge the Royal Society of Chemistry, J.F. Stoddart, 1989.

2   Gutsche C.D. // Top. Curr. Chem. — 1984. — P. 1–47.

3   Shinkai S. // Tetrahedron. — 1993. — No. 49(40). — P. 8933–8968;

4   Shinkai S., Ikeda A. // Chem. Rev. — 1997. —No. 97. — P. 1713–1734.

5   Lhoták P. // Eur. J. Org. Chem. — 2004. — P. 1675–1692.

6   Beer P.D., Gale P. // Angew. Chem. Int. Ed. — 2001. — No. 40. — P. 486–516.

7   Klimentova J., Madlova M., Nemeckova P., Palatinusova L., Vojtisek P., Lukes I. // Bulletin of the Karaganda University. Ser. Chemistry. — 2017. — No. 1(85). — P. 21–46.

8   Klimentova J., Vojtisek P. // Materials Struct. — 2005. —No. 12. — P. 151.

9   Klimentova J., Vojtisek P. // J. Mol. Struct. — 2007. — No. 826(1). — P. 48–63.

10   CSD Version 2.3.6 (update August 2006), Cambridge Crystallographic Data Centre (CCDC).

Я. Климентова, М. Мадлова, П. Немечкова, Л. Палатинусова, П. Войтишек, И. Лукеш

Каликс[4]арендердің конформациялары — CSD мәліметтеріне негізделген зерттеу. ІІ-бөлім. Бөлшектік конус, метиленді және гетероатомды каликс[4]арендердің 1,2-альтернантты және 1,3-альтернантты конформерлері

Бұл зерттеудің бірінші бөлімінде Кембридж құрылымдық мәліметтер базасы (CSD) негізінде метиленді және гетероатомды көпірлері бар каликс[4]арендердің конустық конформерлері зерттелді. Ертерек енгізілген α, β және δ параметрлері жоғарыда келтірілген қосылыстардың көмірсутекті негізі қаңқасының конформациясын сипаттағанда қолданылды. Бұл бөлімде метиленді және гетероатомды каликс[4]арендердің бөлшектік конустық, 1,2-альтернантты және 1,3-альтернантты конформерлері зерттеліп, бұл қосылыстардың конформацияларында молекулаааралық және -ішілік әрекеттесулердің әсері бағаланды.

Кілт сөздер: каликс[4]арен, кристалды құрылымдар, конформациялар, бұрау бұрышы, бұрмалау параметрі.

Я. Климентова, М. Мадлова, П. Немечкова, Л. Палатинусова, П. Войтишек, И. Лукеш

Конформации каликс[4]аренов — исследование, основанное на данных CSD. Часть II. Частичный конус, 1,2-альтернантные и 1,3-альтернантные конформеры метиленовых и гетероатомных каликс[4]аренов

В первой части нашего исследования были рассмотрены конические конформеры каликс[4]-аренов с метиленовыми и гетероатомными мостиками из Кембриджской структурной базы данных (CSD). Ранее вводимые параметры α, β и δ использовались при описании конформаций каркаса углеводородного основания указанных выше соединений. Во второй части исследования изучены частичные конические, 1,2- и 1,3-альтернативные конформеры метилен- и гетероатомно-мостиковых каликс[4]-аренов и оценено влияние меж- и внутримолекулярных взаимодействий на конформации этих соединений.

Ключевые слова: каликс[4]арен, кристаллические структуры, конформация, угол скручивания, параметр искажения.

A.I. Mantel[1], I.S. Irgibayeva[2], I.R. Mukatayev[2]

[1]*Luminescent Materials Research Centre Ltd, Astana, Kazakhstan;*
[2]*L.N. Gumilyov Eurasian National University, Astana, Kazakhstan*
(E-mail: wunderucho@mail.ru)

Modification of solar batteries by polymer fluorescent films

The article describes a method for studying the effect of silicon solar cells´ modification using spectrum shifters, which are polymer films based on polymethylmethacrylate with a thickness of about 4 μm with embedded fluorescent dyes. In the process of work there were obtained spectrum shifters containing commercially available fluorescent dyes Solvent Yellow 160, Coumarin 440 and BBQ. Evaluation of the spectrum shifters´ influence on the efficiency of a solar battery was carried out by comparing the curve of the external quantum yield and the current-voltage characteristics of the latter before and after the modification. Interpretation of the obtained results was based on the absorption and fluorescence spectra of the obtained spectrum shifters. According to the curves of the external quantum yield, a decrease was established in the efficiency of solar cells after the modification by spectrum switches. It is ascertained that the reason for this decrease is the emerging competition in the absorption of incident radiation between the spectrum switch and the solar battery, and the parameters under which this competition would be minimal were determined. According to the data obtained when measuring the volt-ampere characteristics of the obtained modified solar cells, an insignificant increase in the power of the generated electric current was established. A conclusion is made about the contradiction between the results of experiments on measuring the external quantum yield and current-voltage characteristics. With a detailed examination of the features of these research methods it was possible to find the cause for these contradictions. The main conclusions were drawn about the nature of the interaction of spectrum shifters with solar batteries, and the main conditions under which this interaction was effective were determined.

Keywords: solar battery, spectrum switch, external quantum yield, current-voltage characteristics, absorption, fluorescence, fluorescent dye, polymer film.

Introduction

The best efficiency of the experimental device obtained under laboratory conditions reached the conversion efficiency of 25 % for the plates of elements on crystalline silicon [1] and 19.5 % for thin-film technologies [2].

There are two principal approaches for increasing the efficiency of solar cells. The first is to improve the electronic properties of existing devices [3–6]. The second is the use of luminescent low-energy spectrum shifters that absorb short-wavelength photons and re-emit them at more favorable wavelengths (in the long-wavelength region). Luminescent low-energy shifters are a passive approach that involves the use of a luminescent material in a layer located in front of a photocell.

The most common polymers for this purpose are polymethyl methacrylate (PMMA) [7–9] or polyvinyl acetate [10, 11], as well as such inorganic crystalline materials, as Al_2O_3 [3] or SiO_2 [12]. Various types of glasses [13–15] and organic silicates ORMOSIL [16, 17] are also used.

Luminescent materials used for low-energy shifters should ideally demonstrate: the quantum yield of luminescence close to unity; a wide absorption band in the region where the efficiency of photocells is low; high absorption coefficient; a narrow band of radiation coinciding with the maximum effective absorption of the photocell; large Stokes shift to minimize reabsorption; low cost; high photostability.

Organic dyes have relatively high absorption coefficients [18], quantum yield close to one [19], and are easily incorporated into the polymer matrix [18,19]. Their disadvantages are narrow absorption bands and a relatively small Stokes shift, which leads to considerable reabsorption [20]. Several dyes can be introduced into one polymer matrix and mixed with one layer to increase the width of the absorption band and increase the Stokes shift [8]. Their photostability is a matter of debate, although there are reports of significant successes in this direction and similar dyes are commercially available [19].

In this paper it is planned to study the effect of polymer spectrum shifters containing organic dyes on the efficiency of solar cells.

Experimental part

Reagents. The fluorescent dye Solvent Yellow 160 (SY160) (number CAS: 94945-27-4) was purchased from Jinan Junda Industrial Technical Co. Ltd. Fluorescent dyes 7-amino-4-methylcoumarin, coumarin 440 (C440) (Cat. # 04400); and 4,4'''-bis[(2-butyloctyl)oxy]-1,1':4',1'':4'',1'''-quaterphenyl (BBQ) (model number 03800) were purchased from Exciton Inc. [21]. Polymethylmethacrylate, Mw = 996,000, purchased from Aldrich (Cat. # 182265). 1,2-Dichloroethane (DCE), 99+ %, purchased from Acros Organics (Cat. # 406820010. All reagents were used without pre-treatment. The high optical transparency gel of Smartgel OC431A-LVP was purchased from Nyelubricants (Cat. # SM120913).

Equipment. The fluorescence spectra were measured on a USB2000 + spectrometer from Ocean Optics. The transmission and absorption spectra were measured on a Cary 5000 UV-Vis-NIR spectrophotometer from Varian. The profile and thickness of the films were measured on a Dektak 150 profilometer from Veeco. The measurement of the external quantum yield was carried out on a Bentham 218 analyzer equipped with a Bentham TMc300 monochromator and a Bentham PVE30 photovoltaic characterizer and power supplies for a Bentham 605 xenon and halogen lamp. Volt-ampere characteristics were measured on a Keithley 2400 Sourse meter analyzer complete with a Sun 2000 Solar simulator company ABET technologies.

Preparing of polymer films of polymethylmethacrylate

0.5532 g of polymethylmethacrylate (PMMA) were dissolved in 5.7187 g of dichloroethane (DCE), and a stock solution with a mass concentration of PMMA equal to 8.82 % was obtained.

Four working solutions of different concentrations were prepared from the resulting stock solution. The proportions of the base solution (m (PMMA in DCE)) and dichloroethane (m (DCE), as well as the concentration of the obtained samples (W (PMMA)) are presented in Table 1.

Table 1

The concentrations of the PMMA polymer film solutions

Solution	1	2	3	4
m(PMMA in DCE), g	0.1207	0.2535	0.3590	0.4832
m(DCE), g	0.5059	0.3673	0.2395	0.1260
W(PMMA), %	1.70	3.60	5.29	7.00

The resulting working solutions were applied uniformly onto the borosilicate glass with a thickness of 1 mm and an area of 25×35 mm^2. The application area is 25×25 mm^2, the volume of the applied solution for each sample is 0.4 ml. After application, the samples were placed in a draught cupboard to remove the solvent. The resulting films were studied using a profilometer in order to determine their thickness and surface topography. Figure 1 shows the measurements of the profile of all 4 films.
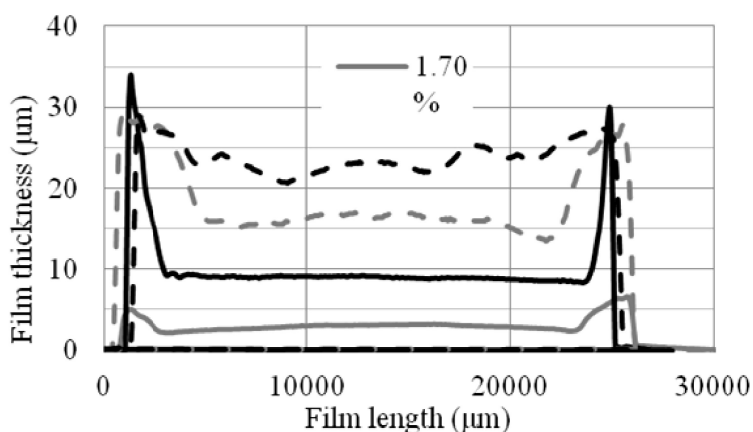
Figure 1. Parameters of the PMMA films profiles obtained from solution in DCE

It can be derived from Figure 1 that the higher is the concentration of the solution from which the film was prepared, the more is the average film thickness, the more is the film thickness, and the worse is its uni-

formity. It should be noted the presence of sharp ups on the boundaries of films. In calculating the average thickness of the films, these sections are not taken into account.

The average thickness of the films was respectively: 3.05; 9.01; 16.01; 24.0 μm.

Based on the results obtained, it was decided to adhere in future studies to a solution concentration of about 4 %, since it allows to obtain the most uniform film surface at its smallest thickness.

General procedure for introducing phosphors into polymer matrices

The PMMA solution is divided into four equal parts by weight. Various proportions of the luminophore solution are added to the each part. To all the obtained solutions additions of pure solvent are added in such a way that the total mass of all solutions is the same. The final concentration of PMMA in working solutions is kept at 4 %.

Discussion of the results

At first to the PMMA film was introduced the dye SY160 having the following structure:
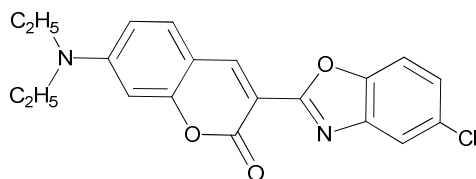
As a result of the introduction, a transparent film with a bright yellow-green fluorescence was obtained, containing 2 % of SY160 based on the PMMA mass. The SY160 dye was selected due to its bright fluorescence with a maximum at 495 nm — the region where the sensitivity of the solar battery is maximal.

The resulting borosilicate glass film was applied to a standard solar cell or solar cell (SC) made of 5×5 mm polycrystalline silicon by gluing through a gel with a high optical clarity and measuring the External Quantum Yield (EQE) of SC with and without the deposited film. The result is shown in Figure 2.
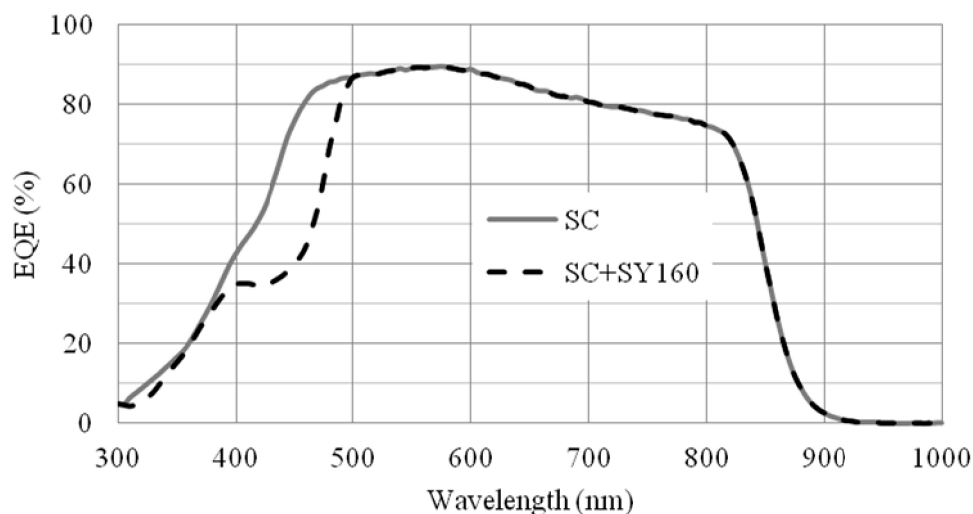
Figure 2. The curves of the BCD of a clean solar cell (SC) and a solar cell
covered with a PMMA film containing the SY160 (SC + SY160) dye

As can be seen from Figure 2, the presence of a fluorescent PMMA film with SY160 leads to a decrease in the SC quantum yield in the ranges of 300–360 nm and 390–500 nm. At first glance, the result is contrary to the theory that the EQE SC should have increased in the wavelength region of 495 nm if a fluorescent film is applied. However, if we consider the absorption and fluorescence spectra of the resulting film (Figure 3), we can explain the obtained result.

As can be seen from Figure 3, the absorption spectrum of SY160 has 2 peaks — from 240 to 340 nm and from 350 to 500 nm. If we look at Figure 2, it is in these areas that we see a drop in the SC VC. This is clearly seen if we compare the absorption spectrum of SY160 with the curve obtained by subtracting the curve SC + SY160 from the curve SC shown in Figure 4.
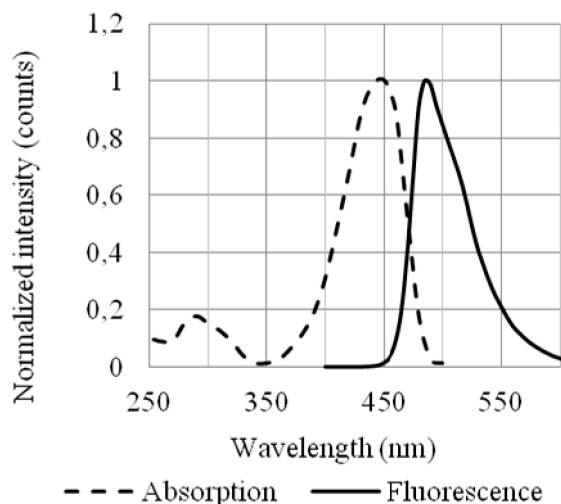
Figure 3. Absorption and fluorescence spectra of the dye SY160
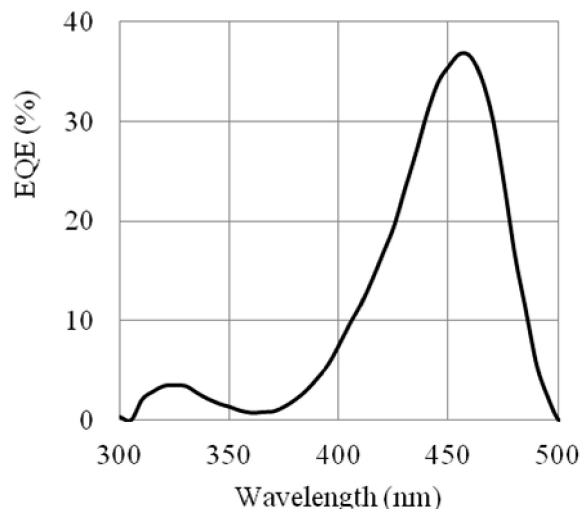
Figure 4. The difference between the EQE SC and SC + SY160 curves from Figure 3

It may seem that in Figures 2 and 3 there is no visible contribution of fluorescence, which should increase the EQE of SC. Comparing Figures 3 and 4, one can see some differences in the ratio of peak intensities and their locations, which is a consequence of the fact that Figure 4 reflects the total contribution from absorption and fluorescence, that is, the difference in absorption and fluorescence intensities at the moment of excitation of the sample at a given wavelength.

From the results obtained, it can be concluded that when light falls on an SC covered with a fluorescent film, a competition arises between the film and SC in absorbing the incident radiation. The SC falls on the radiation that was not absorbed by the film. This competition is the higher, the closer the absorption peak of the dye and the maximum of efficiency are on the SC curve in SC. This loss cannot be compensated by the fluorescence of the film, since the energy absorbed by the film is always greater than the energy transferred to fluorescence or, in other words, the quantum yield of fluorescence is always less than 1.

From the above it follows that as a spectrum shifter for SC it is necessary to use a fluorescent film having an absorption maximum where the EQE SC curve has a minimum.

As fluorophores having absorption in the short-wavelength region of the spectrum, where the EQE SC is the minimum, dyes C440 and BBQ, absorbing shorter than 400 nm, were chosen.

The introduction of dyes into polymer films was carried out according to the procedure described above. For each colorant, 4 films with different weight proportions of the dye in the polymer were prepared. This was done in order to trace the effect of a gradual increase in the concentration of the dye on changes in the EQE SC, as well as to avoid distortion of the results in view of the effect of concentration quenching, which may appear in one of the samples. In this case, the results of this sample will simply not be taken into account.

The first samples of films containing a fluorescent dye C440 were investigated. A summary of the dye is shown in Table 2.

T a b l e 2

Brief information about the dye C440

Full name	7-Amino-4-methylcoumarin			
Abbreviation	C440			
Dye structure				
Weight percent in PMMA films	1	2	3	4
	1.79 %	1.11 %	0.59 %	0.24 %

The absorption and fluorescence spectra are represented by the C440 dye in Figure 5. Figure 6 shows the curves of EQE pure SC, and SC coated with C440 films with a mass concentration of 1.79 % and 0.59 % in the 300–500 nm range. The remaining 2nd concentrations are not indicated in order to avoid cluttering the schedule and loss of informative value.
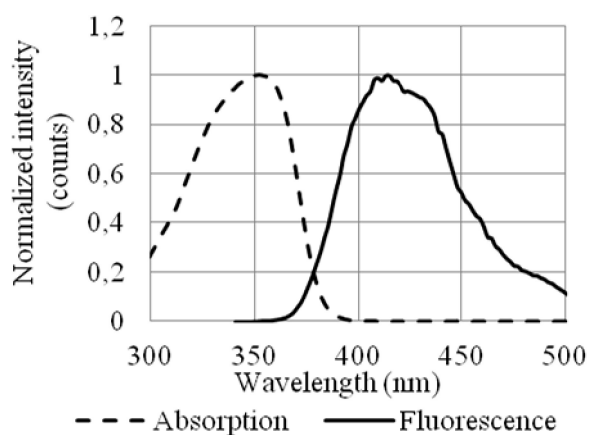
Figure 5. Absorption and fluorescence spectra of the C440 dye
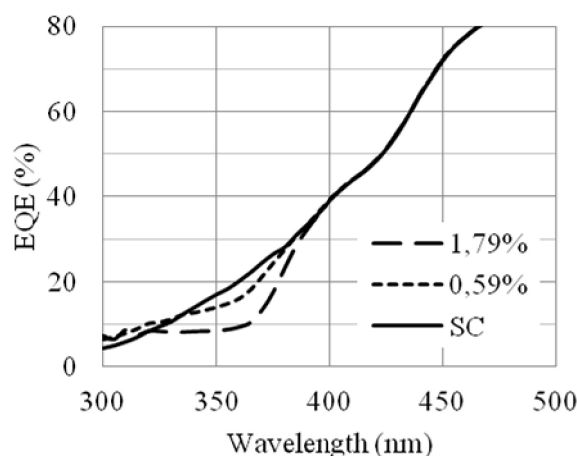
Figure 6. EQE curves of pure SC and SC coated with PMMA films containing C440 dye at concentrations of 1.79 % and 0.59 %

It can be seen from Figure 6 that with an increase in the C440 dye concentration, the SC efficiency in the 320 to 390 nm region decreases. Figure 5 shows that this is the region where the absorption of the dye is located. In the spectral range 300–320 nm, a slight increase in efficiency can be seen, even though in this region the dye has a significant absorption value. This confirms the conclusion made earlier that the smaller the value of the EQE SC in a certain portion of the spectrum, the smaller the fraction of absorbed energy the SC converts into electricity, and the less competition is expressed between the SC and the spectrum switch.

During the research, the current-voltage characteristics of the obtained samples were measured (Table 3).

T a b l e 3

Volt-ampere characteristics of the SC coated with polymer films with C440

Sample	Jsc, mA/cm^2	Pmax, mB/cm^2	Efficiency, %	Relative efficiency[*], %
SC	−23.60	−11.10	11.10	100
1.79 %	−23.62	−11.14	11.14	100.36
1.11 %	−23.49	−11.03	11.03	99.34
0.59 %	−23.41	−11.01	11.01	99.18
0.24 %	−23.49	−10.95	10.95	98.65

Note. [*]Relative efficiency is calculated from the efficiency of the CS, which is assumed to be equal to 100 %.

From Table 3, it is seen that in the case of a concentration of the dye in the PMMA film equal to 1.79 %, an insignificant increase in efficiency with respect to the pure CS is observed, which contradicts the data in Figure 6, where the concentration of the 1.79 % dye leads to the maximum decrease in the CS efficiency. This discrepancy will be considered below.

Hereafter spectrum explorers containing the fluorescent dye BBQ were investigated. A summary of the dye is presented in Table 4.

The absorption and fluorescence spectra of BBQ are shown in Figure 7. The curves of the BCD of a clean solar cell (SC) and a solar cell with overlying PMMA films containing the BBQ dye are shown in Figure 8.

Brief information about the BBQ dye

Full name	4,4'''-bis[(2-butyloctyl) oxy]-1,1':4',1":4",1'''-quaterphenyl			
Abbreviation	BBQ			
Dye structure				
Weight percent in PMMA films	1	2	3	4
	2.63 %	1.33 %	0.67 %	0.34 %
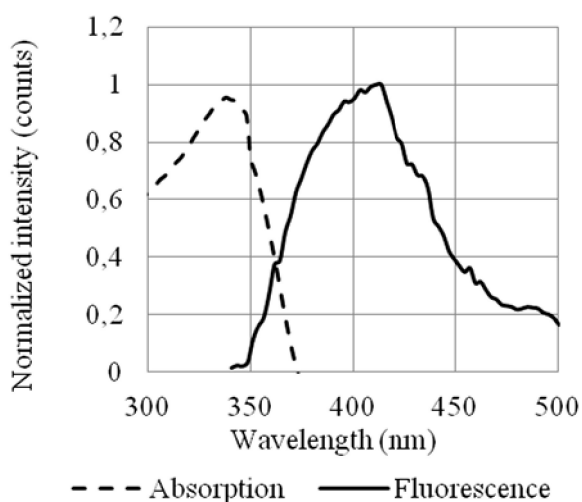
Figure 7. Absorption and fluorescence spectra of the BBQ dye
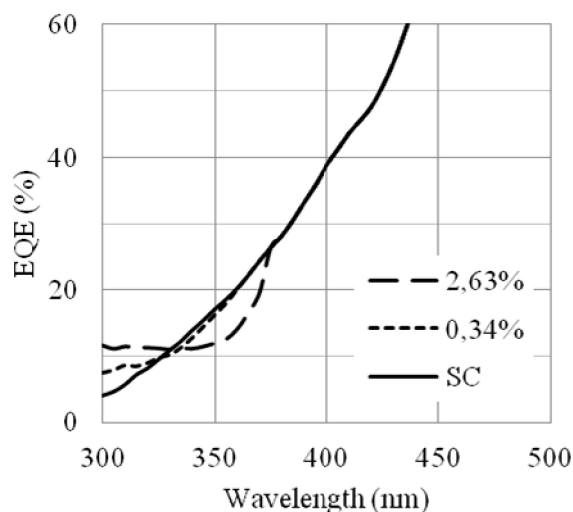
Figure 8. The curves of the DCD of a clean solar cell (SC) and a solar cell coated with PMMA films containing BBQ dye at concentrations of 2.63 % and 0.34 %

It can be seen clearly from Figures 7 and 8 that in the 300–320 nm region the spectrum shifters with the BBQ dye show the most pronounced increase in the EQE SC and a less pronounced decrease in the EQE SC in the 320 to 390 nm region compared to the C440. This is because the absorption bands of the BBQ dye lie in a shorter wavelength range than in the C440, which means that there is less pronounced competition between SC and the spectrum switch. It is expected that measuring the current-voltage characteristics of SC coated with BBQ dye films will show a greater efficiency increase than for samples with C440 dyes (Table 5).

Volt-ampere characteristics of the SC coated with polymer films with BBQ

Sample	Jsc, mA/cm^2	Pmax, mB/cm^2	Efficiency, %	Relative efficiency[*], %
SC	−24.20	−11.14	11.14	100
2.63 %	−23.83	−11.04	11.04	99.10
1.33 %	−23.57	−10.92	10.92	98.02
0.67 %	−23.83	−11.07	11.07	99.37
0.34 %	−23.93	−11.14	11.14	100

Note. [*]Relative efficiency is calculated from the efficiency of the CS, which is assumed to be equal to 100 %.

It can be derived from Table 5 that the efficiency of the SC coated with films with BBQ drops with regard to the clean SC for all concentrations of BBQ, which contradicts the results of Figure 5. This contradiction can be explained by the difference in the operation of the instruments for measuring the BAT and volt-ampere characteristics.

The device for measuring the EQE registers the energy of the radiation incident on the SC at a certain wavelength and the energy produced by the SC when this radiation hits it. The device then calculates the quantum yield as the ratio of the energy generated by SC to the energy of the radiation incident on the SC. Thus, the shape of the incident radiation spectrum on SC does not affect the shape of the EQE curve.

In the instrument for determining the current-voltage characteristics, the radiation from the SC is supplied by a simulator of solar radiation, which produces the radiation similar to sunlight. The instrument measures basic SC parameters, which directly depend on the spectrum and intensity of the incident radiation.

Figure 9 shows the emission spectrum from the solar spectrum simulator, as well as the SC absorption spectrum calculated on the basis of the EQE SC.
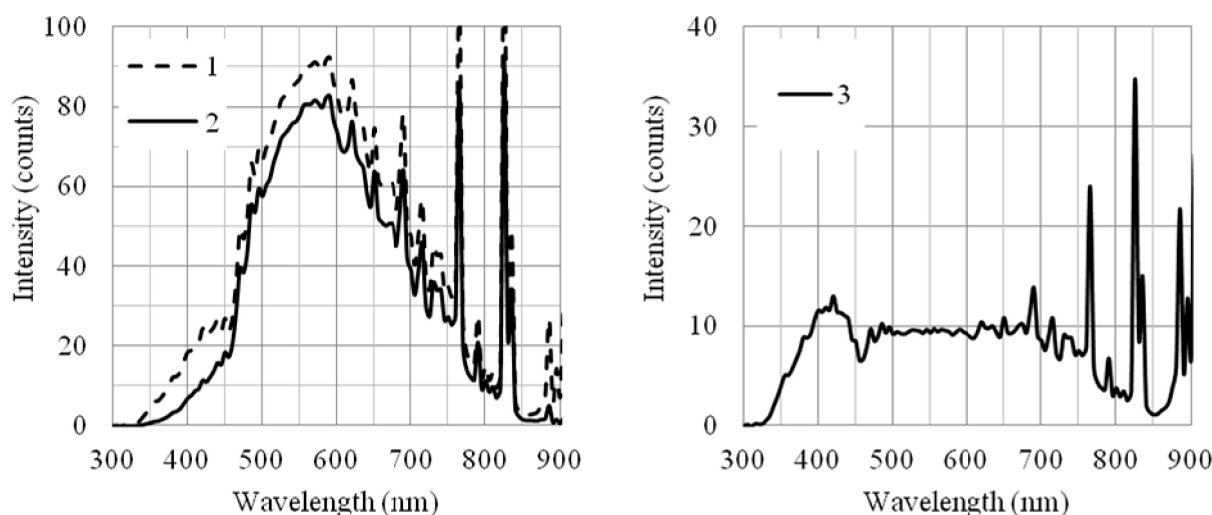
Figure 9. The emission spectrum of the solar simulator (1), calculated on the basis of the BAC, effective absorption spectrum of SC (2) and the difference between spectra 1 and 2 (3)

Figure 9 shows that in the range from 300 to 350 nm, taking into account the low intensity of the incident radiation, as well as the low value of the EQE, the effective absorption of SC is negligible. Since the BBQ dye has an absorbance of up to 350 nm, it is logical that we do not observe any increase in efficiency in the case of spectrum shifters containing BBQ when measuring the volt-ampere characteristics of the samples. If we subtract curve 2 from curve 6 from curve 1, we obtain curve 3 describing the energy of the unused solar battery. The dye BBQ in this case, there is practically nothing to collect, whereas for the C440 dye the absorption spectrum stretches to 380 nm, where there is a larger amount of non-absorbed energy. That is why we see a slight increase in the efficiency of SCs covered by spectrum shifters containing C440, with a simultaneous decrease in efficiency on the BAC curves.

In addition, for some samples there is a slight decrease in efficiency, as can be seen from Table 5, caused not so much by the absorption of the dye as by the scattering of the incident light by the sample.

Conclusion

As a result of the work, spectra based on the PMMA matrix containing fluorescent dyes SY98, C440, and BBQ were obtained. The influence of these shifters on the efficiency of the solar battery on which they were applied was studied.

As a result of the study, the following conclusions were made:

1) there is a competition between the spectrum switch and the solar battery, expressed in the fact that some of the energy absorbed by the switch does not reach the solar battery;

2) the effect of competition between the spectrum switch and the solar battery is much more pronounced than the effect of increasing efficiency due to fluorescence;

3) the absorption region is a more important parameter for the spectrum displacer than the region of its fluorescence;

4) spectrum shifters absorbing shorter than 350 nm do not affect solar batteries.

References

1 Green M.A. Solar cell efficiency tables (version 42) / M.A. Green et al. // Prog. Photovoltaics Res. Appl. — 2013. — Vol. 21, No. 5. — P. 827–837.

2 Klampaftis E. Enhancing the performance of solar cells via luminescent down-shifting of the incident spectrum: A review / E. Klampaftis et al. // Solar Energy Materials and Solar Cells. — 2009. — Vol. 93, No. 8. — P. 1182–1194.

3 Hovel H.J. The effect of fluorescent wavelength shifting on solar cell spectral response / H.J. Hovel, R.T. Hodgson, J.M. Woodall // Sol. Energy Mater. — 1979. — Vol. 2, No. 1. — P. 19–29.

4 Bedair S.M. A two-junction cascade solar-cell structure / S.M. Bedair, M.F. Lamorte, J.R. Hauser // Appl. Phys. Lett. — 1979. — Vol. 34, No. 1. — P. 38–39.

5 Taguchi M. HITTM cells — high-efficiency crystalline Si cells with novel structure / Taguchi M. et al. // Prog. Photovoltaics Res. Appl. — 2000. — Vol. 8, No. 5. — P. 503–513.

6 Luque A. Increasing the efficiency of ideal solar cells by photon induced transitions at intermediate levels / A. Luque, A. Martí // Phys. Rev. Lett. — 1997. — Vol. 78, No. 26. — P. 5014–5017.

7 Maruyama T. Solar cell module colored with fluorescent plate / T. Maruyama, A. Enomoto, K. Shirasawa // Sol. Energy Mater. Sol. Cells. — 2000. — Vol. 64, No. 3. — P. 269–278.

8 Richards B.S. Overcoming the poor short wavelength spectral response of CdS/CdTe photovoltaic modules via luminescence down-shifting: Ray-tracing simulations / B.S. Richards, K.R. McIntosh // Prog. Photovoltaics Res. Appl. — 2007. — Vol. 15, No. 1. — P. 27–34.

9 Slooff L.H. Efficiency Enhancement of solar cells by application of a polymer coating containing a luminescent dye / L.H. Slooff et al. // J. Sol. Energy Eng. — 2007. — Vol. 129, No. 3. — P. 272.

10 Marchionna S. Photovoltaic quantum efficiency enhancement by light harvesting of organo-lanthanide complexes / S. Marchionna et al. // J. Lumin. — 2006. — Vol. 118, No. 2. — P. 325–329.

11 Le Donne A. Enhancement of solar energy conversion efficiency by light harvesting of organo-lanthanide complexes / A. Le Donne et al. // 23rd European photovoltaic solar energy conference and exhibition, 1–5 September 2008, Valencia, Spain. — WIP-Munich, 2008. — P. 269–271.

12 Protti S. Wavelength shifting systems based on flavonols and their metal complexes encapsulated by post-doping in porous SiO_2 xerogel matrices / S. Protti et al. // Journal of Molecular Structure. — 2011. — Vol. 993, No. 1–3. — P. 485–490.

13 Kawano K. Application of rare-earth complexes for photovoltaic precursors / K. Kawano et al. // Sol. Energy Mater. Sol. Cells. — 1997. — Vol. 48, No. 1. — P. 35–41.

14 Švrček V. Silicon nanocrystals as light converter for solar cells / V. Švrček, A. Slaoui, J.C. Muller // Thin Solid Films. — 2004. — Vol. 451–452. — P. 384–388.

15 Yamada K. Improvement of efficiency of solar cells by application of the rare earth ions doped fluorescent glass / K. Yamada et al. // Kidorui (Rare Earths). — 2000. — Vol. 36. — P. 252–253.

16 Machida K. Preparation and application of lanthanide complex incorporated ormosil composite phosphor films / K. Machida et al. // J. Lumin. — 2000. — Vol. 87–89. — P. 1257–1259.

17 Jin T. Photovoltaic cell characteristics of hybrid silicon devices with lanthanide complex phosphor-coating film / T. Jin // J. Electrochem. Soc. — 1997. — Vol. 144, No. 11. — P. 4054.

18 Viehmann W. Thin-film scintillators for extended ultraviolet (UV) response silicon detectors / Ed. H.P. Field, E.F. Zalewski, F.M. Zweibaum // International Society for optics and photonics. — 1979. — Vol. 196. — P. 90–95.

19 Seybold G. New perylene and violanthrone dyestuffs for fluorescent collectors / G. Seybold, G. Wagenblast // Dye. Pigment. — 1989. — Vol. 11, No. 4. — P. 303–317.

20 Sah R.E. Influence of the solvent matrix on the overlapping of the absorption and emission bands of solute fluorescent dyes / R.E. Sah, G. Baur, H. Kelker // Appl. Phys. — 1980. — Vol. 23, No. 4. — P. 369–372.

21 Exciton [ER]. URL: http://www.exciton.com/ (accessed: 04.09.2017).

А.И. Мантель, И.С. Иргибаева, И.Р. Мукатаев

Флуоресцентті полимерлердің қабыршақтарымен күн сәулесі батареяларын түрлендіру

Мақалада флуоресцентті бояғыштар енгізілген, қалыңдығы шамамен 4 мкм, полиметилметакрилат негізіндегі полимерлі қабыршақтар болып табылатын, кремний күн сәулелерінің спектрлі жылжытқыштар көмегімен модификациялаудың әсерін зерттеу әдісі сипатталған. Жұмыс барысында коммерциялық жағынан қолжетімді Solvent yellow 160, Coumarin 440 және BBQ флуоресцентті бояғыштары бар спектрлік жылжытқыштар алынды. Күн батареясының тиімділігіне спектрлік жылжытқыштар әсері сыртқы кванттық шығудың қисық сызығын және модификацияға дейінгі және кейінгі вольтампер сипаттамаларын салыстыру арқылы бағаланды. Алынған нәтижелерді интерпретациялау алынған жылжытқыштардың жұтылу мен флуоресценция спектрлеріне негізделген. Сыртқы кванттық шығудың қисықтарына сәйкес спектрлік жылжытқыштар арқылы модификациядан кейін күн батареяларының тиімділігінің төмендеуі анықталды. Осындай төмендеудің себебі спектралды жылжытқыш пен күн батареясы арасындағы сәулеленудің сіңірілуіндегі пайда болатын

бәсекелестік және оның ең аз болатын параметрлері анықталды. Алынған модификацияланған күн батареяларының вольтампер сипаттамаларын өлшеу кезінде алынған деректерге сәйкес, өндірілетін электр тоғының қуаты шамалы көтерілді. Сыртқы кванттық шығу және вольтампер сипаттамаларын өлшейтін эксперименттердің нәтижелері арасындағы қайшылық туралы қорытынды жасалды. Зерттеу әдістерінің ерекшеліктері егжей-тегжейлі қарастырылғанда осы қарама-қайшылықтардың себебі айқындалды. Негізгі қорытындылар күн батареялары мен спектрлік жылжытқыштардың өзара әрекеттесу сипаты және осы өзара әрекеттесудің тиімді болатын негізгі шарттары туралы жасалды.

Кілт сөздер: күн батареясы, спектрлік жылжытқыш, сыртқы кванттық шығу, вольтампер сипаттамасы, сіңіру, флуоресценция, флуоресценциялық бояғыш, полимерлі қабыршақ.

А.И. Мантель, И.С. Иргибаева, И.Р. Мукатаев

Модификация солнечных батарей полимерными флуоресцентными пленками

В статье описан метод исследования модификации кремниевых солнечных батарей при помощи смесителей спектра, которые представляют собой полимерные пленки на основе полиметилметакрилата толщиной примерно 4 мкм с внедренными флуоресцентными красителями. В процессе работы были получены смесители спектра, содержащие коммерчески доступные флуоресцентные красители Solvent yellow 160, Кумарин 440 и BBQ. Оценку влияния смесителей спектра на эффективность солнечной батареи проводили сравнением кривой внешнего квантового выхода и вольтамперных характеристик последней до и после модификации. Интерпретацию полученных результатов вели с учетом спектров поглощения и флуоресценции полученных смесителей спектра. По данным кривых внешнего квантового выхода было установлено снижение эффективности солнечных батарей после модификации смесителями спектра. Установлено, что причина данного снижения — возникающая конкуренция в поглощении падающего излучения между смесителем спектра и солнечной батареей. Кроме того, определены параметры, при которых данная конкуренция была бы минимальной. По результатам измерения вольтамперных характеристик полученных модифицированных солнечных батарей установлено незначительное увеличение мощности вырабатываемого электрического тока. Сделан вывод о противоречии результатов экспериментов измерения внешнего квантового выхода и вольтамперных характеристик. Причина данных противоречий была установлена при детальном рассмотрении особенностей данных методов исследования. Изучена природа взаимодействия смесителей спектра с солнечными батареями и выведены основные условия, при которых данное взаимодействие было бы эффективным.

Ключевые слова: солнечная батарея, смеситель спектра, внешний квантовый выход, вольтамперные характеристики, поглощение, флуоресценция, флуоресцентный краситель, полимерная пленка.

UDC 544.3:544.412.3:549.743.12/13

D.B. Gogol[1, 2], I.E. Rozhkovoy[2], D.L. Ponomarev[2], V.N. Fomin[2, 3]

[1]*Institute of problems of complex development of mineral resources, Karaganda, Kazakhstan;*
[2]*Public association «Grazhdane Kazakhstana», Karaganda, Kazakhstan;*
[3]*Ye.A. Buketov Karaganda State University, Kazakhstan*
(E-mail: vitfomin@mail.ru)

Investigation of the processes of copper ions transition into a solution from oxide and sulfide compounds under the influence of organic complexing agents

The article describes the results of studying of the process of copper leaching from model grounds containing 0.02 % of copper oxide or copper sulfide, with solutions of natural and chemically modified complexing agents. The total amount of one ground sample was 500 g. The model grounds were placed in columns, and the solutions of complexing agents were passed through the columns at a given rate. Sodium humate, sulfonated and oxidized humic acid, native and oxidized fulvic acid, and sodium lactate were studied as leaching agents. It is shown that solutions of all reagents with a concentration of 0.01 % can produce a transition of copper into the solution from both the oxide and sulfide mixtures. It was established that oxidized and native fulvic acids and sodium lactate are most effective for copper extracting. For oxide copper minerals, the most effective complexing agent is the lactate ion, and an oxidized derivative of fulvic acid has a little lower efficiency. Further, less effective agents are the sulfonated humic derivative and the native fulvic acid which have approximately equal effectiveness. The sodium humate is less active and the oxidized humic derivative has lower efficiency. In the case of sulfide minerals, the most effective complexing agent is the oxidized derivative of fulvic acid. The lactate ion, the sulfonated humic derivative and the native fulvic acid are a little less effective agents. The sodium humate and the oxidized humic derivative have comparatively low efficiency. By the mathematical processing of kinetic data, the rate constants of copper leaching processes from model grounds were estimated. The values of the found constants are in the range from $1.05 \cdot 10^{-7}$ to $1.28 \cdot 10^{-7}$ s^{-1}. The kinetic curves for the transferring of copper ions to the solution under the action of complexing agents are characterized by a relatively small transition period and fast reaching concentrations which are close to equilibrium ones.

Keywords: humic acids, fulvic acids, sulphonated humic acids, oxidized fulvic acids, oxidized humic acids, malachite, kinetics of copper leaching.

Introduction

The development of methods for additional extraction of non-ferrous metals from poor and off-balance ores and dumps is an important and actual task due to permanent decreasing of mineral reserves in rich deposits. The purpose of the research is to develop methods for recovery off-balance metals in depleted copper deposits and dumps by transferring copper minerals to a soluble form with using of complexing agents and followed by fixation of copper ions on carbonate collectors.

The formation of malachite under natural conditions occurs in the presence of carbonate rocks in the zones of oxidation of sulfide copper deposits, as well as in places of development of copper deposits, in waste mines and dumps [1–7]. Earlier it was shown that for the intensification of this process it is expedient to use limestone as a carbonate collector and donor of carbonate ions, as well as the use of environmentally safe organic complexing agents [8, 9]. In order to investigate the processes that affect secondary mineral

formation under these conditions, the effect of organic complexing agents on the solubility of copper minerals has been studied.

The main objective of the research is to describe the dissolution of sulfide and oxidized copper minerals under model conditions for the subsequent accumulation of copper ions on carbonate collectors, with using of various physicochemical methods. The scientific novelty is in the estimation of the efficiency of conversion of copper minerals into solution in the form of complex compounds with chemically modified organic ligands.

Experimental

The experiments were conducted to measure the effect of organic complexing agents and their sulfonated and oxidized derivatives on the process of mineral formation of basic copper carbonates on model grounds. The model grounds were mixtures of copper oxide or copper sulfide with inert filler consisting of a mixture of sand and perlite, the content of copper in the soils was 0.02 %. The total amount of one sample of ground was 500 g. Model grounds were placed in columns, through which solutions of complexing agents were passed at a given rate. Six types of complexing agents were used: the lactate ion in the form of a buffer mixture (conventionally designated as Lac), sodium humate (Hum-Na), free fulvic acid (Ful-H), sulfonated (Hum Sulf) and oxidized (Hum Ox) humic derivatives and oxidized derivative of fulvic acid (Ful Ox). The initial concentration of solutions of complexing agents was 0.01 %; the rate of passage of solutions through the columns was between 30 and 50 ml/h. The controlled parameter in carrying out these experiments was the concentration of copper in the solution. The current analytical control of copper in the solutions was carried out by the photometric method on the KFK-2 colorimeter with using of sodium dithiocarbamate [10].

Synthesis of modified complexing agents

Sodium humate (manufactured by LLC «NVP BashIncom», Ufa, Russia) and free fulvic acid (manufactured by Tagrow Co., Ltd., USA) were used as initial complexing agents. The content of water-soluble fulvates in fulvic acid was 96 % from the dry residue with a fulvic acid content of 70 %, the moisture content was 10 %; for the sodium humate, the content of the main substance was not less than 80 %, the rest 20 % represent mainly with water. To characterize the compounds, infrared spectra were registered (Fig. 1 and 2).
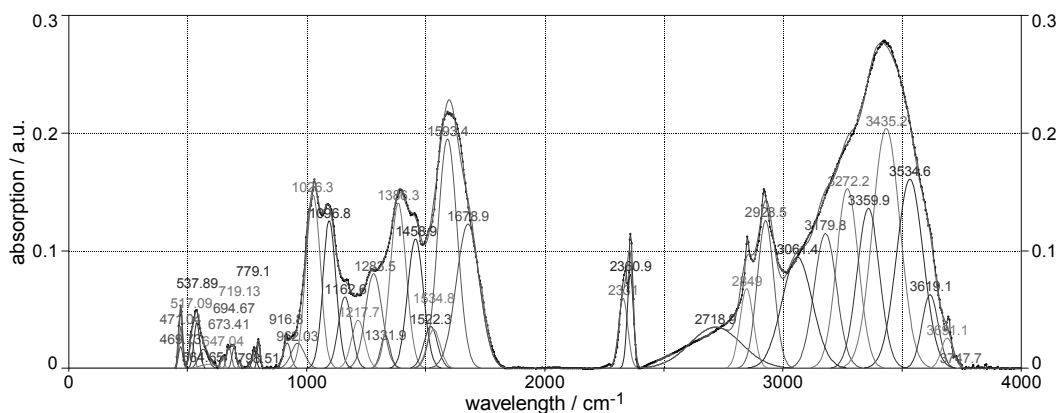
Figure 1. Infrared spectrum of the initial humate
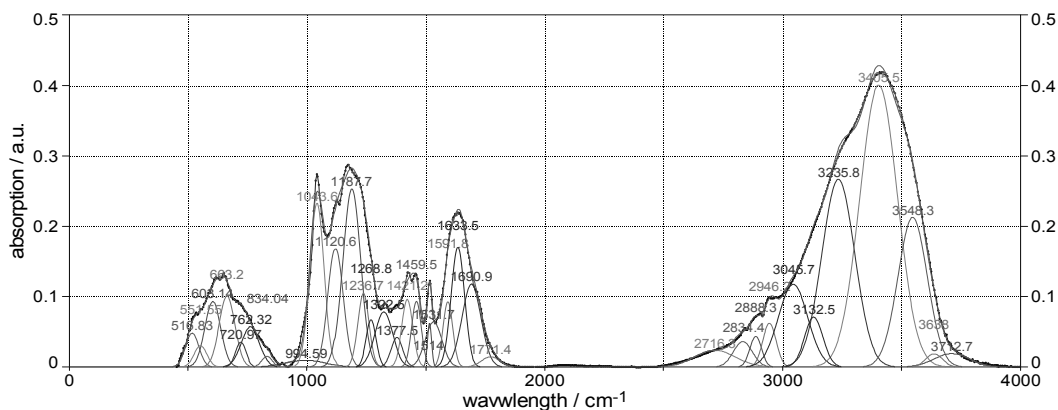
Figure 2. Infrared spectrum of initial fulvic acid

It can be seen from the figures, the starting compounds are characterized by a complex structure of absorption spectra, among which one can distinguish regions related to the vibrations of functional groups (500–1400 cm^{-1}), the range of vibrations of carbonyl groups at 1635–1640 cm^{-1} [11], a wide absorption band of bound water near 3410–3440 cm^{-1}. The IR spectrum of humate also clearly shows the vibrations of free water molecules.

The initial treatment of the starting materials consisted in their heat treatment at 80–90 °C to remove excess moisture and volatile compounds. Two main variants were used for the chemical modification of the starting compounds. First, treatment with oxidants for both a general growth in the number of oxygen-containing functional groups, which, as a rule, exhibit good complexing properties, and to increase the oxygen content in them and, accordingly, to enhance their electron-donating properties and to extend the chemical affinity for metal ions. Second, another variant of the chemical modification involves the introduction of sulfonate groups into the structure of compounds. These groups, in accordance with reference [12], contribute to an increase in the solubility of the humic compounds with content of metals, and, as a result, intensificare their geochemical mobility.

Synthesis of oxidized derivatives from the initial complexing agents

The prepared starting materials were treated with 10 % hydrogen peroxide solution at room temperature for 24 hours. The reaction mixture was evaporated on a sand bath; the residue was dried in a drying oven at 110 °C to constant weight. Infrared spectra of oxidized derivatives of the complexing agents are presented in Figures 3 and 4.
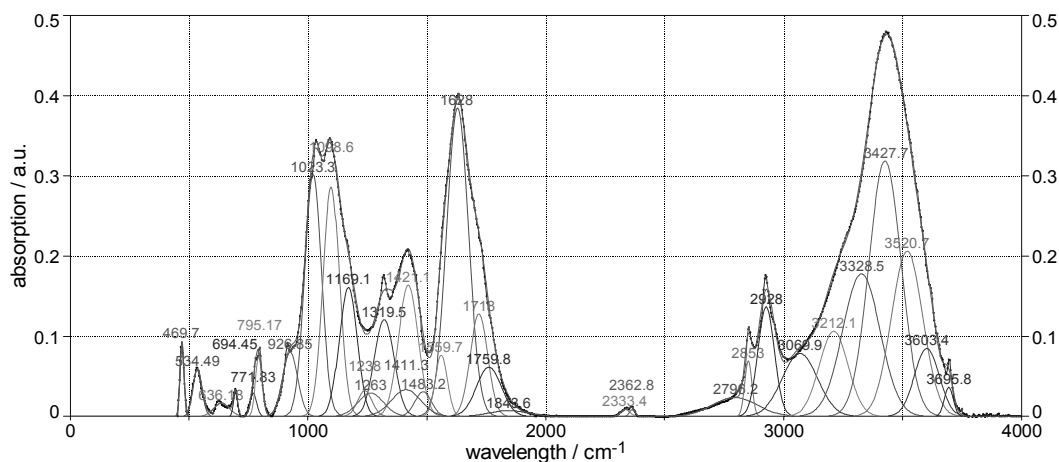
Figure 3. Infrared spectrum of oxidized humate
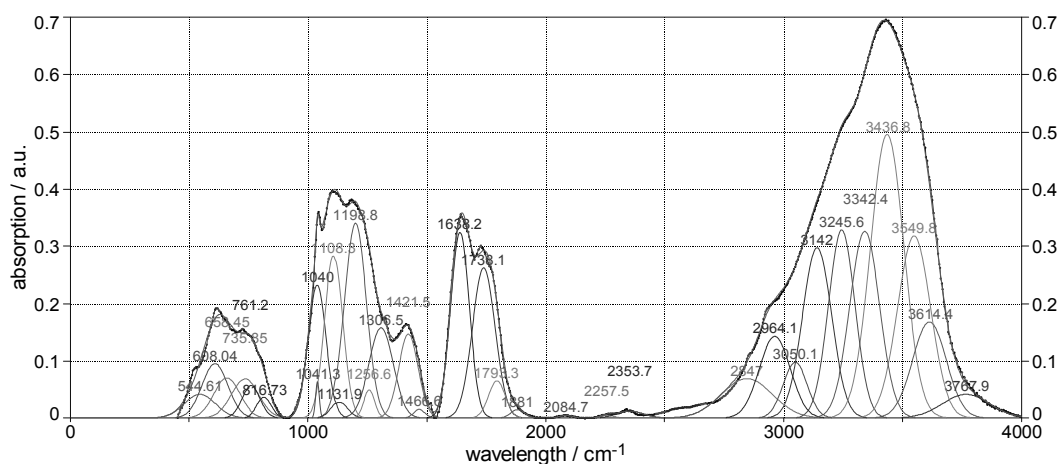
Figure 4. Infrared spectrum of oxidized fulvic acid

The main differences between the spectra of the modified compounds and the spectra of the initial substances consist in an increase in the intensity of absorption of carbonyl groups at 1635–1640 cm^{-1} for humic

and fulvic acids, which indicates an increase in their mole fraction in the oxidation process. For fulvic acid, an additional peak of ketone groups appears at 1730 cm^{-1}. An increase in the number of these functional groups leads to an increase in water solubility and a tendency to formation of complexes with the metal cations that are part of the carbonate collectors, i.e. calcium and magnesium.

Synthesis of sulfonate derivatives from the initial complexing agents

The starting materials were treated with a dilute solution of sulfuric acid (concentration 32 %) at the boiling point of the solution for 4 hours in a cup for evaporation. During the reaction, fulvic acid completely dissolved in the reaction medium, where it could not be isolated. The infrared spectrum of the humic derivative is shown in Figure 5.
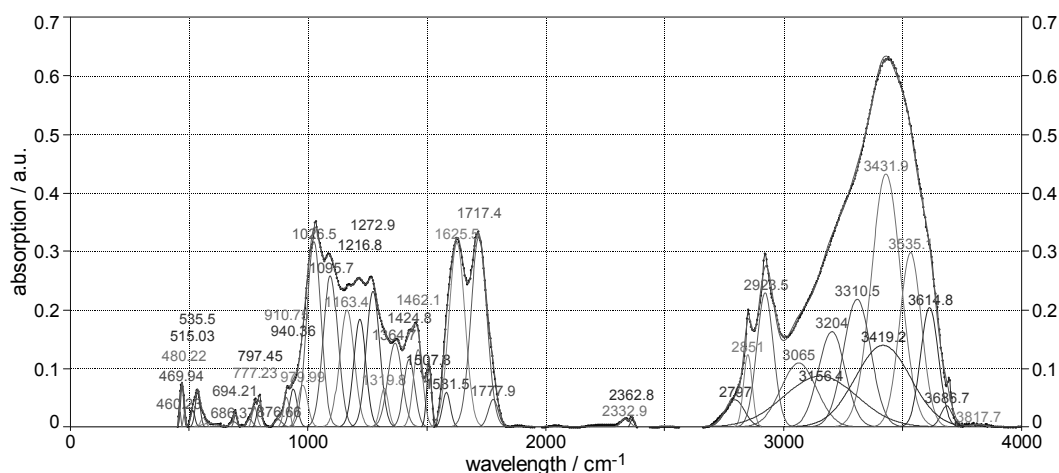
Figure 5. Infrared spectrum of sulfonated humate

The presence of sulfate groups in the structure of the sulfonated derivative is confirmed by an absorption band at 1261 cm^{-1}. It should be noted that along with sulfonation, other processes occur, including the formation of ammonium salts of sulfuric acid with amino groups of humic acid and also the formation of ketone groups (1703 cm^{-1}), apparently in the hydrolysis of unsaturated esters and polysaccharide chains.

Results and discussion

Collection of data on the transfer of copper into a solution from model grounds with the using of complexing agents was carried out over a period of 50 weeks. All types of complexing agents showed appreciable activity for the dissolution of copper from sulfide and oxide minerals. Figures 6–9 show the copper content in solutions passing through the columns. For convenience of perception, the obtained values are divided into four groups: data on the humic complexing agents for the copper oxide and for copper sulfide, and, similarly, on the fulvic complexing agents (together with lactate ion) for copper oxide and copper sulfide. The scale on the ordinate axis is the same for all plots.
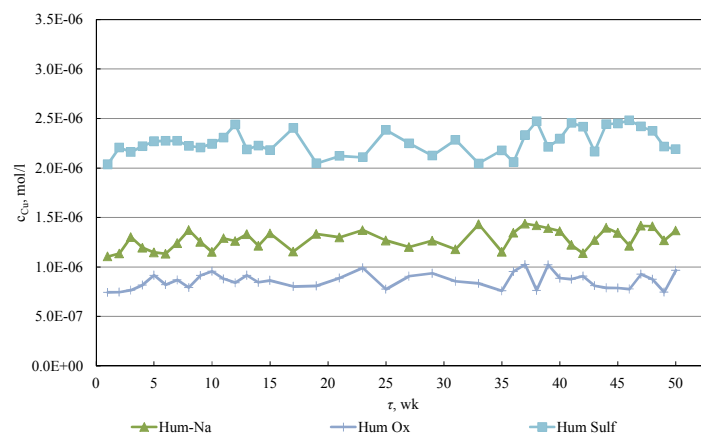
Figure 6. Dependences of copper extraction from copper oxide into solution by humic complexing agents
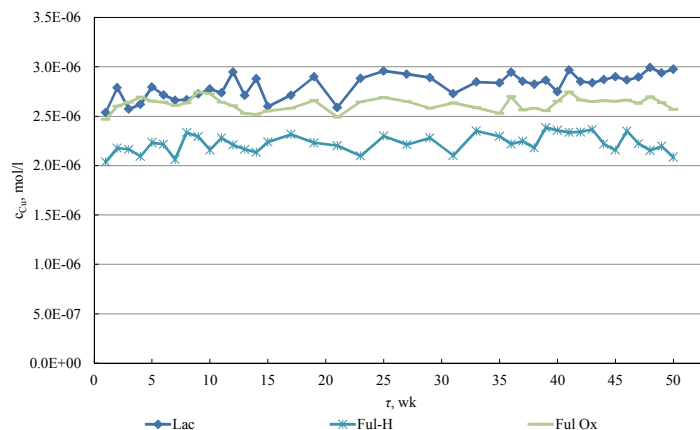
Figure 7. Dependences of copper extraction from copper oxide into solution
by fulvic complexing agents and lactate ion

It can be seen from the graphs given, the copper extraction rates in the solution are quite stable, although they are relatively sensitive to the rate of passage of solutions through the columns, and show a certain tendency to increase with time.

Humic complexants generally show a lower efficiency when copper is transferred to the solution; nevertheless, average values in the transition of copper to solution are observed for the sulfonated humic derivative. At the same time, the humic complexing agents show approximately the same efficiency with respect to the oxide and copper sulfide.
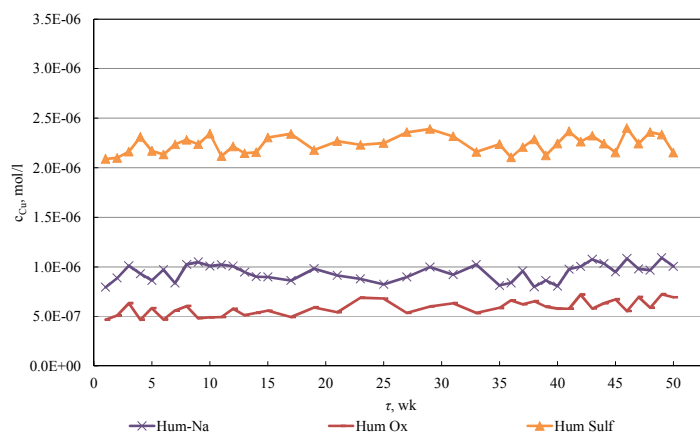
Figure 8. Dependences of copper extraction from copper sulfide into solution by humic complexing agents
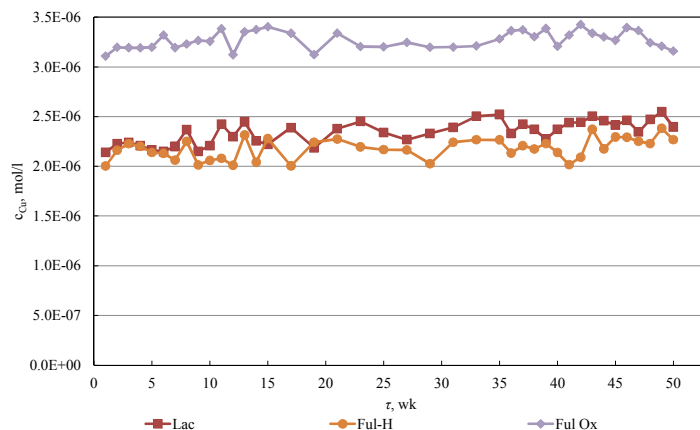
Figure 9. Dependences of copper extraction from copper sulfide into solution
by fulvic complexing agents and lactate ion

For the other group of complexing agents, the oxidized derivative of fulvic acid has higher efficiency for copper sulfide. The lactate ion and the oxidized fulvic acid have a little lower efficiency for copper oxide. For copper sulfide, the lactate ion has less efficiency.

For chemically modified humic derivatives, the sulfonate derivative is more effective than sodium humate, and the oxidized derivative has a little lower efficiency. The oxidized derivative of fulvic acid has a higher efficiency than the native fulvic acid. For these compounds, Figures 10 and 11 show the kinetic curves of the copper ions transition into the solution with complexing agents at the initial stages of time.
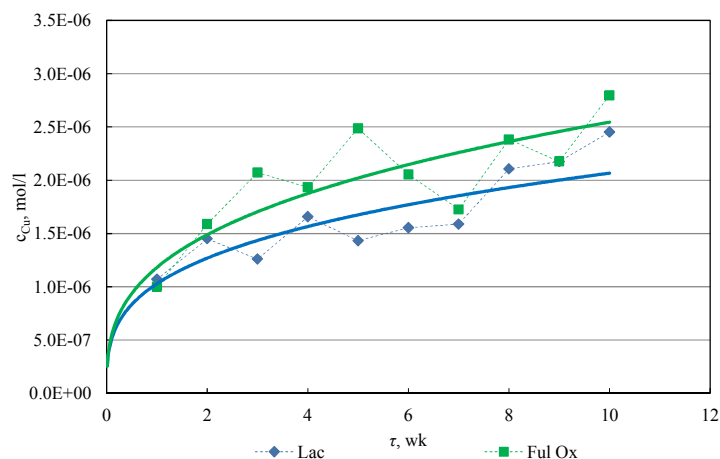
Figure 10. Kinetic curves for the lactate ion and oxidized derivative of fulvic acid for copper oxide
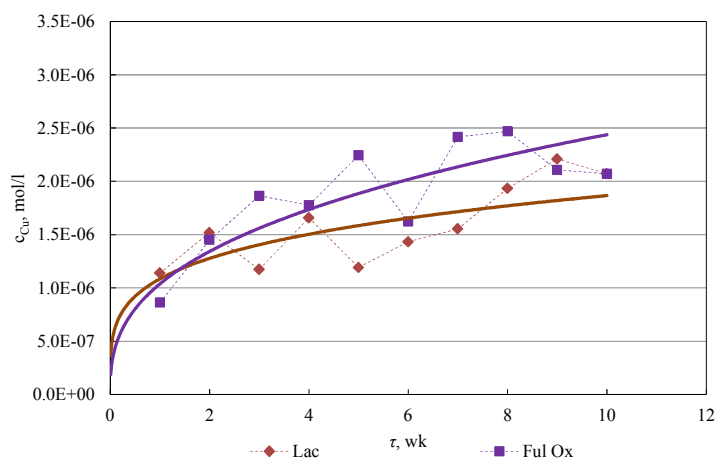
Figure 11. Kinetic curves for the lactate ion and the oxidized derivative of fulvic acid for copper sulfide

It can be seen from the figures, the kinetic curves for the dissolution of copper oxide and sulfide compounds with the participation of the complexing agents are characterized at the initial stage by a very steep rise, followed by a gradual increase in the concentration of copper ions in the solution to equilibrium. Analysis of the graphical shapes of kinetic curves allows us to conclude that the equilibrium value of the concentration of copper ions in solution for the lactate ion is in the range 2.5–3 μmol/l, and for the oxidized derivative of fulvic acid is in the range 3–3.5 μmol/l.

Since the rate of accumulation of products during the dissolution of copper compounds obeys the relations $dc/dt<0$ and $d^2c/dt^2<0$, the processes correspond to a simple chemical reaction with a low order of reaction in the final product, which slowly approaches equilibrium concentrations. Under the considered conditions, the proceeding reaction is heterogeneous, and due to the low dissolution rates of the copper compounds, the interface area can be considered a constant value, and the concentration of the complexing agent in the solution is also maintained at a constant level. Thus, the concentration of the initial substances does not have a decisive influence on the kinetics of the process (that is, they enter the kinetic equation in the form of constants). Formally, the kinetics of the reaction can be described by the reaction product, that is, by the

concentration of copper in the solution, which enters the kinetic equation as the difference between some conditional initial concentration of copper in the solution that is greater than the true equilibrium concentration of copper in the solution:

$$\upsilon = k([Cu]_{init.} - [Cu^{2+}]).$$

When the equation is differentiated, all constants are transformed into a new constant. The linearization of the resulting equation by logarithm gives an array of velocities in the investigated interval (Fig. 12, 13).
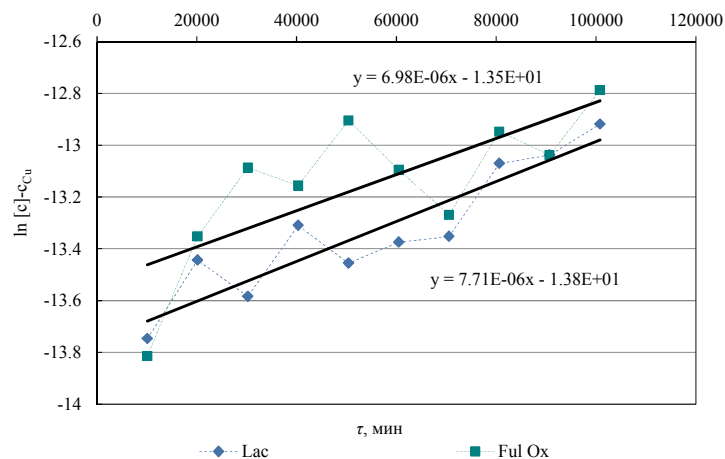
Figure 12. Kinetic equations of lactate ion and oxidized fulvic acid derivative
for copper oxide in logarithmic form
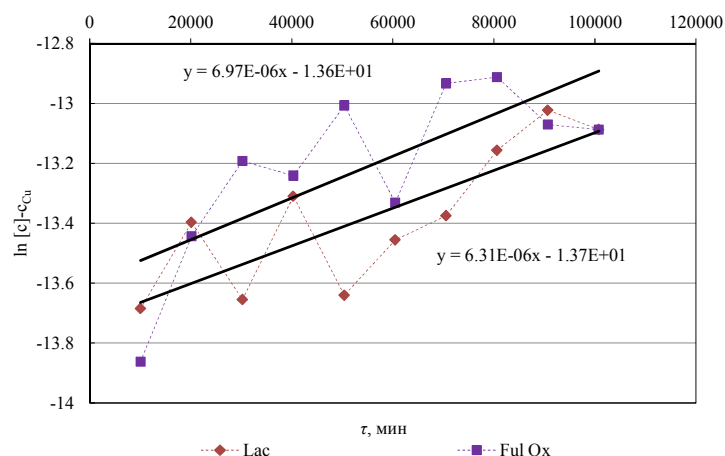
Figure 13. Kinetic equations for the lactate ion and oxidized fulvic acid derivative
for copper sulfide in a logarithmic form

The dependences obtained are satisfactorily described by the equation of a straight line. The rate constant for the reaction involving the oxidized fulvic acid derivative is the same value $1.16 \cdot 10^{-7}$ s^{-1} in both cases, whereas in the lactate-ion reaction the rate constant is $1.28 \cdot 10^{-7}$ s^{-1} for copper oxide and $1.05 \cdot 10^{-7}$ s^{-1} for copper sulfide. Thus, the oxidized derivative of fulvic acid has the same efficiency with respect to oxide and sulfide minerals, and the lactate ion has a somewhat higher efficiency in the case of oxide minerals.

Conclusion

The kinetic curves of the transition of copper ions to the solution under the action of complexing agents are characterized by a relatively small transition period and a rapid yield to the steady-state regime. The absence of an induction period and early attainment of concentrations close to equilibrium indicate a good ability to transfer copper ions to the solution for the selected complexing agents.

The use of chemical modification of chelating agents, as a rule, promoted their effectiveness. Nevertheless, the oxidized humic derivative showed a little lower efficiency than the original sodium humate. In gen-

eral, the investigated complexing agents are placed in following series in accordance with their effectiveness in the case of copper oxide:

Hum Ox < Hum-Na < Ful-H < Hum Sulf < Ful Ox < Lac,
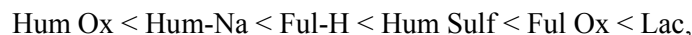
and in the case of copper sulfide:

Hum Ox < Hum-Na < Ful-H < Hum Sulf < Lac < Ful Ox.

For oxide copper minerals, the most effective complexing agent is the lactate ion, and the oxidized derivative of fulvic acid has a little lower efficiency. Less effective agents are the sulfonated humic derivative and the native fulvic acid which have approximately equal effectiveness. The sodium humate and the oxidized humic derivative are least effective agents. In the case of sulfide minerals, the most effective complexing agent is the oxidized derivative of fulvic acid. The lactate ion, the sulfonated humic derivative and the native fulvic acid are a little less effective agents. The sodium humate and the oxidized humic derivative have comparatively low efficiency.

The effectiveness of the complexing agents studied can be given some relative quantitative assessment if it is described their ability to transfer copper ions into solution as compared to the concentration of copper in the solution obtained by passing pure water through the column without the participation of complexing agents. This concentration is 0.15 μmol/l in average. In view of this, the above series can be written for the case of oxide minerals as:

5.6 Hum Ox < 9.1 Hum-Na < 15.1 Ful-H < 15.3 Hum Sulf < 17.6 Ful Ox < 19.6 Lac,
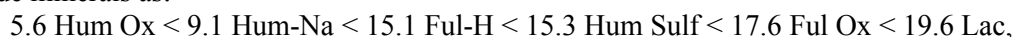
and for the case of sulfide minerals:

4.5 Hum Ox < 6.4 Hum-Na < 14.9 Ful-H < 15.2 Hum Sulf < 16.5 Lac < 22.1 Ful Ox.
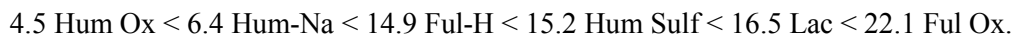
Thus, among studied complexing agents the lactate ion and the oxidized derivative of fulvic acid are the most effective complexants towards both copper oxide and sulfide minerals.

References

1   Woods T.L. Use of oxidized copper minerals as environmental indicators / T.L. Woods, R.M. Garrels // Applied Geochemistry. — 1986. — Vol. 1. — P. 181–187.

2   Sracek O. Geochemistry and mineralogy of Cu and Co in mine tailings at the Copperbelt, Zambia / O. Sracek, M. Mihaljevic, B. Kríbek, V. Majer, F. Veselovsky // Journal of African Earth Sciences. — 2010. — Vol. 57. — P. 14–30.

3   De Putter T. Malachite, an indicator of major Pliocene Cu remobilization in a karstic environment (Katanga, Democratic Republic of Congo) / T. De Putter, F. Mees, S. Decrée, S. Dewaele // Ore Geology Reviews. — 2010. — Vol. 38. — P. 90–100.

4   Yang F. A review of the geological characteristics and geodynamic setting of Late Paleozoic porphyry copper deposits in the Junggar region, Xinjiang Uygur Autonomous Region, Northwest China / F. Yang, J. Mao, F. Pirajno, Sh. Yan, G. Liu, G. Zhou, Zh. Zhang, F. Liu, X. Geng, Ch. Guo // Journal of Asian Earth Sciences. — 2012. — Vol. 49. — P. 80–98.

5   Zheng Y. Geology, fluid inclusion geochemistry, and $^{40}Ar/^{39}Ar$ geochronology of the Wulasigou Cu deposit, and their implications for ore genesis, Altay, Xinjiang, China / Y. Zheng, L. Zhang, Y.-J. Chen, Y.-J. Qin, C.-F. Liu // Ore Geology Reviews. — 2012. — Vol. 49. — P. 128–140.

6   Hazen R.M. Carbon mineral evolution / R.M. Hazen, R.T. Downs, L. Kah, D. Sverjensky // Reviews in Mineralogy & Geochemistry. — 2013. — Vol. 75. — P. 79–107.

7   Seltmann R. Geodynamics and metallogeny of the central Eurasian porphyry and related epithermal mineral systems: A review / R. Seltmann, T.M. Porter, F. Pirajno // Journal of Asian Earth Sciences. — 2014. — Vol. 79. — P. 810–841.

8   Fomin V.N. Thermodynamic parameters of reactions of basic copper carbonates formation with participation of organic complexing agents / V.N. Fomin, I.E. Rozhkovoy, D.B. Gogol, D.L. Ponomarev // Bulletin of the Karaganda University, Chemistry Series. — 2015. — No. 4 (80). — P. 22–26.

9   Fomin V.N. Quantum chemical and thermodynamic calculations of fulvic and humic copper complexes in reactions of malachite and azurite formation / V.N. Fomin, D.B. Gogol, I.E. Rozhkovoy, D.L. Ponomarev // Applied Geochemistry. — 2017. — Vol. 79. — P. 9–16.

10   Марченко З. Фотометрическое определение элементов / З. Марченко. — М.: Мир, 1971. — 502 с.

11   Тарасевич Б.Н. ИК-спектры основных классов органических соединений / Б.Н. Тарасевич. — М.: Изд-во МГУ, 2004. — 55 с.

12   Перминова И.В. Гуминовые вещества в контексте зеленой химии / И.В. Перминова, Д.М. Жилин // Зеленая химия в России / Под ред. В.В. Лунина, П. Тундо, Е.С. Локтевой. — М.: Изд-во МГУ, 2004. — С. 146–162.

Д.Б. Гоголь, И.Е. Рожковой, Д.Л. Пономарев, В.Н. Фомин

Органикалық комплекстүзуші әсерінен тотықты және сульфидті қосылыстардан мыс иондарының ерітіндіге көшу үдерісін зерттеу

Мақалада құрамында 0,02 % оксиді мен сульфиді бар топырақтағы мысты табиғи және химиялық модифицирленген комплекстүзушілердің ерітінділерімен сілтісіздендіру үрдісін зерттеу нәтижелері келтірілген. Грунттың бір үлгісінің жалпы мөлшері 500 г. Комплекстүзуші ерітінділері берілген жылдамдықпен өткізілетін бағаналарға топырақтың үлгілері орналастырылды. Сілтісіздендіргіш агенттер ретінде натрий гуматы, сульфирленген және тотыққан гумин қышқылы, табиғи және тотыққан фульвоқышқыл және натрий лактаты зерттелді. Барлық реагенттердің 0,01 %-дық ерітінділері оксидті және сульфидті қоспалардан мыстың ерітіндіге өтуіне септігін тигізеді. Ең тиімді мысты топырақтан алып шығаруды тотыққан және табиғи фульвоқышқыл мен натрий лактаты көрсетті. Лактат-ион мыстың оксидті минералдары үшін неғұрлым тиімді кешенді түзгіш болып табылады; тотыққан туынды фульвоқышқылының тиімділігі неғұрлым азырақ. Төмен тиімділікке ие агенттер сульфатталған гуматты туынды мен еркін фульвоқышқылы болып табылады, олар тиімділігі бойынша жуықтағанда бірдей. Натрий гуматының белсенділігі баяу, бұл жағдайда тотыққан гуматты туынды неғұрлым аз тиімділікке ие болады. Сульфидті минералдар жағдайында ең тиімді комплекстүзуші болып фульвоқышқылдың тотыққан туындысы табылады. Лактат-ион, сульфатталған гуматты туынды мен еркін фульвоқышқылы тиімділігі неғұрлым төмен агенттер ретінде есептеледі. Натрий гуматы мен тотыққан гуматты туындының тиімділігі салыстырмалы түрде төмен. Кинетикалық мәліметтерді математикалық өңдеу нәтижесінде мысты топырақтардан сілтісіздендіру процестерінің жылдамдықтарының константалары анықталған. Олардың шамалары $1,05 \cdot 10^{-7}$-тен $1,28 \cdot 10^{-7}$ с$^{-1}$ дейін аралығында. Мыстың иондарының ерітіндіге ауысуының кинетикалық қисықтары кешенді түзгіш әсерінен аздаған ауыспалы кезең мен тепе-теңдік күйге жақын концентрацияға жылдам қолжеткізумен сипатталды.

Кілт сөздер: гумин қышқылдары, фульвоқышқылдары, сульфирленген гуминді қышқылдары, тотыққан гуминді қышқылдары, тотыққан фульвоқышқылдары, малахит, минералдар қалыптастыру, мыс шаймалау кинетикасы.

Д.Б. Гоголь, И.Е. Рожковой, Д.Л. Пономарев, В.Н. Фомин

Изучение процессов перехода ионов меди в раствор из оксидных и сульфидных соединений под действием органических комплексообразователей

В статье описаны результаты изучения процесса выщелачивания меди из модельных грунтов, содержащих 0,02 % оксида или сульфида меди, растворами природных и химически модифицированных комплексообразователей. Общее количество одного образца грунта составляло 500 г. Модельные грунты размещались в колонках, через которые с заданной скоростью пропускались растворы комплексообразователей. В качестве выщелачивающих агентов исследованы гумат натрия, сульфированная и окисленная гуминовая кислота, нативная и окисленная фульвокислота, а также лактат натрия. Показано, что растворы всех реагентов с концентрацией 0,01 % вызывают переход меди в раствор как из оксидной, так и из сульфидной смеси. Установлено, что наиболее эффективны для извлечения меди окисленная и нативная фульвокислота и лактат натрия. Для оксидных минералов меди наиболее эффективным комплексообразователем является лактат-ион, окисленное производное фульвокислоты обладает немного меньшей эффективностью. Далее менее эффективными агентами являются сульфированное гуматное производное и свободная фульвокислота, которые приблизительно равны по эффективности. Гумат натрия менее активен, окисленное гуматное производное имеет более низкую эффективность. В случае сульфидных минералов наиболее эффективным комплексообразователем является окисленное производное фульвокислоты. Лактат-ион, сульфированное гуматное производное и свободная фульвокислота являются немного менее эффективными агентами. Гумат натрия и окисленное гуматное производное имеют сравнительно низкую эффективность. Путем математической обработки кинетических данных установлены константы скоростей процессов выщелачивания меди из модельных грунтов. Значения найденных констант находятся в пределах от $1,05 \cdot 10^{-7}$ до $1,28 \cdot 10^{-7}$ с$^{-1}$. Кинетические кривые перехода ионов меди в раствор под действием комплексообразователей характеризуются сравнительно малым переходным периодом и быстрым достижением концентраций, близких к равновесным.

Ключевые слова: гуминовые кислоты, фульвокислота, сульфированные гуминовые кислоты, окисленные гуминовые кислоты, окисленные фульвокислоты, малахит, минералогенез, кинетика выщелачивания меди.

References

1 Woods, T.L., & Garrels, R.M. (1986). *Appl. Geochem.*, *1*, 181–187.

2 Sracek, O., Mihaljevic, M., Kríbek, B., Majer, V., & Veselovsky F. (2010). *J. Afr. Earth Sci.*, *57*, 14–30.

3 De Putter, T., Mees, F., Decrée, S., & Dewaele, S. (2010). *Ore Geol. Rev.*, *38*, 90–100.

4 Yang, F., Mao, J., Pirajno, F., Yan, Sh., Liu, G., & Zhou, et al. (2012). *J. Asian Earth Sci.*, *49*, 80–98.

5 Zheng, Y., Zhang, L., Chen, Y.-J., Qin, Y.-J., & Liu, C.-F. (2012). *Ore Geol. Rev.*, *49*, 128–140.

6 Hazen, R.M., Downs, R.T., Kah, L., & Sverjensky, D. (2013). *Rev. Mineral. Geochem.*, *75*, 79–107.

7 Seltmann, R., Porter, T.M., & Pirajno, F. (2014). *J. Asian Earth Sci.*, *79*, 810–841.

8 Fomin, V.N., Rozhkovoy, I.E., Gogol, D.B., & Ponomarev, D.L. (2015). *Bull. of Karaganda University. Chemistry ser., 4(80)*, 22–26.

9 Fomin, V.N., Gogol, D.B., Rozhkovoy, I.E., & Ponomarev, D.L. (2017). *Appl. Geochem.*, *79*, 9–16.

10 Marczenko, Z. (1971). *Fotometricheskoe opredelenie elementov* [*Photometric determination of elements*]. Moscow: Mir [in Russian].

11 Tarasevich, B.N. (2012). *IK-spektry osnovnykh klassov organicheskikh soedinenii* [*IR spectra of the main classes of organic compounds*], Moscow: MSU Publising [in Russian].

12 Perminova, I.V., & Zhilin, D.M. (2004). Guminovye veshchestva v kontekste zelenoi khimii [Humic substances in the context of green chemistry]. *Zelenaia khimiia v Rossii — Green Chemistry in Russia*. V.V. Lunin, P. Tundo, E.S. Lokteva (Eds.). Moscow: MSU Publising [in Russian].

A.Sh. Kazhikenova, D.B. Alibiyev, E.S. Ibrayeva

Ye.A. Buketov Karaganda State University, Kazakhstan
(E-mail: aigul-kazhikenova@mail.ru)

Efficiency of applying cluster-associated model of viscosity of liquid metals

To describe the viscosity up to the temperature transcendental polynomials with four or five adjustable parameters is often used, which devoid of physical meaning. As it is known, the extrapolation of these approximating dependencies is impossible more than for 25 % of the investigated interval in view unavoidable appearance, it is main characteristic of such polynomials, which are completely contrary to the monotonously decreasing character of the temperature dependence of viscosity. Usually, the experimental points are for the low-temperature region adjacent to the melting point, and especially for high-refractory metals. Meanwhile, the viscosity of each metal strongly depends on the temperature and when it get changed from the melting point to the boiling point decreases about four times. The aim of our research is to develop a generalized cluster-associated model of viscosity of liquid metals based on the concept of chaotized particles according to the degree of clusters association. In this work temperature dependence of viscosity according to the concept of the randomized particles is considered. Models of viscosity dependence on temperature taking into account various maintenance of particles are analysed: crystal-moving, fluid and steam-moving particles. The new cluster model of viscosity temperature dependence allowing to reveal behavior of viscosity in the wide range of temperatures is offered. Applicability of this model on the example of indium fusion is shown.

Keywords: viscosity, chaotized particles, the degree of clusters association, cluster-associated model, liquid metals, reference point, crystal-moving particles, the temperature dependences of the viscosity.

Introduction

In recent years, due to the changing conjunction on the market of non-ferrous and rare earth metals is increasing interest in the study of their physico-chemical properties such as viscosity, plasticity and fusibility and others. In this connection, measurement of physical properties should be considered as a priority of experimental study the structure of real metallic melts.

The melt viscosity is of great practical importance in metal industry. At the same time, the study of the viscosity of molten metal is of great scientific interest, since the viscosity is the most structure-sensitive characteristics of the melt, which gives an idea of the internal forces of interaction of particles.

Expanding the use of liquid metals as working fluids and coolants in nuclear power engineering, chemistry, space technology and other industries, for the needs of metallurgical production and new materials technology make the task of research of their thermal properties, particularly viscosity, urgent. Previous studies found that the temperature dependence of the viscosity is determined by the structure of metals, inter particle connections and interactions between particles [1–3]. This relationship is based on the following theories: theory with effective inter-ion potential; electron theory to the calculation of the generalized pseudo potential; theory based on the methods of quantum chemistry; the theory of quasi-crystalline liquid (Fraenkel equation); semi-empirical model containing two or more adjustable parameters.

Disadvantages of the above theory is that they work in a very narrow temperature range, contain adjustable parameters, which are often no physical meaning. Thus, the main reason for the error correlation temperature dependence of viscosity is that all models of the main studied characteristics (pseudo- or pair potential) either are not changed by increasing temperature, or the models are valid only within a narrow temperature range, thereby not allowing to describe the behavior liquid generally range from melting point to the boiling point, or even to a critical point, ie in the full range of liquid on the basis of continuous change of the status of quasi-crystalline to quasi-gaseous.

The methodology of the research

Employees of the Chemical and Metallurgical Institute J. Abisheva, Doctor of technical sciences, Professor V.P. Malyshev and Doctor of technical sciences A.M. Turdukozhaeva proposed a new approach based on the Boltzmann distribution. According to this approach, all three aggregate states can be viewed from the perspective of subordination Boltzmann distribution and to connect virtually every state with important characteristics of matter on the basis of excess or excess energy barriers melting and boiling. As in all cases con-

sidered particles, differing only in the amount of energy of chaotic motion, then their union and differential display can be described as the concept of chaotized particles [4, 5].

According to the concept of chaotized particles, crystal sliding and steam sliding, liquid sliding particles are present in each of the states of aggregation of matter. However, by increasing temperature, and overcoming various barriers of energy chaotization of ratio of the particles shares changes. Virtual education and the statistical presence of each of the three types of chaotized particles in each aggregate state allows by their balance to determine the role of each species in a particular state of various processes. The authors of the concept of chaotized particles proposed three formulas of temperature dependence of viscosity with the influence of the three classes of chaotized particles. The temperature dependence of the viscosity under the influence of crystal-sliding particle is given by:

$$\nu_1 = \nu_r T_r / T, \tag{1}$$

and formula crystal-sliding and liquid-sliding particles taken into consideration:

$$\nu_2 = \frac{\nu_r T_r \left[\exp\left(-T_m / T_r\right) - \exp\left(-T_b / T_r\right) \right]}{T \left[\exp\left(-T_m / T\right) - \exp\left(-T_b / T\right) \right]}. \tag{2}$$

Under the influence of all the three types of the temperature dependence of the viscosity of the particle is described by the formula:

$$\nu_3 = \frac{\nu_r T_r}{T} \exp\left(\frac{T_m}{T} - \frac{T_m}{T_r} \right). \tag{3}$$

In formulas (1)–(3): T — temperature; T_m — temperature of melting; T_b — temperature of boiling and ν_r, T_r — viscosity and temperature in the reference point.

The proposed equations should be considered as an alternative to existing models of metals viscosity. Extensive testing of these models on the available reference of materials on the viscosity of metal melts allowed to establish the adequacy of the reference data of any of the three species of the proposed models. But the testing necessity of each three models and selecting of the most appropriate complicates the data processing procedure. This made more detailed consider the nature of the liquid state, while remaining within the concept of chaotized particles.

In each of the three states of matter particles chaotized, named crystal, liquid and steam sliding, generally create a more or less orderly set. The concept of chaotized particles based on the virtual presence of each of the three classes of particles in the solid, liquid and gaseous states of matter. Thus, in the solid state, although the crystalsliding particle as a whole and provide along-range order of Communications and stability of the crystal, their presence in the lattice is the exchange with more energy particles–liquid sliding and steam sliding -and there foreshort-lived, the virtual, with ever-changing mosaic of units and vacancies in each cluster formation.

Each individual particle according to the Boltzmann distribution for a short period of time that depends on extremely high frequency vibrations and binary collisions, the order of $10^{12} s^{-1}$, has time to visit all three of its guises. We can say that in the solid state virtually continuously it contains liquid and gaseous state. This virtuality is also characteristic of the liquid and gaseous states, i.e. we can talk about the virtual presence of a solid and gas in the liquid, solid and liquid in gaseous one.

According to the concept of randomized cluster of particles-this is a form of a probability of the existence of various low-energy complexes of the crystal-sliding particles. Calculations of equity and quantitative content of clusters to moles substance at the melting point and boiling point indicate that the concept of randomized particles allows to quantify the formation of clusters with their distribution by number of particles in the fluid at any temperature. The yield on the correlation of viscosity with an average number of particles in a cluster is crucial because it points directly to the lack of considering only the elementary clusters in the case of significant discrepancies with the experimental data on the viscosity. Probably a strong dependence on the temperature, in addition to the diluting effect of liquid sliding and steam sliding particles can be explained by the formation of associated or aggregated elementary clusters, the destruction of which with the temperature rising occur in parallel with the destruction of elementary clusters, which creates the effect of a stronger influence of temperature on the viscosity in the case of the formation of such associations or aggregates.

Therefore, we believe it is necessary to strengthen the fragment (T_r/T) the basic model (1) by raising the probability of an elementary event equal to the number of colliding particles:

$$\nu = \nu_r \left(T_r / T \right)^a. \tag{4}$$

Here indicator a association degree It makes sense to measure a degree n—particle clusters.

A detailed theoretical study of the temperature dependence of viscosity model of liquid metal according to the degree of association of clusters is given in works [4, 5].

The results of research

To pre-test of the applicability for justifying the generalized semi-empirical model of the viscosity of liquid metals on the concept of randomized particles we used well-known experimental and approximation data.

Recieved more generalized form of the temperature dependence of the viscosity can be used to calculate the activation energy of the viscous flow of the melt in combination with Fraenkel equation which is derived for the dynamic viscosity:

$$\eta = A \exp\left(\frac{U}{RT}\right). \qquad (5)$$

Here A and U are respectively constant pre-exponential factor and the activation energy of viscous flow, the meaning of which is interpreted by different authors, depending on the intended nature of the interparticle interaction and quasi-crystalline structure of a liquid [6].

As the kinematic viscosity is related to the dynamic viscosity of the formula $\nu = \eta/\rho$ (ρ — melt density), then, because of the very weak dependence of density on temperature, can be directly replaced in the equation (5) η to ν, respectively, adjusting the parameters A and U by A' and E_a:

$$\nu = A' \exp\left(\frac{E_a}{RT}\right).$$

It should be noted that although the selection of the reference point is not critical, it expedient to fix near (but not at) crystallization, as at lower temperatures, the viscosity is determined more reliably and has the highest value. In the crystallization point itself because of the possible presence of an unspecified number of the equilibrium solid phase viscosity of the emulsion will be inflated against viscosity of the pure liquid state.

Here is the applicability of the proposed model by calculating the viscosity of indium. Indium [6] shows the values of $T_m = 429,56K$ and $T_b = 2273-2373K$ (average 2323 K). It also contains data on the kinematic viscosity, which compared with calculated by model $\nu(1)$–$\nu(4)$ (see Table 1, Fig.). The reference point is a point with $T_r = 443K$ and $\nu_r = 2,433 \cdot 10^{-7}$ m^2/s.

T a b l e 1

Comparison of experimental [6] and calculated by models $\nu(1)$–$\nu(4)$ data
by the kinematic viscosity of indium, $\nu \cdot 10^7$, m^2/s

T	ν(exp)	$\nu(1)$	$\nu(2)$	$\nu(3)$	a	$\nu(4)$
$T_m = 429.6$	–	2.509	2.582	2.586	–	2.506
443	2.433	2.433	2.433	2.433	–	2.433
573	1.809	1.881	1.545	1.510	1.152	1.901
673	1.542	1.602	1.206	1.150	1.091	1.629
773	1.392	1.394	0.995	0.922	1.003	1.427
873	1.288	1.235	0.853	0.766	0.938	1.270
973	1.203	1.108	0.751	0.653	0.895	1.144
1073	1.142	1.004	0.676	0.568	0.855	1.042
1273	1.069	0.847	0.573	0.450	0.779	0.884
$T_b = 2323$	–	0.464	0.374	0.212	–	0.497
R	–	0.981	0.143	< 0	–	0.986

The average value of $\bar{a} = 0,96$. Although India has a sufficient amount of experimental data, $\bar{a} < 1$ due to the fact that it is a chemical analog of gallium and has good fluidity. The homogeneity of the received set for a followed by Nalimov criterion: $S(x) = 0,405$; $r_{\min}^{\max} = 0,514 < r_{cr} = 2,004$.
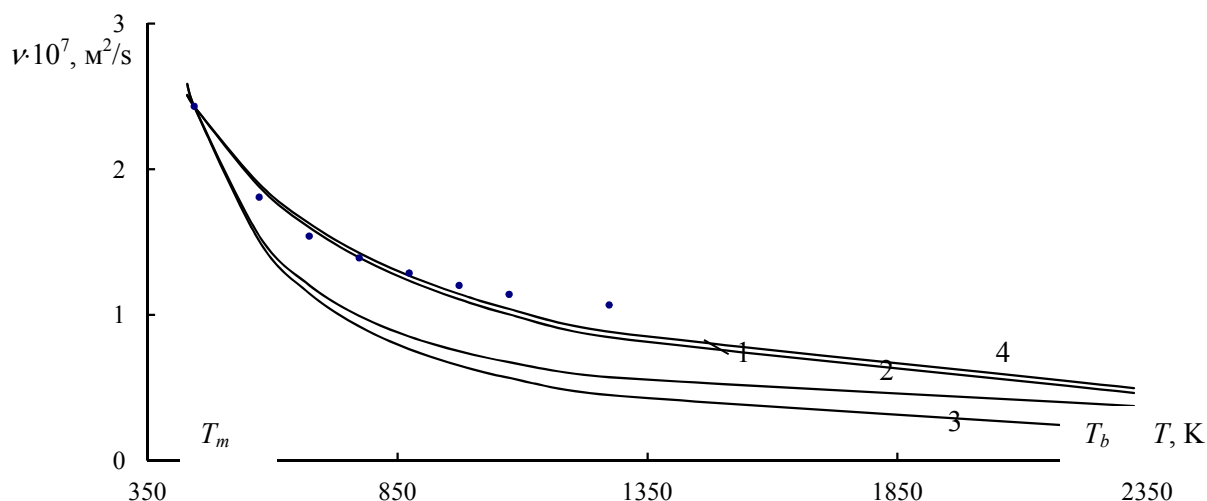
ν — the kinematic viscosity; *T* — temperature; points — experimental data [6];
1 — model (1); *2* — according to (2); *3* — to (3); *4* — to (4)

Figure. Dependence of kinematic viscosity of indium on temperature

Given the degree of association with the cluster reference point in the model (4) can be used as a generalized model indium melt viscosity in the complete range of temperatures near the melting temperature of $T_r = 443 K$ on the kinematic viscosity

$$\nu = 8{,}389 \cdot 10^{-5} / T^{0{,}96} \pm 3{,}06 \cdot 10^{-9}, \text{ m}^2/\text{s}.$$

In this temperature range is calculated activation energy $E_a = 4681$ J/mol , and a generalized model for the activation energy $E_a^{\prime} = 5629$ J/mol .

By the results of comparing the most appropriate are the first and fourth models. The correlation coefficients are respectively 0,981 and 0,986. As can be seen, for the calculation of indium viscosity it is enough to apply the model of general form (4).

Thus, the analysis of these models showed that the generalized model which took into account the degree of association of clusters viscosity molten metal is comparable with the temperature dependence of viscosity based on different content crystal sliding, liquid sliding and steam sliding particles has a high correlation coefficient, and is sufficient to describe the full range from the melting point to boiling point.

The discussion of the results

The new semi-empirical model of viscosity was tested for 28 common metals for which there are reference data about viscosity. With given the degree of association of clusters as the melt viscosity of the generalized model in a full range of temperatures from the melting point T_m till the boiling temperature T_b is possible to use the model (4) from the reference point ν_r and T_r by kinematic viscosity of metal with finding a confidence interval and rounding. These equations are shown in Table 2.

T a b l e 2

The equations of kinematic viscosity of metals

Metal	$T_m,$ K	$T_r,$ K	$\nu_r \cdot 10^7,$ m^2/s	Equation of kinematic viscosity
1	2	3	4	5
Lithium	453.7	500	10.285	$\nu = \left(0.561 \cdot 10^{-3} / T^{1.01} \right) \pm 3.14 \cdot 10^{-9}$
Sodium	371	400	6.603	$\nu = \left(0.216 \cdot 10^{-2} / T^{1.351} \right) \pm 2.74 \cdot 10^{-8}$
Kalium	336.71	350	6.175	$\nu = \left(0.792 \cdot 10^{-3} / T^{1.22} \right) \pm 2.78 \cdot 10^{-9}$
Cuprum	1356	1438	4.85	$\nu = \left(0.080 / T^{1.65} \right) \pm 8.02 \cdot 10^{-9}$

1	2	3	4	5
Rubidium	312.7	350	3.675	$\nu = \left(0.479 \cdot 10^{-3} / T^{1.22}\right) \pm 1.66 \cdot 10^{-9}$
Argentum	1235	1293	3.98	$\nu = \left(0.183 / T^{1.82}\right) \pm 1.57 \cdot 10^{-9}$
Caesium	301.6	350	2.913	$\nu = \left(0.305 \cdot 10^{-3} / T^{1.19}\right) \pm 1.95 \cdot 10^{-9}$
Aurum	1337.59	1336	3.11	$\nu = \left(0.963 \cdot 10^{-2} / T^{1.44}\right) \pm 2.65 \cdot 10^{-9}$
Beryllium	1560	1570	3.494	$\nu = \left(0.864 \cdot 10^{24} / T^{9.51}\right) \pm 0.2$
Magnesium	923	973	7.01	$\nu = \left(0.337 \cdot 10^{2} / T^{2.57}\right) \pm 4.47 \cdot 10^{-9}$
Calcium	1125	1173	10.81	$\nu = \left(0.152 / T^{1.68}\right) \pm 1.37 \cdot 10^{-8}$
Strontium	1043	1073	8.149	$\nu = \left(1.010 / T^{2.01}\right) \pm 3.62 \cdot 10^{-9}$
Barium	983	1073	4.564	$\nu = \left(0.025 / T^{1.56}\right) \pm 1.68 \cdot 10^{-9}$
Zinc	692.7	698	4.5	$\nu = \left(0.117 / T^{1.90}\right) \pm 3.59 \cdot 10^{-9}$
Cadmium	594	603	1.374	$\nu = \left(1.360 \cdot 10^{-2} / T^{1.80}\right) \pm 1.21 \cdot 10^{-9}$
Mercury	234.27	273	1.239	$\nu = \left(0.192 \cdot 10^{-6} / T^{0.90}\right) \pm 1.59 \cdot 10^{-9}$
Aluminium	933.4	973	4.75	$\nu = \left(5.845 \cdot 10^{-4} / T^{1.03}\right) \pm 1.82 \cdot 10^{-11}$
Gallium	302.92	326	3.11	$\nu = \left(6.091 \cdot 10^{-5} / T^{0.91}\right) \pm 3.56 \cdot 10^{-9}$
Indium	429.56	443	2.433	$\nu = \left(8.389 \cdot 10^{-5} / T^{0.96}\right) \pm 3.06 \cdot 10^{-9}$
Thallium	576	579.2	2.328	$\nu = \left(1.001 / T^{1.32}\right) \pm 2.63 \cdot 10^{-9}$
Germanium	1211.41	1218	1.35	$\nu = \left(62.4 / T^{2.81}\right) \pm 7.09 \cdot 10^{-9}$
Tin	505	573	2.23	$\nu = \left(0.102 \cdot 10^{-3} / T^{0.97}\right) \pm 1.56 \cdot 10^{-9}$
Lead	600.6	648	2.05	$\nu = \left(0.341 \cdot 10^{-4} / T^{0.79}\right) \pm 5.75 \cdot 10^{-10}$
Bismuth	544.2	548	1.95	$\nu = \left(1.005 \cdot 10^{-3} / T^{1.36}\right) \pm 1.21 \cdot 10^{-9}$
Tellrium	723.11	733	3.57	$\nu = \left(31.17 / T^{2.77}\right) \pm 0.18 \cdot 10^{-7}$
Ferrum	1811	1838	4.56	$\nu = \left(1.586 \cdot 10^{5} / T^{3.54}\right) \pm 1.86 \cdot 10^{-9}$
Cobalt	1767	1777	7.39	$\nu = \left(5.962 \cdot 10^{3} / T^{3.05}\right) \pm 3.55 \cdot 10^{-9}$
Nickel	1728	1803	6.09	$\nu = \left(1.070 / T^{1.92}\right) \pm 5.98 \cdot 10^{-10}$

5 metals (gallium, indium, tin, lead and mercury) have a mean value $\bar{a} < 1$, when the main cause of it is the capability in supercooling at lower crystallization remain liquid. So gallium is able to remain liquid till –40 ºC (233 K), indium is a chemical analogue of gallium and has good fluidity, tin and lead, also remain liquid at supercooling and mercury — only metal which is liquid in the standard state, has a melting point –38.9 ºC.

Conclusions

1. A new semi-empirical model of viscosity tested on 28 common metals for which there are reference data on the temperature dependence of viscosity. In most cases, generalized model describes the temperature dependence of the viscosity more adequately comparing with the experimental data than previously proposed three alternative models.

2. Obtained high values of correlation coefficients for the proposed model points to its functional characteristics. On this basis there were recommended calculated dependence for each metal.

3. For 5 metals (gallium, indium, tin, lead and mercury) received average meaning $\bar{a} < 1$, which explains their tendency to remain in the supercooling in the liquid state.

References

1 Вертман А.А. К проблеме металлических расплавов / А.А. Вертман // Фундаментальные исследования физикохимии металлических расплавов. Памяти академика А.М. Самарина. — М.: РКЦ «Академкнига», 2001. — 209 с.

2 Herwig F. Eine Schwingtiegelapparatur zur Bestimmung der Viskosität von Flüssigkeiten bei hohen Temperaturen / F. Herwig, M. Wobst // Metallik. — 1991. — Vol. 82, No. 12. — S. 913–916.

3 Bettezzati L. The viscosity of liquid metals and alloys / L. Bettezzati, A. Greer // Acta met. — 1989. — Vol. 37, No. 7. — P. 1791–1802.

4 Малышев В.П. Вязкость расплавов по концепции хаотизированных частиц / В.П. Малышев, А.М. Турдукожаева, А.Ш. Кажикенова // Тяжелое машиностроение. — 2009. — № 6. — С. 37–39.

5 Турдукожаева А.М. Вязкость жидких металлов с учетом природы вещества по концепции хаотизированных частиц / А.М. Турдукожаева, В.П. Малышев, А.Ш. Кажикенова // Новости науки Казахстана. — 2010. — № 2. — С. 32–35.

6 Свойства элементов: Справ. изд.: в 2 кн. Кн. 1 / Под ред. М.Е. Дрица. —3-е изд., перераб. и доп. — М.: Руда и металлы, 2003. — С. 448.

А.Ш. Қажикенова, Д.Б. Әлібиев, Э.С. Ибраева

Тұтқыр сұйық металға кластерлі-ассоциативті модельді қолданудың тиімділігі

Сұйық металдарды ядролық энергетика, химия, космостық техника және өндірістің басқа да салаларында металлургиялық өнеркәсіптің қажеттілігі және заттардың жаңа технологиялары үшін жұмыс денелері мен жылу тасығыштары ретінде қолдану аймақтарының кеңеюі олардың жылу физикалық қасиеттерін, оның ішінде тұтқырлығын зерттеу мәселесінің өзектілігін айқындайды. Температураға байланысты тұтқырлықты сипаттау үшін физикалық мағынасын жоғалтатын төрт-бес жуықтау параметрлері бар трансцендентті полиномдарды қолданады. Осындай аппроксимациялық тәуелділіктерді зерттеген аралықтан оның 25 % артық шамаға экстраполяциялау мүмкін емес екені белгілі. Себебі ондай полиномдарға тән экстремалдылықтардың шығуы мүмкін болады, ал олар тұтқырлықтың температуралық тәуелділігінің біркалыпты кемімелі сипатына қайшы келеді. Әдетте, тәжірибелік нүктелер, әсіресе қиын балқитын және жоғары температурада қайнайтын металдар үшін, балқу нүктесіне түйісетін төменгі температуралық аймақтарға қатысты. Оған қоса әр металдың тұтқырлығы температураға өте тәуелді, сондықтан оның балқу нүктесінен қайнау нүктесіне дейінгі аралықта өзгеру барысында жуықтап алғанда төрт есеге азаяды. Баяндамада байлыныскан кластерлердің сұйық балқымаларға әсер ету деңгейін ескеретін, сұйық металдардың тұтқырлығын есептейтін жалпы модель келтірілген. Кристалданған бөлшектердің біркелкі моделінің сұйық күйіндегі элементарлық кластерінің балқыған металдың температуралық тұтқырлығының тәуелділігі анықталған. Тұтқырлықтың температурадан тәуелділігінің жалпыланған формасы металл ерітіндісінің ағын энергиясының құлшынысын санауға Френкель теңдеуімен бірге қолданылған. Жаңа жартылай эмпирикалық үлгісі тұтқырлық пен температура арасында тәуелділігі анықтамалық индий ерітіндісі арқылы көрсетілген. Ұсынылып отырған модель бойынша есептелген сұйық индий тұтқырлығының салыстырмалы нәтижесі берілген.

Кілт сөздер: тұтқырлық, ретсізделген бөлшектер, ассоцирленген кластердің дәрежесі, кластерлі-ассоциативті моделі, сұйық металдар, реперлік нүкте, кристалқозғалысты бөлшектер, тұтқырлықтың температураға тәуелділігі.

А.Ш. Кажикенова, Д.Б. Алибиев, Э.С. Ибраева

Эффективность применения кластерно-ассоциатной модели кинематической вязкости жидких металлов

Расширение областей использования жидких металлов в качестве рабочих тел и теплоносителей в ядерной энергетике, химии, космической технике и других отраслях промышленности, для потребности металлургического производства и новых технологий материалов делают задачу исследования их теплофизических свойств, и в частности вязкости, актуальной. Для описания вязкости в зависимости от температуры часто используют трансцендентные полиномы с четырьмя-пятью подгоночными параметрами, лишенными физического смысла. Как известно, экстраполяция подобных аппроксимирующих зависимостей невозможна более чем на 25 % от изученного интервала ввиду неизбежных проявлений экстремальностей, характерных для таких полиномов, которые полностью противоречат монотонно убывающему характеру температурной зависимости вязкости. Как правило, экспериментальные точки относятся к низкотемпературной области, примыкающей к точке плавления, особенно

для тугоплавких и высококипящих металлов. Между тем вязкость каждого металла сильно зависит от температуры и при ее изменении от точки плавления до точки кипения уменьшается приблизительно в четыре раза. Целью нашего исследования является разработка кластерно-ассоциатной модели вязкости жидких металлов на основе концепции хаотизированных частиц в зависимости от степени ассоциации кластеров. В статье рассмотрена температурная зависимость вязкости согласно концепции хаотизированных частиц. Проанализированы модели зависимости вязкости от температуры с учетом различного содержания частиц: кристаллоподвижных, жидкоподвижных и пароподвижных частиц. Предложена новая кластерная модель температурной зависимости вязкости, позволяющая выявить поведение вязкости в широком диапазоне температур. Показана применимость данной модели на примере расплава индия.

Ключевые слова: вязкость, хаотизированные частицы, степень ассоциированности кластеров, кластерно-ассоциатная модель, жидкие металлы, реперная точка, кристаллоподвижные частицы, температурная зависимость вязкости.

References

1   Vertman, A.A. (2001). K probleme metallicheskih rasplavov [On the problem of metal melts]. *Fundamentalnye issledovaniia fizikohimii metallicheskih rasplavov. Pamiati akademika A.M. Samarina — Fundamental studies of physical chemistry of metal melts. In memory of Academician A.M. Samarin*. Moscow: Akademkniga [in Russian].

2   Herwig, F., & Wobst, M. (1991). Eine Schwingtiegelapparatur zur Bestimmung der Viskosität von Flüssigkeiten bei hohen Temperaturen. *Metallik, 82, 12*, 913–916.

3   Bettezzati, L., & Greer, A. (1989). The viscosity of liquid metals and alloys. *Acta met., 37, 7,* 1791–1802.

4   Malyshev, V.P., Turdukozhaeva, A.M., & Kazhikenova, A.Sh. (2009). Viazkost rasplavov po konceptsii haotizirovannyh chastits [The viscosity of liquid metals based on the nature of the substance of the concept of randomized particles]. *Tiazheloe mashinostroenie — Heavy Engineering, 6*, 37–39 [in Russian].

5   Turdukozhaeva, A.M., Malyshev, V.P., & Kazhikenova, A.Sh. (2010). Viazkost zhidkih metallov s uchetom prirody veshhestva po konceptsii haotizirovannyh chastits [The viscosity of liquid metals based on the nature of the substance of the concept of randomized particles]. *Novosti nauki Kazakhstana — News of Kazakhstan science, 2*, 32–35 [in Russian].

6   Drits, M.E. (Eds.). (2003). *Svoistva elementov [The properties of the elements]*. (In 2 books. Book 1. 3d ed.). Moscow: Ruda i Metally [in Russian].

UDC 544.46+665.75+662.7

G.R. Nyssanbayeva[1], K.K. Kudaibergenov[1], Ye.K. Ongarbayev[1], Z.A. Mansurov[1,2]

[1]Al-Farabi Kazakh National University, Almaty, Kazakhstan;
[2]Institute of Combustion Problems, Almaty, Kazakhstan
(E-mail: gulnur.83.29@mail.ru)

Obtaining expanded graphite by heat treatment

One of the promising materials of the 21st century is expanded graphite or thermally expanded graphite. The preparation of nanostructure and thermally expanded graphite with improved specific surface, bulk density and expansion along the trigonal axis of the graphite matrix is associated with the thermal shock of intercalated graphite The general principle of these methods is the introduction into graphite of either gaseous substances or compounds that, during thermal heating of the intercalated compound of graphite or their derivatives, transform into a gaseous state and there by create an intralayer pressure that expands the graphite particle. In the given work thermally expanded graphite, obtained during the heat treatment crystalline hydrates of metals and nature graphite obtain expanded graphite material. The expanded graphite obtained was used as a sorbent. The performed studies in this work demonstrated the potential use of the sorbents as adsorbents for the removal of thin oil films. In this paper, it can be seen that the optimum mixture ratio of graphite to other contents (graphite : $Zn(NO_3)_2 \times 6H_2O$: graphite : $FeCl_3 \times 6H_2O$) is 2(g) : 8(g) : 2(g) : 8(g), which obtained the best expansion volume. Here, we propose a simple, effective method to prepare expanded graphite in which the intercalation and expansion of graphite are realized by only one step not involving any sophisticated devices.

Keywords: graphite, expanded graphite, intercalated graphite compound, thermally expanded graphite.

Introduction

In the recent decades expanded graphite (EG) has been one of the major interesting research subjects because of nanostructure. Obtained expanded graphite by heat thermal shock is a low-density carbon material, and it used as a base for sealing and fire-retardant materials. Expanded graphite is a promising material for high temperature. Physicochemical properties of expanded graphite depend from a graphite synthesis condition. While thermal characteristics of EG obtained by the thermal shock of convenient graphite intercalation compounds or their hydrolyzates are well studied [1, 2] the characteristics of EG obtained by thermal shock are scarcely investigated. The synthesis of EG describe through the heat treatment of oxidized graphite and the investigation of thermal properties. The general principle consists in introduction natural graphite of compounds of salts at thermal heat [3, 4].

Experimental part

In this work were used native graphite and crystalline hydrates of metals. The graphite from the Zavalye Graphite Plant (Ukraine) is a large-scaly natural graphite subjected to chemical burning under industrial conditions. The result is achieved by mechanical mixing of powder of initial graphite by the making foam agent by salts of metals for training of porous structure, taken in the quantity of 20–80 % of the mass of mix. The experiment proceeds in two stages: 1) mixing of graphite with salts of metals; 2) and heating of components at a temperature of 350–1000 °C. The mix heats up 5–10 minutes. All process of activation takes from 10 to 20 minutes. In Figure 1 shows scheme of obtaining synthesis of thermally expanded graphite.
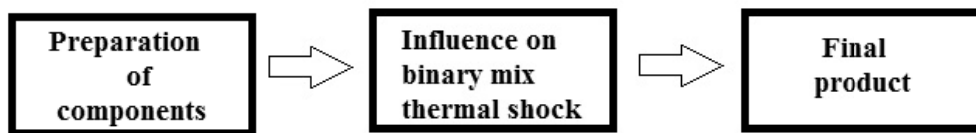
Figure 1. Scheme of the technology of synthesis of the interconnected graphite

Results and their discussion

The single most striking observation to emerge from the comparison, it was formation of the homogeneous melted bubbling mass. After end of this stage there is a sharp foaming of graphite which is followed by allocation of insignificant amount of brown gas (Fig. 2).
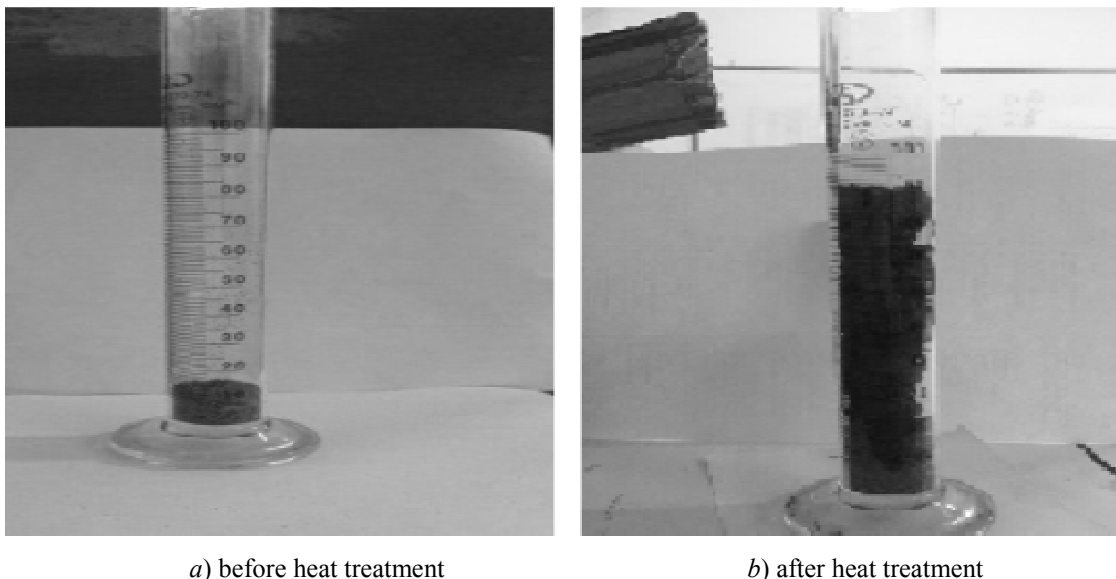

a) before heat treatment   *b*) after heat treatment

Figure 2. Formation of the homogeneous melted bubbling mass

In Table shown main sorption properties of thermally expanded graphite.

T a b l e

Main sorption properties of structure

System «graphite — salt»	Oil capacity, g/g	Water absorption, g/g	Buoyancy, %
Graphite — $FeCl_3 \times 6H_2O$	20	0,5	80
Graphite — $Zn(NO_3)_2 \times 6H_2O$	25	0,1	99

In Table shown that the structure «graphite — $Zn(NO_3)_2 \times 6H_2O$» differs in smaller water absorption, than «graphite — $FeCl_3 \times 6H_2O$». Results of an experiment shown that the reagent structure «graphite — $Zn(NO_3)_2 \times 6H_2O$» adsorbs 25 g of heavy oil.

In details, the mass percent of oxygen in natural graphite increased from 5 to 10 %, the content of carbon decreased from 95 to 46 %. It can be explained with the fact that increased of the temperature causes thermal decomposition of crystalline hydrate in reagent structure, therefore, the relative content of oxygen increases. Qualitative analyses of reagent structures are submitted in the Figure 3.

Figure 4 shows SEM images of the EG samples. The morphology of the EG samples is wormlike and there are a lot of pores that can also be observed on the surface. It is the particular loose and porous structures that would provide EG samples with good adsorption property for the macromolecular compounds.
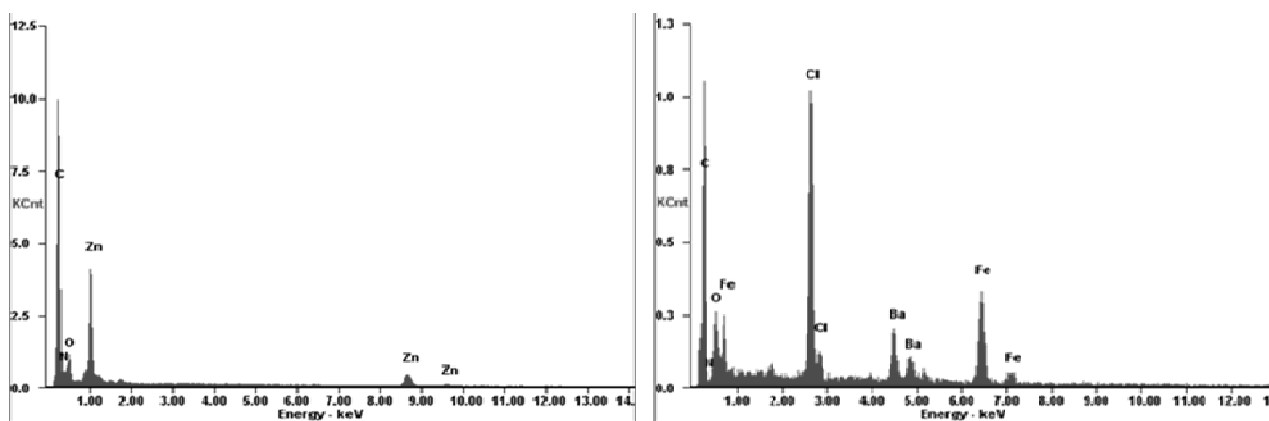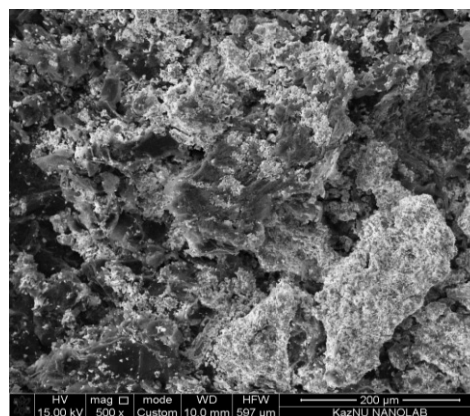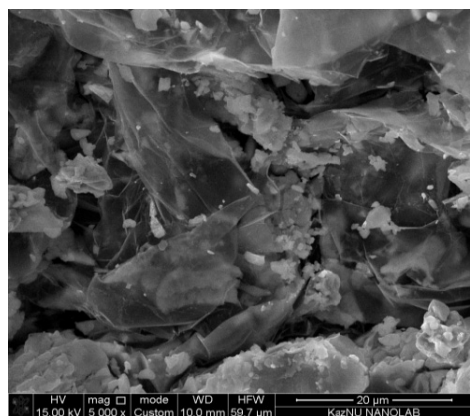
Graphite — $Zn(NO_3)_2 \times 6H_2O$ Graphite — $FeCl_3 \times 6H_2O$

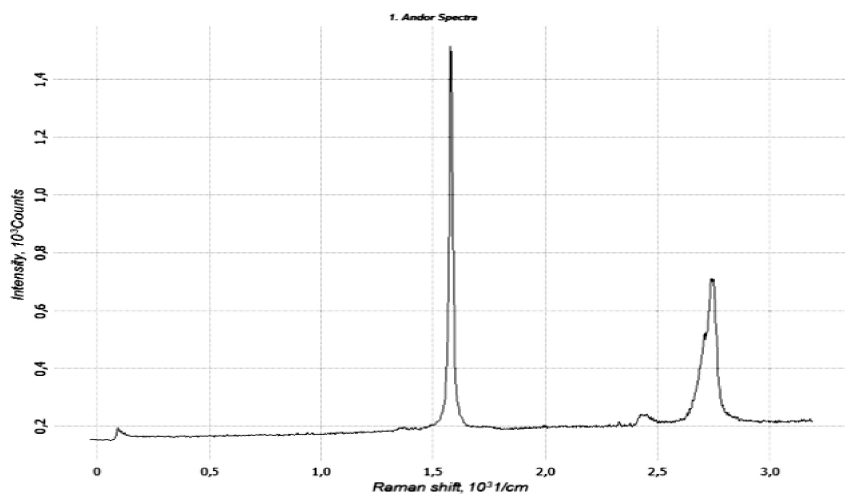Figure 3. Elemental composition of the thermally expanded graphite using SEM/EDAX
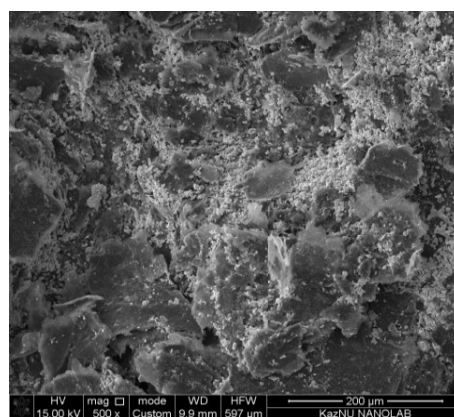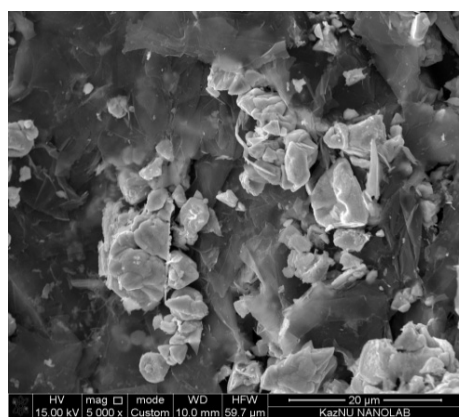
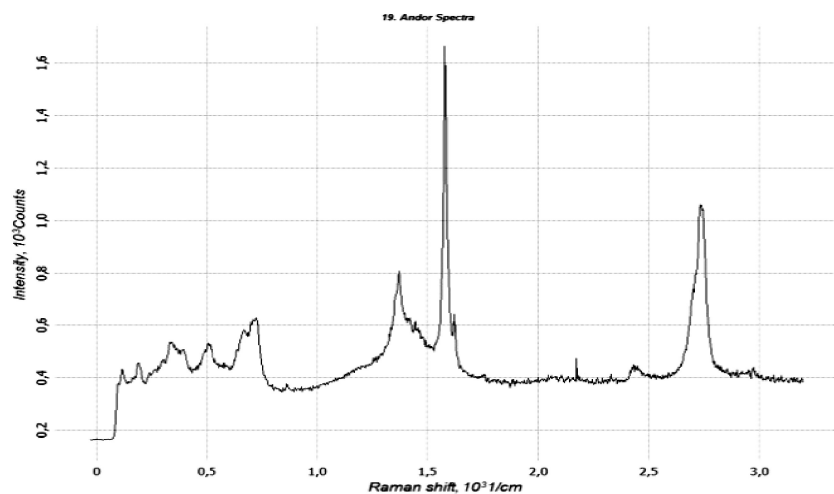*a*) graphite — $Zn(NO_3)_2 \times 6H_2O$

b) graphite — $FeCl_3 \times 6H_2O$

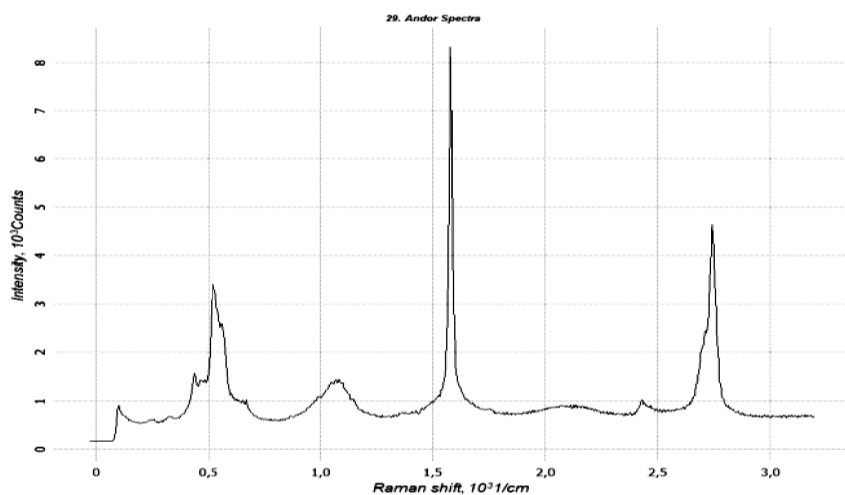Figure 4. (*a*) and (*b*) show the surface morphology of the expanded graphite

Produced samples were also investigated by Raman spectroscopy. As shown in Figure 5, the spectra that all samples have carbon structure.

a)

b)

c)

Figure 5. Raman spectra of natural graphite (*a*), graphite impregnated with salts (*b*, *c*)

In the Figure 6 it is shown oil sorption of TEG in laboratory conditions.

Figure 6. Oil sorption of TEG in laboratory conditions

At the beginning, on the surface of oil a small amount of flammable liquid is sprayed, then fire. During burning of oil we scatter a sorbent on the surface of the poured oil or it is possible to scatter before oil burning, and then to burn out oil. At the combustion of oil porous graphite is formed and in a few minutes there is a full adsorption of oil product.

Conclusions

In this work were to obtain expanded graphite by heat treatment. Morphology of expanded graphite was verified by scanning electron microscopy analysis. Expanded graphite shown outstanding adsorption performance for oil.

References

1   Сорокина Н.Е. Интеркалированные соединения графита акцепторного типа и новые углеродные материалы на их основе: обзор / Н.Е. Сорокина, И.В. Никольская, С.Г. Ионов, В.В. Авдеев // Изв. РАН. Сер. хим. — 2005. — Т. 54, № 8. — С. 1699–1716.

2   Toyoda M. Sorption and recovery of heavy oil by using exfoliated graphite / M. Toyoda, J. Aizawa, M. Inagaki // Desalination. — 1998. — Vol. 4, No. 115. — P. 199–201.

3   Сорокина Н.Е. Композиционные наноматериалы на основе интеркалированного графита: учеб. пособие / Н.Е. Сорокина, В.В. Авдеев. — М.: Изд-во МГУ, 2010. — 100 с.

4   Parvez K. Exfoliation of Graphite into Graphene in Aqueous Solutions of Inorganic Salts / K. Parvez, Z.S. Wu, R. Li, X. Liu, R. Graf, X. Feng, K. Müllen // J. Am. Chem. Soc. — 2014. — Vol. 136, No. 16. — P. 6083–6091. DOI:10.1021/ja5017156.

Г.Р. Нысанбаева, К.К. Кудайбергенов, Е.К. Онгарбаев, З.А. Мансуров

Термиялық өңдеу жолымен кеңейтілген графит алу

ХХІ ғасырда болашағы бар материалдардың бірі кеңейтілген графит, немесе термиялық кеңейтілген графит, болып табылады. Жоғары көрсеткішті беттік ауданы, графит матрицасындағы тригоналды осіндегі кеңейтілген дәрежедегі және сусымалы тығыздығы жоғары наноқұрылымды термокеңейтілген графит алу, әдісінің жалпы қағидасы графитті термиялық қыздыру барысында газ тәрізді немесе қосылысты материалдарды кеңейтілген графиттің ішкі қабаттарына енгізу болып табылады. Мақалада металдың кристалдық гидраттарын және табиғи графитті термиялық өңдеу барысында

термикалық кеңейтілген графит материалын алуға болатындығы айтылған. Алынған кеңейтілген графит сорбент ретінде пайдаланылды. Мұнда графиттің тұздармен қосылысы келесідей (графит : $Zn(NO_3)_2 \times 6H_2O$; графит : $FeCl_3 \times 6H_2O$) 2(г) : 8(г) , 2 (г) : 8 (г), осы қатынастар жақсы кеңейту көлемін алды. Біз кеңейтілген графитті алудың қандай да бір күрделі құрылғыларды қажет етпейтін, бір қадаммен жүзеге асырылатын, қарапайым әрі тиімді әдісін ұсындық.

Кілт сөздер: графит, кеңейтілген графит, интеркалирленген графит, термокеңейтілген графит.

Г.Р. Нысанбаева, К.К. Кудайбергенов, Е.К. Онгарбаев, З.А. Мансуров

Получение расширенного графита путем термической обработки

Одним из перспективных материалов XXI века является пенографит, или терморасширенный графит. Общий принцип получения наноструктурированного терморасширенного графита с улучшенными показателями удельной поверхности, насыпной плотности и степени расширения вдоль тригональной оси графитовой матрицы термического удара интеркалированного графита заключается во внедрении в графит газообразных веществ или соединений, которые переходят в газообразное состояние при термическом нагревании интеркалированного графита или его производных и тем самым создают внутрислоевое давление, расширяющее графитовую частицу. В статье термически вспененный графит получен термообработкой кристаллогидратов металлов и природного графита. Полученный расширенный графит использовали в качестве сорбента. Исследования показали возможность потенциального использования сорбента для удаления тонких масляных пленок. Показано, что оптимальным соотношением компонентов, при котором получен наилучший объем расширения, является: графит : $Zn(NO_3)_2 \times 6H_2O = 2$(г) : 8(г); графит : $FeCl_3 \times 6H_2O = 2$(г) : 8(г). Авторами предложен простой и эффективный способ получения вспененного графита, при котором расширение графита реализуется в одну стадию.

Ключевые слова: графит, расширенный графит, интеркалированное соединение графита, терморасширенный графит.

References

1   Sorokina, N.E., Nikolskaya, I.V., Ionov, S.G., & Avdeev, V.V. (2005). Interkalirovannye soedineniia hrafita aktseptornoho tipa i novye uhlerodnye materialy na ikh osnove [Compounds of graphite of acceptor type and new carbon materials on their basis]. *Izvestiia RAN. Seriia khimiia — Russian Chemical Bulletin, 54, 8*, 1699–1716 [in Russian].

2   Toyoda, M., Aizawa, J., & Inagaki, M. (1998). Sorption and recovery of heavy oil by using exfoliated graphite. *Desalination*, *4, 115,* 199–201.

3   Sorokina, N.E., & Avdeev, V.V. (2010). *Kompozitsionnye nanomaterialy na ocnove interkalirovannoho hrafita [The composite of nanomaterials on a basis intercalated graphite]*. Moscow: MSU Publishing [in Russian].

4   Parvez, K., Wu, Z.S., Li, R., Liu, X., Graf, R., & Feng, X., et al. (2014). Exfoliation of Graphite into Graphene in Aqueous Solutions of Inorganic Salts. *J. Am. Chem. Soc.*, 136, 6083–6091.

ХИМИЯЛЫҚ ТЕХНОЛОГИЯ
ХИМИЧЕСКАЯ ТЕХНОЛОГИЯ
CHEMICAL TECHNOLOGY

M.U. Nurkassimova[1], A.K. Tashenov[1], N.M. Omarova[1], S.V. Morzhuhina[2]

[1]L.N. Gumilyov Eurasian National University, Astana, Kazakhstan;
[2]Dubna State University, Moscow region, Russia
(E-mail: maha.bilan@mail.ru)

Biomonitoring of atmospheric depositions of heavy metals and radionuclides in Irtysh areas of Kazakhstan

This article aims to analyze the data obtained by researching the atmospheric depositions of heavy metals and radionuclides in Irtysh areas of Kazakhstan using the method of moss-biomonitors. This method was applied for the Northeastern and Eastern parts of the Republic of Kazakhstan to assess the environmental situation in these regions. The thirty moss samples were collected in autumn and summer of 2015–2016 growth periods. A total of 42 elements (Na, Mg, Al, Cl, K, Ca, Sc, Ti, V, Cr, Mn, Fe, Ni, Co, Zn, As, Se, Br, Rb, Sr, Zr, Nb, Mo, Ag, Cd, Sb, Ba, La, Ce, Nd, Sm, Eu, Gd, Tb, Dy, Tm, Hf, Ta, W, Au, Th and U) were determined by the epithermal neutron activation analysis, also 14 elements (Ba, Ca, K, Mg, Na, Sr, Cr, Mn, Ni, Co, Zn, Cd, Cu, Pb) were determined by the atomic emission spectrometry with inductively coupled plasma. Multivariate statistical analysis of the obtained results was used to assess the pollution sources in the studied area (Pavlodar, Ust-Kamenogorsk, and Semey regions).

Keywords: biomonitoring, heavy metals, neutron-activation analysis, atomic-emission spectrometry.

Human impact on the natural environment is immense; its power is comparable to natural geological processes and continues to grow with the rate of technological progress. It is especially significantly in the regions of large industrial centers and large cities.

Protection of environment from anthropogenic impacts involves two main activities: monitoring and control. Monitoring should ensure the organization of continuous monitoring of the environment state.

Growth of industrial production in recent decade causes an increase of human affects both components of the environment and public health. Study of atmospheric deposition of trace elements is one of the most important tasks of the environmental protection and collective efforts of scientists from many countries of the world dedicated to this area more than 40 years. Control of air quality requires primarily multi-elemental analysis of the composition of aerosol particles and determination of the concentrations of elements that are recognized as toxic to living organisms.

In Kazakhstan, due to the current socio-economic development, there are disadvantaged regions by state of the environment, which is a unique urbanistic system saturated with varied companies of very different technological orientation. The presence of large number of enterprises and high levels of radiation in Irtysh area of Kazakhstan determine the urgency of these studies.

The state of the environment and thus the health of the population largely depend on the state of the earth's atmosphere. The atmosphere basically consists of a mixture of natural gases. The particulates pass into the air either from natural sources (soil, rocks, water bodies and living organisms) or as a result of anthropogenic activity (industry, transport, fuel, human waste, etc.). Essentially, atmosphere is an aerosol system, where solid particles are dispersed in a mixture of gases. Among the various types of pollutants, the most hazardous are heavy metals.

The use of mosses as biomonitors of atmospheric depositions of trace elements were introduced in Scandinavian countries and shortly after that, usage of the mosses to assess the atmospheric deposition of metals was well proven in the UN Commission of European air [1]. Mosses have only a rudimentary root system and readily take up elements from the atmosphere. The main advantages of the method are the simplicity of sample collection and the relative ease of analysis compared to precipitation samples conventionally used to assess metal deposition. In addition, the abundance and large geographical distribution of mosses is advantageous and provides for an inexpensive and simple alternative to conventional bulk deposition analysis. Thus, a high density network of sampling sites is easily achieved.

The method of moss biomonitoring of atmospheric depositions of trace elements was applied for the first time in Irtysh area to assess the environmental situation in this region.

Theoretical and experimental obtained data from the studying of air depositions of trace elements, based on the moss biomonitors, will make a significant contribution to the level of ecological safety development of Kazakhstan.

This direction seems to be new and highly topical; being that only some regions of the country were previously studied. Based on the small number of studied territories, we can talk about the need to increase the area of sampling and further work on the entire territory of the Republic of Kazakhstan for studying the state of the atmosphere.

Coordination of the European moss survey is since 2014 led by the Joint Institute for Nuclear Research in Dubna, Russian Federation. Kazakhstan joined to the United Nations Program in 2015.

The research results will be used in the preparation of the «Ecological map of the world – 2018» in the «Kazakhstan» section.

Heavy metals are rare elements (scattered, trace), as performing certain biological functions in the body, which are accumulated in high concentrations in the environment.

The main natural source of heavy metals is magmatic and sedimentary rocks and their forming minerals. Many elements enter into the biosphere from cosmic dust, volcanic gases, etc. The entrance of heavy metals into the environment due to industrial pollution carried out in various ways. The most important of these is the release of the processes associated with high temperatures (metallurgy, roasting, burning of fuel). Despite the great diversity of heavy metal compounds, a set of elements in the gas-dust emissions of the ferrous and non-ferrous metallurgy enterprises are the same type; mainly oxides represent them [2].

Heavy metals and other toxic elements emitted into the atmosphere from the industrial constructions, mostly distributed locally around the emission sources. In a real natural environment, it is usually observe a good correlation of the shape and size of areas of contamination with the configuration of the wind rose.

Around large enterprises, ferrous and nonferrous metallurgy formed strong technogenic anomalies of metals. «Characterized by the presence of the zone of maximum concentrations of heavy metals at a distance of 5 km from the source and the zones of high grade at a distance of 20–25 km. Further, the content of heavy metals decreases to the values of the local background. Local anthropogenic anomalies generate around the enterprises that process raw materials containing heavy metals and other contaminants in the form of impurities. Around major thermal power plants, there are zones of contamination with metals 10–20 km in diameter. Any urban areas are a significant source of heavy metal pollution. High pollution found near freeways, especially lead, zinc, cadmium» [3].

Since many heavy metals tend to accumulate, the negative effects of their impact on the environment can occur slowly. Elevated concentrations of heavy metals in soils, groundwater, leading to stunted growth of trees, agricultural crops and accumulation in the human body can have a detrimental effect on the health of future generations. Hence, there is the need for monitoring atmospheric deposition of pollutant elements [4].

Morphological and physiological properties of mosses along with their wide distribution make these plants very useful bio-indicators to assess the state of the environment. They have a number of advantages over other plants biomonitors (lichens, tree bark, grass, etc.): the absence or severe change in the cuticle, thin and close-set leaves, and poorly developed conducting tissue, it leads to efficient accumulation of materials carried by air, and the little direct uptake from the substrate. Mosses are the most effective at concentrating heavy metals and other trace elements from air and precipitation. Moreover, they do not have a root system and, therefore, the contribution of sources other than atmospheric deposition, in most cases is limited. Sample collection is simple, the analysis of mosses is much simpler than precipitation, the period of exposure can be determined accurately [5].

Methods of biomonitoring were developed in the late 70s of the last century as a way to study atmospheric deposition of heavy metals.

The main types of biomonitoring in the European study are the mosses Hylocomium splendens and Pleurozium schreberi. These species of mosses distributed in a wide interval of temperature zones, and annual growth of them can be easily identified. Typically, the analysis takes a three-year growth of moss.

In research were used well-known and widely used physical and chemical methods of analysis, modern statistical and mathematical methods of calculations.

Neutron activation analysis

Determination of the elemental composition of moss samples was carried out by using instrumental neutron activation analysis (NAA).

Neutron activation analysis — analysis in which the identification and quantitative determination of elements in an irradiated sample is carried out selectively, using the variation of irradiation conditions — (energy of bombarding particles, the exposure time), and consider the nuclear-physical properties of elements and the occurring radionuclides (particularly schema-defined decay of radionuclides, half-life).

NAA of moss samples were carried out at the PFR-2 (pulsed fast reactor) using activation of epithermal neutron along with a full range of neutrons [6, 7].

The application of NAA allows to determine up to 45 elements: Ag, Al, As, Au, Ba, Br, Ca, Ce, Cl, Co, Cr, Cs, Dy, Eu, Fe, Hf, Hg, I, In, K, La, Lu, Mg, Mn, Mo, Na, Nd, Ni, Rb, Sb, Sc, Se, Sn, Sm, Sr, Ta, Tb, Th, Ti, V, U, W, Yb, Zn, Zr [2].

Important stages in the analysis are sampling, and sample preparation.

Environmentally important element, lead cannot be identified using the method of neutron activation analysis. Due to low contents of mosses in the samples also hampered the detection of copper and mercury, therefore, to identify these elements, and compare the obtained results, it also was used the method of atomic emission spectrometry with inductively coupled plasma (AES with ICP).

Determination of metals in moss samples by atomic emission spectrometry

Atomic emission spectrometry with inductively coupled plasma is characterized by high sensitivity and ability to detect a range of metals and several nonmetals at concentrations up to 10^{-10} %, i.e. one particle of 10^{12}. The method is based on using inductively coupled plasma as ion source and mass spectrometer for separation and detection. ICP-MS also allows for isotopic analysis of the selected ion.

As the particles of the powdered sample fall in the Central channel of the ICP, it evaporates as the particles are first dissolved therein and disintegrate into atoms. At this temperature, a significant number of the atoms of many chemical elements are ionized, while the atoms lose the least bound electron, moving in a state of the singly charged ion.

Sampling and sample preparation

In compliance with the Moss Manual 2015 (Harmens and Frontasyeva, 2015; http://icpvegetation.ceh.ac.uk/) the three moss species *Hylocomium splendens*, *Pleurozium schreberi*, *Pleurochaete squarrosa* (Fig. 1–3) were collected over the Irtysh area during the period of autumn and summer of 2015–2016. The sampling network with numbered sampling sites is shown in Figures 4–7.
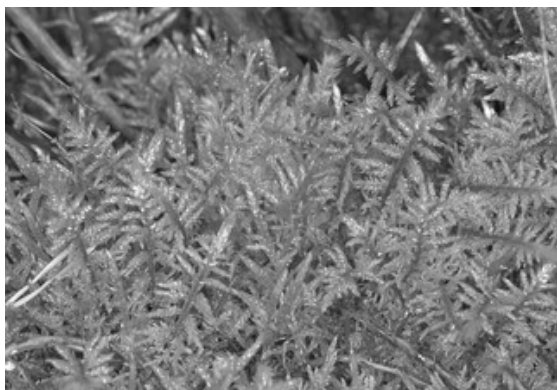

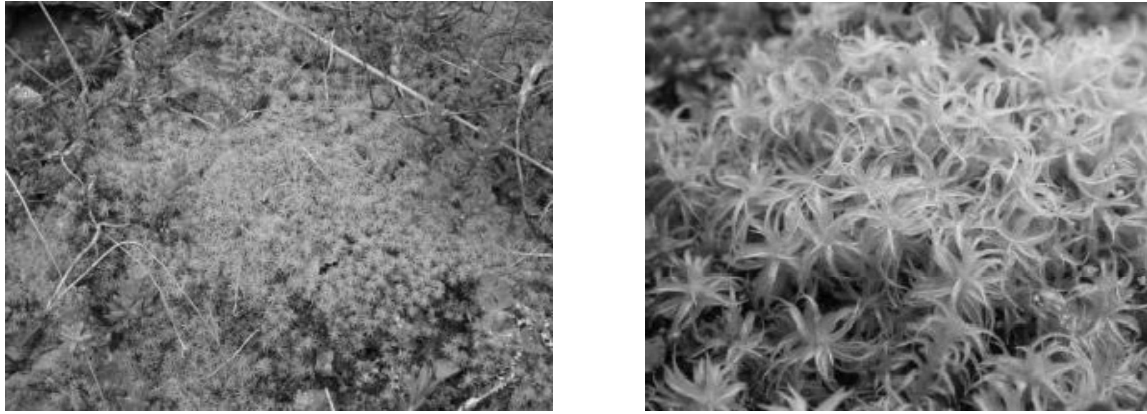Figure 1. Hylocomium splendens

Figure 2. Pleurozium schreberi

Figure 3. Pleurochaete squarrosa

Figure 4. Sampling map (5 samples from Pavlodar)

Figure 5. Sampling map (5 samples from Ust-Kamenogorsk)

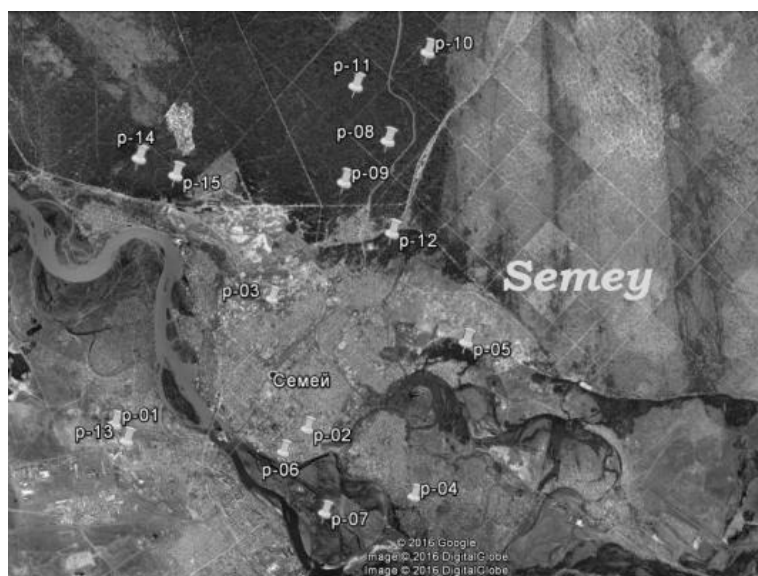Figure 6. Sampling map (5 samples from near the river Irtysh)

Figure 7. Sampling map (15 samples from Semey)

Samples were collected in forest glades or on open heath to reduce through-fall effects from the forest canopy, and the sampling sites were located at least 300 m from main roads, 100 m from local roads, and 200 m from villages. Collected material was stored in paper bags. A separate set of disposable polyethylene gloves was used for collection of each sample.

In the laboratory the samples were cleaned from extraneous plant material and air-dried to constant weight at 30–40 ºC for 48 hours. The samples were neither washed nor homogenized. Green-brown moss shoots representing the last 3 years' growth were subjected to analysis, as they correspond approximately to the deposition over the last 3 years. Previous experience from the use of NAA in moss biomonitoring has shown that samples of 0.3 g are sufficiently large to be used without homogenization.

The concentrations of 42 elements (Na, Mg, Al, Cl, K, Ca, Sc, Ti, V, Cr, Mn, Fe, Ni, Co, Zn, As, Se, Br, Rb, Sr, Zr, Nb, Mo, Ag, Cd, Sb, Ba, La, Ce, Nd, Sm, Eu, Gd, Tb, Dy, Tm, Hf, Ta, W, Au, Th, and U) determined by epithermal neutron activation analysis, also 14 elements (Ba, Ca, K, Mg, Na, Sr, Cr, Mn, Ni, Co, Zn, Cd, Cu, Pb) determined by atomic emission spectrometry with inductively coupled plasma in the moss samples are reported. Multivariate statistical analysis of the obtained results was used to assess the pollution sources in the studied area (Pavlodar, Ust-Kamenogorsk, and Semey regions).

The descriptive statistics of the 42 analysed elements in all collected moss samples (*n*=30) from three different cities are shown in Table 1. All values in Table 1–4 are given in mg·kg^{-1}, dry weight. In Table 3 the me-

dian values and minimum-maximum ranges for the contents of all elements were compared with the data obtained from Georgia (moss survey in 2014) and the data from Norway considered as a pristine area of Europe.

A comparison of concentrations Kazakhstan-Norway showed the increased values for most of heavy metals (Cd, Sm, Ti, V, As, Mo, Mg, Al, Ca, etc) in the studied samples that apparently are due to the state of the industrial sector of Kazakhstan. The main potential sources of air pollution from the industrial sector of Irtysh area are the Aksu ferroalloy plant, aluminium factory, Kazakhstan electrolysis plant, petrochemical plant in Pavlodar region; Ul'binsk metallurgical plant, titanium-magnesium plant in Ust'-Kamenogorsk region; bus factory, engineering plant, silicate plant in Semey region and etc.; also the production of steel and zinc and etc., coal mining, extraction of natural resources.

T a b l e   1

Comparison of the results of NAA for element content in mosses collected in the autumn of 2015
(all data are given in mg·kg⁻¹)

Ele-ments	Region											
	Ust'-Kamenogorsk				Pavlodar				Semey			
	Arithme-tic mean	Average median	C(min.)	C(max.)	Arithme-tic mean	Average median	C(min.)	C(max.)	Arithme-tic mean	Average median	C(min.)	C(max.)
Na	3437.1	3100	2700	3690	2429.2	2400	816	3710	4758	5600	1970	6920
Mg	6248	5900	5760	7170	7106	7550	4910	8220	7250	7790	5470	8480
Al	18260	17800	16500	22000	14356	13900	5380	22300	20420	20800	15300	26500
Cl	140.04	167	36.8	255	312.2	292	45	508	50.26	48.3	42.7	60.9
K	7922	8080	7430	8370	14100	15800	10800	16900	9970	10200	7390	11800
Ca	9328	8790	7790	11700	15290	15100	9550	22800	9666	9820	8020	10700
Sc	4.208	4.09	4.010	4.52	2.924	2.88	1.37	4.1	4.36	4.73	2.56	5.42
Ti	1054.4	970	920	1250	862.6	767	300	1400	1119.8	1170	806	1460
V	25.7	24.7	22.5	30.4	19.258	18.9	7.79	29.5	25.38	24.8	21.2	30.7
Cr	21.06	20.6	19.1	23.5	19.1	20.7	12.6	23.1	20.46	21.1	12.2	26.1
Mn	351.8	219	200	907	376.4	422	228	482	250.4	252	196	313
Fe	7280	7390	5250	9290	6452	6480	3030	8680	7322	7390	5090	9820
Ni	9.968	10.5	8.88	10.8	9.36	8.88	6.87	12.6	9.682	10.8	6.34	12.1
Co	5.610	5.91	4.84	6.4	4.218	4.5	3.07	4.62	6.048	6.74	3.29	7.9
Zn	1.222	1.19	1.05	1.46	404.64	453	87.2	811	1.1226	1.18	0.933	1.27
As	0.130	0.126	0.15	0.17	3.37	3.54	2.51	3.81	0.12658	0.125	0.0909	0.163
Se	0.269	0.293	0.25	0.31	0.3824	0.391	0.275	0.511	0.2502	0.251	0.119	0.351
Br	3.388	4	3	4	5.124	4.64	4.08	7.52	3.286	3.54	2.28	4
Rb	28.32	28.6	26.3	30.1	22.72	23.5	12.1	29.9	33.5	38	19.1	42.3
Sr	53.46	54.7	48.1	57.5	167.22	187	88.1	238	59.98	63.9	39.1	80.1
Zr	69.36	73.3	34.9	94.5	36.6	13.5	10.7	78.4	67.38	54.3	35.3	117
Nb	1.286	1.38	0.73	1.8	4.68	5.02	1.52	7.32	1.075	0.892	0.583	2.14
Mo	0.08	0.08	0.074	0.09	0.8224	0.748	0.369	1.4	0.07438	0.068	0.0639	0.0954
Ag	0.002	0.0	0.002	0.003	0.2738	0.263	0.155	0.436	0.001696	0.00166	0.0014	0.00208
Sb	0.155	0.150	0.134	0.167	1.0604	1.155	0.604	1.77	0.1514	0.15	0.11	0.184
Cd	0.019	0.019	0.0155	0.027	0.0055	0.0055	0.0055	0.0055	0.014226	0.013	0.00973	0.0234
I	2.318	2.37	1.55	3.06	2.846	2.71	1.99	3.64	2.076	2.05	1.83	2.45
Ba	201.4	196	195	222	174.4	174	154	193	236.6	258	149	305
Cs	1.52	1.6	1.34	1.64	1.0922	1.09	0.543	1.5	1.5006	1.59	0.983	1.8
La	8.692	8.8	5.59	12.7	8.754	6.94	2.38	15.4	9.988	10.9	5.98	14.9
Ce	20.02	20.6	12.3	29.5	19.536	15	4.68	34.8	22.5	24.4	13.5	35.2
Nd	8.428	7.37	5.48	12.5	9.698	8.52	3.51	15.5	9.456	11.1	4.63	13.6
Sm	2.59	2.47	1.88	3.28	1.8544	1.37	0.502	3.34	2.722	2.74	1.45	3.95
Eu	0.31	0.35	0.285	0.35	0.2832	0.254	0.202	0.439	0.4074	0.427	0.194	0.591
Tb	0.2632	0.262	0.197	0.377	0.23742	0.178	0.0741	0.411	0.2812	0.311	0.163	0.406
Tm	0.15058	0.147	0.0549	0.257	0.10514	0.0794	0.033	0.179	0.16412	0.144	0.0756	0.297
Yb	0.9264	0.97	0.673	1.35	0.7324	0.659	0.262	1.38	0.9346	0.874	0.529	1.46
Hf	2.474	2.58	1.37	3.41	1.8382	1.7	0.601	3.03	2.27	1.88	1.35	3.99
Ta	0.2204	0.24	0.143	0.281	0.21022	0.212	0.0941	0.319	0.2352	0.29	0.135	0.305
W	0.00504	0.00249	0.00214	0.0159	0.6102	0.593	0.416	0.847	0.008342	0.00286	0.00208	0.0264
Au	0.004404	0.00338	0.00179	0.00772	0.009564	0.00833	0.00681	0.0137	0.0055	0.00589	0.0012	0.0076
Hg	0.07308	0.0923	0.0271	0.0978	0.0436	0.0376	0.0206	0.097	0.06686	0.0791	0.0264	0.0996
Th	3.252	3.59	1.44	5.8	3.2456	2.2	0.768	6.03	3.132	2.63	1.53	6.01
U	0.7882	0.773	0.38	1.34	0.7024	0.602	0.201	1.17	0.7282	0.65	0.419	1.19

T a b l e 2

The results of analysis of moss survey, which were collected in the summer of 2016
(all data are given in mg·kg^{-1})

Elements	Arithmetic mean	Average median	C(min.)	C(max.)	Elements	Arithmetic mean	Average median	C(min.)	C(max.)
Na	2344.69	1540	312	6890	Cd	0.35	0.228	0.12	0.786
Mg	3554.23	2830	918	8370	In	0.26	0.317	0.0528	0.493
Al	10181.53	7400	2240	26000	Sb	0.34	0.23	0.128	0.788
Si	34935.38	25400	5290	116000	I	1.18	1.01	0.305	2.56
Cl	115.30	102	50.2	238	Ba	108.89	81.4	22.5	258
K	6090	5420	1450	10900	Cs	0.81	0.595	0.391	1.5
Ca	5415.38	5510	1100	8670	La	4.37	2.42	0.922	11.7
Sc	2.40	1.35	0.75	6.64	Ce	9.04	5.18	1.93	23.7
Ti	511.92	358	111	1260	Nd	3.96	2.15	0.969	10
V	13.30	8.37	3.74	34.4	Sm	0.82	0.469	0.169	2.11
Cr	16.44	9.62	5.79	49.4	Eu	0.27	0.193	0.0809	0.693
Mn	155.76	117	30.8	349	Gd	0.48	0.283	0.106	1.22
Fe	4098.46	2530	1190	9580	Tb	0.13	0.0823	0.0373	0.353
Ni	6.63	4.1	1.68	19	Dy	0.71	0.451	0.221	1.9
Co	3.50	1.84	0.873	11.5	Tm	0.075	0.0557	0.0276	0.192
Zn	54.63	57.4	26.2	84.3	Yb	0.51	0.312	0.131	1.37
Se	0.30	0.344	0.152	0.409	Lu	0.073	0.0553	0.00782	0.246
As	2.22	1.67	0.823	4.89	Hf	0.617	0.308	0.102	1.53
Br	2.93	2.83	1.39	4.46	Ta	0.112	0.0725	0.0265	0.315
Rb	16.22	11.2	6.64	34.4	W	0.311	0.204	0.0831	0.689
Sr	62.80	47.5	14.8	150	Au	0.0055	0.00415	0.0026	0.00969
Zr	22.22	10.1	4.56	55.7	Hg	0.42	0.402	0.295	0.576
Mo	0.35	0.223	0.0857	0.858	Th	0.975	0.554	0.253	2.44
U	0.29	0.175	0.0568	0.756					

T a b l e 3

Comparison of the median values and ranges of element content in moss from Kazakhstan between data
of the moss survey Norway, Georgia and Kazakhstan (2014–2015) (all data are given in mg·kg^{-1})

	Kazakhstan moss survey 2016–2017		Kazakhstan moss survey 2014–15 (Nazarova. et al. 2015)		Georgia moss survey 2014 (Shetekauri. et al. 2015)		Norway moss survey (Shetekauri. et al. 2015)	
№ of sample	n=30		n=23		n=16		n=100	
Element	Median	Range C(min.)-C(max.)	Median	Range C(min.)-C(max.)	Median	Range C(min.)-C(max.)	Median	Range C(min.)-C(max.)
^{24}Na	2929	312–6920	2000	424–17100	721	268–1990	nd	nd
^{27}Mg	5329	918–8480	6060	1710–24800	4410	2720–11600	1730	940–2370
^{28}Al	14197	2240–26500	9510	33.8–35100	5195	2450–20800	200	67–820
^{38}Cl	143	36.8–508	180	95.5–1270	225	140–465	nd	nd
^{42}K	8540	1450–16900	10800	3820–23200	5875	3080–9040	nd	nd
^{49}Ca	8636	1100–22800	12500	2340–24000	11800	7140–15300	2820	1680–5490
^{51}Ti	779	111–1460	603	99–3920	547	216–2070	23.5	12.4–66.4
^{52}V	18.7	3.74–34.4	13	1.7–56.7	11.8	6.2–54.0	0.92	0.39–5.1
^{56}Mn	247	30.8–907	178	70.5–1260	158	70–592	256	22–750
^{76}As	1.68	0.0909–4.89	1.92	0.80–8.1	0.88	0.33–2.87	0.093	0.020–0.505
^{82}Br	3.46	1.39–7.52	4.67	2.3–31.3	4.545	2.3–9.8	4.5	1.4–20.3
^{99}Mo	0.34	0.0639–1.4	0.69	0.21–2.03	0.35	0.24–0.77	0.135	0.065–0.70
^{115}Cd	0.17	0.0055–0.7865	0.75	0.02–2.74	0.25	0.12–0.56	0.058	0.025–0.171
^{140}La	6.9	0.922–15.4	6.4	1.35–37.3	59.28	18.8–138	17.1	5.6–50.5
^{153}Sm	1.66	0.169–3.95	1.05	0.198–7.09	2.13	0.92–6.28	0.189	045–2.56
^{187}W	0.25	0.00208–0.847	0.44	0.12–1.42	0.43	0.035–0.945	0.33	0.05–1.34
^{198}Au	0.00584	0.0012–0.0137	0.00145	0.00023–0.00441	0.13	0.06–0.27	0.127	0.009–1.23

The average concentrations of elements are given in Table 4 to compare two different methods: NAA and AES with ICP, and was found a correlation coefficient, which is 0,7784.

The average concentrations of elements, determined by two different methods

Elements	Ba	Ca	Cd	Co	Cr	K	Mg	Mn	Na	Ni	Sr	Zn
C(average), mcg/kg by NAA	170	8909	0.3	4.9	19.9	8762	5716	247	3178	9.1	86.6	146.2
C(average), mcg/kg by AES	114	12720	2.0	5.4	33.7	5316	2971	473	1868	172.3	76.6	225.1

The performed preliminary investigation shows that the moss biomonitoring of atmospheric deposition of heavy metals is an efficient technique to study the environmental situation in the Kazakhstan. The experience of this study can be successfully used in the other regions of the Kazakhstan. Also, there will be maps of the spatial distribution of elements and radionuclides in the study area, based on the statistical analysis of the data created with the use of maps of the distribution of elements, will assess potential sources of pollutants into the environment.

References

1   Moss survey protocol. [ER]. Access mode: http://icpvegetation.ceh.ac.uk/manuals/moss_survey.html.

2   Kuznetsov D.Yu. Cluster analysis and its application / D.Yu. Kuznetsov, T.L. Troshina // Yaroslavl pedagogical Bulletin. — 2006. — Vol. 4. — P. 103–107.

3   Frontasyeva M.V. Analytical Investigations at the IBR-2 reactor in Dubna / M.V. Frontasyeva, S.S. Pavlov // Preprint of JINR, E14–2000–177, Dubna, 2000 (submitted to the Proc. VIII Int. Seminar on Interaction of Neutrons with Nuclei (Dubna, May 17–20, 2000).

4   Steinnes E. Large Scale Multi-Element Survey of Atmospheric Deposition Using Naturally Growing Moss as Biomonitor / E. Steinnes, J.P. Rambaek, J.E. Hanssen // Chemosphere. — 1992. — Vol. 25. — P. 735–752.

5   Frontasyeva M.V. A study of atmospheric deposition of heavy metals in the southern Urals / M.V. Frontasyeva, L.I. Smirnov, E. Steinnes, S.M. Lyapunov, V.D. Cherchintsev // Preprint JINR, D-14–2002–69. — Dubna, 2002.

6   Frontasyeva M.V. Neutron activation analysis for the Life Sciences. A review / M.V. Frontasyeva // Physics of Particles and Nuclei. — 2011. — Vol. 42, No. 2. — P. 332–378. http://www.springerlink.com/content/f836723234434m27/M.V.

7   Makhambet A.Zh. First moss survey in Kazakhstan / A.Zh. Makhambet, N.M. Omarova, M.V. Frontasyeva // ICP Vegetation. The 29th Task Force Meeting: Book of Abstracts. — 2016.

М.У. Нуркасимова, А.К. Ташенов, Н.М. Омарова, С.В. Моржухина

Қазақстан Республикасының Ертіс өңіріндегі ауыр металдар мен радионуклидтердің ауадан түсулерінің биомониторингі

Мақалада мүк-биомониторлар талдауы негізінде Қазақстанның Ертіс өңіріндегі ауыр металдар мен радионуклидтердің атмосфералық түсулерін зерттеу барысында алынған мәліметтер талқыланған. Бұл әдіс Қазақстан Республикасының Солтүстік-Шығыс және Солтүстік аймақтарының экологиялық жағдайын бағалау мақсатында қолданылды. 30 мүк үлгілері 2015–2016 жж. өсу кезеңінің күз және жаз мезгілдерінде жиналған. Жалпы, 42 элемент (Na, Mg, Al, Cl, K, Ca, Sc, Ti, V, Cr, Mn, Fe, Ni, Co, Zn, As, Se, Br, Rb, Sr, Zr, Nb, Mo, Ag, Cd, Sb, Ba, La, Ce, Nd, Sm, Eu, Gd, Tb, Dy, Tm, Hf, Ta, W, Au, Th және U) эпижылулық нейтрон-белсенділік талдау әдісімен, сонымен қатар 14 элемент (Ba, Ca, K, Mg, Na, Sr, Cr, Mn, Ni, Co, Zn, Cd, Cu, Pb) индуктивті байланысқан плазмалы атом-эмиссиялық спектрометрия әдісімен анықталды. Алынған нәтижелердің көпфункционалды статистикалық талдауы зерттелген территориядағы (Павлодар, Өскемен және Семей аймақтары) ластану көздерін бағалау мақсатында қолданылды.

Кілт сөздер: биомониторинг, ауыр металдар, нейтрон-белсенділік талдау, атом-эмиссиялық спектрометрия.

М.У. Нуркасимова, А.К. Ташенов, Н.М. Омарова, С.В. Моржухина

Биомониторинг воздушных выпадений тяжелых металлов и радионуклидов в Прииртышье Республики Казахстан

В статье проанализированы данные, которые были получены при изучении атмосферных выпадений тяжёлых металлов и радионуклидов в Прииртышье на основе анализа мхов-биомониторов. Данный метод был применён для оценки экологической ситуации в Северо-восточных и Восточных регионах Республики Казахстан. 30 образцов мхов были собраны осенью и летом 2015–2016 гг. растительного периода. В целом, 42 элемента (Na, Mg, Al, Cl, K, Ca, Sc, Ti, V, Cr, Mn, Fe, Ni, Co, Zn, As, Se, Br, Rb, Sr, Zr, Nb, Mo, Ag, Cd, Sb, Ba, La, Ce, Nd, Sm, Eu, Gd, Tb, Dy, Tm, Hf, Ta, W, Au, Th и U) были определены с помощью эпитеплового нейтронно-активационного анализа, а также 14 (Ba, Ca, K, Mg, Na, Sr, Cr, Mn, Ni, Co, Zn, Cd, Cu, Pb) — с помощью атомно-эмиссионной спектрометрии с индуктивно-связанной плазмой. Многофункциональный статистический анализ полученных результатов был использован для оценки источников загрязнения на исследованной территории (регионы Павлодара, Усть-Каменогорска и Семея).

Ключевые слова: биомониторинг, тяжелые металлы, нейтронно-активационный анализ, атомно-эмиссионная спектрометрия.

N.I. Kopylov

Institute of Solid State Chemistry and Mechanochemistry
of the Siberian Branch of the Russian Academy of Sciences, Novosibirsk, Russia
(E-mail: kolyubov@narod.ru)

Thermolysis of brown coal from the Baganursky deposit (Mongolia)

The process of thermolysis of brown coal from the Baganursky deposit of Mongolia has been studied. These coals are characterized by high content of gas component (up to 40 %) and low content of liquid fraction. The decomposition begins at ~200 ºC. At temperatures up to ~700 ºC there is no sintering. In the solid residue, only relics of the individual hydrocarbon constituents of the original coal are retained. The liquid condensate of sublimates (up to 19 % by weight of the initial) contains 0.78 % of the organic extract (96–98 % of the phenolic mass with a maximum boiling point of 360 °C) and 92.2 % of the aqueous solution (with a boiling range of 115–130 ºC). The initial aggregate state (the particle size of the material, the effect on it of the external medium) not only affects the yield of the gas constituent of coal during thermolysis, but also determines the impurity composition of the organic extract of the condensate liquid sublimates.

Keywords: thermolysis, brown coals, solid residue, sublimates, condensate, hydrocarbons, phenols, thermal analysis.

Introduction

Fossil coals are subdivided into anthracites, stone and brown coals. Depending on the composition, physical and technological properties, as well as economic, social and other factors, the coals of particular deposits can be used as energy or technological raw materials. Currently, they mainly serve as a fuel resource. At the end of the last century, up to 73 % of the extracted fossil coals were used for this purpose in the USSR [1].

When burning in the furnaces of boiler houses and domestic ovens, a large amount of volatile components is released and incomplete coal burnout spores are formed, which leads to a systemic release of environmentally hazardous combustion products into the atmosphere. In the conditions of the mountainous terrain and the continental climate in Central Asia, for example, on the territory of the Republic of Tuva, stagnant zones, smog in the surface space of the «wind shadow effect» and pollution of the atmosphere of cities and settlements of the region with harmful products of flue gases: carcinogens and other highly toxic substances [2].

Similarly, an analogical adverse environmental situation is observed in the adjacent coal-mining regions of Mongolia. For example, at the Khushut coal deposit of lean coal, production is conducted only for the energy needs of the local population [3]. Also, mainly for domestic needs and thermal power engineering, deposits of a number of brown and hard coals of Mongolia are being developed [4]. At the same time, environmental problems of flue emissions have not been solved, both for large stationary TS and TPPs, and for private sector furnaces of cities and settlements of regions that use coal to be extracted as a source of thermal energy.

In this regard, within the framework of the comprehensive Program for the Creation of Technologies for the Efficient and Environmentally Safe Processing of Mineral Raw Materials (SB RAS project No. 28.4.8, 2004–2006) in TuVIKOPR SB RAS, (Kyzyl) in cooperation with ISTTM SB RAS (Moscow). Novosibirsk), investigations were carried out on the dynamics of thermolysis of coals of Tuva with the aim of working out a process for obtaining environmentally friendly fuel material [5]. Interest in this topic from Mongolian specialists served as a basis for research on the thermal decomposition of coals of Mongolian deposits. Within the framework of the program of these investigations, work was carried out to investigate the thermolysis of coals of individual deposits in Mongolia [6, etc.].

This report is devoted to the results of investigations of the thermal decomposition of brown coals of the Baganursky deposit.

Experimental part

The technical characteristics of the samples of this coal are given in Table 1.

Technical characteristics of the samples of coal

Sample of Baganur stone coal	Technical analysis, %			Elemental composition on dax				Calorie Q^s, kg/cal
	W^s	A^d	V^{dax}	C	H	S	O+S+N	
Sample 1	8.4	10.4	41.1	72.0	4.9	0.36	22.9	5034.4
Sample 2	9.3	10.2	42.5	70.0	4.1	0.49	21.5	4991.0

The material for the investigation was initially presented in the form of a single sample, and then in addition — an aggregate batch weighing about 3 kg, which was a mixture of lumps of various sizes mixed with a small rash. At the first stage, the dynamics of thermal decomposition were investigated by differential thermal analysis (DTGA) using the MOM-1000 derivatograph (type «Paulik, Paulik-Erdei», Hungary). The weight of the sample was ~1 g. The starting material was previously divided into three fractions: free-flowing, medium-sized (5–20 mm) and lump (> 20 mm). Heating was carried out to 650–700 ºC at a rate of 10 °C/min. The experimental conditions provided for the free diffusion of gaseous constituents of coal formed in the sample upon heating, but excluding contact with the air medium.

Determination of the quantitative characteristics of the process was carried out in a laboratory facility with the capture of gas and light boiling condensates, including a container placed in the furnace, into which a crucible with a sample was connected, connected by a branch pipe with a system for capturing sublimations. The mass of samples in these experiments was in the range of 50–100 g.

Investigations of thermolysis products were carried out by a number of methods of instrumental analysis: DTGA, IR spectroscopy, chromatography-mass spectroscopy.

DTGA single sample. Figure 1 and Table 2 show the data of the DTGA of samples of material of various sizes.
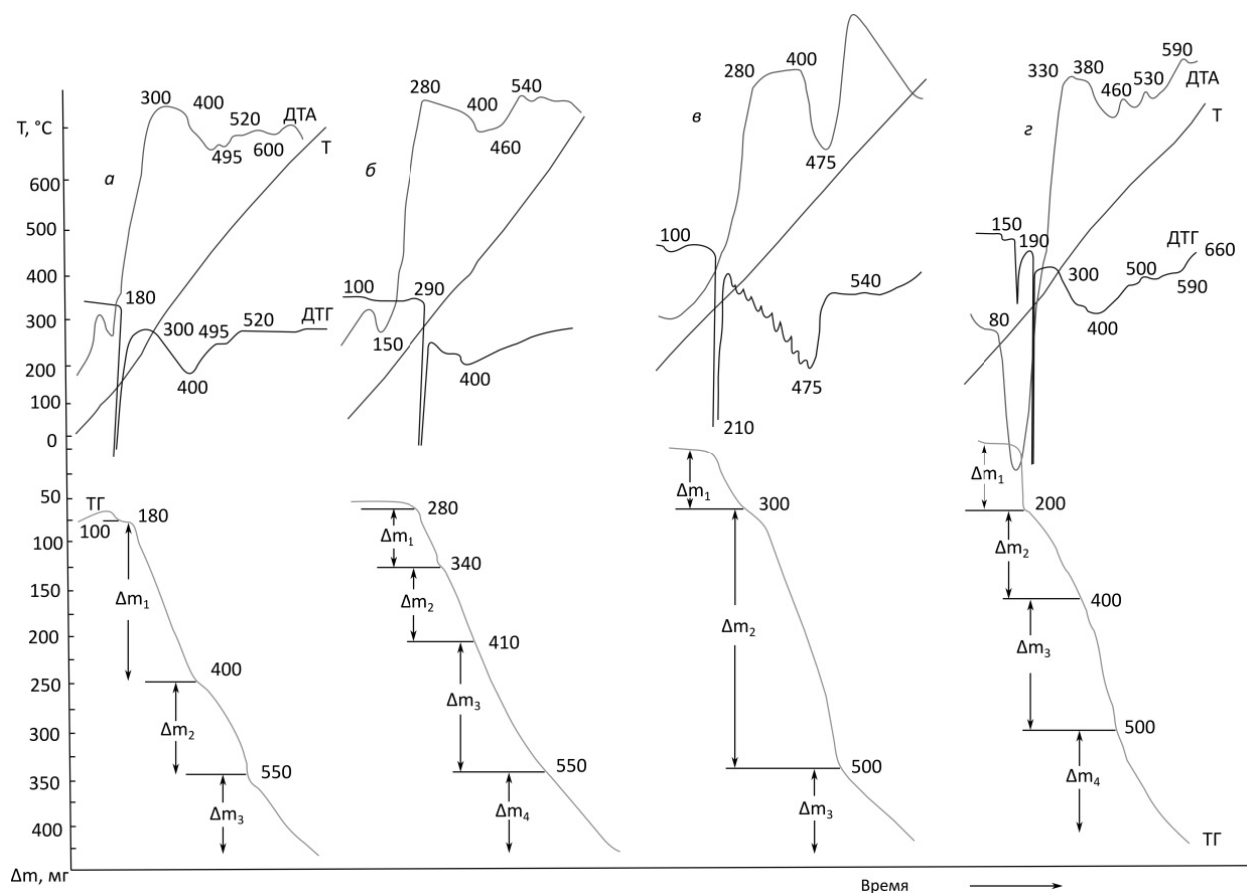
Figure 1. DTGA of a single (initial) coal sample: *a-g* (see Table 2)

Thermal decomposition of brown coal from the Baganursky deposit

Steps of decomposition	Initial sample*)							
	a		b		c		d	
	Interval, t °C	Weight loss from the initial, %	Interval, t °C	Weight loss from the initial, %	Interval, t °C	Weight loss from the initial, %	Interval, t °C	Weight loss from the initial, %
1	80–100	0.2	100–150	0.5	100	-	80–150	5.5
2	180–300	17.1	280–300	6.5	210–300	7.0	150–200	
3	300–400		300–400	10.5	300–400	27.5	200–400	11.2
4	400–550	10	410–500	21.5	400–500		400–500	12.4
5	550–700	12	500–700		500–700	8.0	500–650	7.0
Σ	700	~39 %	700	~40 %	700	~42.5	650	~36.1

Note. *) _a_ — lump sample, fresh prepared; _b_ — lump, previously prepared; _c_ — fresh prepared rash sample; _d_ — rash sample, previously prepared.

It can be seen that with the general identity of the results of individual samples on the curves, there are differences in the course of their sections characterizing the individual stages of thermolysis. On the DTA curves for samples in experiments with samples _a_, _b_, _d_ (see Fig. 1), a clear cascade of endoeffects is fixed in the interval 380–600 °C, corresponding to the phased removal of gaseous and low-boiling decomposition products from the material. However, in the case of a sample in (Fig. 1), instead of a cascade of thermal effects, only one large endopic is observed in the range of ~ 400–540 °C. Such a variety of curves on thermograms at the initial stage of heating can be explained by the initial state of the material: the size, the conditions of its content from the time of extraction to sampling (contact with the air medium and storage time). Nevertheless, the decomposition sequence is the same for all samples (Table 2): the process begins with explosive gas evolution at relatively low temperatures in the amount of 5.5–7.0 % of the initial one. For trials a and c, the association is combined into a single stage with the subsequent or with the previous stage. The total weight loss varies between 36.1–42.5 %, depending on the final temperature of the experiment.

DTGA samples of the coarse lot. The results of the experiments (Fig. 2) basically agree with the data of the experiments of a single sample (Fig. 1). Thus, the loss of the mass of the samples upon heating (TG and DTG curves) is carried out step-by-step at 80–200 and 300–470 °C: by 9.4 and 14.7 %, respectively (for small intermediate loss $\Delta m^2 = 2.7$ %). With further heating, the monotonic mass loss (Δm^4) is 14.1 %. The total mass loss of the sample reaches ~ 41 %, and in some experiments — 47 %.

Consistency of the decomposition products of coal. Determination of the consistency of the decomposition products was carried out in the following modes: 1) continuous heating to 600–650 °C with an exposure of 1–2 hours at a finite temperature; 2) stage-by-stage heating (with a 2-hour exposure through 100 °C) to 600–650 °C (see Table 3).

The results of thermolysis of brown coal with a gradual aging

t, °C	Experiment 1, monolith sample			Experiment 2, intermediate sample		
	ΔP, %	Condensate, %	Gas fraction, %	ΔP, %	Condensate, %	Gas fraction, %
200	18.73	0.28	18.44	9.5	6	3.5
300	9.3	1.5	7.54	10.04	4.04	6
400	10.2	3.65	6.6	9.74	4.14	5.6
500	6.58	0.64	5.94	7.7	2	5.7
600	5.03	0.37	4.66	–	–	–
650	–	–	–	5.05	1.9	3.15
Σ	49.94	6.39	43.55	42.03	18.08	23.95

The results of the experiments of regimes 1 and 2 differ somewhat, but on the whole they correlate according to the main parameters. Thus, in the case when the initial sample was an initial coal monolith (experiment No. 1, Table 3), a significant loss of mass (18.73 %) was observed already at 200 °C, mainly as a gas

component. At the same time, in an experiment with an average breakdown of fines (experiment No. 2, Table 3) at a holding temperature of 200 ºC, the mass loss is only 9.5 %. Extracts at subsequent temperature stages in both experiments lead to comparable mass losses, differing only in the gaseous components. The final results differ only due to the mass loss at 200 °C.

a — monolith; *b* — average
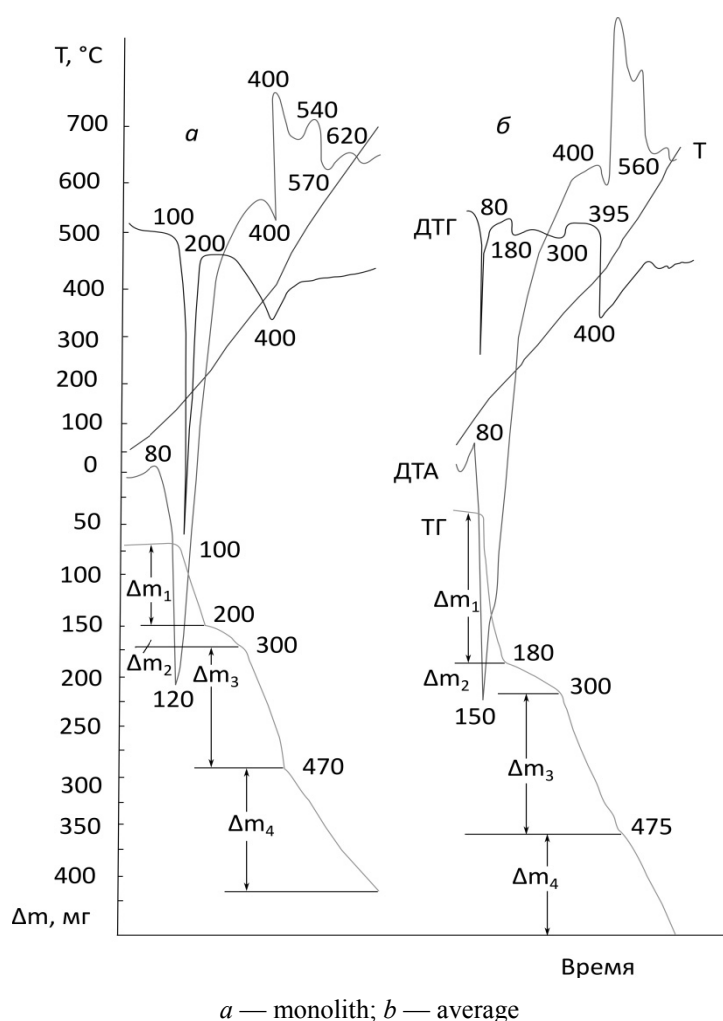
Figure 2. DTGA of the coarse coal lot

The total loss of mass of experiment No. 1 is 49.94 % and is determined primarily by the gas component (43.55 %), and the total loss in experiment No. 2 is 42.03 % and is determined by equally condensed sublimates (18.08 %) and gas constituents (23, 95 %), while the number of the latter is almost half that of experiment No. 1. This difference is due to the partial loss of gaseous components in the case of sample No. 2 due to diffusion weathering during storage under conditions of free contact with the environment.

In the investigation, along with the study of the dynamics of the thermal decomposition of coal, quantitative characteristics of the decomposition process were determined and a solid residue and liquid condensates of the sublimes of the low-boiling constituents of coal were obtained.

For a comparative evaluation of the thermolysis result, an X analysis of the average initial lot of coal and its solid thermolysis product was carried out.

The IR spectrum of the initial coal sample (Fig. 3, curve 1) includes absorption bands corresponding to out-of-plane vibrations of aromatic CH bonds in the range 1000–1100 cm^{-1}; ether in the region of 1150–1350 cm^{-1}; C–O phenolic in the region 1550–1650 cm^{-1}; C=O quinolones in the region of 2845–2020 cm^{-1}; CH-aliphatic and OH groups of phenols and carboxylic acids in the region of 3100–3400 cm^{-1} and their peripheral groups in the 3500–3600 cm^{-1} region. The IR spectra of the material after thermolysis (Fig. 3, curve 2), as a rule, have relict absorption bands corresponding to weakly pronounced vibrations, and in regions of 2500 cm^{-1} there are no vibrational bands.
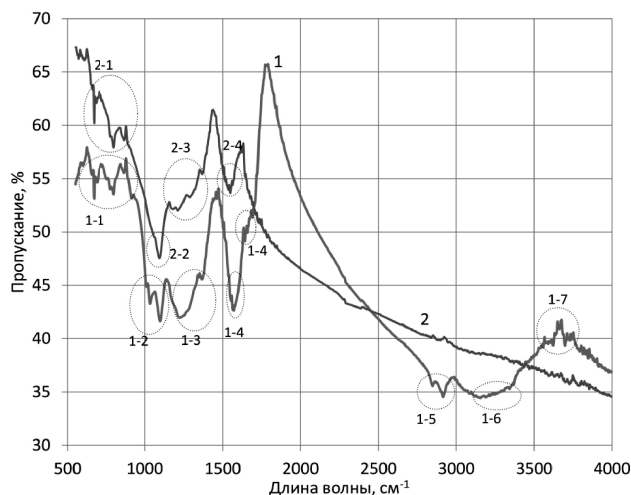
Figure 3. IR spectrograms of the average initial sample of brown coal (1) and the product of its thermolysis (2)

The results of DTGA liquid condensate sublimation of coal thermolysis (samples I, II and average en-larged lot) obtained after holding at 600, 300 and 400 ºC (Fig. 4) showed that in the temperature range 115–130 °C all the sample material passes into vapor. In this case, the complete identity of the thermograms of all samples is noted.

The liquid condensate of the thermolysis of the average sample of the coarse lot of coal was extracted with chloroform, extracting an extract in an amount of 0.78 % of the mass of the liquid condensate. The main part of the liquid condensate of sublimates is an aqueous solution. IR spectra of the extract of the middle sample contain the following characteristic absorption bands: 1 — saturated fragments of molecules (maxima 1377, 1463, 2728, 2854 cm^{-1}); 2 — aromatic structures (722, 744, 812, 874, 1604 cm^{-1}); 3 — oxygen-containing compounds (1032, 1167, 1706 cm^{-1}). This thermolysis product contains phenol, two isomers of methylphenols and two isomers of ethylphenols, as well as n-alkanes and α-olefins (in minimal amounts).
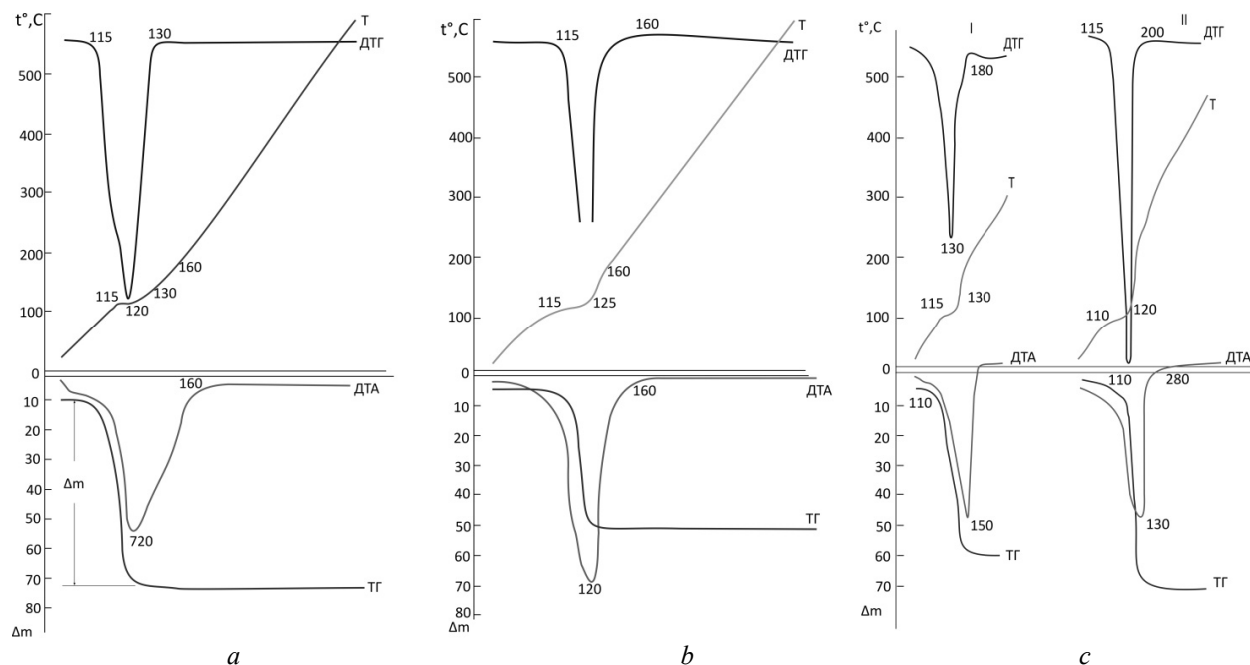
Figure 4. DTGA of the liquid extract of the sublimations of thermolysis of samples I (*a*) and II (*b*) in the temperature range up to 600 ºC, and also of the average coal sample (*c*) in the temperature range up to 300 (I) and 400 ºC (II)

The results of chromatographic determination of the consistency of organic products of the extract of the sublimations of thermolysis of samples I and II are given in Table. 4. The bulk of the extracted organic component is also represented by phenol and its derivatives.

T a b l e 4

Material composition of the extract of the condensate of the sublimes of thermolysis of the Baganurian coal

Peak No.	Substance	Retention time, minutes	Relative content, %
	Sample I		
1	Phenol	4.6	36.45
2	2-Methylphenol	5.3	14.45
3	3-Methylphenol	5.5	32.57
4	2,6-Dimethylphenol	5.9	0.45
5	2-Ethylphenol	6.1	0.90
6	2,4-Dimethylphenol	6.3	5.03
7	3-Ethylphenol	6.4	7.27
8	2,3-Dimethylphenol	6.6	0.74
9	3,4-Dimethylphenol	6.7	1.44
10	3-Propylphenol	7.4	0.69
	Sample II		
1	3-Methylpyridine	5.0	0.2
2	2,6-Dimethylpyridine	5.8	0.08
3	2-Methyl-2-cyclopentene-1-one	6.1	0.3
4	3-Methyl-2-cyclopentene-1-one	7.0	1.12
5	Phenol	7.3	60.26
6	2,3-Dimethyl-2-cyclopentene-1-one	8.2	0.71
7	2-Methylphenol	8.5	6.21
8	4-Methylphenol	9.0	27.25
9	2,5-Dimethylphenol	10.2	1.06
10	3-Ethylphenol	10.8	2.69

In the extract of condensate, there are also small amounts of cyclopentene and pyridine derivatives, there is an insignificant amount of the phase relating to alkanes and olefins.

Within a general identity of the phase composition of the extracts of the average sample of the aggregated lot, samples I and II (96–99 % phenol and its derivatives), the proportions of the constituent phases are slightly different. Also, in the extract of sample II there is an admixture of the cyclopentene derivative, and in the extract of the intermediate sample condensate, an admixture of naphthalene derivatives. This is probably due to the different initial aggregate state of the materials of these samples: the particle size, which determines the contact surface with the external medium of the starting material, and the degree of reaction of this factor to it.

Based on the investigation data, it is possible to imagine the thermal decomposition of the Baganur brown coal by the following scheme:

Initial brown coal of the Baganursky deposit (average sample)
650 ºC, 2 hours

Sublimation (42,03%)   Solid residue (57,97%)

Gas (23,95%)   liquid product (condensate)   Partially preserved relicts: aromatic
to the atmosphere   hydrocarbons, ethereal groups, phenol and
                                                     quinol derivatives

H₂O (92,22 %) + Organic constituent
(0,78 %)

Phenol and its derivatives
average (98,3 %)

130 ºC

Gas to the atmosphere

Conclusion

The conducted study of the thermolysis of brown coal from the Baganursky deposit showed that it is characterized by a high content (> 40 %) of gaseous components, which are removed from the material when heated in the range of ~ 200 ℃, minor admixtures of liquid condensate and absence of astringent constituents. The material does not cake. The solid-phase residual thermolysis product is a free-flowing graphite-like material, which can be briquetted only by the introduction of astringent formulations. Liquid condensate consists of 99.22 % of the aqueous solution and 0.78 % of the organic component — phenol and its derivatives. The condensate boils away without residue in the range 115–130 ℃. Investigation on samples of a material with various sizes: medium sample of a coarse batch, fine (sample I — size < 5 mm) and large (sample II — diagonal size > 30 mm) fractions showed that the initial aggregate state of the material, the degree of environmental impact on it influence not only the yield of the gas component during thermolysis, but also the phase composition of the extract of the condensate of sublimation.

References

1 Горная энциклопедия. — Т. 5. — М.: Сов. энцикл., 1991. — С. 227.

2 Шабанов В.И. Марочный состав углей пласта Улуг Улуг-Хемского бассейна / В.И. Шабанов, И.Ю. Яковлев // Химия твердого топлива. — 1989. — № 6. — С. 52–55.

3 Bat-Orahikh Erdenetsogt, Insung Lee, Belegiin Bat-Erdene, Luvsanhultem Jargal // Int. J. Coal Geol. — 2009. — Vol. 80. — P. 87.

4 Геология Монгольской народной республики / Под ред. Н.А. Миронова, Р.А. Хасина, Ч. Хурц. — М.: Недра, 1977, 125 с.

5 Копылов Н.И. Термическое разложение углей Тувинского месторождения / Н.И. Копылов, Ю.Д. Каминский // Химия в интересах устойчивого развития. — 2013. — Т. 21, № 3. — С. 319–327.

6 Копылов Н.И. Термолиз бурого угля Баганурского месторождения (Монголия) / Н.И. Копылов, Ю.Д. Каминский, Ж. Дугаржав, Б. Авид, Ю.В. Патрушев // Химия в интересах устойчивого развития. — 2013. — Т. 21, № 5. — С. 499–504.

Н.И. Копылов

Баганур кен орнының (Монғолия) қоңыр көмірінің термолизі

Баганур кен орнының (Монғолия) қоңыр көмірінің термолизі үрдісі зерттелді. Бұл көмірлер газдардың көп мөлшерімен (40 % дейін) және сұйық фракцияның ~200 ℃ басталады. ~700 ℃ дейінгі температурада пісу болмайды. Қатты қалдықта бастапқы көмірдің тек жеке көмірсутекті құрамдастарының реликтері кездеседі. Айдаудың сұйық конденсатында (бастапқы мөлшерден 19 % дейін) 0,78 % органикалық экстракт (96–98 % фенолды масса, максималды қайнау температурасы 360 ℃) және 92,2 % сулы ерітінді (қайнаудың температуралық интервалы 115–130 ℃) болады. Бастапқы агрегаттық күй (материал бөлшектерінің ірілігі, оған қоршаған ортаның әсері) термолиз кезінде көмірдің газдық құрамдасының шығымына әсер етіп қана қоймай, айдаудың сұйық конденсатының қоспалық құрамына да ықпал етеді.

Кілт сөздер: термолиз, қоңыр көмірлер, қатты қалдық, айдау, конденсат, көмірсутектер, фенолдар, термиялық талдау.

Н.И. Копылов

Термолиз бурого угля Баганурского месторождения (Монголия)

Изучен процесс термолиза бурого угля Баганурского месторождения Монголии. Данные угли отличаются высоким содержанием газовой составляющей (до 40 %) и низким содержанием жидкой фракции. Разложение материала начинается при ~200 ℃. При температурах вплоть до ~700 ℃ спекание отсутствует. В твёрдом остатке сохраняются только реликты отдельных углеводородных составляющих исходного угля. Жидкий конденсат возгонов (до 19 % мас. от исходного) содержит 0,78 % органического экстракта (96–98 % фенольной массы с максимальной температурой выкипания 360 ℃) и 92,2 % водного раствора (с температурным интервалом кипения 115–130 ℃). Исходное агрегатное состояние (крупность частиц материала, воздействие на него внешней среды) не только влияет на выход газовой составляющей угля при термолизе, но и определяет примесный состав органического экстракта жидкого конденсата возгонов.

Ключевые слова: термолиз, бурые угли, твёрдый остаток, возгоны, конденсат, углеводороды, фенолы, термический анализ.

References

1 *Gornaia entsyclopediia [Mountain encyclopedia]*. (1991). (Vol. 5). Moscow: Sovetskaia entsiklopediia [in Russian].

2 Shabanov, V.I., & Yakovlev, I.Yu. (1989). Marochnyi sostav uhley plasta Uluh Uluh-Khemskoho basseina [Vintage composition of coals of the Ulugh Ulug-Khem basin]. *Khimiia tverdoho topliva — Solid Fuel Chemistry, 6,* 52–55 [in Russian].

3 Bat-Orahikh Erdenetsogt, Insung Lee, Belegiin Bat-Erdene, & Luvsanhultem Jargal (2009). *Int. J. Coal Geol., 80,* 87.

4 Mironova, N.A., Khasina, R.A., & Khurts, Ch. (Eds.). (1977). *Heolohiia Monholskoi Narodnoi Respubliki [Geology of the Mongolian People's Republic]*. Moscow: Nedra [in Russian].

5 Kopylov, N.I., & Kaminskii, Yu.D. (2013) Termicheskoe razlozhenie uhlei Tuvinskoho mestorozhdeniia [Thermal decomposition of coals of the Tuva deposit]. *Khimiia v interesakh ustoychivoho razvitiia — Chemistry for Sustainable Development, 21, 3,* 319–327 [in Russian].

6 Kopylov, N.I., Kaminskiy, Yu.D., Dugarzhav, Zh., Avid, B., & Patrushev, Yu.V. (2013). Termoliz buroho uhlia Bahanurskoho mestorozhdeniia (Monholiia) [Thermolysis of brown coal from Boganursky deposit (Mongolia)]. *Khimiia v interesakh ustoichivoho razvitiia — Chemistry for Sustainable Development, 21, 5,* 499–504 [in Russian].

G. Burkitseterkyzy, G.L. Katkeeva, I.M. Oskembekov,
D.R. Gizatullina, A.M. Zhunussov

Zh. Abishev Chemical-Metallurgical Institute, Karaganda, Kazakhstan
(E-mail: katkeeva@mail.ru)

Study of the material composition of raw materials and the thermodynamic analysis of ore sulphidization

This research is aimed at a complex solution of two problems — increasing the efficiency of processing of oxidized copper ores and utilization of sulfur-containing waste from oil and gas processing. By the methods of chemical, mineralogical and granulometric analyzes the composition of the Sayak ore and waste sulfur was examined. It was found that the total copper content in the ore made 2.7 %, 1.8 % of which is represented by oxidized minerals. The main ore minerals are malachite, azurite, brochantite and chrysocolla. A thermodynamic analysis of the interaction of oxidized copper minerals with dissolved elemental sulfur possessing the properties of nanoparticles was carried out. The possibility in principle of copper sulfidization was established. Based on the obtained data on the thermodynamic properties of polysulfide systems, $\Delta_f H^0_{298.15}$, $S^0_{298.15}$, $\Delta_f G^0_{298.15}$, $C_p^0{}_{298.15}$ of eight polysulfides — CaS_2, CaS_3, CaS_4, CaS_5, CaS_6, CaS_7, CaS_8 и CaS_9 were defined. The temperature dependences of the standard Gibbs energy of the reaction of dissolved sulfur with oxidized copper minerals — malachite, azurite, brochantite and chrysocolla — were defined. The possibility in principle of sulfidization of oxidized copper minerals with dissolved elemental sulfur possessing the properties of nanoparticles was established. It is shown that in the temperature range 298.15–500 K the formation of copper (II) sulfide and sulfur (IV) oxide in the interaction of oxidized copper minerals with elemental nano-sized sulfur is most likely. As the standard Gibbs energy of the sulfidation reaction increases, the minerals can be arranged in a row up to 400 K: azurite; malachite; brochantite; chrysocolla, after 400 K: azurite; brochantite; malachite; chrysocolla. In these rows, the probability of interaction with sulfur decreases.

Keywords: oxidized copper ore, sulfidization, polysulfides, sulfur-containing waste.

The problem of processing oxidized copper ores is urgent in the copper industry of Kazakhstan. It is caused by the lack of cost-effective technology for concentration of this type of raw materials. Relatively cheap flotation methods of concentration, which are traditional in the processing of sulphide raw materials, are ineffective in view of the natural hydrophilicity of oxidized copper minerals. As a result, about 20 % of the total volume of mined copper mineral products that fall to the share of oxidized ores accumulate in the form of dumps and are on the balance sheet of the corresponding enterprises, requiring maintenance costs, which leads to an increase in the cost price of the final product of these enterprises [1].

The problem of sulfur utilization is caused by the excess of supply over demand in the elemental sulfur market. This is caused by the increase in the production of associated sulfur in the processing of constantly increasing volumes of sulfur-containing oil and gas raw materials and deeper purification from sulfur of the off-gases and flue gases of the coke-chemical, metallurgical and energy industries, which is dictated by the toughening of requirements for environmental protection. Forced storage of non-distributed surplus commodity sulfur, as well as storage of sulfur-containing waste in the form of dumps require large areas of territory and financial costs for maintenance by oil and gas processing enterprises. In addition, these warehouses and dumps are sources of soil and air pollution [2, 3].

The solution of the problem of oxidized ores concentration is seen in the change in the properties of oxidized minerals towards the hydrophobization of the surface, which would improve the efficiency of the flotation method. One of the methods of solving the problem is chemical modification of minerals by means of sulphidization, as a result of which oxidized minerals are converted to sulphide minerals with the hydrophobic surface. For this transformation nanosized element waste sulfur can be used. In addition to the sulfiding role, nano-sulfur, depositing on the mineral surface, plays an additional hydrophobization role [4].

To determine the principle possibility of the sulfidation of oxidized copper minerals, a thermodynamic analysis of their interaction with sulfur was carried out.

Chemical composition of Sayak ore

The technological sample of Sayak deposit ore, according to mineralogical composition and genetic characteristics, also falls to the oxidized type of copper ore. The main ore minerals are malachite, azurite and chalcopyrite, the secondary ones are pyrite, magnetite, hematite, iron hydroxides.

The chemical composition of the studied ore samples was determined by chemical and spectral analysis methods. The results are shown in Table 1.

Chemical composition of copper ore of Sayak deposit

Component	Content, %	Component	Content, %
$Cu_{общ.}$	2.7	CaO	2.79
$Cu_{окисл.}$	1.80	MgO	2.40
SiO_2	56.60	Pb	1.01
Al_2O_3	14.42	Zn	–
$Fe_{общ.}$	6.18	$S_{общ.}$	0.13

In the ore, the content of oxidized copper made 66.7 % of its total amount. In terms of copper, the ore is mixed.

Thermodynamic analysis of the interaction of ore components with elemental sulfur

Thermodynamic analysis of the interaction of ore components with elemental sulfur was carried out. When preparing the investigated ores for flotation concentration, their preliminary sulphidization was provided. The main sulphiding chemical is dissolved elemental sulfur, which possesses the properties of nanoparticles. The possibility in principle of interaction of this sulfur with the raw materials oxidized copper minerals is considered in the thermodynamic analysis of possible sulfidization reactions and calculation of the temperature dependence of the standard Gibbs energy of the reaction.

Initial thermodynamic data

The temperature dependences of the standard Gibbs energy of compound formation is calculated according to the equation

$$\Delta_f G^0_T = \Delta_f H^0_0 - T\Delta_f \Phi^*_T, \tag{1}$$

on the basis of the data [5–8] for the reduced Gibbs energy and the standard enthalpy of formation at 0 K (Tables 2, 3).

Temperature dependence of the change in the reduced Gibbs energy of the formation of compounds

Substance	T, K					
	298.15	300	350	400	450	500
	$\Delta\Phi^*_T$, $J\cdot mol^{-1}\cdot K^{-1}$					
S	22.9	22.9	22.3	22.1	22.1	20.2
H_2O	−164.7	−164.7	−164.5	−34.5	−37.1	−39.7
SO_2	19.5	19.5	18.0	16.7	14.9	13.1
SO_3	−63.9	−64.0	−66.3	−69.6	−71.0	−74.9
CO_2	4.1	4.1	4.0	3.8	3.7	3.5
SiO_2	−165.7	−165.8	−166.9	−170.1	−169.2	−172.6
Cu_2S	13.2	13.3	13.5	15.1	16.9	17.4
CuS	20	2.0	2.0	1.8	1.1	0.4

Standard enthalpy of formation of compounds at 0 K

Substance	$\Delta_f H^0_0$, $kJ\cdot mol^{-1}$	Substance	$\Delta_f H^0_0$, $kJ\cdot mol^{-1}$
S	13.2	CO_2	−393.1
H_2O	−286.3	SiO_2	−906.0
SO_2	−294.3	Cu_2S	−81.1
SO_3	−390.1	CuS	−55.0

The required values of the standard enthalpy of formation at 298.15 K [8, 9] for calculating the temperature dependence of the standard Gibbs energy of formation by the equation are given in Table 4.

$$\Delta_f G^0_T = \Delta_f H^0_{298.15} - T\Delta_f S^0_{298.15} - TM\Delta_f C^0_{p\,298.15}. \tag{2}$$

Standard enthalpy of formation of substances at 298.15 K

Substance	$\Delta_f H^0_{298.15}$, kJ·mol⁻¹
$Cu_2CO_3(OH)_2$	−1051.0
$Cu_3(CO_3)_2(OH)_2$	−1631.3
$CuSiO_3·2H_2O$	−1747.3
$Cu_4SO_4(OH)_6$	−2179.9

The values of the standard entropy of the formation of substances calculated using the data [8] are given in Table 5.

The standard heat capacity of compound formation was calculated using the data [8]. Its values are given in Table 6. Data on the chrysocolla standard heat capacity are taken from [10]. The standard heat capacity of the formation of azurite, malachite and brochantite was calculated through the standard heat capacity, which was estimated using the Kumok's heat capacity increment system [11, 12] by the formula

$$C^0_{p\,298.15}(A_mB_n) = mC^i_{p\,298,15}(A^{n+}) + nC^i_{p\,298,15}(B^{m-}). \tag{3}$$

Standard entropy of formation of substances

Substance	$\Delta_f S^0_{298.15}$, J·mol⁻¹·K⁻¹
$Cu_2CO_3(OH)_2$	−503.5
$Cu_3(CO_3)_2(OH)_2$	−671.5
$CuSiO_3·2H_2O$	−629.3
$Cu_4SO_4(OH)_6$	−1211.0

Standard heat capacity of formation of substances

Substance	$\Delta_f C^0_{p\,298.15}$, J·mol⁻¹·K⁻¹
$Cu_2CO_3(OH)_2$	−4.5
$Cu_3(CO_3)_2(OH)_2$	−4.2
$CuSiO_3·2H_2O$	45.3
$Cu_4SO_4(OH)_6$	−21.4

On the basis of the obtained data, the temperature dependence of the standard Gibbs energy for the formation of all participants in the investigated interactions was calculated by the formulas (1, 2). The results are given in Table 7.

Temperature dependence of the standard Gibbs energy of formation of substances

Substance	T, K					
	298.15	300	350	400	450	500
	$\Delta_f G^0_T$, kJ·mol⁻¹					
1	2	3	4	5	6	7
S	6.4	6.4	5.4	4.4	3.3	3.1
H_2O	−237.2	−236.9	−228.7	−225.1	−222.1	−219.1
CO_2	−394.4	−394.4	−394.5	−394.7	−394.8	394.9
SiO_2	−856.6	−856.2	−847.5	−837.9	−829.8	−819.7
SO_2	−300.2	−300.2	−300.6	−301.0	−301.1	−300.9
SO_3	−371.1	−370.9	−366.9	−362.3	−358.2	−352.7

1	2	3	4	5	6	7
Cu_2S	−85.0	−85.0	−85.8	−87.1	−88.7	−89.7
CuS	−55.6	−55.6	−55.7	−55.7	−55.5	−55.2
$Cu_2CO_3(OH)_2$	−900.9	−900.0	−874.8	−849.5	−824.3	−799.0
$Cu_3(CO_3)_2(OH)_2$	−1431.1	−1429.9	−1396.3	−1362.7	−1329.0	−1295.4
$CuSiO_3 \cdot 2H_2O$	−1559.7	−1558.5	−1527.2	−1496.3	−1465.6	−1435.2
$Cu_4SO_4(OH)_6$	−1818.8	−1816.5	−1755.9	−1695.1	−1634.2	−1573.1

The temperature dependences of the standard Gibbs energy of the reaction of dissolved sulfur with oxidized copper minerals — malachite, azurite, brochantite and chrysocolla — were defined.

Thermodynamic analysis of the interaction of sulfur with brochantite

The following four interactions of dissolved sulfur with brochantite were considered:

$$Cu_4SO_4(OH)_6 + 4S = 2Cu_2S + SO_3 + 2SO_2 + 3H_2O \tag{4}$$

$$3Cu_4SO_4(OH)_6 + 10S = 6Cu_2S + 7SO_3 + 9H_2O \tag{5}$$

$$Cu_4SO_4(OH)_6 + 6S = 4CuS + SO_3 + 2SO_2 + 3H_2O \tag{6}$$

$$3Cu_4SO_4(OH)_6 + 16S = 12CuS + 7SO_3 + 9H_2O \tag{7}$$
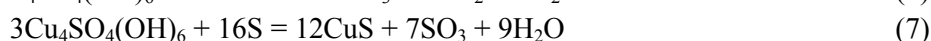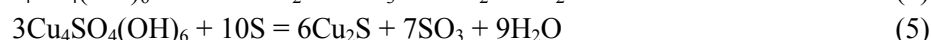
The probability of these interactions was judged by the change in the standard Gibbs energy:

$$\Delta_r G^0_T = 2\Delta_f G^0_T(Cu_2S) + \Delta_f G^0_T(SO_3) + 2\Delta_f G^0_T(SO_2) + 3\Delta_f G^0_T(H_2O) - $$
$$- \Delta_f G^0_T(Cu_4SO_4(OH)_6) - 4\Delta_f G^0_T(S); \tag{8}$$

$$\Delta_r G^0_T = 6\Delta_f G^0_T(Cu_2S) + 7\Delta_f G^0_T(SO_3) + 9\Delta_f G^0_T(H_2O) - $$
$$- 3\Delta_f G^0_T(Cu_4SO_4(OH)_6) - 10\Delta_f G^0_T(S); \tag{9}$$

$$\Delta_r G^0_T = 4\Delta_f G^0_T(CuS) + 1\Delta_f G^0_T(SO_3) + 2\Delta_f G^0_T(SO_2) + 3\Delta_f G^0_T(H_2O) - $$
$$- \Delta_f G^0_T(Cu_4SO_4(OH)_6) - 6\Delta_f G^0_T(S); \tag{10}$$

$$\Delta_r G^0_T = 12\Delta_f G^0_T(CuS) + 7\Delta_f G^0_T(SO_3) + 9\Delta_f G^0_T(H_2O) - $$
$$- 3\Delta_f G^0_T(Cu_3(Cu_4SO_4(OH)_6) - 16\Delta_f G^0_T(S). \tag{11}$$

Substituting the values of the corresponding quantities from Table 7 to the equations, we obtained the temperature dependence of the standard Gibbs energy of the reactions (4–7). By the formula

$$\lg K_{P(T)} = -\Delta_r G^0_T/(2{,}303RT) \tag{12}$$

the temperature dependence of the reaction equilibrium constant was calculated. The results are given in Table 8.

Table 8

Temperature dependence of the standard Gibbs energy and the equilibrium constant of the reaction of dissolved sulfur with brochantite

Reaction	T, K	298.15	300	350	400	450	500
4	$\Delta_r G^0_T$, kJ·mol⁻¹	−59.9	−61.1	−91.5	−136.3	−183.1	−230.5
	Equation	$\Delta_r G^0_T = -0.843T + 195.8$					
	$\lg K_P$	10.5	10.6	13.6	17.8	21.2	24.1
5	$\Delta_r G^0_T$, kJ·mol⁻¹	50.0	49.0	24.1	−14.4	−56.3	−96.9
	Equation	$\Delta_r G^0_T = -0.727T + 271.0$					
	$\lg K_P$	−8.8	−8.5	−3.6	1.9	6.5	10.1
6	$\Delta_r G^0_T$, kJ·mol⁻¹	−125.1	−126.3	−153.5	−193.7	−234.3	−278.1
	Equation	$\Delta_r G^0_T = -0.753T + 103.2$					
	$\lg K_P$	21.9	22.0	22.9	25.3	27.2	29.0
7	$\Delta_r G^0_T$, kJ·mol⁻¹	−15.2	−16.2	−37.9	−71.8	−107.5	−144.5
	Equation	$\Delta_r G^0_T = -0.637T + 178.5$					
	$\lg K_P$	2.7	2.8	5.6	9.4	12.5	15.1

Based on the data in Table 8, the temperature dependences of the standard Gibbs energy of the reaction of dissolved sulfur with brochantite are shown in Figure.

◇— reaction (4); ☐— reaction (5); Δ — reaction (6); × — reaction (7)
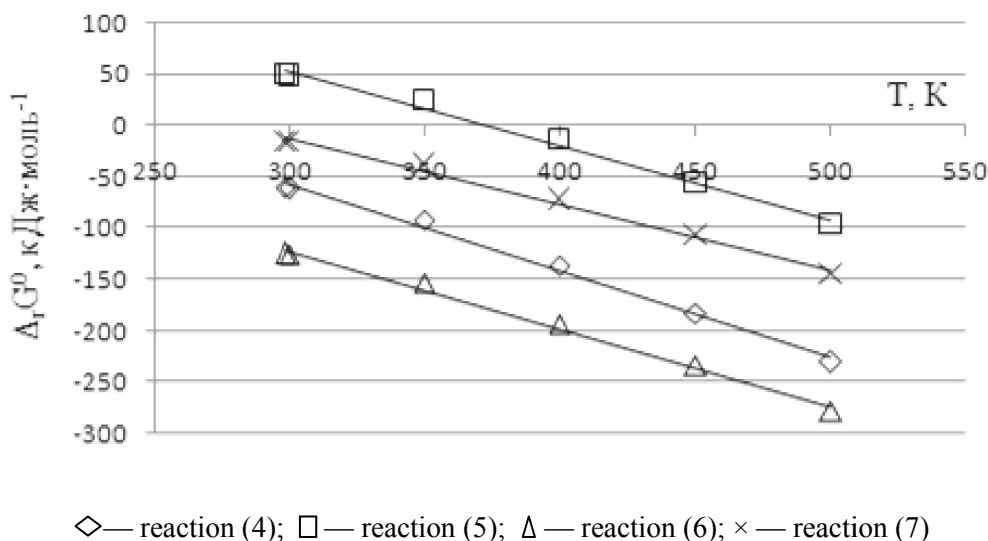
Figure. Temperature dependences of the standard Gibbs energy
of the reaction of dissolved sulfur with brochantite

According to the temperature dependence of the standard Gibbs energy of the reaction, the formation of copper (II) sulphide and sulfur (IV) oxide is most likely in the interaction of brochantite with elemental nano-sized sulfur. Temperature rise increases the probability of this interaction.

The probability of reactions (4) and (7) is also high. Reaction (5) is likely with a temperature of 100 ℃ and higher.

Conclusions

The studies of the chemical, mineralogical and granulometric composition of the copper ore of Sayak deposit have been carried out. It has been established that the examined ore with the content of $Cu_{tot/ox}$=2.7/1.8 is oxidized by 67 %.

According to the mineralogical analysis in the Sayak ore, the main ore minerals are the oxidized minerals of copper — malachite and azurite. Iron is represented in the form of minor minerals — pyrite, magnetite, hematite and iron hydroxides. According to the X-ray diffraction analysis, silicon and aluminum form non-metallic minerals in the form of quartz, feldspar, chlorite and mica.

The results of thermodynamic analysis indicate a possibility in principle of sulfidization of oxidized copper minerals — malachite, azurite, brochantite and chrysocolla, dissolved by elemental sulfur, which possesses the properties of nanoparticles.

References

1   Смирнов С. Медные проблемы цветной металлургии / С. Смирнов // Kazakhstan. — 2010. — № 3.

2   Мировой рынок серы. [ЭР]. — Режим доступа: http://www.webeconomy.ru/index.php?newsid=1300&page=cat&type= news.

3   Елюбаева Ж.С. Правовые аспекты производства, хранения и транспортировки серы в Казахстане и странах СНГ / Ж.С. Елюбаева // Химическая и нефтехимическая промышленность в СНГ: III конф. — Амстердам, 2006.

4   Шайке Ж.А. Выбор оптимального режима сульфидизации окисленной медной руды / Ж.А. Шайке, Г.Л. Каткеева, И.М. Оскембеков, Д.Р. Гизатуллина, М.А. Акубаева // Промышленность Казахстана. — 2014. — № 4. — С. 68–71.

5   Гурвич Л.В. Термодинамические свойства индивидуальных веществ / Л.В. Гурвич, И.В. Вейц, В.А. Медведев и др. — М.: Наука, 1978. — Т. I, Кн. 2. — 328 с.

6   То же, 1966. — Вып. II. — 96 с.

7   Термодинамические свойства индивидуальных веществ. [ЭР]. — Режим доступа: http://www.chem.msu.su/Zn/ welcome.html.

8   Термические константы веществ. [ЭР]. — Режим доступа: http://www.chem.msu.su/cgi-bin/tkv.pl?show=welcom.html.

9   Свойства минералов. [ЭР]. — Режим доступа: http://www.74rif.ru/mineral-gl.html.

10   Бабушкин В.И. Термодинамика силикатов / В.И. Бабушкин, Г.М. Матвеев, О.П. Мчедлов-Петросян. — М.: Стройиздат, 1986. — 408 с.

11 Кумок В.Н. Проблема согласования методов оценки термодинамических характеристик / В.Н. Кумок // Прямые и обратные задачи химической термодинамики. — Новосибирск: Наука, 1987. — С. 108–123.

12 Касенов Б.К. Термодинамические методы в химии и металлургии / Б.К. Касенов, А.С. Пашинкин, М.К. Алдабергенов. — Алматы: Рауан, 1994. — 256 с.

Г. Бүркітсетерқызы, Г.Л. Каткеева, И.М. Оскембеков, Д.Р. Гизатуллина, А.М. Жунусов

Шикізаттың заттық құрамын зерттеу және кенді сульфидтеудің термодинамикалық талдауы

Мақала тотыққан мыс кендерін байытудың тиімділігін арттыру және мұнай мен газ қалдықтарын өндеу кезіндегі күкіртқұрамды қалдықтарды кәдеге жарату мәселелерін кешенді шешуге бағытталған. Химиялық, минералогиялық және гранулометриялық талдау әдістері бойынша Саяқ кенінің және қалдық күкірттің құрамдары зерттелді. Кендегі жалпы мыстың құрамы 2,7 %, оның ішінде 1,8 % тотыққан минералдар екендігі анықталды. Негізгі кен минералдары малахит, азурит, брошантит және хризоколла болып табылады. Тотыққан мыс минералдарының, нанобөлшектік қасиеттерге ие, еріген элементтік күкіртпен әсерлесуінің термодинамикалық талдауы жүргізілді. Мыс сульфидтенуінің басты мүмкіндігі анықталды. Полисульфидтік жүйелердің термодинамикалық қасиеттері бойынша алынған нәтижелер негізінде CaS_2, CaS_3, CaS_4, CaS_5, CaS_6, CaS_7, CaS_8 және CaS_9 полисульфидтерінің $\Delta_f H^0_{298,15}$, $S^0_{298,15}$, $\Delta_f G^0_{298,15}$, $C^0_{p\,298,15}$ көрсеткіштері алынды. Еріген күкірттің тотыққан мыс минералдары — малахит, азурит, брошантит және хризоколламен әсерлесу реакциялары бойынша стандартты Гиббс энергиясының температуралық тәуелділіктері белгіленді. Тотыққан мыс минералдарының, нанобөлшектік қасиеттерге ие, еріген элементтік күкіртпен сульфидтенуінің негізгі мүмкіндіктері зерттелді. 298,15–500 К температура интервалында тотыққан мыс минералдарының элементтік наномөлшерлі күкіртпен әсерлесуі кезінде мыс (II) сульфиді мен күкірт (IV) оксиді түзілуінің мүмкіндігі жоғары екені анықталды. Сульфидтеу реакцияларындағы стандартты Гиббс энергияларының артуы бойынша 400 К-ге дейін мынадай қатарға орналастыруға болады: азурит, малахит, брошантит, 400 К-нен кейін: азурит, брошантит, малахит, хризоколла. Осы қатарда күкіртпен әрекеттесу ықтималдылығы азаяды.

Кілт сөздер: тотыққан мыс кені, сульфидтеу, полисульфидтер, күкіртқұрамды қалдықтар.

Г. Буркитсетеркызы, Г.Л. Каткеева, И.М. Оскембеков, Д.Р. Гизатуллина, А.М. Жунусов

Изучение вещественного состава сырья и термодинамический анализ сульфидизации руды

Статья направлена на комплексное решение двух проблем — повышение эффективности обогащения окисленных медных руд и утилизацию серосодержащих отходов переработки нефти и газа. Методами химического, минералогического, гранулометрического анализов исследованы составы саякской руды и отходной серы. Установлено, что содержание общей меди в руде 2,7 %, из них 1,8 % представлено окисленными минералами. Главные рудные минералы представлены малахитом, азуритом, брошантитом и хризоколлой. Проведен термодинамический анализ взаимодействия окисленных медных минералов с растворенной элементной серой, обладающей свойствами наночастиц. Установлена принципиальная возможность сульфидизации меди. На основе полученных данных по термодинамическим свойствам полисульфидных систем определены $\Delta_f H^0_{298,15}$, $S^0_{298,15}$, $\Delta_f G^0_{298,15}$, $C^0_{p\,298,15}$ восьми полисульфидов — CaS_2, CaS_3, CaS_4, CaS_5, CaS_6, CaS_7, CaS_8 и CaS_9. Кроме того, установлены температурные зависимости стандартной энергии Гиббса реакции растворенной серы с окисленными медными минералами — малахитом, азуритом, брошантитом и хризоколлой. Указана принципиальная возможность сульфидизации окисленных медных минералов растворенной элементной серой, обладающей свойствами наночастиц. Показано, что в температурном интервале 298,15–500 К при взаимодействии окисленных медных минералов с элементной наноразмерной серой наиболее вероятно образование сульфида меди (II) и оксида серы (IV). По мере возрастания стандартной энергии Гиббса реакции сульфидирования минералы можно расположить в ряд до 400 К: азурит, малахит, брошантит, хризоколла, после 400 К: азурит, брошантит, малахит, хризоколла. В данных рядах уменьшается вероятность взаимодействия с серой.

Ключевые слова: окисленная медная руда, сульфидизация, полисульфиды, серосодержащие отходы.

References

1 Smirnov, S. (2010). Mednye problemy tsvetnoi metallurhii [Copper Problems of Non-Ferrous Metallurgy]. *Kazakhstan*, 3 [in Russian].

2 Mirovoi rynok sery [Global sulfur market] (n.d.). *www.webeconomy.ru.* Retrieved from http://www.webeconomy.ru /index.php?newsid= 1300&page=cat&type=news [in Russian].

3 Yelyubayeva, Zh.S. (2006). Pravovye aspekty proizvodstva, khraneniia i transportirovki sery v Kazakhstane i stranakh SNG [Legal aspects of sulfur production, storage and transportation in Kazakhstan and CIS countries]. Proceedings from Chemical and petrochemical industry in the CIS '06: *III konferentsiia — IIIrd Conference.* Amsterdam [in Russian].

4 Shaike, Zh.A., Katkeyeva, G.L., Oskembekov I.M., Gizatullina, D.R., & Akubayeva, M.A. (2014). Vybor optimalnoho rezhima sulfidizatsii okislennoi mednoi rudy [Choice of optimal mode of sulfidization of oxidized copper ore]. *Promyshlennost Kazakhstana — Industry of Kazakhstan, 4,* 68–71 [in Russian].

5 Gurvich, L.V., Veits, I.V., Medvedev, V.A. et al. (1978). *Termodinamicheskie svoistva individualnykh veshchestv [Thermodynamic properties of individual substances].* (Iss. I, Book 2). Moscow: Nauka [in Russian].

6 As above (1966). (Iss. II) [in Russian].

7 Termodinamicheskie svoistva individualnykh veshchestv [Thermodynamic properties of individual substances] (n.d.). *www.chem.msu.su* Retrieved from http://www.chem.msu.su/ Zn/welcome.html [in Russian].

8 Termicheskie konstanty veshchestv [Thermal constants of substances] (n.d.). *www.chem.msu.su* Retrieved from http://www.chem.msu.su/cgi-bin/tkv.pl? show=welcom.html [in Russian].

9 Svoistva mineralov [Properties of minerals] (n.d.). *www.74rif.ru* Retrieved from http://www.74rif.ru/mineral-gl.html [in Russian].

10 Babushkin, V.I., Matveyev, G.M., & Mchedlov-Petrosyan, O.P. (1986). Termodinamika silikatov [Thermodynamics of silicates]. Moscow: Stroiizdat [in Russian].

11 Kumok, V.N. (1987). Problema sohlasovaniia metodov otsenki termodinamicheskikh kharakteristik [The problem of coordination of methods for estimating thermodynamic characteristics]. *Priamye i obratnye zadachi khimicheskoi termodinamiki — Direct and inverse problems of chemical thermodynamics.* Novosibirsk: Nauka [in Russian].

12 Kassenov, B.K., Pashinkin, A.S., & Aldabergenov, M.K. (1994). *Termodinamicheskie metody v khimii i metallurgii [Thermodynamic methods in chemistry and metallurgy].* Almaty: Rauan [in Russian].

S.A. Vizer, N.O. Akimbayeva, K.B. Yerzhanov

A.B. Bekturov Institute of Chemical Sciences, Almaty, Kazakhstan
(E-mail: s-w07@bk.ru)

«Green» chemistry methods in synthesis of flotation agents

A review of the authors' own works devoted to the development of «green» methods of chemistry in the synthesis of various derivatives of monoethanolamine and diethanolamine, which are potential surface active substances and flotation agents, is made up. It is shown that the application of the «green» chemistry principles, for example, implication of 5 molar % an organic phase transfer catalyst — tetrabutylammonium iodide in alkylation reactions makes it possible to significantly increase (in two to three times) the yields of target substances N-alkylated derivatives of diethanolamine and monoethanolamine with a tenfold reduction in the duration of reactions and a lowering of the process temperature, which leads to a significant reduction in energy and labor costs. Synthesis of target flotation agents, for example, O-2-((dimethoxyphosphoryl)-(2-hydroxyethyl)amino)ethylxanthate and sodium 2-dimethoxyphosphoryloxyethyl carbamate by the atom-economic method — four-component reaction of the one-reactor interaction with a reduction in the number of stages from two to one also contributes to an increase in the total yield of target substances by 2–3 times.

Keywords: surface active substances, flotation agents, «green» chemistry, monoethanolamine and diethanolamine alkyl and dialkoxyphosphoryl derivatives, xanthate, carbamate.

Introduction

It is known, «green» chemistry means chemistry that efficiently processes raw materials (preferably renewable), excludes drains, avoids the use of toxic and harmful reagents and solvents in the production of chemical products and their application [1–3]. Acquiring new positions in technology development, «green» chemistry in the 21st century has become a truly new way of thinking, a new philosophy, a new language that allows us to look at chemistry not only from utilitarian positions (production of products that have demand), but above all with humanitar positions [2]. It should be emphasized that «green» chemistry and ecology are not the same thing. On the contrary, the final goal of «green» chemistry is to negate the efforts of ecologists to remove those harmful emissions that are the main problem of almost all chemical (and not only chemical) industries. If ecologists try to neutralize the consequences created by chemistry, then the task of «green» chemistry is to provide such production in which harmful consequences are generally absent or minimized. The basic principles of «green» chemistry were formulated at the beginning of the 21st century by Paul Anastas, one of the leaders of the US Environmental Protection Agency [3].

The current state of the technology of mineral processing makes it possible to ensure a fairly high degree of complex utilization of raw materials [4]. However, the further solution of the interrelated problems of more rational use of natural resources, ecology, energy and production management requires technologies for processing and enriching the mineral and other types of raw materials of a qualitatively new level [5]. Successful solution of the above problems is impossible without further improvement of the theory of enrichment processes, including selective opening and separation of minerals, separation of components of organic and inorganic substances from water [6]. The creation of new and modification of traditional flotation agents will allow increasing the extraction of target components from ores of nonferrous, noble and rare metals. In addition, from the economic point of view, the principle of creating new flotation agents should be the availability of starting reagents, which are easily obtained from petroleum hydrocarbons. In this regard, the problem of developing an efficient technology for the enrichment of polymetallic ores and the creation of highly effective, original and affordable flotation agents continues to be very actual [7].

It is known that the main groups of reagents used in the flotation of polymetallic sulphide ores are sulfhydryl anionic collectors — alkylxanthates, dithiocarbamates [5, 8] and dialkyldithiophosphates. Their collective ability largely depends on the structure and location of the hydrocarbon radical. This dependence has been studied in detail in a number of papers, from which it can be seen that a relatively small change in the structure of the collector molecule (for example, the elongation or isomerization of the hydrocarbon radical) leads to a significant change in the collection ability of the reagent [9−13].

The study of the properties of modified alkyl xanthates and dialkyl dithiophosphates is especially interesting, because a very limited number of publications are devoted to the study of the flotation properties of reagents of this kind, both in domestic and foreign literature.

«Green» synthesis of alkyl diethanolamine derivatives

As a result of our previous studies, high flotation activity and the selectivity of the action of a number of alkyl diethanolamine derivatives as additional collectors in flotation enrichment of sulfide polymetallic ores have been established. The disodium salt of N-octyl-N,N-bis(2-xanthateethyl)amine [14] and 2-[N-heptyl-N-(2-hydroxyethyl)amino]ethylxanthate sodium [15] significantly improve the quality of copper-lead concentrate at the processing of copper-lead-zinc-pyrite ore. N,N-Di(2-hydroxyethyl)aminononane [16] shows a high collecting activity in the flotation of lead-zinc-silver-containing ore, significantly increasing the extraction of lead, zinc and silver into the collective concentrate.

These reagents-collectors are obtained from commercially available diethanolamine in two stages via intermediate N-alkyldi(2-hydroxyethyl)amines.

In order to increase the yields of intermediate N-alkyldi(2-hydroxyethyl)amines in the preparation of compounds having flotation activity, an alkylation reaction of diethanolamine (DEA) with alkyl C_4-C_7 bromides (AB) was carried out. Previously, the alkylation reaction of DEA was usually carried out by heating (50–60 °C) in a water-alcohol medium for 3 days in the presence of a stoichiometric amount of potash [17]. At the same time, the yields of C_4-C_7 alkylated DEA derivatives ranged from 42 to 72 %.

Using one of the principles of «green» chemistry: «Catalytic systems and processes (as selective as possible) are better in all cases than stoichiometric ones» [2, 3] alkylation of DEA in the presence of an organic phase transfer catalyst — tetrabutylammonium iodide was carried out. As a result of the reactions of alkylation of DEA at room temperature for 2 hours in an aqueous alcohol medium and a molar ratio of DEA:AB:K_2CO_3: n-Bu$_4$NI = 1:1:1:0.1 reagents, 81 % of N-butyl-N,N-di(2-hydroxyethyl)amine, 87 % of N-pentyl-N,N-di(2-hydroxyethyl)amine, 87 % of N-hexyl-N,N-di(2-hydroxyethyl)amine, 92 % of N-heptyl-N,N-di(2-hydroxyethyl)amine were obtained (Fig. 1).

R = C_4H_9, C_5H_{11}, C_6H_{13}, C_7H_{15}
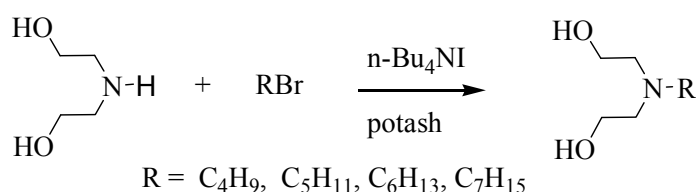
Figure 1. Synthesis of N-alkyl-N, N-diethanolamines

Based on the results obtained, it can be concluded that the alkylation reaction of DEA in accordance with the principles of «green» chemistry makes it possible to obtain N-alkyldi(2-hydroxyethyl)amines selectively and in a high yield, with a significant reduction in the reaction time and a 30 ℃ decrease in the process temperature, it leads to a reduction in energy and labor costs. At the same time, the yield of the target alkylaminoglycols almost doubles increases [18].

Application of the principles of «green» chemistry in the synthesis
of sodium O-2-((dimethoxyphosphoryl)(2-hydroxyethyl)amino)ethylxanthate

In continuation of our research to obtain new diethanolamine-based surfactants, we performed a diethanolamine phosphorylation reaction by dialkyl phosphites, as shown in the diagram in Figure 2.

R = CH_3, C_2H_5
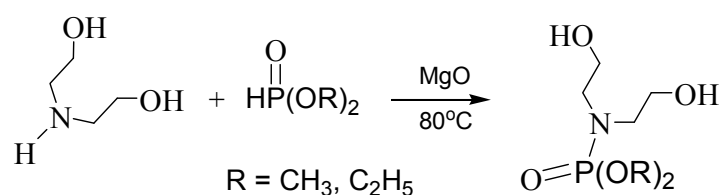
Figure 2. Scheme of phosphorylation of diethanolamine by dialkyl phosphites

The diethanolamine phosphorylation reaction was carried out by reacting diethanolamine with a dialkyl phosphite in a benzene medium in the presence of magnesium oxide at a temperature of 80 ºC. As a result, dialkyl bis (2-hydroxyethyl) phosphoramidates were obtained in the yields of 67 % and 65 %, respectively. The composition of the obtained phosphoramidates was confirmed on the basis of elemental analysis data, and the structure was confirmed on the basis of IR and NMR data of ^{1}H and ^{13}C, ^{31}P spectra [19]. In the IR spectra of synthesized phosphoramidates, intense bands of characteristic stretching vibrations of P=O and P–O–C bonds in the region 1196, 1162 cm^{-1} are observed, confirming the presence of a phosphorus-containing radical in the molecule of the obtained compounds. The presence in the spectra of intense absorption bands in the region of 3267±3387 cm^{-1} confirms the presence of hydroxyl groups in the structure of phosphoramidates. In the PMR spectrum of dimethyl-bis(2-hydroxyethyl)phosphoramidate in D$_2$O the protons of the OCH$_3$ substituents are observed as a doublet at 3.20 and 3.23 ppm, the protons of NCH$_2$ groups are resonated at 2.80–2.92 ppm, protons of OCH$_2$ groups at 3.48 ppm, protons of OH groups at 4.70 ppm in the form of a broadened singlet, which also confirms the reaction of the amine group.

In the PMR spectrum of diethyl-bis(2-hydroxyethyl)phosphoramidate in DMSO-d$_6$, the protons of ethyl substituents manifest themselves as two groups of signals: a triplet at 1.15 ppm with J = 7.3 Hz and two quartets at 3.85 ppm and 3.87 ppm with the same SSIC, the protons of NCH$_2$ groups are resonated at 2.95 and 2.98 ppm in the form of two triplets with SSIC 6.1 Hz, protons of CH$_2$OH groups at 3.41 ppm in the form of a triplet with J = 6.3 Hz, protons of OH groups at 4.70 ppm in the form of a broadened singlet.

The two-dimensional COSY spectrum of dimethyl-bis(2-hydroxyethyl)phosphoramidate, shown in a Figure 3, made it possible to establish the homonuclear interactions of H-H through three bonds and unambiguously confirm the structure of the obtained phosphamidate.

Figure 3. The two-dimensional COSY spectrum of dimethyl bis(2-hydroxyethyl)phosphamidate in D$_2$O

In the ^{13}C NMR spectrum of dimethyl-bis(2-hydroxyethyl)phosphoramidate, resonance signals in the region of 50.61 ppm corresponding to the OCH$_3$ groups, 57.44 and 59.82 ppm corresponding to the CH$_2$OH groups and the signals in the 39.87 and 41.05 ppm which belong to the groups CH$_2$N are observed. In the ^{13}C NMR spectrum of diethyl-bis(2-hydroxyethyl)phosphoramidate resonance signals are observed in the 16.4 ppm region corresponding to the OCH$_2$CH$_3$ groups, at 60.28 ppm. −OCH$_2$CH$_3$ groups and signals in the region of 49.28 ppm belong to the CH$_2$N groups, the signals at 61.78 ppm. — to CH$_2$OH groups.

In the ^{31}P spectrum of dimethyl-bis(2-hydroxyethyl)phosphoramidate, only one signal is observed in the region of 8.86 ppm, and in the ^{31}P spectrum of diethyl-bis(2-hydroxyethyl)phosphoramidate — one signal in the region of 11.17 ppm corresponding to the dialkoxyphosphamide group is observed.

Further conversion of dimethyl bis(2-hydroxyethyl)phosphamidate to sodium xanthate was carried out by reacting phosphamidate (FA) with carbon disulphide and sodium hydroxide at room temperature and the molar ratio of FA:CS$_2$:NaOH = 1:1:1 reagents in an alcohol medium, as shown in Figure 4. Sodium O-2-((dimethoxyphosphoryl)(2-hydroxyethyl)amino)ethylxanthate was obtained in a yield of 28 %, m.p. 78 °C. Since the yield of dimethyl-bis(2-hydroxyethyl)phosphamidate in the first stage was 67 %, the total yield of xanthate in two stages is 19 %.
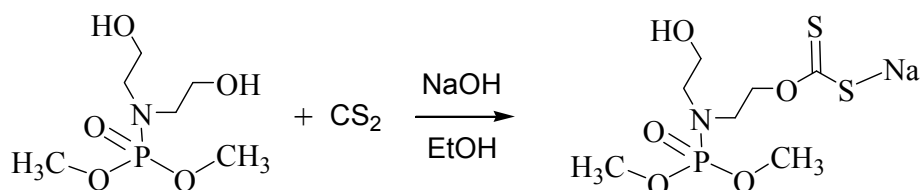
Figure 4. Scheme of dimethyl-bis(2-hydroxyethyl)phosphamidate reaction
with carbon disulphide and sodium hydroxide

Since the development of «green» methods for the synthesis of diethanolamine derivatives is one of the goals of our studies, we studied a one-reactor method for carrying out a four-component reaction of diethanolamine, dimethyl phosphite, carbon disulfide and sodium hydroxide, as the reduction in the number of stages of obtaining the target substance corresponds to a number of principles of «green» chemistry, and namely, principle 2, which reads: «*The synthesis strategy must be chosen in such a way that all materials used in the synthesis process are maximized were included in the product*», and also to principle 5, which reads: «*The use of auxiliary substances (solvents, extractants, etc.) should be minimized whenever possible*» [2, 3].

A four-component reaction of a single-reactor reaction of diethanolamine, dimethyl phosphite, carbon disulfide and sodium hydroxide, taken in a molar ratio of 1:1:1:1, was carried out in a ethyl alcohol medium at room temperature, as shown in the diagram in Figure 5. After appropriate treatment of the reaction mixture, sodium O-2-((dimethoxyphosphoryl)(2-hydroxyethyl)amino)ethylxanthate was isolated in a yield of 65 %, m.p. 78 °C.
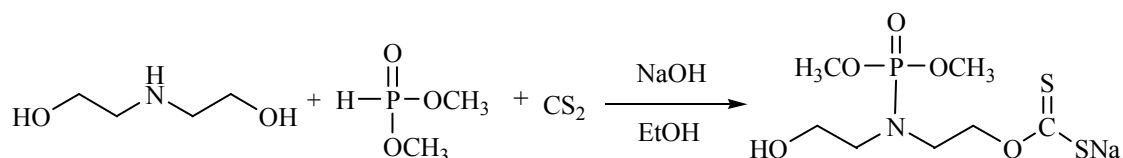
Figure 5. Scheme of a four-component reaction of a single-reactor interaction of diethanolamine,
dimethylphosphite, carbon disulfide and sodium hydroxide

The structure of the synthesized samples of O-2-((dimethoxyphosphoryl)(2-hydroxyethyl)amino)ethyl xanthogenate was established on the basis of the IR and ^{1}H NMR spectra analysis [19]. In the IR spectra of both xanthate samples in the region of 2847 ± 2952 cm^{-1}, absorption bands characteristic for valence vibrations of CH$_2$ and CH$_3$ groups of saturated hydrocarbons are observed. A wide strong OH band absorption band is manifested in the 3300 cm^{-1} region. The absorption band of medium intensity in the region of 1201 cm^{-1} is attributed to the stretching vibrations of the P=O group. Strong bands of stretching vibrations of P–O–C bonds are observed in the region of 1050 cm^{-1}. The presence of the C=S group is confirmed by the presence of very strong absorption bands in the spectrum at 1063 and 1070 cm^{-1}, weak bands in the 781 and 575 cm^{-1} regions correspond to vibrations of the C–S bond.

As a result of our studies, we have established that both the sequential reactions of diethanolamine phosphorylation and the interaction of the dimethylbis(2-hydroxyethyl)phosphoramide formed with the carbon disulphide and the four-component reaction of the one-reactor interaction of diethanolamine, dimethylphosphite, carbon disulfide and sodium hydroxide form sodium O-2-((dimethoxyphosphoryl)-(2-hydroxyethyl)amino)ethyl xanthate. The coincidence of the physicochemical characteristics of both xanthate samples confirms that in both cases the same substance was obtained.

Consequently, the practical application of the principles of «green» chemistry leads to the synthesis of the desired compound: sodium O-2-((dimethoxyphosphoryl)(2-hydroxyethyl)amino)ethylxanthate by the atom economical method — with a reduction in the number of stages from two to one, and increase of the total yield of the target substance more than three times (from 19 to 65 %).

The «green» method of monoethanolamine N-alkylation

Continuing the search for highly effective flotation agents among amino alcohol derivatives, we investigated the «green» methods for the alkylation of monoethanolamine (MEA) in order to increase the yield of target products while reducing energy and labor costs [20]. Previously, the alkylation reaction of MEA was carried out by the usual method of amine reaction with alkyl bromide in the presence of potassium acetate in anhydrous alcohol at 50–55 ℃ [21]. As a result of prolonged heating (20–30 h), corresponding N-monosubstituted MEA derivatives with the yields of 27–42 % and N,N-disubstituted derivatives of MEA with the yields of 7–10 % are formed. Obviously, the use of the conventional alkylation process gives a rather low yield of the target amino alcohols with a total reaction time of 3–5 days. Therefore, a search for a more economical method of synthesis was carried out.

In order to optimize the conditions for the interaction of MEA with alkyl halides and increase the yield of N-alkylation products, the reaction was carried out in various solvents — alcohol, acetone, dioxane, tetrahydrofuran, benzene. It has been experimentally established that 90 % alcohol is the most suitable solvent. In fact, the solubility of the initial reagent — MEA in alcohol is greatest. While in other polar solvents such as sulfuric ether, ethyl acetate, dioxane, tetrahydrofuran, MEA is practically insoluble, or dissolves poorly at room temperature, which consequently affects the yield of the final product.

Among the tested binding agents of hydrogen bromide, which was released in the reaction, — NaOH, KOH, sodium and potassium acetate, potash, the best yields of alkylated ethanolamines were obtained by using potash. Based on the analysis of scientific chemical literature on the application of «green» chemistry methods, it has been shown that one of the main principles of «green» chemistry is the use of catalysts in order to shorten the time of synthesis, reduce energy costs and increase the selectivity of reactions for rational use of initial reagents and reduce the costs of target products [1–3].

Since the MEA alkylation reaction is carried out in a two-phase liquid-solid system, an organic catalyst for the interfacial transfer the tetrabutylammonium iodide was used. With the addition of five mole percent catalyst, the alkylation process is significantly accelerated, and the reaction ends after two hours at room temperature. As a result of the reaction, monosubstituted N-alkyl-N-ethanolamines in the yields of 72–81 % and disubstituted N,N-dialkyl ethanolamines in the yields of 7–19 % were obtained under the conditions obtained (Fig. 6). The composition of the obtained compounds was confirmed on the basis of elemental analysis data, and the structure was based on IR and NMR data of ^{1}H and ^{13}C spectroscopy [20].

$$R = C_3H_7, \ C_4H_9, \ C_5H_{11}$$
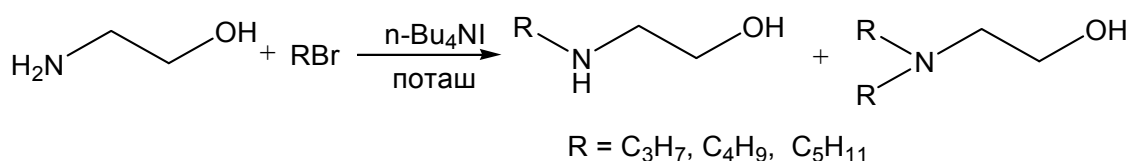
Figure 6. Synthesis of C_3–C_5 alkylated derivatives of MEA in «green» conditions

Thus, using the principles of «green» chemistry, carrying out the alkylation reaction of MEA in aqueous alcohol under organocatalysis conditions makes it possible to obtain N-alkylated derivatives of MEA selectively and in high yield, with an almost doubling of the yield of the target substances and a reduction in the reaction time by a factor of ten.

«Green» chemistry in the synthesis of sodium dimethoxyphosphoryloxyethyl carbamate

With the aim of developing new highly effective flotation reagents-collectors, we investigated the reaction of phosphorylation of MEA [22]. In the study of various reaction conditions, the best conversion of the initial MEA was achieved by phosphorylation with dimethyl phosphite (DMF) at 80 ℃ in benzene using magnesium oxide as the catalyst and a molar ratio of reagents MEA:DMF:MgO = 1:1:1. As a result of the reaction, 2-aminoethyldimethylphosphate (ADMP) was obtained in a yield of 65 % (Fig. 7). 2-Aminoethyldimethylphosphate is an oil, that is highly soluble in water.
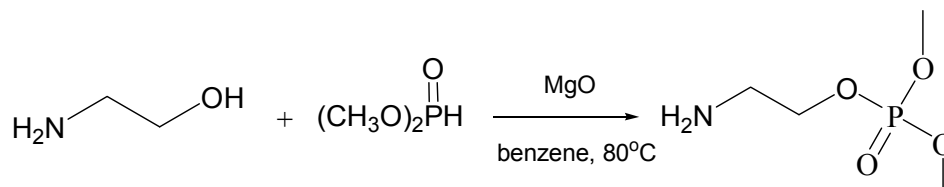
Figure 7. Phosphorylation of MEA by dimethyl phosphite

The composition and individuality of synthesized 2-aminoethyldimethylphosphate are confirmed by thin-layer chromatography and physicochemical characteristics. The structure of the compound was established on the basis of an analysis of the IR and NMR spectra of ^{1}H and ^{13}C, [31]P [22]. In the IR spectrum of the synthesized phosphate, given in a Table, there is an absorption band of the characteristic vibrations of the NH_2 group at 3440 cm^{-1}, in the region of 1190 cm^{-1} a characteristic band of the P=O group is observed, in the 1070 cm^{-1} the absorption band of P–O–C. In the [31]P 2-aminoethyldimethyl phosphate spectrum, only one signal is observed in the 6.72 ppm region corresponding to the phosphate group.

In order to obtain new surfactants, we investigated the reaction of 2-aminoethyldimethylphosphate with carbon disulfide. The reaction was carried out in the presence of an equimolar amount of sodium hydroxide in an ethyl alcohol medium at room temperature, as shown in Figure 8. The reaction yielded a crystalline product in 48 % yield, which is sodium 2-dimethoxyphosphoryloxyethylcarbamate (DMPC-1). At the same time, its total yield with respect to the initial MEA is 31 %.
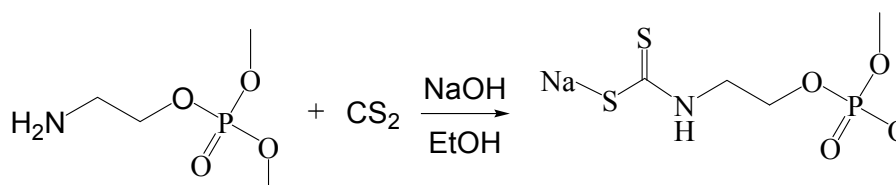
Figure 8. Interaction of 2-aminoethyldimethylphosphate with carbon disulfide

The structure and individuality of the synthesized compound — sodium 2-dimethoxyphosphoryloxy-ethylcarbamate — are confirmed by the data of physicochemical methods, IR and PMR spectroscopy [22], presented in Table.

In order to develop a «green» method for the synthesis of sodium 2-dimethoxyphosphoryloxy-ethylcarbamate, we carried out a four-component reaction of monoethanolamine, dimethylphosphite, carbon disulfide and sodium hydroxide, due to the fact that the reduction in the number of stages of obtaining the target substance corresponds to a number of principles of «green» chemistry [2, 3].

The four-component reaction of single-reactor method of MEA, DMF, carbon disulfide and sodium hydroxide in a molar ratio of 1:1:1:1 interaction was carried out in an ethyl alcohol medium at room temperature, as shown in the scheme in Figure 9. After the appropriate treatment of the reaction mixture, 2-dimethoxyphosphoryloxyethylcarbamate (DMFC-2) in 78 % yield.
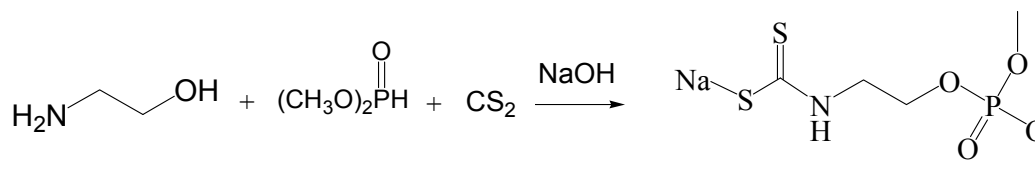
Figure 9. The single-reactor method of four-component reaction of MEA, DMF,
carbon disulfide and sodium hydroxide

As can be seen from the data in Table, the infrared spectra and nuclear magnetic resonance spectra of ^{1}H and ^{13}C of the sample of sodium 2-dimethoxyphosphoryloxyethyl carbamate (DMPC-2) obtained in the four-component reaction coincide with the spectra of the sample obtained in the reaction of 2-aminoethyldimethylphosphate with carbon disulfide DMPC-1.

T a b l e

Physico-chemical characteristics of synthesized MEA derivatives

MEA derivatives	A yield %	R_f	PMR spectra data, δ, ppm			IR spectra data, ν, sm^{-1}		
			CH_2NH_2 (CH_2NH)	OCH_3	OCH_2	P=O	P-O-C	$NH_2(NH)$
ADMP	65	0.17	2.95	3.24–3.27	3.58	1190	1070	3440
DMPC-1	48	0.28	(4.50)	3.26–3.28	3.62	1163	1050	(3414)
DMPC-2	78	0.29	(4.50)	3.27–3.31	3.62	1200	1053	(3425)

Thus, we have established that as a result of sequential reactions of phosphorylation of mono-ethanolamine and subsequent reaction of the 2-aminoethyldimethylphosphate formed with carbon disulphide and the four-component reaction of monoethanolamine, dimethyl phosphite, carbon disulfide and sodium hydroxide, a sodium 2-dimethoxyphosphoryloxyethyl carbamate is formed. In the latter case, its total yield increases in 2.5 times. Consequently, the application of the principles of «green» chemistry makes it possible to carry out the synthesis by an atom-economic method with a reduction in the number of stages from two to one and a significant increase in the yield of the target substance.

References

1 Шелдон Р.А. Каталитические превращения в воде и сверхкритическом диоксиде углерода с позиций концепции устойчивого развития / Р.А. Шелдон // Рос. хим. журн. — 2004. — Т. 48, № 6. — С. 74–83.

2 Кустов Л.М. «Green Chemistry» — новое мышление / Л.М. Кустов, И.П. Белецкая // Рос. хим. журн. — 2004. — Т. 48, № 6. — С. 3–12.

3 Anastas P. The Role of Catalysis in the Design, Development and Implementation of Green Chemistry / P. Anastas, L.B. Bartlett, M.M. Kirchhoff, T.C. Williamson // Catalysis Today. — 2000. — Vol. 55, No. 1–2. — P. 11–22.

4 Абрамов А.А. Флотационные методы обогащения / А.А. Абрамов. — М.: Изд-во Моск. гос. горного ун-та; Горная кн.; Мир горной кн., 2008. — 710 с.

5 Абрамов А.А. Собрание сочинений. Т.7. Флотация. Реагенты-собиратели / А.А. Абрамов. — М.: Изд-во Моск. гос. горного ун-та, 2010. — 656 с.

6 Абрамов А.А. Пути развития теории обогатительных процессов и создания инновационных технологий комплексного использования сырья / А.А. Абрамов // Физико-технические проблемы разработки полезных ископаемых. — 2012. — № 1. — С. 165–178.

7 Калугин С.Н. Химия и технология получения флотореагентов / С.Н. Калугин. — Алматы: Каз. ун-т, 2014. — 230 с.

8 Шубов Л.Я. Флотационные реагенты в процессах обогащения минерального сырья / Л.Я. Шубов, С.И. Иванков, Н.К. Щеглова. — В 2 кн. Кн. 1. — М.: Недра, 1990. — 400 с.

9 Абрамов А.А. Принципы выбора и синтеза более селективных собирателей во флотации / А.А. Абрамов, М.М. Сорокин // Цветные металлы. — 2009. — № 4. — С. 35–40.

10 Игнаткина В.А. Выбор селективных собирателей для флотации сульфидных минералов / В.А. Игнаткина // Цветные металлы. — 2009. — № 6. — С. 14–19.

11 Рябой В.И. Создание и применение более эффективных реагентов на основе физико-химических представлений / В.И. Рябой // Обогащение руд. — 2002. — № 1. — С. 19–23.

12 Чантурия В.А. Химия поверхностных явлений при флотации / В.А. Чантурия, Р.Ш. Шафеев. — М.: Недра, 1977. — 191 с.

13 Рубцов Н.В. Эффективность сочетаний ксантогенатов / Н.В. Рубцов, В.М. Усова // Технология обогащения полиметаллических руд: сб. науч. тр. ВНИИцветмет. — М.: Недра, 1972. — С. 132–136.

14 Ержанов К.Б. Инновационный патент РК № 26888. Динатриевая соль N-октил-N,N-бис(2-ксантогенатэтил)амина, обладающая флотационной активностью при обогащении сульфидных руд / К.Б. Ержанов, Н.О. Акимбаева, И.Н. Ануарбекова, Н.К. Тусупбаев, Ж.А. Ержанова, А.А. Муханова // БИ. — 2013. — № 5.

15 Ержанов К.Б. Инновационный патент РК № 28114. 2-[N-гептил-N-(2-гидроксиэтил)амино] этилксантогенат натрий, обладающий флотационной активностью / К.Б. Ержанов, Н.О. Акимбаева, И.Н. Ануарбекова, Н.К. Тусупбаев, Ж.А. Ержанова, А.А. Муханова // БИ. — 2014. — № 2.

16 Ергожин Е.Е. Инновационный патент РК № 26889. N,N-Ди(2-гидроксиэтил)аминононан, обладающий флотационной активностью при обогащении сульфидных руд / Е.Е. Ергожин, К.Б. Ержанов, Н.О. Акимбаева, И.Н. Ануарбекова, Н.К. Тусупбаев, Ж.А. Ержанова, А.А. Муханова // БИ. — 2013. — № 5.

17 Ержанов К.Б. Отчет о научно-исследовательской работе «Разработка технологии получения новых поверхностно-активных веществ на основе продуктов переработки углеводородного сырья», по научно-технической программе О.0537–03 «Научное обеспечение развития химической промышленности Республики Казахстан на 2010–2012 годы», 1 направление — переработка углеводородного сырья и нефтехимия, раздел 3 «Разработка и реализация технологий переработки углеводородного сырья с целью получения мономеров, полимеров и поверхностно-активных веществ». № Гос. регистрации 0110РК00199, отчеты в НЦНТИ под инв. номерами 0210РК01118 (2010 г.), 211РК00730 (2011 г.) 0212РК00833 (2012 г.) / К.Б. Ержанов, Н.Б. Курманкулов, С.А. Визер и др.

18 Akimbaeva N.O. Application of «green» chemistry's principles at the N-alkylation of diethanolamine / N.O. Akimbaeva, I.N. Anuarbekova, S.A. Vizer, K.B. Yerzhanov // Хим. журн. Каз. — 2016. — № 2(54). — С. 183–188.

19 Акимбаева Н.О. Промежуточный отчет по гранту «Исследование и разработка «зеленых» условий синтеза отечественных высокоэффективных и селективных флотореагентов на основе местного сырья для обогащения труднообогатимых полиметаллических и золотосодержащих руд» по бюджетной программе Г.2015 «Развитие науки», № гос. регистрации 0115РК00252, отчет в НЦНТИ, инв. номер 0216РК01536 (2016 г.) / Н.О. Акимбаева, К.Б. Ержанов, С.А. Визер, И.Н. Ануарбекова, М.С. Муканова, Е.С. Сычева.

20 Акимбаева Н.О. Изучение «зеленых» методов N-алкилирования моноэтаноламина / Н.О. Акимбаева, С.А. Визер, И.Н. Ануарбекова, Т.М. Сейлханов, К.Б. Ержанов // Хим. журн. Каз. — 2016. — № 4. — С. 302–308.

21 Ануарбекова И.Н. Синтез N(алкил)-N-моноэтаноламинов на основе первичного амина / И.Н. Ануарбекова, Н.О. Акимбаева, Н.Б. Курманкулов // Инновационные технологии и исследования, направленные на развитие «зеленой» энергетики и глубокую переработку продукции: сб. материалов междунар. шк.-семинара. — Усть-Каменогорск, 2013. — С. 64.

22 Акимбаева Н.О. Применение методов «зеленой» химии в синтезе фосфорилоксиэтилкарбамата натрия / Н.О. Акимбаева, Е.С. Сычева, С.А. Визер, К.Б. Ержанов // Хим. журн. Каз. — 2017. — № 2. — С. 243–250.

С.А. Визер, Н.О. Әкімбаева, Қ.Б. Ержанов

Флотореагенттер синтезіндегі «жасыл» химия әдістері

Мақалада потенциалды беттік белсенді заттар және флотореагенттер болып табылатын моноэтаноламин мен диэтаноламиннің әртүрлі туындыларының синтезіне «жасыл» химия әдістерін жасауға арналған авторлардың өз жұмыстарына шолу жүргізілген. Онда «жасыл» химия принциптерін қолданғанда мақсатталған өнімнің шығымдары біршама (екі-үш есеге) жоғарылайтыны және процесті жүргізу температурасы мен реакция жүргізу ұзақтығы он есе төмендеуі біршама энергетикалық және еңбек шығындардың қысқаруына әкелген. Атомэкономды әдіспен мақсатталған флотореагенттердің синтезі — саты саны екіден бірге дейін қысқартып, сонымен қатар мақсатталған заттың жалпы шығымын 2-3 есеге дейін жоғарылатуға қабілеттілігін көрсеткен.

Кілт сөздер: беттік белсенді заттар, флотореагенттер, «жасыл» химия, моноэтаноламин және диэтаноламиндердің алкилді және диалкоксифосфорил туындылары, ксантогенат, карбамат.

С.А. Визер, Н.О. Акимбаева, К.Б. Ержанов

«Зеленые» методы химии в синтезе флотореагентов

В статье проведен обзор собственных работ авторов, посвященных разработке «зеленых» методов химии в синтезе разнообразных производных моноэтаноламина и диэтаноламина, являющихся потенциальными поверхностно-активными веществами и флотореагентами. Показано, что применение принципов «зеленой» химии позволяет значительно (в два-три раза) повысить выходы целевых веществ при десятикратном сокращении продолжительности проведения реакций и снижении температуры проведения процессов, что приводит к значительному сокращению энергетических и трудовых затрат. Синтез целевых флотореагентов атомэкономным методом — с сокращением числа стадий от двух до одной также способствует повышению общего выхода целевых веществ в 2-3 раза.

Ключевые слова: поверхностно-активные вещества, флотореагенты, «зеленая» химия, алкильные и диалкоксифосфорильные производные моноэтаноламина и диэтаноламина, ксантогенат, карбамат.

References

1 Sheldon, R.A. (2004). Kataliticheskie prevrashcheniia v vode i sverkhkriticheskom diokside uhleroda s pozitsii kontseptsii ustoichivoho razvitiia [Catalytic transformations in water and supercritical carbon dioxide from the standpoint of the concept of sustainable development]. *Rossiiskii khimicheskii zhurnal — Russian Chemical Journal, 48, 6,* 74–83 [in Russian].

2 Kustov, L.M., & Beletskaya, I.P. (2004). «Green Chemistry» — novoe myshlenie [«Green Chemistry» — a new thinking]. *Rossiiskii khimicheskii zhurnal — Russian Chemical Journal, 48, 6,* 3–12 [in Russian].

3 Anastas, P., Bartlett, L.B., Kirchhoff, M.M., & Williamson, T.C. (2000). The Role of Catalysis in the Design, Development and Implementation of Green Chemistry. *Catalysis Today, 55, 1–2,* 11–22.

4 Abramov, A.A. (2008). *Flotatsionnye metody obohashcheniia [Flotation methods of enrichment]*. Moscow: Publ. house of Moscow State Mining University; Publishing house «Hornaia kniga», «Mir hornoi knigi» [in Russian].

5 Abramov, A.A. (2010). *Sobranie sochinenii. T. 7. Flotatsiia. Reagenty-sobirateli [Collected works. Vol. 7. Flotation. Reagents-collectors]*. Moscow: Publ. house of Moscow State Mining University [in Russian].

6 Abramov, A.A. (2012). Puti razvitiia teorii obohatitelnykh protsessov i sozdaniia innovatsionnykh tekhnolohii kompleksnoho ispolzovaniia syria [Ways of development of the theory of enrichment processes and the creation of innovative technologies for the integrated use of raw materials]. *Fiziko-tekhnicheskie problemy razrabotki poleznykh iskopaemykh — Physico-technical problems of mining, 1*, 165–178 [in Russian].

7 Kalugin, S.N. (2014). *Khimiia i tekhnolohiia polucheniia flotoreahentov [Chemistry and technology of obtaining flotation agents]*. Almaty: Kazakh University [in Russian].

8 Shubov, L.Ya., Ivankov, S.I., & Scheglova, N.K. (1990). *Flotatsionnye reahenty v protsessakh obohashcheniia mineralnoho syria [Flotation reagents in the processes of mineral dressing]*. (In 2 books. Book 1). Moscow: Nedra [in Russian].

9 Abramov, A.A., & Sorokin, M.M. (2009). Printsipy vybora i sinteza bolee selektivnykh sobiratelei vo flotatsii [Principles of selection and synthesis of more selective collectors in flotation]. *Tsvetnye metally — Non-ferrous metals, 4*, 35–40 [in Russian].

10 Ignatkina, V.A. (2009). Vybor selektivnykh sobiratelei dlia flotatsii sulfidnykh mineralov [Selection of selective collectors for the flotation of sulphide minerals]. *Tsvetnye metally — Non-ferrous metals, 6*, 14–19 [in Russian].

11 Riaboy, V.I. (2002). Sozdanie i primenenie bolee effektivnykh reagentov na osnove fiziko-khimicheskikh predstavlenii [Creation and application of more effective reagents on the basis of physical and chemical representations]. *Obogashchenie rud — Enrichment of ores, 1*, 19–23 [in Russian].

12 Chanturia, V.A., & Shafeev, R.Sh. (1977). *Khimiia poverkhnostnykh yavlenii pri flotatsii [Chemistry of surface phenomena in flotation]*. Moscow: Nedra [in Russian].

13 Rubtsov, N.V., & Usova, V.M. (1972). Effektivnost sochetanii ksantohenatov [Efficiency of combinations of xanthates]. *Tekhnolohiia obohashcheniia polimetallicheskikh rud — Technology of enrichment of polymetallic ores.* Moscow: Nedra [in Russian].

14 Erzhanov, K.B., Akimbaeva, N.O., Anuarbekova, I.N., Tusupbaev, N.K., Yerzhanova, Zh.A., & Mukhanova, A.A. (2013). Innovatsionnyi patent RK № 26888. Dinatrievaia sol N-oktil-N,N-bis(2-ksantogenatetil)amina, obladaiushchaia flotatsionnoi aktivnostiu pri obohashchenii sulfidnykh rud [Innovation Patent of the Republic of Kazakhstan No. 26888. Disodium salt of N-octyl-N,N-bis(2-xanthate ethyl)amine, which has flotation activity in the enrichment of sulphide ores]. *Biulleten izobretenii — Bulletin*, 5 [in Russian].

15 Erzhanov, K.B., Akimbaeva, N.O., Anuarbekova, I.N., Tusupbaev, N.K., Erzhanova Zh.A., & Mukhanova A.A. (2014). Innovatsionnyi patent RK № 28114. 2-[N-geptil-N-(2-gidroksietil)amino]etilksantohenat natrii, obladaiushchii flotatsionnoi aktivnostiu [Innovation Patent of the Republic of Kazakhstan No. 28114. 2-[N-heptyl-N-(2-hydroxyethyl)amino]ethylxanthate sodium, having flotation activity]. *Biulleten izobretenii — Bulletin*, 2 [in Russian].

16 Ergozhin E.E., Erzhanov K.B., Akimbaeva N.O., Anuarbekova I.N., Tusupbaev N.K., Erzhanova Zh.A., & Mukhanova A.A. (2013). Innovatsionnyi patent RK № 26889. N,N-Di(2-gidroksietil)aminononan, obladaiushchii flotatsionnoi aktivnostiu pri obohashchenii sulfidnykh rud [Innovation patent of Republic of Kazakhstan № 26889. N,N-Di(2-hydroxyethyl)aminononane, which has a flotation activity in the enrichment of sulphide ores]. *Biulleten izobretenii — Bulletin*, 5 [in Russian].

17 Erzhanov, K.B., Kurmankulov, N.B., & Vizer, S.A., et al. (2012). *Otchet o nauchno-issledovatelskoi rabote «Razrabotka tekhnolohii polucheniia novykh poverkhnostno-aktivnykh veshchestv na osnove produktov pererabotki uhlevodorodnoho syria», po nauchno-tekhnicheskoi prohramme O.0537–03 «Nauchnoe obespechenie razvitiia khimicheskoi promyshlennosti Respubliki Kazakhstan na 2010–2012 hody», 1 napravlenie — pererabotka uhlevodorodnoho syria i neftekhimiia, razdel 3 «Razrabotka i realizatsiia tekhnolohii pererabotki uplevodorodnoho syria s tseliu polucheniia monomerov, polimerov i poverkhnostno-aktivnykh veshchestv». № Gos. rehistratsii 0110RK00199, otchety v NTsNTI pod inv. nomerami 0210RK01118 (2010 g.), 211RK00730 (2011 g.) 0212RK00833 (2012 g.)* [Report on the research work «Development of technology for obtaining new surfactants based on hydrocarbon feedstock products», on the scientific and technical program O.0537–03 «Scientific provision of development of the chemical industry of the Republic of Kazakhstan for 2010–2012», 1st direction — Processing of hydrocarbon raw materials and petrochemistry, Section 3 — Development and implementation of hydrocarbon processing technologies for the production of monomers, polymers and surfactants. State. registration No. 0110RK00199, reports in the NCSTI under Inv. numbers 0210RK01118 (2010), 0211RK00730 (2011) 0212RK00833] [in Russian].

18 Akimbaeva, N.O., Anuarbekova, I.N., Vizer, S.A., & Yerzhanov, K.B. (2016). Application of «green» chemistry's principles at the N-alkylation of diethanolamine. *Chem. J. Kaz.*, 2(54), 183–188.

19 Akimbaeva, N.O., Erzhanov, K.B., Vizer, S.A., Anuarbekova, I.N., Mukanova, M.S., & Sycheva, E.S. (2016). *Promezhutochnyi otchet po hrantu «Issledovanie i razrabotka «zelenykh» uslovii sinteza otechestvennykh vysokoeffektivnykh i selektivnykh flotoreahentov na osnove mestnoho syria dlia obohashcheniia trudnoobohatimykh polimetallicheskikh i zolotosoderzhashchikh rud» po biudzhetnoi programme G.2015 «Razvitie nauki», № hos. rehistratsii 0115RK00252, otchet v NTsNTI, inv. nomer 0216RK01536* [Interim report on the grant «Research and development of» green «conditions for the synthesis of domestic highly effective and selective flotation agents based on local raw materials for the enrichment of difficult-to-digestible polymetallic and gold-bearing ores» under the budget program G.2015 «Development of Science», registration No. 0115RK00252, report in the NCISTI, inv. number 0216PK01536] [in Russian].

20 Akimbaeva, N.O., Vizer, S.A., Anuarbekova, I.N., Seilkhanov, T.M., & Erzhanov, K.B. (2016). Izuchenie «zelenykh» metodov N-alkilirovaniia monoetanolamina [The study of «green» methods of N-alkylation of monoethanolamine]. *Khimicheskii zhurnal Kazakhstana — Chem. J. Kaz., 4*, 302–308 [in Russian].

21 Anuarbekova, I.N., Akimbaeva, N.O., & Kurmankulov, N.B. (2013). Sintez N(alkil)-N-monoetanolaminov na osnove pervichnoho amina [Synthesis of N(alkyl)-N-monoethanolamines based on the primary amine]. Proceedings from Innovative technologies and research aimed at the development of green energy and deep processing of products'13: *Mezhdunarozhdnaia shkola-seminar — Int. school-seminar* (p. 64). Ust-Kamenogorsk [in Russian].

22 Akimbaeva, N.O., Sycheva, E.S., Vizer, S.A., & Erzhanov, K.B. (2017). Primenenie metodov «zelenoi» khimii v sinteze fosforiloksietilkarbamata natriia [Application of the methods of «green» chemistry in the synthesis of sodium phosphoryloxyethylcarbamate]. *Khimicheskii zhurnal Kazakhstana — Chem. J. Kaz., 2,* 243–250 [in Russian].

G.G. Baikenova[1], T.V. Benz[1], L.M. Sugralina[2]

[1]*Karaganda Economic University of Kazpotrebsouyz, Kazakhstan;*
[2]*Ye.A. Buketov Karaganda State University, Kazakhstan*
(E-mail: murzabek_b@mail.ru)

Analysis of the quality of water resources of the Republic of Kazakhstan

The article summarizes and analyzes the data of observations on the condition of water resources of the Republic of Kazakhstan. The rivers and lakes of Kazakhstan are sources of water consumed by the population of the country for various needs, while the availability of water is reduced, and the demand for it is growing due to the development of large cities and expansion of business in various regions of the country. Therefore the problem of saving and rational usage of available water resources is topical. The article shows the factors affecting the quality of water in open reservoirs as well as the results of observations of fresh water sources for five years. The analysis of data presented testifies to the deterioration of the environmental situation as a whole. The number of water resources having class of hazard «pure» is decreasing, and the number of water sources of «dirty» and «very dirty» classes is increasing. It is noted that the most contaminated areas are the territories of East Kazakhstan and Karaganda, Aktobe and Zhambyl regions. The level of pollution of fifteen water resources was determined, it was noted that the main pollutants are zinc, manganese, nickel and nitrogen compounds. The analysis of the data presented indicates the need to address the serious problem caused by fresh water pollution due to an increase in the amount of sewage, and ways to solve this problem should have a legislative basis that will protect the environment from the harmful effects of anthropogenic factors.

Keywords: water resources of the Republic of Kazakhstan, rivers, pollution, pollutants, environmental protection.

Water occupies a special place among the natural resources of our planet. It is known that less than 30 % of the Earth's surface is land, and everything else is the World Ocean. And although there is a lot of water on the globe, it is not evenly distributed across the countries and regions of the Earth. It should be borne in mind that fresh water is negligible, it means about 3 % together with the ice of the Arctic, Greenland and Antarctica in relation to the general water resources of our planet.

Resources of surface river waters of the Republic of Kazakhstan according to the State Committee of the Republic of Kazakhstan on average are estimated at 100.9 billion m^3 per year of which 56.5 % are formed in Kazakhstan and 44.4 % amount comes from adjacent territories such as China, Republic of Uzbekistan, Republic of Kyrgyzstan and the Russian Federation [1, 2].

Our country occupies the last rating among the former Soviet Union republics for water availability. Specific water availability is about 36,000 per 1 km^2 and 6,000 m^3 per person per year [2].

There are eight river basins on the Kazakhstan territory, the largest of which are Irtysh, Balkhash-Alakol, Aral-Syrdarya and Zhayik-Caspian, it consists more than 90 % of water resources in total.

In general Kazakhstan water resources are unevenly distributed across regions. Thus 34.5 % of all water resources are in the Eastern region, 4.2 % in the North, 2.6 % in the Central region, 24.1 % in the South, 21.2 % in the Western South, 13.4 % in the West.

Total resources of fresh water are estimated at 524 km^3 including 80 km^3 of water locating on the glaciers, 190 km^3 of water are concentrated in lakes, the resources of the rivers contain 101 km^3. Reserves of groundwater make up 7.6 km^3, including next points: for domestic and drinking water supply — 5.6 km^3; for household, drinking and industrial and technical water supply — 0.4 km^3; for domestic and drinking water supply together with irrigation of land — 1.3 km^3 [3].

At present 67 % of the population of Kazakhstan can use the central system of drinking water supply, while in Russia this figure is 89 %, in Great Britain, Germany, France, Singapore and Israel it is almost 100 %. Access to the centralized system of water disposal is less than half of the country's population, in Germany and France — 93 %, the UK — 98 %. By 2040 it is expected to increase the irretrievable consumption of water for public utilities up to 1.4 km^3 (an average of 1.9 % per year). The population growth is projected to 20.8 million people, which will lead to an increase in water consumption up to 35 %, while the urban population will increase from the current 53 % to 73 % due to the formation of agglomeration centers on the basis of the largest cities of Kazakhstan such as Astana, Almaty and Shymkent with a population of at least two million people as well as Aktobe and Aktau which have a high proportion of the able-bodied population and where small and medium businesses are most actively developing. As the country develops other

major cities of Kazakhstan may become centers of agglomeration, which will require the construction of a new water infrastructure to meet the needs of the growing population of agglomerations in water supply and sanitation [3].

The situation with lack of affordable drinking water, waste water and waste water treatment is aggravated by the backlog in the technical support and repair of the existing infrastructure of centralized water supply. A significant part of the communal infrastructure is in a dilapidated state, which leads to high water losses. On a nationwide scale they account for about 40 % of the total amount which is significantly higher than in countries such as the USA (11 %), Russia (21 %), the UK (23 %). One of the reasons for the backlog in infrastructure development is the weak tariff setting mechanism, which does not allow covering operational and investment costs [4].

The general unsatisfactory state of assets (over 60 % worn ones) worsens the quality of the services of centralized water supply. The efficiency of public services in Kazakhstan lags behind those of the United Kingdom, Italy, and Russia: there are 1.5 to 4 employees per thousand water users, while it is 0.3 to 1.3 person in other countries [5].

In general the gradual economic recovery of the demand for water will increase as the population becomes larger. In this connection it is necessary to carry out large-scale works on saving and rational use of water resources [5].

Parameters of drinking water quality standards in Kazakhstan generally correspond to European standards and the World Health Organization, but the levels of the maximum allowable values of international standards, for example, for turbidity, are often more stringent.

According to the Committee for Consumer Protection of the Ministry of National Economy of the Republic of Kazakhstan, the main reasons affecting the quality of water in open reservoirs are:

− non-observance of the size of water protection zones,

− the formation of spontaneous household dumps,

− effluent of industrial and agricultural objects,

− accommodation of residential and industrial facilities on the banks of river beds without coordination with the sanitary epidemiological service, accidents on sewer networks, and others [3].

The level of surface water pollution was estimated from the complex index of water pollution (IWM), which is used to compare and identify the dynamics of water quality changes and varies insignificantly from year to year (Table 1).

T a b l e   1

Distribution of water bodies with a class of hazard

Class of hazard	Amount of water bodies				
	2011	2012	2013	2014	2015
«Pure»	13 (15.3 %)	23 (21.5 %)	25 (22.9 %)	18 (16.2 %)	10 (9.9)
«Moderately polluted»	52 (61.2 %)	49 (45.8 %)	52 (47.7 %)	49 (44,1 %)	65 (60.8)
«Polluted»	12 (14.1 %)	26 (24.3 %)	17(15.6 %)	28 (25.2 %)	–
«Dirty»	5 (5.9 %)	6 (5.6 %)	6 (5.5 %)	11(9.9 %)	–
«Very dirty»	1 (1.2 %)	2 (1.9 %)	9 (8.3 %)	3 (2.7 %)	33 (28.3)
«Extremely dirty»	2 (2.35 %)	1 (0.9 %)	–	2 (1.8 %)	1 (1.0)

In 2014–2015 the number of water bodies of the class «pure» has decreased compared with 2012–2013.

In 2015 the number of water bodies with the class «very dirty»(33) increased compared with 2011–2013 (2011 — 1, 2013 — 2, 2013 — 9).

The observations on the quality of surface waters by hydro chemical indicators were carried out at 215 hydro chemical stations, which were distributed in 88 water bodies in 2011; then 240 hydro chemical sections were distributed for 104 water bodies in 2012. In 2013–2015 observations were made on 240 hydro chemical stations, which were distributed on 109 water bodies, namely 71 rivers, 16 lakes, 14 reservoirs, 3 canals, 1 sea [3].

Constant water pollution occurs in water bodies on the territory of the East Kazakhstan area, Karaganda, Aktobe, Zhambyl regions by heavy metals, nutrients and organic substances, in connection with the historical discharges of chemicals (the river Ilekbor, pollutant is chrome), a historical accident at a chemical plant (Lake. Biilikol — increase in BOD5), obtaining of purification discharges from mining and mining enterprises (the rivers Cherubaynura, Kara-Kengir, Sokyr, Nura, pollutants are nitrogen nitrite, ammonium salt,

copper, zinc, oil products, phenol S), (the rivers Krasnoyarka, Breksa, Tikhaya, Glubochanka, pollutants are zinc, cadmium, copper, iron, manganese, ammonium salt) (Table 2).

In addition, excess MPCs are fixed due to high background concentrations of chemicals in the regions. For example, in the basin of the river Tobyl there were manganese, nickel, iron; in the mountain rivers of the Ile river basin copper, fluorides were; In Balkash – Alakol systems of lakes and lakes of Shchuchinsk – Borovoe resort zone there was high mineralization.

T a b l e 2

Information on pollution of surface waters of the Republic of Kazakhstan

Name of water body, region	Level of pollution	Name of pollutants
Elek river (Aktobe region)	«Very dirty»	Boron, chromium (6+), ammonium saline
Esil river (Akmola region)	«Very dirty»	Nitrogen, manganese
Glubochanka river (East Kazakhstan)	«Very dirty»	Zinc, manganese
Brex river (East Kazakhstan)	«Very dirty»	Zinc, manganese
Tikhaya river (East Kazakhstan)	«Very dirty»	Zinc, manganese
Krasnoyarka river (East Kazakhstan)	«Very dirty»	Zinc, manganese
Ulba river (East Kazakhstan)	«Very dirty»	Zinc, manganese
Tobyl river (Kostanay region)	«Very dirty»	Manganese, nickel
Nura river (Karaganda region)	«Very dirty»	Manganese, nitrite nitrogen
Kara Kengir river (Karaganda region)	«Extremely dirty»	Ammonium saline, manganese, nitrite nitrogen
Kokpekty river (Karaganda region)	«Very dirty»	Manganese
Samarkand Reservoir (Karaganda region)	«Very dirty»	Manganese
Sokyr river (Karaganda region)	«Very dirty»	Manganese, nitrite nitrogen, ammonium salt
Cherubai-nura river (Karaganda Region)	«Extremely dirty»	Manganese, nitrite nitrogen, ammonium salt
Nura-Yesil Channel (Karaganda region)	«Very dirty»	Manganese

Pollution and scarcity of water resources constitute a serious environmental problem for the sustainable development of Kazakhstan. Currently rational use of water resources is an extremely urgent problem. This, above all, protecting water areas from pollution, and since industrial wastewater is the first in terms of the volume and damage that they cause, it is first of all necessary to solve the problem of dumping them into rivers. In particular, it is necessary to limit discharges into reservoirs, as well as improvement of production, purification and utilization technologies. Also it is important to collect charges for the discharging sewage and pollutants and to transfer levied funds for the development of new non-waste technologies and treatment facilities.

Apparently, the ways to solve the problem of water resources pollution in Kazakhstan lie primarily in the development of a developed legislative framework that would allow to really protect the environment from harmful anthropogenic impact, as well as to find ways to implement these laws in practice.

References

1   Берденов Ж.Г. Источники загрязнения водных ресурсов как одна из главных проблем рационального природопользования в Казахстане / Ж.Г. Берденов, Е.Х. Мендыбаев, Г.М. Джаналеева // Науки о Земле: вчера, сегодня, завтра: материалы Междунар. науч. конф. (Казань, 20–23 мая 2015 г.). — Казань: Бук, 2015. — С. 78–84.

2   Нечаева В.Л. Водные ресурсы как фактор сохранения национальной безопасности Республики Казахстан: дис. … канд. полит. наук / В.Л. Нечаева. — Астана, 2006. — С. 65–70.

3   [ЭР]. Режим доступа: http://ecodoklad.kz

4 Гусева Л.Ю. // Аналитический обзор. — 2010. — № 1. — С. 56–58.

5 Байкенова Г.Г., Тусупова К.М. // Вестн. КЭУ. — 2012. — № 4. — С. 122–124.

Г.Г. Байкенова, Т.В. Бенц, Л.М. Сугралина

Қазақстан Республикасының жерүсті суларының сапасын сараптау

Мақалада Қазақстан Республикасының су қорларының жағдайын бақылау мәліметтері сарапталды және қорытылды. Қазақстанның өзендері мен көлдері ел халқымен әртүрлі қажеттеліктерге қолданылатын су көзі, сондықтан жарамды сулар қоры азаюда, ал оған деген қажеттілік елдің әртүрлі аймақтарында бизнестің кеңеюімен және ірі қалалардың дамумен артуда. Сондықтан бар су қорларын сақтау және тиімді қолдану өзекті болып табылады. Мақалада ашық резервуарлардағы су сапасына әсер ететін факторлар және соңғы бес жылда тұщы су қорларын бақылау нәтижелері келтірілген. Мәліметтерді сараптау жалпы экологиялық жағдайдың нашарлағанын көрсетті. «Таза» санаттағы су қорларының саны азайып, ал «лас» және «өте лас» санаттағы су қорларының мөлшері артуда. Шығыс Қазақстан аудандары және Қарағанды, Ақтөбе және Жамбыл облыстары ең ластанған аймақтар болып табылды. Он бес су қорларының ластану дәрежесі анықталды, негізгі ластандырғыштар болып мырыш, марганец, никель және азот қосылыстары екені табылды. Көрсетілген мәліметтер ағынды сулардың артуымен тұщы судың ластануына негізделген күрделі мәселелерді шешу қажеттігінің дәлелі және бұл мәселені шешу қоршаған ортаны антропогенді фактордың зиянды әсерінен қорғауға мүмкіндік беретін заңдық тұрғыда болуы қажет.

Кілт сөздер: Қазақстан Республикасының су қорлары, өзендер, ластану, ластаушы заттар, қоршаған ортаны қорғау.

Г.Г. Байкенова, Т.В. Бенц, Л.М. Сугралина

Анализ качества поверхностных вод Республики Казахстан

В статье обобщены и проанализированы данные наблюдений о состоянии водных ресурсов Республики Казахстан. Реки и озера Казахстана являются источниками воды, потребляемой населением страны для различных нужд, при этом запасы пригодной воды уменьшаются, а потребность в ней растет в связи с развитием крупных городов и расширением бизнеса в различных регионах страны. Поэтому проблема сохранения и рационального использования имеющихся водных ресурсов является актуальной. В статье указаны факторы, влияющие на качество воды в открытых резервуарах, а также результаты наблюдений за источниками пресной воды за пять лет. Анализ представленных данных свидетельствует об ухудшении экологической обстановки в целом. Число водных ресурсов класса «чистый» уменьшается, а количество источников воды класса «грязный» и «очень грязный» увеличивается. Отмечено, что наиболее загрязненными регионами являются территории Восточного Казахстана, Карагандинской, Актюбинской и Жамбылской областей. Был определен уровень загрязнения пятнадцати водных источников. Отмечено, что основными загрязнителями являются цинк, марганец, никель и соединения азота. Анализ представленных данных свидетельствует о необходимости решения серьезной проблемы, обусловленной загрязнением пресной воды из-за увеличения количества сточных вод, причем пути решения этой проблемы должны иметь законодательную основу, что позволит защитить окружающую среду от вредного влияния антропогенного фактора.

Ключевые слова: водные ресурсы Республики Казахстан, реки, загрязнения, загрязняющие вещества, защита окружающей среды.

References

1 Berdenov, Zh.G., Mendybaev, E.Kh., & Dzhanaleeva, G.M. (2015). Istochniki zahriaznzeniya vodnykh resursov kak odna iz hlavnykh problem ratsionalnoho prirodopolzovaniia v Kazakhstane [Sources of water resources pollution as one of the main problems of rational nature management in Kazakhstan]. Proceedings from Earth Sciences: Yesterday, Today, Tomorrow' 15: *Mezhdunarodnaia nauchnaia konferentsiia (20–23 maia) — International Scientific Conference* (pp. 78–84). Kazan: Buk [in Russian].

2 Nechaeva, V.L. (2006). Vodnye resursy kak faktor sokhraneniia natsionalnoi bezopasnosti Respubliki Kazakhstan [Water Resources as the Factor of Maintenance of National Safety of Republic Kazakhstan]. *Candidate's thesis*. Astana [in Russian].

3 (n.d.). Retrieved from http://ecodoklad.kz [in Russian]

4 Guseva, L.Yu. (2010). *Analiticheskii obzor — Analytical Review, 1*, 56–58 [in Russian].

5 Baikenova, G.G., & Tusupova, K.M. (2012). *Vestnik KEU — Bulletin of KEU, 4*, 122–124 [in Russian].

ХИМИЯНЫ ОҚЫТУ ӘДІСТЕМЕСІ
МЕТОДИКА ОБУЧЕНИЯ ХИМИИ
METHODS OF TEACHING CHEMISTRY

G.T. Kokibasova, K.K. Serikova, M.M. Abisheva, S.H. Kaztayeva, A.Zh. Beisova

Ye.A. Buketov Karaganda State University, Kazakhstan
(E-mail: kokibasova@mail.ru)

Implementation of new forms of works for formation of skills of information critical analysis

Technology of critical thinking development aimed at gaining new knowledge, including on the basis of knowledge which is already available through its critical analysis. The main condition for the development of critical thinking is not a presentation of a specific and limited amount of information, but motivation of interest in the Chemistry study, the critical assessment of the proposed theoretical and empirical material by students and then synthesizing them in their activities. To develop skills of critical analysis the new forms of independent work have been introduced. With the aid of reflexive questions the students' attitude have been ascertained. There are many techniques and strategies to generate critical thinking. In this paper we have highlighted some of the most popular and productive methods, besides it was necessary to take into account the possibility of its use in Chemistry lessons. Each method allows diversifying the learning process, which often consists of one activity: written or oral.

Keywords: critical thinking, modernization, analysis, reflection, Venn diagram, techniques, strategies, presentation.

Creation of conditions and the use of various learning tools that can generate students' critical thinking is one of the main tasks of the successful implementation of the modernization of education, so now many educators and psychologists conducted theoretical and empirical search for the creation of these conditions.

Students themselves should set goals and choose ways to achieve them, to use the knowledge acquired at school in real life, beyond the educational process.

Critical thinking development technology aimed at obtaining new knowledge, also on the basis of knowledge already available through its critical analysis. In more detail about technology of development of critical thinking, about the methods and strategies proposed by it, it is described in this source [1; 89]. For example, an effective study of the theme pH of the solutions is possible only with thorough knowledge of such concepts as hydrolysis, dissociation, strong, weak acids and bases. I.e. studied information should have a causal relationships and a logical sequence. It is also important that students do not perceive the information received from the teachers as undeniable truth without the possibility of its sequential analysis. For example, when studying the theme «The structure of electron shells» distribution of electrons along energy levels (electron arrangement in cells) is perceived as a given, or that in a molecule consisting of two different kinds of atoms, such as CO_2, is polar covalent bond, although this oxide is not pole.

With the development of information technology, the Internet, everyone can access the specialized knowledge at any point and almost instantly. Simultaneously with the appearance of unlimited access absolutely to all information, is increasing the risk of links, the study of unreliable sources with not quite trustworthy information.

Considering all the above arguments, first-year students need to develop the ability to critical analysis of information. For this you can use new forms of independent work, contributing to the development of critical thinking.

We carried out a pedagogical experiment on the subject «Chemistry of elements» classes, in which took part first-year students. Earlier we have written an article about implementation of techniques and strategies proposed by technology of development of critical thinking and the impact of these forms of work on the learning activities of schoolchildren [2]. Only the first year students were selected to participate in the experiment, as schools still maintained the linear system of training represented by a class-and-lesson form of organization of educational process, where students study subjects strictly sequentially in a specific amount for a certain period in the classroom. Universities Students use a credit system, which is aimed at increasing the level of self-education, and to individualization student learning pace. Therefore, first-year students are less prepared for the individual form of organization of learning, where they have to develop knowledge on their own. It is also one of the reasons why the first year students took part in the experiment is that at school students use one or two books, when they come to University, they do not have a unified textbook for learning. This is also one of the difficulties in finding and studying the information.

The aim of the pedagogical experiment was to teach the students a critical analysis of incoming information. The experiment was conducted in a period of 4 months, 24 people were involved. According to the program of the discipline at every lesson describes a specific group of elements, such as group 15, group 16 and their separate agents, the compounds which they form and characteristic properties of these compounds. To maximize the assimilation of information flow through its critical analysis, we decided to use the group training that has allowed us to analyze simultaneously emotional and functional comfort of students when training in groups.

Before reading every lecture on the topic of discipline students write their own abstracts. To evaluate the effectiveness of composed abstracts the students were asked to answer a number of questions on the topic, using only their abstracts. At the end of the lesson the students were asked the following questions:

1. Do you consider your abstracts effective?

2. The abstracts helped you when answering the questions?

3. Do you consider you need to learn how to compose more effective abstracts?

The survey revealed that the majority of students believe that their abstracts were imperfect. For most students abstracts are mechanical rewriting of the text from the textbook, without analyzing the information, which entails a lack of systemacy of knowledge For example, students describe the sectors that use nitrogen, but they cannot explain why it is used, due to what property it is widely used in a particular sector.

Before the start of the experiment we have chosen the form of independent work that promote the development of critical thinking skills, that as a result would have led to mastering the skills of presenting the results of their analysis in a variety of forms: a collective presentation, a Venn diagram and schemes.

Presentation (duration 15–20 minutes) is prepared by students who were previously divided into groups. For example, in the lesson on the topic «15 group», where the main members are nitrogen and phosphorus, as the basis for the dividing of students into groups, we used the degree of oxidation of specific for the given elements. If a student receives a card with a «+5», then he falls into the group, which had to characterize all nitrogen compounds, where it has an oxidation state +5. The main requirements for the presentation were: own critical analysis of information, close contact with the audience, persuasiveness and creative presentation of information using the examples. Perhaps, work on a collective presentation helps to gain the greatest number of skills and competencies, as besides analytical skills also develops an ability to assign responsibilities, skills of oral effective presentation.

After the completion of work the students have been proposed a number of issues for introspection, where the students had to answer yes or no:

1. I analyze in detail the content of the training material and carry out its selection.

2. I propose to the group the ideas to maximize the presentation effectiveness of the material.

3. Build the logic and sequence of presentation of educational material in preparation for presentation.

4. Plan my speech according to the requirements of the presentation.

After processing the survey results, the following data were obtained: 62 % of students rate their educational activity as high, 38 % — as low.

For clarity the results of the responses to questions for introspection are presented in Figure 1.
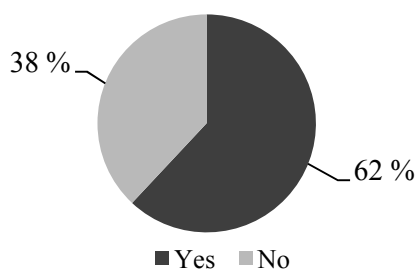
Figure 1. Student's introspection

Also one of the new forms of work has been the development of schemes. The scheme is used for the visual structuring of a theme, allocation of the main structural elements and establishing links between them. These schemes help the students to see not only the features of the objects, but also allow you to memorize the information faster. The scheme allows preparing homework more qualitatively, since it is already a finished reminder that was made on the lesson. It is necessary to ask questions to those who made the scheme. These questions should be free-response questions. This work has allowed to develop in students besides the ability to work to the text, the following skills: highlight keywords, organize the necessary information, analyze, compare and summarize information, development of monologic speech, as well as the students have a need to look for additional information, as it happens that not all the issues are covered in class. These questions remain as homework, which takes the form of fascinating work with information.

Another form, used by us for individual work of students is Venn diagram. The first technique was described by English scientist John Venn in his book «Symbolic Logic». This is a graphical way that is used when you need to compare two or more concepts, methods, objects. «Venn diagram « help to identify common in two or more events, highlight the differences and summarize knowledge on the stated topic [3; 175]. A lesson identifies two or more concepts, terms, events that you need to compare. For example, it is possible to compare the structure and properties that are inherent in nitrogen and phosphorus (Fig. 2). Students draw diagrams, fill the graphs. At the stage of comprehension takes place a discussion of diagrams in groups.
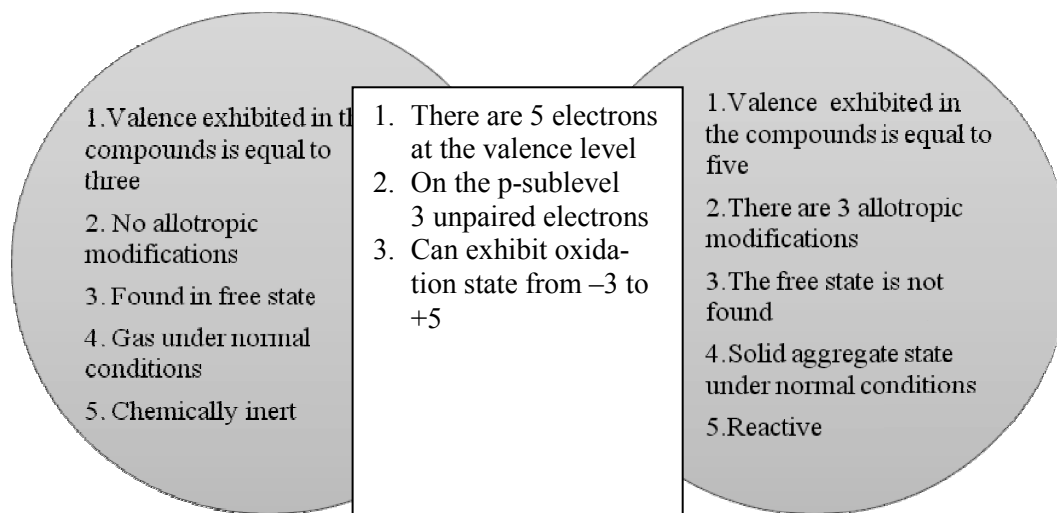
Figure 2. Venn diagram for nitrogen and phosphorus

At the last lesson we carried out self-reflection in order to identify the perception of students of new forms of work. For this the students were given questionnaires with the following questions:

1. Did you like the new ways of working with information?

2. Did you easily manage with providing information in the form of schemes, diagrams and presentations?

3. What do you think, whether this ways of work help to improve the quality of knowledge in the discipline?

4. Would you like to continue to use these ways of work on the lessons?

After processing the survey results, the following data were obtained (see Table).

The results of survey

Answers	Number of students	%
Yes	14	59
No	8	33
Difficult to answer	2	8

The results of this survey are shown in a Figure 3.
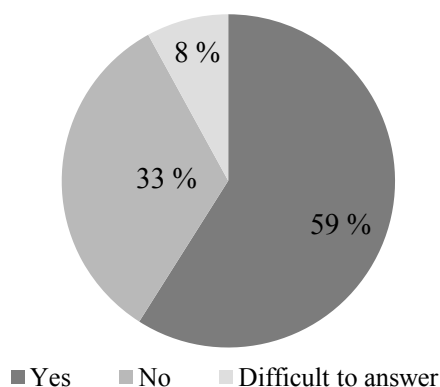
Figure 3. The results of survey

As the results of the survey, most students liked the new ways of work, and they would like to use them in future.

Despite the variety of approaches to the study of the problem and opinions of different scientists, there is a common opinion that critical thinking which is developed enough is an integral part of an effective teaching, good training material possession and use of the information obtained in ordinary life.

There are many techniques and strategies to generate critical thinking. In this paper we have highlighted some of the most popular and productive methods, besides it was necessary to take into account the possibility of its use in Chemistry lessons. Each method allows diversifying the learning process, which often consists of one activity: written or oral.

When using this program, the teacher is not just a source of new information, but also helps in a quality assimilation of information.

References

1   Кокибасова Г.Т. Новые технологии в обучении химии / Г.Т. Кокибасова. — Караганда: Изд-во КарГУ, 2016. — 141 с.

2   Кокибасова Г.Т. Формирование критического мышления учащихся в процессе обучения химии / Г.Т. Кокибасова, М.М. Абишева, К.К. Серикова //Вестник Караганд. ун-та. Сер. Химия. — 2016. — № 2(82). — С. 89–94.

3   Заир-Бек С.И. Развитие критического мышления на уроке / С.И. Заир-Бек, И.В. Муштавинская. — М.: Просвещение, 2011. — 223 с.

Г.Т. Кокибасова, К.К. Серикова, М.М. Абишева, С.Х. Казтаева, А.Ж. Беисова

Ақпаратты сын тұрғыдан талдау дағдыларын қалыптастыру үшін жұмыстың жаңа түрлерін енгізу

Сын тұрғыдан ойлауды дамыту технологиясы жаңа білім алуға, оның ішінде оны сын тұрғыдан талдау көмегімен алынған білім негізіне бағытталған. Ақпаратты шектелген көлемде және толықтай баяндамау, ал олардың химияны зерттеуге деген ынтасының оянуына итермелеу, берілген теориялық және эмпирикалық мәліметтерді оқушылардың сын тұрғысынан бағалауы және бұдан әрі оларды өз мүддесіне қолдануға жинақтау алуы сын тұрғысынан ойлаудың негізгі шарты болып табылады. Сын

тұрғыдан талдау дағдыларын қалыптастыру үшін өзіндік жұмыстың жаңа түрі енгізілді. Рефлексивті сұрақтардың көмегімен студенттердің жұмыстың жаңа түріне деген көзқарастары анықталды. Сын тұрғысынан ойлауды қалыптастыруға мүмкіндік беретін амалдар мен жұмыс түрлері жеткілікті. Тәжірибеде таныс, түсінікті, әрі өнімді бірнеше жұмыс түрлері қолданылды, мұнымен қоса олардың химия сабақтарында қолданылу мүмкіндіктерін ескеру қажет болды. Бұл амал-тәсілдердің әрқайсысы оқыту үрдісін түрлендіруге мүмкіндік беретін бір жұмыс түрінен құралған (жазбаша немесе ауызша).

Кілт сөздер: сын тұрғыдан ойлау, жаңарту, талдау, рефлексия, Венн диаграммасы, тәсілдер, стратегия, тұсаукесер.

Г.Т. Кокибасова, К.К. Серикова, М.М. Абишева, С.Х. Казтаева, А.Ж. Беисова

Внедрение новых форм работы для формирования навыков критического анализа информации

Технология развития критического мышления направлена на получение нового знания, в том числе и на основе уже имеющегося знания при помощи его критического анализа. Главным условием развития критического мышления является не изложение конкретного и ограниченного объема информации, а провоцирование побуждения интереса к изучению химии, критического оценивания учениками предложенного теоретического и эмпирического материала и далее синтезирование их в своей деятельности. Для формирования навыков критического анализа были внедрены новые формы самостоятельной работы. С помощью рефлексивных вопросов установлено отношение студентов к новым формам работы. Существует огромное количество приемов и форм работы, позволяющих сформировать критическое мышление. В данном эксперименте были применены несколько наиболее популярных и продуктивных форм работы, к тому же необходимо было учитывать возможность их применения на занятиях по химии. Каждый из приемов позволял разнообразить учебный процесс, который зачастую состоит из одного вида деятельности: письменного или устного.

Ключевые слова: критическое мышление, модернизация, анализ, рефлексия, диаграмма Венна, приемы, стратегии, презентация.

References

1   Kokibasova, G.T. (2016). Novye tekhnolohii v obuchenii khimii [New technologies while teaching Chemistry]. Karaganda: KarSU Publ. [in Russian].

2   Kokibasova, G.T., Serikova, K.K., & Abisheva, M.M. (2016). Formirovanie kriticheskoho myshleniya uchashchikhsia v protsesse obucheniia khimii [Formation of students' critical thinking in the process of teaching Chemistry]. *Vestnik Karahandinskoho universiteta — Bulletin of Karaganda State University, 2(82)*, 89–94 [in Russian].

3   Zair-Beck, S.I., & Mushtavinskaya, I.V. (2011). Razvitie kriticheskoho myshleniia na uroke [Development of the critical thinking at the lesson]. Moscow: Prosveshchenie [in Russian].

АВТОРЛАР ТУРАЛЫ МӘЛІМЕТТЕР
СВЕДЕНИЯ ОБ АВТОРАХ
INFORMATION ABOUT AUTHORS

Abisheva, M.M. — Master student, Ye.A. Buketov Karaganda State University, Kazakhstan.

Akimbayeva, N.O. — Candidate of chemical sciences, Senior Researcher of the Laboratory of Physiologically Active Compounds Chemistry, A.B. Bekturov Institute of Chemical Sciences, Almaty, Kazakhstan.

Alibiyev, D.B. — Dean of faculty of mathematics and information technologies, Candidate of physical and mathematical sciences, Ye.A. Buketov Karaganda State University, Kazakhstan.

Baikenova, G.G. — Head of Chair of ecology and estimation, Associated Professor, Doctor of chemical sciences, Karaganda Economic University of Kazpotrebsoyuz, Kazakhstan.

Beisova, A.Zh. — Master student, Ye.A. Buketov Karaganda State University, Kazakhstan.

Benz, T.V. — Head of Laboratory, Master of ecology, Karaganda Economic University of Kazpotrebsoyuz, Kazakhstan.

Burkitseterkyzy, G. — Engineer, Zh. Abishev Chemical-Metallurgical Institute, Karaganda, Kazakhstan.

Fomin, V.N. — Associate professor of inorganic and technical chemistry Department, Candidate of chemical sciences, Ye.A. Buketov Karaganda State University, Kazakhstan.

Gizatullina, D.R. — Junior researcher, Zh. Abishev Chemical-Metallurgical Institute, Karaganda, Kazakhstan.

Gogol, D.B. — Leading scientist, Candidate of chemical sciences, Institute of problems of complex development of mineral resources, Karaganda, Kazakhstan.

Ibrayeva, E.S. — Teacher of Chair of Foreign Languages, Ye.A. Buketov Karaganda State University, Kazakhstan.

Irgibayeva, I.S. — Professor, L.N. Gumilyov Eurasian National University, Astana, Kazakhstan.

Katkeeva, G.L. — Candidate of science (Engineering), Ph.D., Assistant professor, Zh. Abishev Chemical-Metallurgical Institute, Karaganda, Kazakhstan.

Kazhikenova, A.Sh. — Associate professor of chair of technique of teaching of mathematics and informatics, Candidate of technical sciences, Ye.A. Buketov Karaganda State University, Kazakhstan.

Kaztayeva, S.H. — Master student, Ye.A. Buketov Karaganda State University, Kazakhstan.

Klimentova, J. — Researcher, Charles University, Prague, Czech Republic.

Kokibasova, G.T. — Senior lecturer, Associate professor, Candidate of chemical sciences, Chair of inorganic and technical chemistry, Ye.A. Buketov Karaganda State University, Kazakhstan.

Kopylov, N.I. — Institute of solid state chemistry and mechanochemistry of the Siberian branch of the Russian Academy of Sciences, Novosibirsk, Russia.

Kudaibergenov, K.K. — PhD, Senior lecturer, al-Farabi Kazakh National University, Almaty, Kazakhstan.

Lukes, I. — Researcher, Charles University, Prague, Czech Republic.

Madlova, M. — Researcher, Charles University, Prague, Czech Republic.

Mansurov, Z.A. — Doctor of chemical sciences, Professor, General director of the Institute of Combustion Problems, Almaty, Kazakhstan.

Mantel, A.I. — Researcher, Luminescent Materials Research Centre Ltd, Astana, Kazakhstan.

Morzhuhina, S.V. — PhD, Head of the Department of Chemistry, new technologies and materials of «Dubna» State University, Moscow region, Russia.

Mukatayev, I.R. — Researcher, L.N. Gumilyov Eurasian National University, Astana, Kazakhstan.

Nemeckova, P. — Researcher, Charles University, Prague, Czech Republic.

Nurkassimova, M.U. — Master of natural sciences, Teacher of the Department of Chemistry, L.N. Gumilyov Eurasian National University, Astana, Kazakhstan.

Nyssanbayeva, G.R. — PhD student, al-Farabi Kazakh National University, Almaty, Kazakhstan.

Omarova, N.M. — PhD, Associate Professor of the Department of Chemistry, L.N. Gumilyov Eurasian National University, Astana, Kazakhstan.

Ongarbayev, Ye.K. — Doctor of chemical sciences, Professor, al-Farabi Kazakh National University, Almaty, Kazakhstan.

Oskembekov, I.M. — Senior researcher, Zh. Abishev Chemical-Metallurgical Institute, Karaganda, Kazakhstan.

Palatinusova, L. — Researcher, Charles University, Prague, Czech Republic.

Ponomarev, D.L. — Senior researcher, Public association «Grazhdane Kazakhstana», Karaganda, Kazakhstan.

Rozhkovoy, I.E. — Junior researcher, Magister of chemistry, Public association «Grazhdane Kazakhstana», Karaganda, Kazakhstan.

Serikova, K.K. — Master student, Ye.A. Buketov Karaganda State University, Kazakhstan.

Sugralina, L.M. — Professor of Chair of Organic Chemistry and Polymers, Associated Professor, Candidate of chemical sciences, Ye.A. Buketov Karaganda State University, Kazakhstan.

Tashenov, A.K. — Doctor of chemical sciences, Professor, Head of the Department of Chemistry, L.N. Gumilyov Eurasian National University, Astana, Kazakhstan.

Vizer, S.A. — Doctor of chemical sciences, Associate Professor, Principal Researcher of the Laboratory of Physiologically Active Compounds Chemistry, A.B. Bekturov Institute of Chemical Sciences, Almaty, Kazakhstan.

Vojtisek, P. — Department of Inorganic Chemistry, Faculty of Science, Charles University, Prague, Czech Republic.

Yerzhanov, K.B. — Doctor of chemical sciences, Professor, Head of the Laboratory of Physiologically Active Compounds Chemistry, A.B. Bekturov Institute of Chemical Sciences, Almaty, Kazakhstan.

Zhunussov, A.M. — Technician of the highest category, Zh. Abishev Chemical-Metallurgical Institute, Karaganda, Kazakhstan.

ФИЗИКАЛЫҚ ЖӘНЕ АНАЛИТИКАЛЫҚ ХИМИЯ

ХИМИЯЛЫҚ ТЕХНОЛОГИЯ ЖӘНЕ МҰНАЙ ХИМИЯСЫ

ХИМИЯНЫ ОҚЫТУ ӘДІСТЕМЕСІ

Указатель статей, опубликованных в «Вестнике Карагандинского университета» в 2017 году. Серия «Химия»

ФИЗИЧЕСКАЯ И АНАЛИТИЧЕСКАЯ ХИМИЯ

ХИМИЧЕСКАЯ ТЕХНОЛОГИЯ И НЕФТЕХИМИЯ

МЕТОДИКА ОБУЧЕНИЯ ХИМИИ

Index of articles published in
«Bulletin of the Karaganda University» in 2017.
«Chemistry» Series

	№	p.

INORGANIC CHEMISTRY

Abdurazova P.A., Sataev M.S., Koshkarbayeva Sh.T., Raiymbekov Ye.B., Nazarbek U.B. Method for determining the thickness of metal coating deposited on the surface of dielectric material 2 85

Abdurazova P.A., Satayev M.S., Koshkarbayeva Sh.T., Raiymbekov Ye.B., Nazarbek U.B. Research of bactericidal properties of nanoparticles of copper, gold and silver deposited on the surface of non-metallic products... 2 78

Bekturganova A.Zh., Rustembekov K.T., Kasenov B.K., Stoyev M., Toibek A.A. Calorimetric research of a heat capacity of a triple lanthanum tellurite in the range of 298.15–673 K 2 68

Nyssanbayeva G.R., Kudaibergenov K.K., Ongarbayev Ye.K., Mansurov Z.A. Obtaining expanded graphite by heat treatment.. 4 65

Rustembekov K.T., Lazareva Ye.S., Stoev M., Fomin V.N., Kaykenov D.A. Thermochemistry of new holmium-calcium tellurite 3 108

Matayev M.M., Abdraimova M.R., Saksena S.M., Kezdikbayeva A.T. Synthesis and X-ray analysis of complex ferrites $BiMe_3^{II}Fe_5O_{12}$ (M^{II} = Mg, Ca, Ba) 2 73

ORGANIC CHEMISTRY

Akhmetova G.S., Sadyrbayeva F.M., Issayeva U.B., Praliyev K.D., Seilkhanov T.M., Yu V.K., Sultanova D.A. Target synthesis of C- and N-subsituted phenyloxypropynylpiperidines possessing an anti-infective action 3 56

Burkeev M.Zh., Kreuter J., Tazhbayev Y.M., Zhaparova L.Zh., Zhumagalieva T.S., Arystanova Zh.T., Mukhanova D.A. Preparation, characterization and investigation of *in vitro* release of anti-tuberculosis drug p-amino salicylic acid based on human serum albumin 3 38

Burkeev M.Zh., Tazhbaev E.M., Davrenbekov S.Zh., Negim E.M., Kazhmuratova A.T., Khamitova T.O., Ibrayeva L.T., Kozhabekova G.E., Imanbekova Zh.K., Shaiahmetova A.S. Simulation of the synthesis reaction conditions of organic compounds and the behavior of the polymer complex under these conditions 3 50

Burkeyev M.Zh., Tazhbayev E.M., Davrenbekov S.Zh., Bakibayev A.A., Kazhmuratova A.T., Khamitova T.O., Ibrayeva L.T., Kozhabekova G.E., Tolendi Zh.A., Imanbekova Zh.K. Selection of optimal conditions for obtaining of Co nanoparticles in the matrix of polymeric hydrogels............................. 2 23

Burkeyeva G.K. Investigation of copolymers based on unsaturated polyester resins 2 15

Burkeyeva G.K. Terpolymerization of polyethylene glycol maleate with acrylamide and monovinyl ether of monoethanolamine 2 8

Kaliyeva S.S., Mamayeva E.A., Ye.E.Nurpeiis, Bakibayev A.A., Tashenov A.K., Zamanova M.K., Kets T.S. Methods for treating some pentacyclic triterpenoids.. 2 35

Klimentova J., Madlova M., Nemeckova P., Palatinusova L., Vojtisek P., Lukes I. Conformations of calix[4]arenes — an investigation based on CSD data. Part I. Cone conformers of methylene- and heteroatom-bridged calix[4]arenes 1 21

Klimentova J., Madlova M., Nemeckova P., Palatinusova L., Vojtisek P., Lukes I. Conformations of calix[4]arenes — an investigation based on CSD data. Part II. Partial cone, 1,2-alternate and 1,3-alternate conformers of methylene- and heteroatom-bridged calix[4]arenes.. 4 8

Mambetova A.M., Irgibaeva I.S., Mantel A.I. A method of producing fluorescent pigment having a high resistance to organic solvents 1 8

Mantel A.I., Irgibayeva I.S., Mukatayev I.R. Modification of solar batteries by polymer fluorescent films .. 4 39

Mussabayeva B.Kh., Murzagulova K.B., Izumrudov V.A., Kim M.E., Dinzhumanova R.T. Polyelectrolytic multilayers as drug delivery system.. 3 45

Muzychkina R.A., Korulkin D.Yu., Gemedzhieva N.G., Kurbatova N.V. Qualitative and quantitative analysis of biologically active compounds of *Rheum tataricum* L. Roots from Southern Balkhash 1 14

Nurkenov O.A., Fazylov S.D., Seilkhanov T.M., Arinova A.E., Issayeva A.Zh., Satpaeva Zh.B., Karipova G.Zh. Synthesis and structure of condensed biheterocycles on the basis of 3-amino-1,2,4-triazole. 3 9

PHYSICAL AND ANALYTICAL CHEMISTRY

CHEMICAL TECHNOLOGY AND OILCHEMISTRY

METHODS OF TEACHING CHEMISTRY